

---

# Lattice Perturbation Theory of Brillouin Fermions, Stout Smearing, and Wilson Flow and its Application to the Fermion Self-Energy and $c_{SW}$ at One-Loop Order

---

Dissertation im Fach Physik

MAXIMILIAN AMMER

Eingereicht: Juni 2024

Betreuer:  
PD. Dr. Stephan Dürr

*Institut für theoretische Teilchenphysik  
Fakultät für Mathematik und Naturwissenschaften  
Bergische Universität Wuppertal*



**BERGISCHE  
UNIVERSITÄT  
WUPPERTAL**



## **Eidesstattliche Erklärung**

Hiermit versichere ich, dass ich die vorliegende Arbeit selbständig verfasst habe und dass ich keine anderen Quellen und Hilfsmittel als die angegebenen benutzt habe und dass die Stellen der Arbeit, die anderen Werken – auch elektronischen Medien – dem Wortlaut oder Sinn nach entnommen wurden, auf jeden Fall unter Angabe der Quelle als Entlehnung kenntlich gemacht worden sind. Ich erkläre weiterhin, dass die vorliegende Arbeit nicht anderweitig als Dissertation eingereicht wurde.

---

(Datum, Unterschrift)

---

## Abstract

In this thesis the Feynman rules of the Brillouin action are derived. Furthermore stout smearing and the gradient flow of the Wilson gauge action are perturbatively expanded to order  $g_0^3$ . It is shown how to include perturbative stout smearing or the Wilson flow in the Feynman rules of a fermion action. These are then applied to the one-loop calculations of the fermion self energy and the clover improvement coefficient  $c_{\text{SW}}$  for both Wilson and Brillouin fermions and with both Wilson and Lüscher-Weisz gauge background.

---

## Acknowledgements

I thank my advisor, Stephan Dürr, for the support and guidance throughout my time working on the subjects of this thesis. For being patient and understanding and for giving me the initial ideas and letting me run with it.

Thank you to my family. Thank you to my child for brightening my life and often reminding me of myself and the truly important things like rainbows and finding out how cheese gets its holes. Thank you for always asking questions I do not yet know the answers to.

Thank you to my amazing partner for being by my side through all of it. For planning things and keeping our life together. Thank you for the weekends and vacations spent as a family. Thank you for forcing me to go outside and enjoy myself from time to time. Thank you for showing me how to finish a PhD. Thank you for growing with me. I am so glad to have done this parenting PhD-thing with you.

# Contents

<b>1</b>	<b>Introduction</b>	<b>1</b>
<b>2</b>	<b>QFT and the Standard Model</b>	<b>4</b>
2.1	Gauge Theories . . . . .	4
2.2	The Standard Model of Particle Physics . . . . .	8
2.3	Quantum Chromodynamics . . . . .	9
2.3.1	Path Integrals . . . . .	9
2.3.2	Gauge Fixing . . . . .	10
2.3.3	Perturbation Theory . . . . .	11
2.3.4	Renormalization . . . . .	13
2.3.5	Asymptotic Freedom . . . . .	14
<b>3</b>	<b>Lattice Gauge Theory</b>	<b>16</b>
3.1	The naive lattice fermion action . . . . .	16
3.2	The lattice gauge action . . . . .	17
3.3	The lattice path integral . . . . .	19
3.4	Wilson Fermions . . . . .	19
3.5	Brillouin Fermions . . . . .	21
3.6	Improvement . . . . .	24
3.6.1	Clover Improvement . . . . .	24
3.6.2	Improvement of the Gauge Action . . . . .	26
3.7	Smearing and Gradient Flow . . . . .	26
3.7.1	Stout Smearing . . . . .	29
3.7.2	Wilson Flow . . . . .	29
<b>4</b>	<b>Lattice Perturbation Theory (LPT)</b>	<b>32</b>
4.1	The Gauge Action . . . . .	33
4.1.1	Improvement . . . . .	37
4.2	The Fermion Action . . . . .	38
4.2.1	Clover Improvement . . . . .	39
4.3	Fermion Self-Energy . . . . .	40
4.4	Perturbative Determination of $c_{\text{SW}}$ . . . . .	42
<b>5</b>	<b>LPT of Brillouin Fermions</b>	<b>48</b>
5.1	Feynman Rules . . . . .	48
5.2	Self-Energy of the Brillouin Clover Fermion . . . . .	54
5.3	$c_{\text{SW}}^{(1)}$ for Brillouin Fermions . . . . .	56

<b>6 LPT of Stout Smearing and WF</b>	<b>59</b>
6.1 Perturbative Stout Smearing . . . . .	59
6.1.1 Leading Order . . . . .	64
6.1.2 Next-to-Leading Order . . . . .	65
6.1.3 Next-to-Next-to-Leading Order . . . . .	68
6.2 Perturbative Wilson Flow . . . . .	75
6.2.1 Leading Order . . . . .	76
6.2.2 Next-to-Leading Order . . . . .	77
6.2.3 Next-to-Next-to-Leading Order . . . . .	79
6.2.4 Continuum Limit . . . . .	81
6.3 Feynman Rules . . . . .	82
<b>7 Fermion Self-Energy with Stout Smearing and Wilson Flow</b>	<b>84</b>
7.1 $\Sigma_0$ with Stout Smearing . . . . .	84
7.2 $\Sigma_1$ with Stout Smearing . . . . .	94
7.3 $\Sigma_0$ with Wilson Flow . . . . .	102
7.4 $\Sigma_1$ with Wilson Flow . . . . .	108
<b>8 One-Loop <math>c_{\text{SW}}</math> with Stout Smearing and Wilson Flow</b>	<b>114</b>
8.1 $c_{\text{SW}}^{(1)}$ with Stout Smearing . . . . .	116
8.2 $c_{\text{SW}}^{(1)}$ with Wilson Flow . . . . .	123
<b>9 Summary and Conclusion</b>	<b>128</b>
<b>Appendix A Additional Data</b>	<b>132</b>
A.1 $c_{\text{SW}}^{(1)}$ with Brillouin Fermions . . . . .	132
A.2 $\Sigma_0$ with Stout Smearing . . . . .	136
A.3 $\Sigma_1$ with Stout Smearing . . . . .	140
A.4 $\Sigma_0$ and $\Sigma_1$ with Wilson Flow . . . . .	143
A.5 $c_{\text{SW}}^{(1)}$ with Stout Smearing . . . . .	148
A.6 $c_{\text{SW}}^{(1)}$ with Wilson Flow . . . . .	156
<b>Bibliography</b>	<b>156</b>

**Notation and conventions:**

*In Chapter 2:*

*In the continuum we use greek letters  $\mu, \nu, \rho, \sigma \dots$  for space-time indices. The zeroth component of a four-vector is the time component*

$$x^\mu = (x^0, x^1, x^2, x^3) = (ct, x, y, z) .$$

*The Einstein summation convention is used, where summation over repeated indices is implied. We write contra-variant vectors or tensors with lower indices  $x_\mu = \eta_{\mu\nu} x^\nu$  and use the “mostly minus” convention for the Minkowski metric tensor*

$$\eta_{\mu\nu} = \text{diag}(1, -1, -1, -1) .$$

*From Chapter 3 onward:*

*For the lattice we use Greek letters  $\alpha, \beta, \gamma, \dots, \mu, \nu, \rho, \sigma, \dots \in \{1, 2, 3, 4\}$  for euclidean space time indices. The fourth component being the euclidean time component. We only use lower indices*

$$x_\mu = (x, y, z, t_E)$$

*and repeated indices are not automatically summed over. Due to the breaking of Lorentz symmetry on the lattice, expressions where a space-time index appears more than twice are common and we always indicate sums explicitly.*

*We denote colour indices by lower case Latin letters  $a, b, c, \dots$  and sums over repeated indices are implied*

$$T^a T^a = \sum_a T^a T^a .$$

# 1 Introduction

Lattice QCD is a formulation of quantum chromodynamics on a four-dimensional euclidean lattice with lattice spacing  $a$ . The lattice not only acts as a UV regulator but allows access to the non-perturbative regime of QCD through computer simulation. This is achieved by treating the space of field configurations on the lattice as a statistical system with a probability distribution given by the classical action of the theory [1, 2]. The fermion fields are defined on the discrete lattice points  $x$ , while the gauge variables  $U_\mu(x)$  are parallel transporters of the gauge group. Physical results are obtained by evaluating expectation values on lattices with varying lattice spacing  $a$ , while keeping the physical volume constant, and extrapolating to  $a = 0$ .

Lattice operators often involve discretized versions of derivatives, which are not unique, acting on the quark fields. Additionally lattice actions suffer from broken symmetries and doublers, i.e. they describe multiple copies of a fermion field. Therefore there exist many different lattice actions, each with different advantages or disadvantages. For example the Wilson fermion action [3] is able to get rid of all the doublers but thereby breaks chiral symmetry and introduces additive renormalization of the quark mass.

Hence strategies to alleviate such disadvantages and improve the performance of a lattice formulation are very important to producing and understanding lattice results. Some of these strategies, that are important to this thesis include:

- Using better discretizations of derivatives. The “Brillouin action” [4] is a Wilson-like fermion action which uses more favourable approximations of the derivative and Laplace operators in the Wilson action.
- On-shell improvement of lattice actions [5]. By adding terms to the action that vanish in the limit  $a \rightarrow 0$  their scaling behaviour can be improved (for example from  $\mathcal{O}(a)$  to  $\mathcal{O}(a^2)$  for fermion actions or from  $\mathcal{O}(a^2)$  to  $\mathcal{O}(a^4)$  for gauge actions). The clover term [6] is a widely used improvement term for fermion actions and we will determine its coefficient  $c_{\text{sw}}$  perturbatively in different contexts.
- Smearing or smoothing techniques. By replacing the gauge links  $U_\mu(x)$  by smeared links  $U_\mu^{(n)}(x)$ , which are usually constructed from averages over gauge paths in the vicinity of the original link, the gauge background is smoothed. This improves the evaluation of fermionic operators on it. The procedure can be iterated to increase its effectiveness. The perturbative expansion of so called stout smearing [7] is one of the main goals of this thesis.
- Gradient flow. Here the gauge links are replaced by flowed links  $U_\mu(x, t)$ . They are solutions to a diffusion-type differential equation in the flow time  $t$ . The effect is similar to that of smearing. In fact the Wilson flow, i.e. the gradient flow of the Wilson gauge action is generated by infinitesimal stout smearing steps [8]. The perturbative expansion of the Wilson flow is one of the main goals of this thesis.

All four of these concepts are brought together in this thesis in the context of lattice perturbation theory (LPT). Lattice perturbation theory is perturbation theory with a finite lattice spacing  $a$  and even though the lattice is introduced specifically to do calculations in the non-perturbative regime of QCD, it is an important tool for many aspects of lattice theory.

The fundamental principle of lattice perturbation theory is to expand the link variables

$$U_\mu(x) = e^{i a g_0 A_\mu(x)} \quad (1.1)$$

in the bare coupling constant  $g_0$ . This introduces new interaction terms between the quark fields and the gluon fields  $A_\mu$  at each order of  $g_0$ . For one-loop calculations at order  $g_0^3$  there is not only the quark-quark-gluon ( $\bar{q}qg$ ) vertex, familiar from continuum QCD, but also a  $\bar{q}qgg$  and a  $\bar{q}qggg$  vertex. This increases the number of diagrams to be considered immensely. Additionally the expressions for the Feynman rules can become very large depending on how many products of link variables are present in the action. Hence, deriving Feynman rules involving any of the strategies to ameliorate lattice actions mentioned above, becomes very cumbersome.

In this thesis we take on the task of deriving Feynman rules for the Brillouin fermion action, perturbatively expanding stout smearing and the Wilson flow and applying them to the calculation of the one-loop fermion self-energy and the one-loop value of  $c_{\text{SW}}$ .

The structure of the thesis is as follows.

We begin by recalling some basics of quantum field theory, the standard model and QCD in particular in Chapter 2. Following that, we introduce the general concepts of Lattice QCD in Chapter 3 along with the topics integral to the work presented in later chapters (Brillouin fermions are introduced in Section 4.4, clover improvement in Section 3.6, and stout smearing and the Wilson flow in Section 7.3).

Chapter 4 gives the fundamentals of lattice perturbation theory including a lot of the Feynman rules, we will use in calculations. The perturbative determinations of the self energy and the one-loop value of the improvement coefficient  $c_{\text{SW}}$  are explained in Sections A.3 and A.6 respectively.

In Chapter 5 we present our results for the perturbation theory of Brillouin fermions. We give the Feynman rules of the Brillouin action in Section 9. Then we apply them by calculating the divergent part  $\Sigma_0$  of the fermion self energy, i.e. the critical mass  $am_{\text{crit}}$  at one loop order in Section 9 and the one-loop value of  $c_{\text{SW}}$  in Section A.1. These results have been published in Ref. [9], along with the additional data given in Appendix A.1.

We lay out the perturbative expansion of stout smearing and the Wilson flow in some detail in Chapter 6. We analytically derive the expressions of the new, smeared or flowed, gluon fields up to order  $g_0^3$ , which suffices for one-loop calculations. The results of both are related to each other by the appropriate limits (see Section 6.2.4). We conclude the chapter by showing how to couple stout smearing with any parameter  $\varrho$  and any number of steps  $n_{\text{stout}}$  or the Wilson flow for any flow time  $t/a^2$  to the Feynman rules of any lattice fermion action (Section 9). The contents of Chapter 6 have appeared in [10] (so far) in preprint form.

In Chapter 7 we apply our new Feynman rules to the relatively simple calculation of the one-loop fermion self energy. It has two parts:  $\Sigma_0$ , which is proportional to the

additive mass shift of the Wilson (or Brillouin) fermion, and  $\Sigma_1$ , which gives the one-loop correction to the fermion propagator. We present results for up to four steps of stout smearing in Sections 7.1 and 7.2 and with Wilson flow for a flow time  $t \in [0, 1]$  in Sections 7.3 and 7.4. The results in Chapter 7 and Appendices A.3, A.3, and A.4 with Wilson fermions have also appeared in Ref. [10].

In Chapter 8 we move on to the determination of the one-loop value of the clover coefficient  $c_{\text{SW}}$  with stout smearing and Wilson flow. We present results with all four combinations of the Wilson and Brillouin fermion actions and the plaquette and Lüscher-Weisz gauge action. We give values for  $N_c = 3$  as well as for general  $N_c$  and have repeated the calculations for several values of the Wilson parameter  $r$ . More data for  $c_{\text{SW}}^{(1)}$  is given in Appendices A.5 and A.6.

Finally Chapter 9 contains a summary and concluding remarks.

## 2 Quantum Field Theory and the Standard Model of Particle Physics

In this chapter we give a short summary of the basics of quantum field theory (QFT) and the standard model of particle physics. The topics presented have been chosen based on their pertinence for the following introduction to lattice gauge theory and the main topics of this thesis. We mainly follow Refs. [11–14] in this chapter.

### 2.1 Gauge Theories

Quantum field theory is the language in which the standard model of particle physics is expressed. It is the combination of quantum mechanics and special relativity and describes relativistic quantum fields on a flat Minkowski space-time. The Lorentz group is the symmetry group of Minkowski space-time which leaves the distance of two space-time points  $\Delta s$ , with

$$\Delta s^2 = x^\mu x_\mu = \eta_{\mu\nu} x^\mu x^\nu = (ct)^2 - x^2 - y^2 - z^2 \quad (2.1)$$

invariant, i.e. with a Lorentz-transformation  $x'^\mu = \Lambda^\mu_\nu x^\nu$

$$\Delta s^2 = \eta_{\mu\nu} x^\mu x^\nu = \eta_{\mu\nu} \Lambda^\mu_\rho x^\rho \Lambda^\nu_\sigma x^\sigma = \eta_{\mu\nu} x'^\mu x'^\nu \quad (2.2)$$

remains unchanged. Particle fields with different spins are expressed in different irreducible unitary representations of the Poincaré group, which in addition to the Lorentz transformations includes translations in Minkowski space. Spin-zero fields are scalar fields, fields with spin-one-half are spinors, and spin-one fields are described by vector fields. Fields with higher spins (i.e. tensor fields) do not appear in the standard model.

For spin one fields this correspondence is, however, not as straight forward. A vector field in Minkowski space has four components, whereas a massive (massless) spin-one particle has only three (two) degrees of freedom (polarisations). Indeed the four-dimensional vector representation of the Poincaré group is the sum of the spin-one and spin-zero representations of  $SO(3)$ . For massless spin-one fields the extra degrees of freedom manifest as the so called gauge invariance of the Lagrangian [11], i.e. the free Lagrangian

$$\mathcal{L}_g = -\frac{1}{4} F_{\mu\nu} F^{\mu\nu}, \quad F_{\mu\nu} = \partial_\mu A_\nu(x) - \partial_\nu A_\mu(x) \quad (2.3)$$

is invariant under gauge transformations

$$A_\mu(x) \rightarrow A_\mu(x) + \partial_\mu \phi(x) \quad (2.4)$$

for any scalar field  $\phi$ . Reversely, we can say that the gauge potential  $A_\mu(x)$  which we use to describe the spin-one gauge boson does not transform as a Lorentz-vector and the

difference is given by a gauge transformation.

Massive spin-one-half fields are used to describe the fundamental particles that make up matter. They are represented as spinors. One such representation is the Dirac-spinor

$$\psi = \begin{pmatrix} \psi_R \\ \psi_L \end{pmatrix}, \quad \bar{\psi} = (\psi_R^\dagger \quad \psi_L^\dagger) \quad (2.5)$$

which is made up from a right-handed and a left-handed two-component spinor. Its free Lagrangian is the Dirac-Lagrangian

$$\mathcal{L}_f = \bar{\psi}(i\gamma^\mu \partial_\mu - m)\psi \quad (2.6)$$

with the four-by-four gamma-matrices  $\gamma^\mu$  which fulfil  $\{\gamma^\mu, \gamma^\nu\} = 2\eta^{\mu\nu}$ . If we want to include an interaction between a fermion and a gauge boson, such that the interacting Lagrangian reads

$$\mathcal{L}_{\text{int}} = -\frac{1}{4}F^{\mu\nu}F_{\mu\nu} - m\bar{\psi}\psi + i\bar{\psi}\not{D}\psi - iq\bar{\psi}A_\mu\psi \quad (2.7)$$

$$= -\frac{1}{4}F^{\mu\nu}F_{\mu\nu} + \bar{\psi}(i\not{D} - m)\psi, \quad (2.8)$$

Lorentz invariance of the Lagrangian requires the fermion to transform under gauge transformations as

$$\psi \rightarrow e^{iq\phi}\psi \quad (2.9)$$

to compensate the gauge transformation of the interaction term. We write  $D_\mu = \partial_\mu - iqA_\mu$  for the covariant derivative and  $q$  is a charge that governs the interaction strength.

The Lagrangian in Eq. (2.8) is the Lagrangian of quantum electrodynamics (QED), if we set  $q = e$  as the charge of the electron. The symmetry group of the gauge transformations (2.9) is that of rotations in the complex plane  $U(1)$ . It is therefore called an abelian gauge theory.

Non-abelian gauge theories are gauge theories with non-commutative transformations. So called Yang-Mills theories are non-abelian gauge theories with a Lie group as the gauge group, specifically an  $SU(N)$  gauge group. In such a theory there are  $N$  copies of the fermion field, and  $N^2 - 1$  gauge bosons. The gauge potential  $A_\mu$  becomes an element of the algebra  $\mathfrak{su}(N)$  and can be written as a linear combination of the generators  $T^a$  as

$$A_\mu(x) = \sum_{a=1}^{N^2-1} T^a A_\mu^a(x). \quad (2.10)$$

**Reminder on Lie groups** *Lie groups are infinite groups that are also differentiable manifolds. Its elements*

$$U = e^{i\alpha^a T^a} \quad (2.11)$$

*are parametrised by a linear combination of the generators  $T^a$ , which form the Lie*

algebra. They fulfil

$$[T^a, T^b] = if^{abc}T^c, \quad (2.12)$$

where  $[., .]$  is a Lie bracket (which in matrix representations becomes the commutator  $[A, B] = AB - BA$ ), and the  $f^{abc}$  are the structure constants.

A representation of a Lie algebra is an embedding of the generators into matrices. The fundamental representation is the smallest non-trivial representation; for  $SU(N)$  groups these are the special Hermitian  $N \times N$  matrices. The adjoint representation acts on the vector space spanned by the generators. For  $SU(N)$  they are  $(N^2 - 1) \times (N^2 - 1)$  matrices given by

$$(t^a)^{bc} := (T_{\text{adj}}^a)^{bc} = -if^{abc}. \quad (2.13)$$

Some important Casimir identities are

$$T^a T^a = C_F = \frac{N^2 - 1}{2N} \quad (2.14)$$

$$f^{abc} f^{abc} = C_A = N. \quad (2.15)$$

We use the common normalisation

$$\text{Tr}(T^a T^b) = T_R \delta^{ab} \quad (2.16)$$

with  $T_F = 1/2$  (fundamental representation) and  $T_A = N$  (adjoint representation).

The covariant derivative

$$D_\mu = \partial_\mu - igT^a A_\mu^a \quad (2.17)$$

acts, in geometric terms, as a *connection* on the group and the field strength

$$F_{\mu\nu} = T^a F_{\mu\nu}^a = \frac{i}{g}[D_\mu, D_\nu] = \partial_\mu A_\nu - \partial_\nu A_\mu - ig[A_\mu, A_\nu] \quad (2.18)$$

$$= T^a (\partial_\mu A_\nu^a - \partial_\nu A_\mu^a + gf^{abc} A_\mu^b A_\nu^c) \quad (2.19)$$

as the *curvature*.

**Wilson lines and Wilson loops** are a nice way to illustrate this [11] and will prepare us for the discretized version of a gauge action on the lattice.

We start from a free theory of  $N$  fermions,

$$\mathcal{L} = \bar{\psi}(i\cancel{D} - m)\psi = \sum_{i=1}^N \bar{\psi}_i(i\cancel{D} - m)\psi_i, \quad (2.20)$$

which is invariant under a global  $SU(N)$  symmetry. In order to compare field values at different space-time points  $x$  and  $y$ , a parallel transporter is needed. This is given

by the Wilson line

$$W(x, y) = P \exp \left( ig \int_y^x A_\mu(z) dz^\mu \right), \quad (2.21)$$

where  $P$  is a path ordering operator, and  $A_\mu = T^a A_\mu^a$  an element of the algebra. It transforms as

$$W(x, y) \rightarrow U(x) W(x, y) U^\dagger(y) \quad (2.22)$$

under gauge transformations. Being able to compare fields at different points allows us to define a (covariant) derivative

$$D_\mu \psi(x) = \lim_{\epsilon^\mu \rightarrow 0} \frac{W(x^\mu, x^\mu + \epsilon^\mu) \psi(x^\mu + \epsilon^\mu) - \psi(x^\mu)}{\epsilon^\mu}. \quad (2.23)$$

Expanding  $W(x, x + \epsilon)$  to first order in  $\epsilon$  gives

$$W(x^\mu, x^\mu + \epsilon^\mu) = 1 - igT^a A_\mu^a(x) \epsilon^\mu + \mathcal{O}(\epsilon^2), \quad (2.24)$$

and thus  $D_\mu = \partial_\mu - igT^a A_\mu^a$ . If the Wilson line is along a closed path  $\gamma$ , it is called a Wilson loop

$$W^{\text{loop}} = P \exp \left( ig \oint_\gamma T^a A_\mu^a(z) dz^\mu \right). \quad (2.25)$$

If we choose the path along an infinitesimal square with side lengths  $\epsilon$  in the  $\mu\nu$ -plane, we get

$$W^{\text{loop}} = 1 + igT^a \epsilon^2 F_{\mu\nu}^a + \mathcal{O}(\epsilon^4). \quad (2.26)$$

While the field strength  $F_{\mu\nu}^a$  is gauge invariant, the generators  $T^a$  are not, thus in order to get a gauge invariant quantity we can take the trace of the Wilson loop. In the trace, the leading order vanishes because the  $T^a$  are traceless

$$\text{Tr}[W^{\text{loop}}] = N - \frac{g^2}{2} \epsilon^4 F_{\mu\nu}^a F^{a\mu\nu} + \mathcal{O}(\epsilon^6) \quad (2.27)$$

Thus we have found one of two terms that are permissible by Lorentz and gauge invariance and renormalizability for a gauge action; the second term being

$$\varepsilon^{\mu\nu\rho\sigma} F_{\mu\nu}^a F_{\rho\sigma}^a, \quad (2.28)$$

with the completely anti-symmetric Levi-Cevita symbol  $\varepsilon$ . This term is CP-odd and its coefficient is constrained to be extremely small in the standard model [11, 12].

## 2.2 The Standard Model of Particle Physics

The standard model describes all the known fundamental particles and their interactions as a gauge theory. Each particle is uniquely identified by its mass and spin. The interactions are characterised by the product of three gauge groups

$$SU_c(3) \times SU_L(2) \times U_Y(1). \quad (2.29)$$

The strong interaction is governed by  $SU_c(3)$  with three color-charges and eight gauge bosons called gluons. The electro-weak interaction with symmetry group  $SU_L(2) \times U_Y(1)$  is the unification of the weak interaction and electro-magnetism. It is a chiral theory, meaning the left handed components form doublets under  $SU(2)$ , while the right handed components form singlets. Its four initially massless gauge bosons combine in the process of spontaneous symmetry breaking involving the scalar Higgs-field to form the three massive  $W^+$ ,  $W^-$ , and  $Z^0$ -bosons, and the massless photon. The remaining gauge symmetry is the  $U(1)$  group of electro-magnetism.

The fermions of the standard model are divided into two groups depending on whether or not they interact with the strong force. Leptons do not and are comprised of the electrically charged electron and its two heavier copies, the muon and the tau, as well as the uncharged and (at least in the standard model) massless electron-, muon-, and tau-neutrinos.

The fermions that do take part in the strong interactions are the six flavours of quarks. They are grouped into up-type quarks with electric charge  $+2/3e$  and down-type quarks with  $-1/3e$ . Like the leptons, they come in three generations with increasing masses. However, mass terms of the form  $-m\bar{\psi}\psi$  are not gauge invariant under  $SU_L(2)$ , as the weak interaction only couples to left handed spinors. Rather, in the standard model the fermions receive their masses through Yukawa couplings to the Higgs-doublet  $H$  (here as an example for the quarks):

$$\mathcal{L}_{\text{Yukawa}} = -Y_{ij}^d (\bar{u}_L^i \bar{d}_L^j) H d_R^j - Y_{ij}^u (\bar{u}_L^i \bar{d}_L^j) \tilde{H} u_R^j + h.c. \quad (2.30)$$

Here,  $u_{L/R}^i$  and  $d_{L/R}^i$  stand for the left/right handed spinors of the up- or down-type quark of generation  $i$ . The Higgs doublet (after symmetry breaking) can be written in terms of the *vacuum expectation value*  $v$  and the real scalar field  $h$  as

$$H = \frac{1}{\sqrt{2}} \begin{pmatrix} 0 \\ v+h \end{pmatrix}, \quad \tilde{H} = i\sigma_2 H^\star \quad (2.31)$$

This results in terms of the form

$$-\frac{v}{\sqrt{2}} Y_{ij}^d \bar{d}_L^i d_R^j - \frac{v}{\sqrt{2}} Y_{ij}^u \bar{u}_L^i u_R^j + h.c. \quad (2.32)$$

By rotating the quark fields in flavour-space, the Yukawa-matrices  $Y^u$  and  $Y^d$  can be diagonalised, thus giving mass terms for the rotated fields

$$-m_{ii}^d \bar{d}_L^i d_R^i - m_{ii}^u \bar{u}_L^i u_R^i + h.c. \quad (2.33)$$

These rotations, however, also affect the kinetic terms and cause the mixing of flavours in the interactions with the  $W^\pm$  bosons leading to CP-violation. The mixing is summarized in the *Cabbibo-Kobayashi-Maskawa* (CKM) matrix, which is almost diagonal, meaning the flavour and mass bases are very close to each other [11, 12, 15].

el. charge	1st generation	2nd generation	3rd generation
$2/3e$	up (2.16 MeV)	charm (1.27 GeV)	top (172.69 GeV)
$-1/3e$	down (4.67 MeV)	strange (93.4 MeV)	bottom (4.18 GeV)

**Table 2.1:** The six flavours of quarks and their approximate masses [15].

## 2.3 Quantum Chromodynamics

Quantum Chromodynamics (QCD) is the isolated theory of the strong interaction. With  $N_f$  flavours and  $N_c$  colour charges the Lagrangian looks like

$$\mathcal{L}_{\text{QCD}} = -\frac{1}{4} \sum_{a=1}^{N_c^2-1} F^{a\mu\nu} F_{\mu\nu}^a + \sum_{i,j=1}^{N_c} \sum_{f=1}^{N_f} \bar{\psi}_i^f (iD_{ij} - \delta_{ij} m_f) \psi_j^f , \quad (2.34)$$

with  $D_{\mu,ij} = \delta_{ij} \partial_\mu - ig T_{ij}^a A_\mu^a$ .

### 2.3.1 Path Integrals

The path integral formalism is a way to quantize gauge theories (here specifically QCD). Expectation values are expressed as integrals over all possible classical field configurations and a phase factor given by the classical action of the theory

$$S_{\text{QCD}} = \int d^4x \mathcal{L}_{\text{QCD}}(x) \quad (2.35)$$

and normalised by the path integral of 1, thus

$$\langle \mathcal{O} \rangle = \frac{\int \mathcal{D}A_\mu \mathcal{D}\bar{\psi} \mathcal{D}\psi \mathcal{O} e^{iS_{\text{QCD}}[A_\mu, \bar{\psi}, \psi]}}{\int \mathcal{D}A_\mu \mathcal{D}\bar{\psi} \mathcal{D}\psi e^{iS_{\text{QCD}}[A_\mu, \bar{\psi}, \psi]}} . \quad (2.36)$$

The  $\mathcal{D}$  symbol is short for integrations over all components of a field at every space time point.

A *generating functional* is a path integral

$$Z[J_\mu, \eta, \bar{\eta}] = \int \mathcal{D}A_\mu \mathcal{D}\bar{\psi} \mathcal{D}\psi e^{iS_{\text{QCD}}[A_\mu, \bar{\psi}, \psi] + i \int d^4x (J^\mu A_\mu + \bar{\psi}\eta + \bar{\eta}\psi)} \quad (2.37)$$

with external currents  $J_\mu$ ,  $\bar{\eta}$ , and  $\eta$ , which couple to the fields. By defining appropriate derivatives with respect to these currents, any  $n$ -point functions can be derived from the generating functional. For example the fermionic two-point correlator

$$\langle \bar{\psi}(x)\psi(y) \rangle = \frac{1}{Z[0]} \frac{\partial^2}{\partial \eta(x) \partial \bar{\eta}(y)} Z[J_\mu, \bar{\eta}, \eta] \Big|_{J, \bar{\eta}, \eta=0} . \quad (2.38)$$

The resulting path integral would however, not be convergent. To make it convergent and fulfil *time reflection positivity*, i.e. the theory being unitary and having a positive definite Hamiltonian, the Lagrangian is being deformed by the term  $i\varepsilon\bar{\psi}\psi$ . This is equivalent to

choosing the forward propagator or the fields at  $t = \pm\infty$  [11]. With this, the fermion propagator (i.e. the two point function of the free theory) becomes

$$D_F(x, y) = \frac{1}{Z[0]} \frac{\partial^2}{\partial \eta(x) \partial \bar{\eta}(y)} Z[\bar{\eta}, \eta] \Big|_{\bar{\eta}, \eta=0} = \frac{i\delta(x-y)}{i\cancel{D} - m + i\varepsilon} \quad (2.39)$$

$$= \int \frac{d^4 p}{(2\pi)^4} \frac{ie^{-ip(x-y)}}{\cancel{p} - m + i\varepsilon} = \int \frac{d^4 p}{(2\pi)^4} \frac{i(\cancel{p} + m)e^{-ip(x-y)}}{p^2 - m^2 + i\varepsilon}. \quad (2.40)$$

The small  $\varepsilon$  is understood to be taken to zero eventually.

### 2.3.2 Gauge Fixing

The Lagrangian (2.34) is still completely invariant under full gauge transformations. This is a problem when one wants to derive unique results for physical quantities from it; for example via perturbation theory [11]. In the formalism of path integrals, the equivalence class of all possible gauges (or *gauge orbits*) leads to over-counting in the resulting physical results. By adding a gauge fixing term to the Lagrangian

$$\mathcal{L}_{\text{gf}} = \frac{1}{2\xi} (\partial^\mu A_\mu)^2, \quad (2.41)$$

the path integral becomes unique. Gauges characterised by the gauge fixing term (2.41) are called  $R_\xi$ -gauges. It can be shown (see *Faddeev-Popov procedure* below) that the difference between the original and the gauge-fixed path integral can be expressed as the addition of scalar Grassmann-valued fields  $\bar{c}$ ,  $c$ , called (*Faddeev-Popov*) *ghosts* to the Lagrangian

$$\mathcal{L}_{\text{gh}} = -\bar{c}^a \partial^\mu D_\mu c^a. \quad (2.42)$$

These ghosts do not appear as asymptotic states but are simply a computational tool to remove the over-counting problem from Feynman diagrams. They are ultimately due to the Lagrangian formulation of a Lorentz invariant field theory.

**The Faddeev-Popov procedure** [11, 16] We start by expressing the gauge fixing condition as

$$\partial^\mu A_\mu - \frac{1}{g} \partial^\mu D_\mu \alpha^a = 0 \quad (2.43)$$

Next, we write a path integral of the form

$$f[A] = \int \mathcal{D}\pi e^{-i \int dx \frac{1}{2\xi} (\partial^\mu D_\mu \pi^a)^2} \quad (2.44)$$

for some fields  $\pi^a$ , which also parametrise a gauge transformation  $A_\mu^a \rightarrow A_\mu^a + D_\mu \pi^a$ . Shifting  $\pi^a$  by  $-\frac{1}{g} \alpha^a$  we can get

$$f[A] = \int \mathcal{D}\pi e^{-i \int dx \frac{1}{2\xi} (\partial^\mu A_\mu^a - \partial^\mu D_\mu \pi^a)^2}. \quad (2.45)$$

Because  $f[A]$  is a Gauss integral, we can multiply the full QCD path integral by

$$1 = C \cdot \det(\partial^\mu D_\mu) \int \mathcal{D}\pi e^{-i \int dx \frac{1}{2\xi} (\partial^\mu A_\mu^a - \partial^\mu D_\mu \pi^a)^2}, \quad (2.46)$$

where  $C$  is a constant that drops out in physical expectation values. Shifting

$$A_\mu^a \rightarrow A_\mu^a + D_\mu \pi^a \quad (2.47)$$

removes  $\pi$  from the Lagrangian, while leaving  $\mathcal{L}_{\text{QCD}}$  invariant. The determinant can be written as a path integral over non-commuting scalar fields, thus giving us

$$\det(\partial^\mu D_\mu) = \int \mathcal{D}\bar{c} \mathcal{D}c e^{-i \int dx \bar{c} \partial^\mu D_\mu c}, \quad (2.48)$$

the Lagrangian of the ghost fields.

### 2.3.3 Perturbation Theory

The perturbation theory of a quantum field theory is the expansion around the free theory for small coupling constant(s). Thereby it is only valid when the coupling is actually small. We have seen that any operator can be derived from the generating functional. Thus, by expanding the generating functional for a small coupling, we can get order by order expressions for the operator in terms of path integrals of the *free* theory. This means any higher order terms can be constructed from free propagators and leading order  $n$ -point vertices. This can be visualised as *Feynman diagrams* and the order of the coupling constant becomes synonymous with the number of closed loops in the diagram. The *Feynman rules* are the building blocks of Feynman diagrams corresponding to factors in the Feynman integrals. They can be read off of the interaction terms of a Lagrangian.

For QCD, we split the Lagrangian into a free and an interaction part

$$\mathcal{L}_{\text{QCD}} = \mathcal{L}_0 + \mathcal{L}_{\text{int}}, \quad (2.49)$$

with

$$\mathcal{L}_0 = -\frac{1}{4}(\partial_\mu A_\nu^a - \partial_\nu A_\mu^a)^2 - \frac{1}{2\xi}(\partial_\mu A_\mu^a)^2 = \bar{c}^a \partial^2 c^a + \bar{\psi}(i\cancel{\partial} - m)\psi. \quad (2.50)$$

and

$$\begin{aligned} \mathcal{L}_{\text{int}} = & -\frac{1}{4}g^2 f^{abc} f^{ade} A_\mu^b A_\nu^c A_\mu^d A_\nu^e - g f^{abc} (\partial_\mu A_\nu^a) A_\mu^b A_\nu^c + g f^{abc} (\partial_\mu \bar{c}^a) A_\mu^b c^c \\ & + g A_\mu^a \bar{\psi} \gamma_\mu T^a \psi. \end{aligned} \quad (2.51)$$

From the free Lagrangian (2.50) we get the quark, gluon and ghost propagators in mo-

momentum space:

$$a \xrightarrow{p} b \quad S^{ab}(p) = i\delta^{ab} \frac{\not{p} + m}{p^2 - m^2 + i\varepsilon} \quad (2.52)$$

$$\mu, a \xrightarrow{k} \nu, b \quad G_{\mu\nu}^{ab}(k) = -i\delta^{ab} \frac{1}{k^2 + i\varepsilon} \left( \eta_{\mu\nu} - (1 - \xi) \frac{k_\mu k_\nu}{k^2} \right) \quad (2.53)$$

$$a \xrightarrow{q} b \quad G_{gh}^{ab}(q) = i\delta^{ab} \frac{1}{q^2 + i\varepsilon} . \quad (2.54)$$

We can read off the interaction Feynman rules directly in momentum space, where a derivative  $\partial_\mu$  becomes a four-momentum  $ip_\mu$ . The first two terms of (2.51) give the self interaction of the gluons; the four- and three-gluon vertices:

$$\begin{aligned} V_{4g\mu\nu\rho\sigma}^{abcd}(k_1, k_2, k_3, k_4) &= -ig^2 \left[ f^{abe} f^{cde} (\eta_{\mu\rho} \eta^{\nu\sigma} - \eta_{\mu\sigma} \eta_{\nu\rho}) \right. \\ &\quad + f^{ace} f^{bde} (\eta_{\mu\nu} \eta_{\rho\sigma} - \eta_{\mu\sigma} \eta_{\nu\rho}) \\ &\quad \left. + f^{ade} f^{bce} (\eta_{\mu\nu} \eta_{\rho\sigma} - \eta_{\mu\rho} \eta_{\nu\sigma}) \right] \end{aligned} \quad (2.55)$$

$$V_{3g\mu\nu\rho}^{abc}(k_1, k_2, k_3) = g f^{abc} \left[ \eta_{\mu\nu} (k_{1\rho} - k_{2\rho}) + \eta_{\nu\rho} (k_{2\mu} - k_{3\mu}) + \eta_{\mu\rho} (k_{3\nu} - k_{1\nu}) \right] . \quad (2.56)$$

The other two terms give the anti-quark-quark-gluon ( $\bar{q}qg$ ) and anti-ghost-ghost-gluon ( $\bar{cc}g$ ) vertices

$$V_{1\mu}^a(p, q) = ig\gamma_\mu T^a \quad (2.57)$$

$$V_{1gh\mu}^{abc}(p) = -g f^{abc} p_\mu . \quad (2.58)$$

These are all the Feynman rules of continuum QCD. Feynman diagrams with an arbitrary number of loops can be constructed from them. The main difference to perturbation theory on the lattice is, that there new Feynman rules will appear at each order of the coupling constant  $g$ .

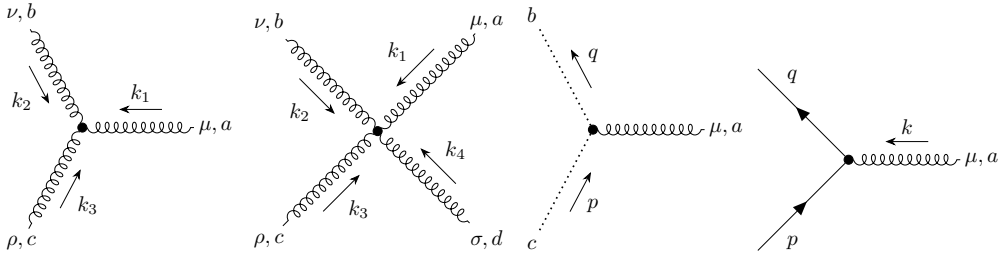


**Figure 2.1:** The vertices of QCD. From left to right: three-gluon, four gluon, anti-ghost-ghost-gluon, and anti-quark-quark-gluon vertex. We use the convention were all gluon momenta are going into the vertex.

### 2.3.4 Renormalization

Non-physical quantities and individual Feynman diagrams are infinite. In particular all Green's functions are infinite but can be made finite by renormalization. We call the fields, masses and, coupling constants that we have had in the Lagrangian so far *bare* and denote them by a subscript of 0. We define their renormalized versions with a subscript of  $R$  and *renormalization coefficients*  $Z_i$  such that

$$m = m_0 = Z_m m_R \quad g = g_0 = Z_g g_R \quad (2.59)$$

$$\bar{\psi} = \bar{\psi}_0 = \sqrt{Z_2} \bar{\psi}_R \quad \psi = \psi_0 = \sqrt{Z_2} \psi_R \quad (2.60)$$

$$\bar{c}^a = \bar{c}_0^a = \sqrt{Z_{3c}} \bar{c}_R^a \quad c^a = c_0^a = \sqrt{Z_{3c}} c_R^a \quad (2.61)$$

$$A_\mu^a = A_{0\mu}^a = \sqrt{Z_3} A_{R\mu}^a . \quad (2.62)$$

The  $Z_i$  are meant to absorb the infinities such that the Green's functions of the renormalised fields become finite [11].

For one-loop perturbation theory we expand the renormalization factors according to

$$Z_i = 1 + g_0^2 \delta_i . \quad (2.63)$$

The  $\delta_i$  are called *counter terms*, which must be calculated to remove the divergencies coming from the Feynman diagrams.

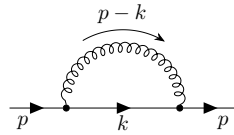


**Figure 2.2:** The one loop correction to the quark propagator.

**Example: The fermion self-energy** The fermion self energy is the one-loop correction to the fermion propagator

$$G_0(x - y) = \langle \bar{\psi}_0(x) \psi_0(y) \rangle = \int \frac{dp}{(2\pi)^4} i G_0(p) e^{-i(x-y)} \quad (2.64)$$

with

$$G(p) = \frac{1}{\not{p} - m} - \frac{1}{\not{p} - m} \Sigma(p) \frac{1}{\not{p} - m} , \quad (2.65)$$

where  $\Sigma(p)$  is the one-loop integral

$$\Sigma(p) = ig_0^2 T^a T^a \int \frac{dk}{(2\pi)^4} \gamma^\mu \frac{i(\not{k} + m)}{k^2 - m^2 + i\varepsilon} \gamma^\mu \frac{-i}{(k - p)^2 + i\varepsilon} . \quad (2.66)$$

The renormalized Green's function is

$$G_R(p) = \frac{1}{Z_2} G_0(p) . \quad (2.67)$$

Then, with  $Z_2 = 1 + g_0^2 \delta_2$  and  $m_0 = (1 + g_0^2 \delta_m) m_R$ , we get up to order  $g_0^2$

$$G_R(p) = \frac{1}{\not{p} - m_R} - g_0^2 \frac{1}{\not{p} - m_R} (\delta_2 \not{p} - (\delta_2 + \delta_m) m_R) \frac{1}{\not{p} - m_R} \quad (2.68)$$

$$- \frac{1}{\not{p} - m_R} \Sigma_R(p) \frac{1}{\not{p} - m_R} + \mathcal{O}(g_0^4). \quad (2.69)$$

The integral can be evaluated, for example by using a small un-physical photon mass  $\mu$  (Pauli-Villars regularisation) to give

$$\Sigma_R(p) = \frac{g_0^2 C_F}{16\pi^2} \left( (\not{p} - 4m_R) \ln(\mu^2) + S \right), \quad (2.70)$$

where  $S$  is a finite number. Thus by setting

$$\delta_2 = -\frac{C_F}{16\pi^2} \ln(\mu^2), \quad \delta_m = -\frac{3C_F}{16\pi^2} \ln(\mu^2), \quad (2.71)$$

we can remove all divergencies from  $G_R(p)$  up to one-loop order.

Similar calculations can be done to determine the other counter terms; for example  $\delta_3$  from the gluon vacuum polarisation [11] etc.

### 2.3.5 Asymptotic Freedom

Gauge theories with massless gauge bosons describe interactions that are classically given by  $1/r^2$  potentials (or  $1/p^2$  in momentum space). Quantum effects change this behaviour and introduce an additional dependence on  $r$  (or  $p^2$ ). Thus, the coupling constant is effectively changing with the scale  $p^2$  at which the process is taking place. This is called a *running coupling*.

When renormalizing couplings (or charges) one is effectively setting them at a certain scale (e.g. through defining a potential at a certain distance or momentum). This scale  $\mu$  is arbitrary and physical results should not depend on it. This independence can be expressed in so called *renormalisation group equations*

$$\mu \frac{d}{d\mu} g_0 = 0 \Leftrightarrow \mu \frac{d}{d\mu} g_R = \beta(g_R). \quad (2.72)$$

The *beta function* on the right hand side determines the behaviour of the running coupling. In QCD, the one-loop beta function is [11]

$$\beta(g_R) = -\frac{g_R^3}{16\pi^2} \left( 11 - \frac{2}{3} N_f \right) \quad (2.73)$$

The solution of the differential equation is then

$$\alpha_s(\mu) := \frac{g_R^2(\mu)}{4\pi} = \frac{2\pi}{11 - \frac{2}{3} n_f} \cdot \frac{1}{\ln(\frac{\mu}{\Lambda_{\text{QCD}}})}, \quad (2.74)$$

where  $\Lambda_{\text{QCD}}$  is the dimension-full parameter of QCD. Measuring  $\alpha_s$  at any scale  $\mu$  determines  $\Lambda_{\text{QCD}}$ .

Thus, for any number of flavours  $N_f < 17$ , the strong coupling increases for small energies and decreases for large energies. This is called *asymptotic freedom* and explains why the strong interaction is short ranged, contrary to QED, which is relatively much weaker but long ranged due to a different running of the coupling.

Asymptotic freedom also means that low energy observables such as bound states of quarks (hadrons) are not accessible to perturbative calculations. It is for this reason, that non-perturbative methods such as lattice QCD are needed.

### 3 Lattice Gauge Theory

A lattice gauge theory is a gauge theory formulated on a regular lattice  $\Lambda$  of discrete points in euclidean space. The physical distance between the points in each direction is called the lattice constant  $a$ . The lattice acts as a UV-regularization, providing an energy cut-off  $\sim 1/a$ . For computer simulations only finite lattices can be realised (often lattices with  $|\Lambda| = N^d$  points, sometimes the extent in the temporal direction is chosen differently to the spatial directions  $|\Lambda| = N^{d-1} \times N_t$ ) and boundary conditions need to be specified. The simplest are periodic boundary conditions where the lattice forms a (hyper-)torus.

Euclidean lattice path integrals can be evaluated numerically through importance sampling methods because of their structural similarity to statistical systems. By performing multiple simulations at different lattice spacings, while keeping the physical size of the lattice constant, the continuum result is extrapolated by performing the *continuum limit*. The results can then be related to the corresponding continuum theory in Minkowski space.

In the following, we will be discussing Lattice QCD in particular, i.e. the lattice gauge theory of  $SU(N_c)$  with  $N_f$  flavours of quarks. However, we will later consider massless quarks (which is a good approximation for QCD with only the up and down quarks) and drop the factor of  $N_f$ .

In this chapter we mainly follow Refs. [1, 2].

#### 3.1 The naive lattice fermion action

The lattice quark fields  $\bar{\psi}(x)$ ,  $\psi(x)$  are defined on the lattice points, where  $x$  is no longer a continuous variable, but

$$x \in \Lambda = \{(an_1, an_2, an_3, an_4) | n_i = 0, 1, \dots, N-1\} \quad (3.1)$$

for an  $N \times N \times N \times N$  lattice. Simply discretizing the continuum fermion action could look like

$$S_F = a^4 \sum_{x \in \Lambda} \left( \bar{\psi}(x) \sum_{\mu=1}^4 \gamma_\mu \nabla_\mu \psi(x) + m \cdot \bar{\psi}(x) \psi(x) \right), \quad (3.2)$$

with  $\nabla_\mu$  being a symmetric discretization of the derivative

$$\nabla_\mu \psi(x) = \frac{\psi(x + a\hat{\mu}) - \psi(x - a\hat{\mu})}{2a}, \quad (3.3)$$

where  $\hat{\mu}$  is the euclidean unit vector in direction  $\mu$ . The gamma-matrices also have to be adjusted here such that they obey the euclidean anti-commutation rules

$$\{\gamma_\mu, \gamma_\nu\} = 2\delta_{\mu\nu}. \quad (3.4)$$

**Euclidean  $\gamma$ -matrices** By defining the euclidean gamma matrices as

$$\gamma_i = -i\gamma_i^M, \quad i = 1, 2, 3 \quad (3.5)$$

$$\gamma_4 = \gamma_0^M \quad (3.6)$$

in terms of the Minkowski matrices  $\gamma_\mu^M$ , they obey (3.4). An explicit representation is the chiral representation

$$\gamma_1 = \begin{pmatrix} 0 & 0 & 0 & -i \\ 0 & 0 & -i & 0 \\ 0 & i & 0 & 0 \\ i & 0 & 0 & 0 \end{pmatrix}, \quad \gamma_2 = \begin{pmatrix} 0 & 0 & 0 & -1 \\ 0 & 0 & 1 & 0 \\ 0 & 1 & 0 & 0 \\ -1 & 0 & 0 & 0 \end{pmatrix}, \quad (3.7)$$

$$\gamma_3 = \begin{pmatrix} 0 & 0 & -i & 0 \\ 0 & 0 & 0 & i \\ i & 0 & 0 & 0 \\ 0 & -i & 0 & 0 \end{pmatrix}, \quad \gamma_4 = \begin{pmatrix} 0 & 0 & 1 & 0 \\ 0 & 0 & 0 & 1 \\ 1 & 0 & 0 & 0 \\ 0 & 1 & 0 & 0 \end{pmatrix}. \quad (3.8)$$

Demanding the fermion action to be gauge invariant under  $SU(N_c)$  color rotations

$$\psi(x) \rightarrow \Omega(x)\psi(x), \quad \bar{\psi}(x) \rightarrow \bar{\psi}(x)\Omega^\dagger(x). \quad (3.9)$$

requires a gauge transporter  $U_\mu(x)$  which transforms as

$$U_\mu(x) \rightarrow \Omega(x)U_\mu(x)\Omega^\dagger(x + a\hat{\mu}) \quad (3.10)$$

Then

$$\nabla_\mu \psi(x) = \frac{U_\mu(x)\psi(x + a\hat{\mu}) - U_\mu^\dagger(x - a\hat{\mu})\psi(x - a\hat{\mu})}{2a} \quad (3.11)$$

is a covariant derivative and the fermion action becomes gauge invariant. The transporter  $U_\mu(x)$  is an element of the gauge group (not the algebra, as  $A_\mu$  was in the continuum) and is called a *link variable*. Were the lattice embedded into continuous space, it would be given by the Wilson line (2.21) connecting the points  $x$  and  $x + a\hat{\mu}$ . Therefore we can write

$$U_\mu(x) = e^{iag_0 A_\mu(x)}, \quad (3.12)$$

such that in the limit  $a \rightarrow 0$  we recover the continuum fermion action with the correct interaction term  $ig_0 \bar{\psi} A_\mu \psi$ .

There are problems that arise from the naive lattice fermion action presented here and we will address them in section 4.2.

## 3.2 The lattice gauge action

We have seen in the continuum how one can derive a gauge invariant term for the gauge part of the Lagrangian from an infinitesimal Wilson loop. On the lattice, the smallest Wilson loop is the *plaquette*

$$P_{\mu\nu}(x) = U_\mu(x)U_\nu(x + a\hat{\mu})U_\mu^\dagger(x + a\hat{\nu})U_\nu^\dagger(x), \quad (3.13)$$

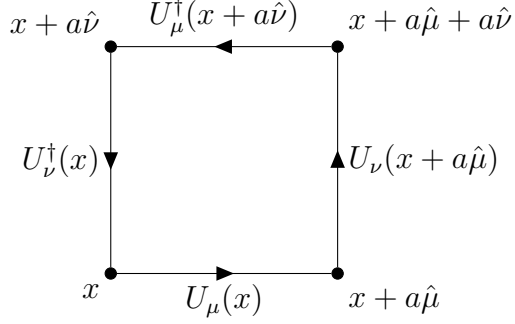


**Figure 3.1:** The gauge links that make up the plaquette  $P_{\mu\nu}(x)$  in the  $\mu\nu$ -plane.

which is the Product of link variables along the edges of a one-by-one square in the  $\mu\nu$ -plane starting from  $x$  (see Figure 3.1).

The lattice gauge action,

$$\mathcal{S}_G = \frac{2}{g_0^2} \sum_{x \in \lambda} \sum_{\mu < \nu} \text{ReTr} [1 - P_{\mu\nu}(x)] , \quad (3.14)$$

was first given by Wilson [3] and reproduces the continuum version in the limit  $a \rightarrow 0$ .

**Proof [1]** Expanding the plaquette according to (3.12) and using the Baker-Campbell-Hausdorff formula  $e^X e^Y = e^{X+Y+\frac{1}{2}[X,Y]+\dots}$ , gives

$$\begin{aligned} P_{\mu\nu}(x) = & \exp \left( i g_0 \left( A_\mu(x) + A_\nu(x+a^{\hat{\mu}}) - A_\mu(x+a^{\hat{\nu}}) - A_\nu(x) \right) \right. \\ & - \frac{a^2 g_0^2}{2} \left( [A_\mu(x), A_\nu(x+a^{\hat{\mu}})] - [A_\mu(x), A_\mu(x+a^{\hat{\nu}})] \right. \\ & - [A_\mu(x), A_\nu(x)] - [A_\nu(x+a^{\hat{\mu}}), A_\mu(x+a^{\hat{\nu}})] \\ & \left. \left. - [A_\nu(x+a^{\hat{\mu}}), A_\nu(x)] + [A_\mu(x+a^{\hat{\nu}}), A_\nu(x)] \right) + \mathcal{O}(a^3) \right) . \end{aligned} \quad (3.15)$$

For small  $a$ , we can write  $A_\mu(x+a^{\hat{\nu}}) - A_\mu(x) = a \partial_\nu A_\mu(x) + \mathcal{O}(a^2)$  and

$$P_{\mu\nu}(x) = \exp \left( i g_0 a^2 \left( \partial_\mu A_\nu(x) - \partial_\nu A_\mu(x) + i g_0 [A_\mu, A_\nu] \right) + \mathcal{O}(a^3) \right) \quad (3.16)$$

$$= \exp \left( i g_0 a^2 F_{\mu\nu} + \mathcal{O}(a^3) \right) \quad (3.17)$$

$$= 1 + i g_0 a^2 F_{\mu\nu} - \frac{g_0^2 a^4}{2} F_{\mu\nu}^2 + \mathcal{O}(a^5) , \quad (3.18)$$

where  $F_{\mu\nu}$  is the (euclidean) field strength in the continuum. Taking the trace of  $1 - P_{\mu\nu}$  and recalling  $F_{\mu\nu} = T^a F_{\mu\nu}^a$  and  $\text{Tr}[T^a] = 0$ ,  $\text{Tr}[T^a T^b] = 1/2 \delta^{ab}$ , we get

$$S_G = a^4 \sum_{x \in \lambda} \sum_{\mu < \nu} \text{Tr}[F_{\mu\nu}^2] + \mathcal{O}(a^2) = \frac{a^4}{2} \sum_{x \in \lambda} \sum_{\mu < \nu} \text{Tr}[F_{\mu\nu}^2] + \mathcal{O}(a^2) \quad (3.19)$$

$$\rightarrow \int dx \text{Tr}[F_{\mu\nu}^2] + \mathcal{O}(a^2) . \quad (3.20)$$

Note that by taking the real part in  $S_G$ , the lattice corrections are of order  $a^2$  while for the naive fermion action (3.2), the leading corrections are of order  $a$  [1].

### 3.3 The lattice path integral

With the basic principles of how to put QCD on a lattice established, we can construct a lattice path integral [1, 2]

$$\langle \mathcal{O} \rangle = \frac{\int \mathcal{D}\bar{\psi} \mathcal{D}\psi \mathcal{D}U \mathcal{O} e^{-S_F - S_G}}{\int \mathcal{D}\bar{\psi} \mathcal{D}\psi \mathcal{D}U e^{-S_F - S_G}} . \quad (3.21)$$

The measures are now finite products

$$\mathcal{D}\bar{\psi} = \prod_{x \in \Lambda} d\bar{\psi}(x) , \quad \mathcal{D}\psi = \prod_{x \in \Lambda} d\psi(x) , \quad \mathcal{D}U = \prod_{x \in \Lambda} \prod_{\mu=1}^4 dU_\mu(x) , \quad (3.22)$$

and the Wick rotation from Minkowski space to euclidean space has removed the  $i$  from the exponential. This makes these integrals much better mathematically defined than the continuum path integrals [1].

It is important to note that the integration over the gauge links  $U$  is over the manifold of the group  $SU(N_c)$ . Thus,  $dU$  is a *Haar measure*. This will be important for lattice perturbation theory when relating the  $U_\mu$  to the  $A_\mu$ .

The Form of (3.21) is that of a statistical system with

$$Z = \int \mathcal{D}\bar{\psi} \mathcal{D}\psi \mathcal{D}U e^{-S_F - S_G} , \quad (3.23)$$

its partition function and  $e^{-S_F - S_G}$  taking on the role of the Boltzmann factor. This opens up the possibility to evaluate expectation values by numerical Monte Carlo simulations [1, 2].

### 3.4 Wilson Fermions

The problem with the naive fermion action (3.2) becomes apparent when deriving the propagator, i.e. the inverse of the free Dirac operator, free meaning all  $U_\mu = 1$ . The free naive action for a massless quark is

$$\mathcal{S}_N = a^4 \sum_{x,y \in \Lambda} \bar{\psi}(x) D_0(x,y) \psi(y) , \quad (3.24)$$

with the Dirac operator

$$D_0(x,y) = \sum_\mu \gamma_\mu \frac{\delta(x + a\hat{\mu}, y) - \delta(x - a\hat{\mu}, y)}{2a} . \quad (3.25)$$

Its Fourier transform is

$$D_0(p, q) = \sum_{x, y \in \Lambda} \sum_{\mu} \gamma_{\mu} \frac{\delta(x + a\hat{\mu}, y) - \delta(x - a\hat{\mu}, y)}{2a} e^{-ixp} e^{-iyq} \quad (3.26)$$

$$= \sum_{x \in \Lambda} \sum_{\mu} \gamma_{\mu} \frac{1}{2a} (e^{-ia\hat{\mu}q} - e^{ia\hat{\mu}q}) e^{-ix(p-q)} \quad (3.27)$$

$$= \frac{1}{2a} \sum_{\mu} \gamma_{\mu} (e^{-iap_{\mu}} - e^{iap_{\mu}}) \delta(p, q) \quad (3.28)$$

$$= \frac{i}{a} \sum_{\mu} \gamma_{\mu} \sin(ap_{\mu}) \delta(p, q) . \quad (3.29)$$

**Fourier transformations on the lattice** For an  $N^4$  lattice with periodic boundary conditions, the set of discrete momenta in the Brillouin zone is

$$\tilde{\Lambda} = \left\{ k = (k_1, k_2, k_3, k_4) \mid k_{\mu} = -\frac{\pi}{a} + \frac{2\pi}{aN}, \dots, \frac{\pi}{a} - \frac{2\pi}{aN}, \frac{\pi}{a} \right\} . \quad (3.30)$$

Then, the Fourier transform of a function  $f(x)$  and its inverse are

$$f(p) = \sum_{x \in \Lambda} f(x) e^{-ixp} \quad (3.31)$$

$$f(x) = \frac{1}{N^4} \sum_{p \in \tilde{\Lambda}} f(p) e^{ixp} . \quad (3.32)$$

We use the normalization, where

$$\delta(x, y) = \frac{1}{N^4} \sum_{p \in \tilde{\Lambda}} e^{ip(x-y)} , \quad \delta(p, q) = \sum_{x \in \Lambda} e^{ix(p-q)} . \quad (3.33)$$

In lattice perturbation theory we will assume an infinite lattice volume, which will turn the sum in (3.32) into a momentum space integral

$$\frac{1}{N^4} \sum_{p \in \tilde{\Lambda}} \rightarrow \int_{-\frac{\pi}{a}}^{\frac{\pi}{a}} \frac{dp}{(2\pi)^4} . \quad (3.34)$$

Inverting  $D_0(p, q)$  gives us the momentum space propagator

$$S_{\text{naive}}(p) = a \frac{-i \sum_{\mu} \gamma_{\mu} \sin(ap_{\mu})}{\sum_{\alpha} \sin(ap_{\alpha})^2} . \quad (3.35)$$

This propagator has poles not only for  $p = 0$ , but for any  $p_{\mu} = \pi/a$ , i.e. at the 16 corners of the Brillouin zone, whereas the continuum propagator only has the one pole at  $p = 0$ .

Each pole represents one propagating particle. Hence the naive fermion action includes 16 unwanted so called *doublers*.

Wilson solved this problem [3], by adding another term to the action that vanishes for  $a \rightarrow 0$ ,

$$\mathcal{S}_W = a^4 \sum_{x \in \Lambda} \left( \sum_{\mu=1}^4 \bar{\psi}(x) \gamma_\mu \nabla_\mu \psi(x) - \frac{ra}{2} \bar{\psi}(x) \Delta \psi(x) \right), \quad (3.36)$$

where  $\Delta$  is a discretized covariant Laplace operator

$$\Delta \psi(x) = \sum_{\mu} \frac{U_{\mu}(x)\psi(x+a\hat{\mu}) - 2\psi(x) + U_{\mu}^{\dagger}(x-a\hat{\mu})\psi(x-a\hat{\mu})}{a^2}. \quad (3.37)$$

The pre-factor  $r$  is called the Wilson parameter and usually set to one. Now the momentum space Dirac operator is

$$D_W(p) = \frac{i}{a} \sum_{\mu} \gamma_{\mu} \sin(ap_{\mu}) + \frac{r}{a} \sum_{\mu} (1 - \cos(ap_{\mu})). \quad (3.38)$$

For the doublers with  $p_{\mu} = \pi/a$ , the Wilson term adds an (extra) mass term which is proportional to  $1/a$ . Thus, the doublers become very heavy and decouple in the continuum limit.

Finally, the Propagator of the Wilson fermion is

$$S_W(p) = a \frac{-i \sum_{\mu} \gamma_{\mu} \sin(ap_{\mu}) + 2r \sum_{\mu} \sin^2(\frac{a}{2} p_{\mu}) + am}{\sum_{\mu} \sin^2(ap_{\mu}) + (2r \sum_{\mu} \sin^2(\frac{a}{2} p_{\mu}) + am)^2}, \quad (3.39)$$

where we have included the fermion mass again.

There are many other fermion actions in use with different ways to deal with the doublers and different advantages or disadvantages over the Wilson formulation. The Wilson term for example breaks chiral symmetry. Indeed, the *Nielsen-Ninomiya theorem* [17–20] states that a local unitary lattice fermion action with both chiral symmetry and no doublers is not possible. Some prominent examples of other fermion actions are staggered (or Kogut-Susskind) fermions [21], domainwall fermions [22] and overlap fermions [23]. Some recent development includes Boriçi-Kreutz fermions [24, 25], Karsten-Wilczek fermions [26, 27], and Brillouin/hypercube fermions [4, 28].

From this point onward we will be using lattice units and setting  $a = 1$ .

### 3.5 Brillouin Fermions

As we have seen in the previous section, the (massless) Wilson Dirac operator consists of a term involving the “standard” two-point covariant derivative and the “standard” nine-point covariant Laplace operator

$$D_W(x, y) = \sum_{\mu} \gamma_{\mu} \nabla_{\mu}^{\text{std}}(x, y) - \frac{r}{2} \Delta^{\text{std}}(x, y). \quad (3.40)$$

In the Brillouin Dirac operator these derivatives are replaced by the 54-point “isotropic” derivative  $\nabla_\mu^{\text{iso}}$  and the 81-point “Brillouin” Laplacian  $\Delta^{\text{bri}}$  as defined in Ref. [4], hence

$$D_B(x, y) = \sum_\mu \gamma_\mu \nabla_\mu^{\text{iso}}(x, y) - \frac{r}{2} \Delta^{\text{bri}}(x, y) . \quad (3.41)$$

The Brillouin operator takes the explicit form

$$\begin{aligned} D_B(x, y) = & -r \frac{\lambda_0}{2} \delta(x, y) \\ & + \sum_{\mu=\pm 1}^{\pm 4} \left( \rho_1 \gamma_\mu - r \frac{\lambda_1}{2} \right) W_\mu(x) \delta(x + \hat{\mu}, y) \\ & + \sum_{\substack{\mu, \nu = \pm 1 \\ |\mu| \neq |\nu|}}^{\pm 4} \left( \rho_2 \gamma_\mu - r \frac{\lambda_2}{4} \right) W_{\mu\nu}(x) \delta(x + \hat{\mu} + \hat{\nu}, y) \\ & + \sum_{\substack{\mu, \nu, \rho = \pm 1 \\ |\mu| \neq |\nu| \neq |\rho|}}^{\pm 4} \left( \frac{\rho_3}{2} \gamma_\mu - r \frac{\lambda_3}{12} \right) W_{\mu\nu\rho}(x) \delta(x + \hat{\mu} + \hat{\nu} + \hat{\rho}, y) \\ & + \sum_{\substack{\mu, \nu, \rho, \sigma = \pm 1 \\ |\mu| \neq |\nu| \neq |\rho| \neq |\sigma|}}^{\pm 4} \left( \frac{\rho_4}{6} \gamma_\mu - r \frac{\lambda_4}{48} \right) W_{\mu\nu\rho\sigma}(x) \delta(x + \hat{\mu} + \hat{\nu} + \hat{\rho} + \hat{\sigma}, y) , \end{aligned} \quad (3.42)$$

where  $|\mu| \neq |\nu| \neq \dots$  is used in a transitive way, i.e. the sums are over indices with pairwise different absolute values. In this way, the four sums in (3.42) include all *off-axis* points that are one, two, three, or four hops away from  $x$  (but at most one unit in each direction), and

$$W_\mu(x) = U_\mu(x) \quad (3.43)$$

$$W_{\mu\nu}(x) = \frac{1}{2} \left( U_\mu(x) U_\nu(x + \hat{\mu}) + \text{perm} \right) \quad (3.44)$$

$$W_{\mu\nu\rho}(x) = \frac{1}{6} \left( U_\mu(x) U_\nu(x + \hat{\mu}) U_\rho(x + \hat{\mu} + \hat{\nu}) + \text{perms} \right) \quad (3.45)$$

$$W_{\mu\nu\rho\sigma}(x) = \frac{1}{24} \left( U_\mu(x) U_\nu(x + \hat{\mu}) U_\rho(x + \hat{\mu} + \hat{\nu}) U_\sigma(x + \hat{\mu} + \hat{\nu} + \hat{\rho}) + \text{perms} \right) \quad (3.46)$$

are gauge-covariant averages of the connecting paths.

The contributing points in (3.42) are weighted by the coefficients

$$(\rho_1, \rho_2, \rho_3, \rho_4) = \frac{1}{432} (64, 16, 4, 1) \quad (3.47)$$

$$(\lambda_0, \lambda_1, \lambda_2, \lambda_3, \lambda_4) = \frac{1}{64} (-240, 8, 4, 2, 1) \quad (3.48)$$

in the Brillouin action, whereas with

$$(\rho_1, \rho_2, \rho_3, \rho_4) = (1/2, 0, 0, 0) \quad (3.49)$$

$$(\lambda_0, \lambda_1, \lambda_2, \lambda_3, \lambda_4) = (-8, 1, 0, 0, 0) , \quad (3.50)$$

$\nabla_\mu^{\text{std}} \sim \frac{1}{2}$	<table border="1"> <tr><td>0 0 0</td><td>0 0 0</td><td>0 0 0</td></tr> <tr><td>0 0 0</td><td>-1 0 1</td><td>0 0 0</td></tr> <tr><td>0 0 0</td><td>0 0 0</td><td>0 0 0</td></tr> </table>	0 0 0	0 0 0	0 0 0	0 0 0	0 0 0	0 0 0	0 0 0	0 0 0	0 0 0	0 0 0	0 0 0	0 0 0	0 0 0	0 0 0	0 0 0	0 0 0	0 0 0	0 0 0	0 0 0	-1 0 1	0 0 0	0 0 0	0 0 0	0 0 0	0 0 0	0 0 0	0 0 0	0 0 0	0 0 0	0 0 0	0 0 0	0 0 0	0 0 0	0 0 0	0 0 0	0 0 0	0 0 0	0 0 0	0 0 0	$\Delta^{\text{std}} \sim$	<table border="1"> <tr><td>0 0 0</td><td>0 0 0</td><td>0 0 0</td></tr> <tr><td>0 0 0</td><td>0 1 0</td><td>0 0 0</td></tr> <tr><td>0 0 0</td><td>0 0 0</td><td>0 0 0</td></tr> <tr><td>0 0 0</td><td>0 1 0</td><td>0 1 0</td></tr> <tr><td>0 1 0</td><td>1 -8 1</td><td>0 1 0</td></tr> <tr><td>0 0 0</td><td>0 1 0</td><td>0 0 0</td></tr> <tr><td>0 0 0</td><td>0 0 0</td><td>0 0 0</td></tr> <tr><td>0 0 0</td><td>0 0 0</td><td>0 0 0</td></tr> <tr><td>0 0 0</td><td>0 1 0</td><td>0 0 0</td></tr> <tr><td>0 0 0</td><td>0 0 0</td><td>0 0 0</td></tr> </table>	0 0 0	0 0 0	0 0 0	0 0 0	0 1 0	0 0 0	0 0 0	0 0 0	0 0 0	0 0 0	0 1 0	0 1 0	0 1 0	1 -8 1	0 1 0	0 0 0	0 1 0	0 0 0	0 0 0	0 0 0	0 0 0	0 0 0	0 0 0	0 0 0	0 0 0	0 1 0	0 0 0	0 0 0	0 0 0	0 0 0
0 0 0	0 0 0	0 0 0																																																																						
0 0 0	0 0 0	0 0 0																																																																						
0 0 0	0 0 0	0 0 0																																																																						
0 0 0	0 0 0	0 0 0																																																																						
0 0 0	0 0 0	0 0 0																																																																						
0 0 0	0 0 0	0 0 0																																																																						
0 0 0	-1 0 1	0 0 0																																																																						
0 0 0	0 0 0	0 0 0																																																																						
0 0 0	0 0 0	0 0 0																																																																						
0 0 0	0 0 0	0 0 0																																																																						
0 0 0	0 0 0	0 0 0																																																																						
0 0 0	0 0 0	0 0 0																																																																						
0 0 0	0 0 0	0 0 0																																																																						
0 0 0	0 0 0	0 0 0																																																																						
0 0 0	0 1 0	0 0 0																																																																						
0 0 0	0 0 0	0 0 0																																																																						
0 0 0	0 1 0	0 1 0																																																																						
0 1 0	1 -8 1	0 1 0																																																																						
0 0 0	0 1 0	0 0 0																																																																						
0 0 0	0 0 0	0 0 0																																																																						
0 0 0	0 0 0	0 0 0																																																																						
0 0 0	0 1 0	0 0 0																																																																						
0 0 0	0 0 0	0 0 0																																																																						
$\nabla_\mu^{\text{iso}} \sim \frac{1}{432}$	<table border="1"> <tr><td>-1 0 1</td><td>-4 0 4</td><td>-1 0 1</td></tr> <tr><td>-4 0 4</td><td>-16 0 16</td><td>-4 0 4</td></tr> <tr><td>-1 0 1</td><td>-4 0 4</td><td>-1 0 1</td></tr> <tr><td>-4 0 4</td><td>-16 0 16</td><td>-4 0 4</td></tr> <tr><td>-16 0 16</td><td>-64 0 64</td><td>-16 0 16</td></tr> <tr><td>-4 0 4</td><td>-16 0 16</td><td>-4 0 4</td></tr> <tr><td>-1 0 1</td><td>-4 0 4</td><td>-1 0 1</td></tr> <tr><td>-4 0 4</td><td>-16 0 16</td><td>-4 0 4</td></tr> <tr><td>-1 0 1</td><td>-4 0 4</td><td>-1 0 1</td></tr> </table>	-1 0 1	-4 0 4	-1 0 1	-4 0 4	-16 0 16	-4 0 4	-1 0 1	-4 0 4	-1 0 1	-4 0 4	-16 0 16	-4 0 4	-16 0 16	-64 0 64	-16 0 16	-4 0 4	-16 0 16	-4 0 4	-1 0 1	-4 0 4	-1 0 1	-4 0 4	-16 0 16	-4 0 4	-1 0 1	-4 0 4	-1 0 1	$\Delta^{\text{bri}} \sim \frac{1}{64}$	<table border="1"> <tr><td>1 2 1</td><td>2 4 2</td><td>1 2 1</td></tr> <tr><td>2 4 2</td><td>4 8 4</td><td>2 4 2</td></tr> <tr><td>1 2 1</td><td>2 4 2</td><td>1 2 1</td></tr> <tr><td>2 4 2</td><td>4 8 4</td><td>2 4 2</td></tr> <tr><td>4 8 4</td><td>8 -240 8</td><td>4 8 4</td></tr> <tr><td>2 4 2</td><td>4 8 4</td><td>2 4 2</td></tr> <tr><td>1 2 1</td><td>2 4 2</td><td>1 2 1</td></tr> <tr><td>2 4 2</td><td>4 8 4</td><td>4 2 4</td></tr> <tr><td>1 2 1</td><td>2 4 2</td><td>1 2 1</td></tr> </table>	1 2 1	2 4 2	1 2 1	2 4 2	4 8 4	2 4 2	1 2 1	2 4 2	1 2 1	2 4 2	4 8 4	2 4 2	4 8 4	8 -240 8	4 8 4	2 4 2	4 8 4	2 4 2	1 2 1	2 4 2	1 2 1	2 4 2	4 8 4	4 2 4	1 2 1	2 4 2	1 2 1															
-1 0 1	-4 0 4	-1 0 1																																																																						
-4 0 4	-16 0 16	-4 0 4																																																																						
-1 0 1	-4 0 4	-1 0 1																																																																						
-4 0 4	-16 0 16	-4 0 4																																																																						
-16 0 16	-64 0 64	-16 0 16																																																																						
-4 0 4	-16 0 16	-4 0 4																																																																						
-1 0 1	-4 0 4	-1 0 1																																																																						
-4 0 4	-16 0 16	-4 0 4																																																																						
-1 0 1	-4 0 4	-1 0 1																																																																						
1 2 1	2 4 2	1 2 1																																																																						
2 4 2	4 8 4	2 4 2																																																																						
1 2 1	2 4 2	1 2 1																																																																						
2 4 2	4 8 4	2 4 2																																																																						
4 8 4	8 -240 8	4 8 4																																																																						
2 4 2	4 8 4	2 4 2																																																																						
1 2 1	2 4 2	1 2 1																																																																						
2 4 2	4 8 4	4 2 4																																																																						
1 2 1	2 4 2	1 2 1																																																																						

**Figure 3.2:** Stencil representation of the derivatives (left) and the Laplacians (right) of the Wilson (top) and Brillouin actions (bottom). The numbers are the weights ( $\rho_1, \rho_2, \rho_3, \rho_4$ ) for  $\nabla_\mu$  and ( $\lambda_0, \lambda_1, \lambda_2, \lambda_3, \lambda_4$ ) for  $\Delta$ . The point in the centre of the centre panel represents the point  $x$  where the operator is defined. Around it are the weights of its neighbours in the  $\mu\nu$ -plane. Moving in the remaining two dimensions means moving to a neighbouring panel.

we recover the Wilson action.

Other values for the weights  $\rho_{1,\dots,4}$  and  $\lambda_{0,\dots,4}$  are possible, as long as they satisfy certain conditions outlined in Ref. [4]. One example are the “hypercube fermions” introduced in Ref. [28].

The formulation in Eq. (3.42) is chosen for clarity and the purpose of doing perturbative (analytical) calculations. An effective way to implement the Brillouin operator on modern computer architectures has been presented in Ref. [29].

The derivatives used in the Brillouin action are obviously better discretizations than the ones used in the Wilson action. They were found to be the most promising candidates out of a number of similar possible discretizations [4]. Figure 3.3 shows the eigenvalue spectrum and free field dispersion relations of both operators. The eigenvalues of the Brillouin operator form an almost circular shape in the complex plane closer to the origin, while the ones from the Wilson action form its signature “burger”-like form. The Brillouin dispersion relation follows the continuum line for much longer than the Wilson one.

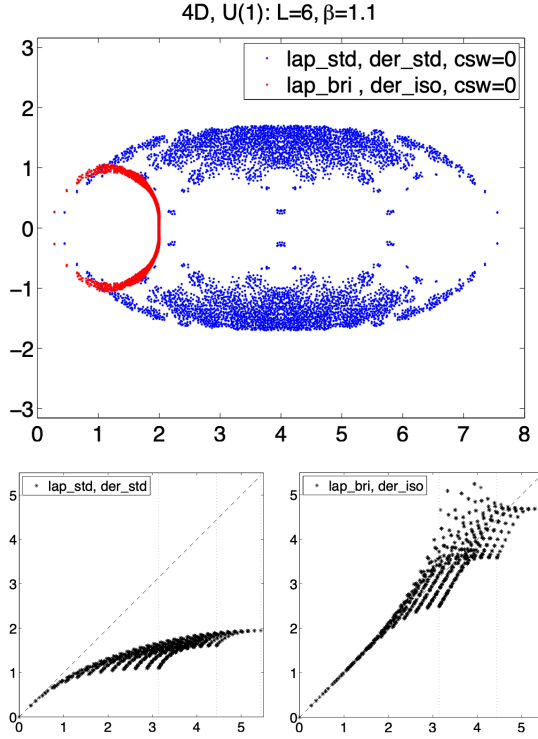


**Figure 3.3:** Comparison of the eigenvalue spectra of the Wilson and Brillouin operators (top) and their respective free field dispersion relations (Wilson bottom left, Brillouin bottom right). Pictures taken from [4].

## 3.6 Improvement

Doing calculations on the lattice introduces discretization errors. As we have mentioned before, fermion actions usually have discretization errors of order  $a$  while the Wilson gluon action has errors of order  $a^2$ . By adding higher dimensional operators to a lattice action, the order of the discretization errors can be improved similarly to how a derivative can be improved by including more lattice points [1]

$$\begin{aligned} \partial_\mu f(x) &= \frac{f(x + \epsilon) - f(x - \epsilon)}{2\epsilon} \\ &\quad - \frac{\epsilon^2}{6} \frac{f(x + 2\epsilon) - 2f(x - \epsilon) + 2f(x - \epsilon) - f(x - 2\epsilon)}{2\epsilon^3} + \mathcal{O}(\epsilon^4). \end{aligned} \quad (3.51)$$

The systematic improvement of lattice actions and on-shell observables is called the *Symanzik (on-shell) improvement program* [5].

### 3.6.1 Clover Improvement

Out of the possible dimension five operators that could be added to the Wilson fermion action, only one actually contributes on-shell [1, 6], namely

$$\mathcal{S}_{W,\text{clover}} = \mathcal{S}_W + c_{SW} \frac{a^5}{2} \sum_{x \in \Lambda} \sum_{\mu < \nu} \bar{\psi}(x) \sigma_{\mu\nu} F_{\mu\nu}(x) \psi(x), \quad (3.52)$$

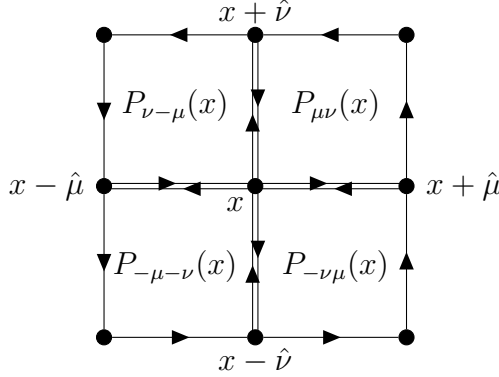


**Figure 3.4:** The clover term  $C_{\mu\nu}$  consists of four plaquettes in the  $\mu\nu$ -plane.

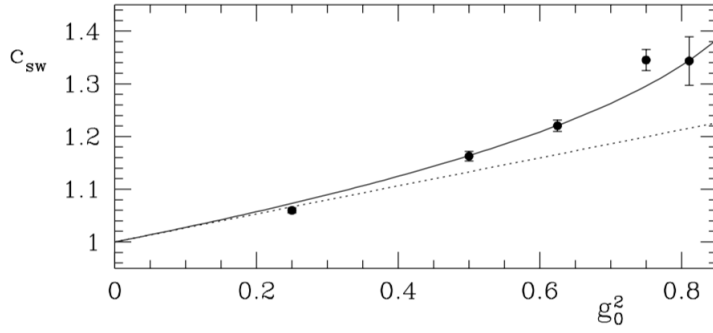


**Figure 3.5:** Non-perturbative determination of  $c_{SW}$  (data points), one-loop value (dashed line) and rational fit (solid line). Graphic taken from Ref. [33].

where  $\sigma_{\mu\nu} = \frac{i}{2}\{\gamma_\mu, \gamma_\nu\}$  and  $F_{\mu\nu}$  is a discretization of the continuum field strength tensor. A good choice for  $F_{\mu\nu}$  is the so called *clover term* (see Figure 3.4)

$$F_{\mu\nu}(x) = -\frac{i}{8a^2}(C_{\mu\nu}(x) - C_{\nu\mu}(x)) \quad (3.53)$$

$$C_{\mu\nu} = P_{\mu\nu}(x) + P_{\mu\nu}(x - \hat{\mu}) + P_{\mu\nu}(x - \hat{\nu}) + P_{\mu\nu}(x - \hat{\mu} - \hat{\nu}) . \quad (3.54)$$

The coefficient  $c_{SW}$  is named after *Sheikholeslami and Wohlert*, the authors of [6]. It has a perturbative expansion

$$c_{SW} = c_{SW}^{(0)} + g_0^2 c_{SW}^{(1)} + \mathcal{O}(g_0^4) \quad (3.55)$$

with a tree-level value of  $c_{SW}^{(0)} = r$  [6, 30]. The determination of  $c_{SW}^{(1)}$  in lattice perturbation theory for various improved actions and including stout smearing or gradient flow is a main part of this thesis (see Chapter 8).

In the non-perturbative regime,  $c_{SW}$  can be determined for example through simulations that probe the PCAC-relation with the Schrödinger functional [1, 31–37]. Figure 3.5 shows an example of non-perturbative data for  $c_{SW}$ . Knowing the tree-level value  $c_{SW}^{(0)} = 1$  and the one-loop value  $c_{SW}^{(1)} = 0.2659$ , improve the quality of the fit function considerably.

### 3.6.2 Improvement of the Gauge Action

The Wilson gauge action was constructed from the smallest possible loop on the lattice, the plaquette. Higher dimensional operators can be obtained from larger loops. A basis for suitable dimension six operators is given by  $L_1^{(6)}$  (2 by 1 rectangle),  $L_2^{(6)}$  (twisted loop along six edges of a cube), and  $L_3^{(6)}$  (L-shaped loop along six edges of a cube). Hence the improved gauge action looks like

$$\mathcal{S}_G = \frac{2}{g_0^2} \left( c_0 L_0^{(4)} + a^2 \sum_{i=1}^3 c_i L_i^{(6)} \right), \quad (3.56)$$

with  $L_0^{(4)}$  the plaquette operator. Lüscher and Weisz [38] showed that the coefficients are constrained by

$$c_0 + 8c_1 + 8c_2 + 16c_3 = 1 \quad (3.57)$$

and determined the tree level condition

$$c_1 - c_3 = -\frac{1}{12}, \quad c_2 = 0. \quad (3.58)$$

The choice  $c_3 = 0$  is the most convenient. Then

$$\mathcal{S}_G = \frac{2}{g_0^2} \sum_x \sum_{\mu < \nu} \left( c_0 \cdot \text{ReTr}[1 - P_{\mu\nu}] + c_1 a^2 \cdot \text{ReTr}[1 - P_{\mu\mu\nu}] \right) \quad (3.59)$$

(where  $P_{\mu\mu\nu}$  is the product of link variables along the  $2 \times 1$  loop in the  $\mu\nu$ -plane) removes order  $a^2$  corrections at tree level for the choice

$$c_0 = \frac{5}{3}, \quad c_1 = -\frac{1}{12}. \quad (3.60)$$

We call the action with (3.60) *Lüscher Weisz action* or *tree-level improved Symanzik gauge action* and denote it by “sym”. The un-improved action with  $c_0 = 1$ ,  $c_1 = 0$  we denote by “plaq”.

## 3.7 Smearing and Gradient Flow

Smearing or filtering strategies are procedures to replace the gauge links  $U_\mu(x)$  by “smeared” or “fattened” gauge links which involve averages over gauge links in the vicinity of the original link. Thereby the gauge configuration is smoothed before the Dirac operator is evaluated on it. This avoids *exceptional configurations*, where an eigenvalue of the Dirac operator becomes very small, making its numerical inversion impossible.

Some prominent smearing strategies are APE-smearing [39], HYP-smearing [40] and stout smearing [7], which we will discuss in detail below.

The *gradient flow* of continuum QCD is defined through the differential equation

$$\partial_t A_\mu(x, t) = D_\nu F_{\nu\mu}(x, t) + \alpha D_\mu \partial_\nu A_\nu(x, t) \quad (3.61)$$

$$A_\mu(x, 0) = g_0 A_\mu(x), \quad (3.62)$$

where  $t > 0$  is called the *flow time*,  $\alpha$  is a gauge parameter and

$$D_\mu = \partial_\mu + [A_\mu(x, t), \cdot] \quad (3.63)$$

$$F_{\mu\nu}(x, t) = \partial_\mu A_\nu(x, t) - \partial_\nu A_\mu(x, t) + [A_\mu(x, t), A_\nu(x, t)] \quad (3.64)$$

are the covariant derivative and field strength of the flowed fields. The right hand side of (3.61) is proportional to the gradient of the gauge action and the action itself is monotonously decreasing for positive flow time. Thus the Wilson flow has the effect of transporting the gauge fields towards a smooth classical field configuration. In this way its effect is very similar to smearing.

**Perturbative gradient flow in the continuum** As a preparation for the perturbative treatment of the lattice gradient flow, we review here some results from the continuum [8, 41–43]. We start by perturbatively expanding the flowed fields to third order in  $g_0$ :

$$T^a A_\mu^a(x, t) = g_0 T^a A_{1,\mu}^a(x, t) + g_0^2 T^a A_{2,\mu}^a(x, t) + g_0^3 T^a A_{3,\mu}^a(x, t) + \mathcal{O}(g_0^4), \quad (3.65)$$

and inserting this into the flow equation (3.61) resulting at first order in

$$\partial_t A_{1,\mu} = (\delta_{\mu\nu} \partial_\rho \partial_\rho + (1 - \alpha) \partial_\mu \partial_\nu) A_{1,\nu}. \quad (3.66)$$

Going to momentum space

$$A_\mu(x, t) = \int \frac{dp}{(2\pi)^4} A_\mu(p, t) e^{ipx}, \quad (3.67)$$

the solution is

$$A_{1,\mu}(p, t) = B_{\mu\nu}(p, t) A_\nu(p, 0) \quad (3.68)$$

$$B_{\mu\nu}(p, t) = \delta_{\mu\nu} e^{-p^2 t} - \frac{p_\mu p_\nu}{p^2} (e^{-p^2 t} - e^{-\alpha p^2 t}). \quad (3.69)$$

At second order the differential equation is

$$\begin{aligned} \partial_t A_{2,\mu} &= (\delta_{\mu\nu} \partial_\rho \partial_\rho + (1 - \alpha) \partial_\mu \partial_\nu) A_{2,\nu} \\ &+ 2[A_{1,\nu}, \partial_\nu A_{1,\mu}] - [A_{1,\nu}, \partial_\mu A_{1,\nu}] \\ &+ (\alpha - 1)[A_{1,\mu}, \partial_\nu A_{1,\nu}], \end{aligned} \quad (3.70)$$

and in momentum space

$$\begin{aligned} \partial_t A_{2,\mu}(p, t) &= -(\delta_{\mu\nu} p^2 + (1 - \alpha) p_\mu p_\nu) A_{2,\nu}(p, t) \\ &+ i \int \frac{dk_1 dk_2}{(2\pi)^8} \left( 2\delta_{\mu\rho} k_{2\nu} - \delta_{\nu\rho} k_{2\mu} + (\alpha - 1) \delta_{\mu\nu} k_{2\rho} \right) \\ &\times \delta(p - k_1 - k_2) [T^a, T^b] A_{1,\nu}^a(k_1, t) A_{1,\rho}^b(k_2, t). \end{aligned} \quad (3.71)$$

An ansatz of the form  $A_{2,\mu}(p, t) = B_{\mu\nu}(p, t)C_\nu(p, t)$  gives the solution

$$\begin{aligned} A_{2,\mu}^a(k_1 + k_2, t) &= f^{abc} \int_0^t ds B_{\mu\alpha}(k_1 + k_2, t-s) g_{\alpha\beta\gamma}(k_1, k_2) \\ &\quad \times B_{\beta\nu}(k_1, s) B_{\gamma\rho}(k_1, s) A_\nu^b(k_1, 0) A_\rho^c(k_1, 0) \end{aligned} \quad (3.72)$$

with

$$g_{\mu\nu\rho}(k_1, k_2) = \delta_{\mu\rho}k_{2\nu} - \delta_{\mu\nu}k_{1\rho} - \frac{1}{2}\delta_{\nu\rho}(k_{2\mu} - k_{1\mu}) + \frac{1}{2}(\alpha - 1)(\delta_{\mu\nu}k_{2\rho} - \delta_{\mu\rho}k_{1\nu}). \quad (3.73)$$

At third order we have

$$\begin{aligned} \partial_t A_{3,\mu} &= (\delta_{\mu\nu}\partial_\rho\partial_\rho - (1-\alpha)\partial_\mu\partial_\nu)A_{3,\nu} \\ &\quad + 2[A_{1,\nu}, \partial_\nu A_{2,\mu}] + 2[A_{2,\nu}, \partial_\nu A_{1,\mu}] \\ &\quad - [A_{1,\nu}, \partial_\mu A_{2,\nu}] - [A_{2,\nu}, \partial_\mu A_{1,\nu}] \\ &\quad + (\alpha - 1)([A_{1,\mu}, \partial_\nu A_{2,\nu}] + [A_{2,\mu}, \partial_\nu A_{1,\nu}]) \\ &\quad + [A_{1,\nu}, [A_{1,\nu}, A_{1,\mu}]], \end{aligned} \quad (3.74)$$

and the solution in momentum space is

$$\begin{aligned} A_{3,\mu}^a(k_1 + k_2 + k_3, t) &= f^{abc} \int_0^t ds B_{\mu\alpha}(k_1 + k_2 + k_3, t-s) g_{\alpha\nu\rho}(k_1, k_2 + k_3) A_{1,\nu}^b(k_1) A_{2,\rho}^c(k_2 + k_3) \\ &\quad + f^{abc} \int_0^t ds B_{\mu\alpha}(k_1 + k_2 + k_3, t-s) g_{\alpha\nu\rho}(k_1 + k_2, k_3) A_{2,\nu}^b(k_1 + k_2) A_{1,\rho}^c(k_3) \\ &\quad + f^{abe} f^{cde} \delta_{\nu\rho} \delta_{\mu\sigma} A_{1,\nu}^b(k_1) A_{1,\rho}^c(k_2) A_{1,\sigma}^d(k_3). \end{aligned} \quad (3.75)$$

Structurally we will find very similar solutions on the lattice, but with much more complicated functions  $g$ .

On the lattice the gradient flow of the plaquette gauge action is called *Wilson flow*. It has found many applications beyond the smoothing of gauge configurations, for example in scale setting [8, 44, 45], determining the running coupling [46] and many more [47].

### 3.7.1 Stout Smearing

Stout smearing is a unitary transformation of the link variable  $U_\mu(x)$ , which depends on the plaquettes containing  $U_\mu(x)$ . Thereby the configuration of link variables is smoothed. Often multiple smearing steps are performed to increase the smoothing effect. We write  $U_\mu^{(n)}(x)$  for the link variable after  $n$  smearing steps. The transformation to obtain  $U_\mu^{(n+1)}(x)$  is given by

$$U_\mu^{(n+1)}(x) = \exp \{ i\varrho Q_\mu^{(n)}(x) \} U_\mu^{(n)}(x) \quad (3.76)$$

$$U_\mu^{(0)}(x) = U_\mu(x), \quad (3.77)$$

with the smearing parameter  $\varrho$  and the hermitian operator  $Q_\mu^{(n)}(x)$ , which is constructed from link variables of the previous smearing step according to

$$Q_\mu^{(n)}(x) = \frac{1}{2i} \left( W_\mu^{(n)}(x) - \frac{1}{N_c} \text{Tr} [W_\mu^{(n)}(x)] \right) \quad (3.78)$$

$$W_\mu^{(n)}(x) = S_\mu^{(n)}(x) U_\mu^{(n)\dagger}(x) - U_\mu^{(n)}(x) S_\mu^{(n)\dagger}(x) \quad (3.79)$$

$$\begin{aligned} S_\mu^{(n)}(x) = & \sum_{\nu \neq \mu} \left( U_\nu^{(n)}(x) U_\mu^{(n)}(x + \hat{\nu}) U_\nu^{(n)\dagger}(x + \hat{\mu}) \right. \\ & \left. + U_\nu^{(n)\dagger}(x - \hat{\nu}) U_\mu^{(n)}(x - \hat{\nu}) U_\nu^{(n)}(x + \hat{\mu} - \hat{\nu}) \right). \end{aligned} \quad (3.80)$$

The superscript  $(n)$  denotes quantities that are constructed from link variables after  $n$  smearing steps. The quantity  $S_\mu^{(n)}(x)$  is referred to as the sum of *staples* (products of three links connecting the end-points of  $U_\mu^{(n)}(x)$ ) and  $iQ_\mu^{(n)}(x)$  is constructed as the projection of the product  $S_\mu^{(n)}(x) U_\mu^{(n)\dagger}(x)$  onto the algebra  $\mathfrak{su}(N_c)$ . Thus, the smeared link is by construction a valid group element and no further projection step is necessary as with other smearing procedures.

### 3.7.2 Wilson Flow

The lattice gradient flow was first introduced in the context of trivialising maps (and their flows) by Lüscher in Ref. [48]. Trivialising maps are maps that map the pure gauge theory onto its strong coupling limit, where the link variables decouple from one-another, i.e. a field transformation whose Jacobian cancels the gauge action in the path integral. Such maps can be generated by a continuous flow on the manifold of field configurations, the trivialising flow. Lüscher showed that, to first order in the flow time  $t$ , the trivialising flow of the Wilson gauge action is given by the Wilson flow defined through

$$\partial_t U_\mu(x, t) = -g_0^2 \{ \partial_{\mu, x} \mathcal{S}_G[U(t)] \} U_\mu(x, t) \quad (3.81)$$

$$U_\mu(x, 0) = U_\mu(x). \quad (3.82)$$

On the right-hand side,  $\partial_{\mu, x} \mathcal{S}_G[U(t)]$  is the  $\mathfrak{su}(N_c)$  algebra valued derivative of the Wilson gauge action  $\mathcal{S}_G$  with respect to the link variable  $U_\mu(x, t)$ . It is given by

$$\partial_{\mu, x} \mathcal{S}_G[U(t)] = -\frac{i}{g_0^2} Q_\mu(x, t). \quad (3.83)$$

Here  $Q_\mu$  is the same, as in the definition of stout smearing but made up from the “flowed” fields  $U_\mu(x, t)$  instead of the smeared fields.

**Proof** The differential operator is given by

$$\partial_{\mu, x} f(U) = T^a \partial_{\mu, x}^a f(U) \quad (3.84)$$

$$= T^a \frac{d}{ds} f(X^a U) \Big|_{s=0}, \quad X_\nu^a(y) = \begin{cases} e^{sT^a}, & \mu = \nu, x = y \\ 1, & \text{else} \end{cases} \quad (3.85)$$

In the sum over all plaquettes the link  $U_\mu(x)$  appears in one plaquette in each 2D-

plane containing the  $\mu$  direction, i.e. in three plaquettes. Thus the derivative of the Wilson gauge action is

$$T^a \text{Tr} \left[ \frac{d}{ds} \sum_{\nu \neq \mu} \left( e^{sT^a} U_\mu(x) U_\nu(x + \hat{\mu}) U_\mu^\dagger(x + \hat{\nu}) U_\nu^\dagger(x) \right) \Big|_{s=0} \right] \quad (3.86)$$

$$= T^a \text{Tr} \left[ \sum_{\nu \neq \mu} \left( T^a U_\mu(x) U_\nu(x + \hat{\mu}) U_\mu^\dagger(x + \hat{\nu}) U_\nu^\dagger(x) \right) \right]. \quad (3.87)$$

This is a projection of  $\sum_{\nu \neq \mu} U_\mu(x) U_\nu(x + \hat{\mu}) U_\mu^\dagger(x + \hat{\nu}) U_\nu^\dagger(x) = U_\mu(x) S_\mu^\dagger(x)$  onto  $\mathfrak{su}(N_c)$  and we can use instead the projector

$$\mathcal{P}_{\mathfrak{su}(N_c)}(M) = \frac{1}{2} \left( M - M^\dagger - \frac{1}{N_c} \text{Tr}[M - M^\dagger] \right) \quad (3.88)$$

giving  $iQ_\mu(x)$  with  $Q$  defined in (3.78).

Thus, the Wilson flow is given by

$$\partial_t U_\mu(x, t) = iQ_\mu(x, t) U_\mu(x, t) \quad (3.89)$$

$$U_\mu(x, 0) = U_\mu(x) \quad (3.90)$$

and it is easy to see that it is generated by infinitesimal stout smearing.

**Explicitly** One stout smearing step with an infinitesimal  $\varrho = \epsilon$  gives

$$U_\mu^{(1)}(x) = U_\mu^{(0)}(x) + i\epsilon Q_\mu^{(0)}(x) U_\mu^{(0)}(x) \quad (3.91)$$

while for an infinitesimal flow time  $t = \epsilon$

$$\frac{U_\mu(x, \epsilon) - U_\mu(x, 0)}{\epsilon} = iQ_\mu(x, 0) U_\mu(x, 0) \quad (3.92)$$

$$\Leftrightarrow U_\mu(x, \epsilon) = U_\mu(x, 0) + i\epsilon Q_\mu(x, 0) U_\mu(x, 0) \quad (3.93)$$

generates the same right hand side. Performing a second smearing step and expanding to order  $\epsilon^2$  gives us

$$U_\mu^{(2)}(x) = \left( 1 + i\epsilon Q_\mu^{(1)}(x) - \frac{\epsilon^2}{2} (Q_\mu^{(1)}(x))^2 \right) U_\mu^{(1)}(x) + \mathcal{O}(\epsilon^3) \quad (3.94)$$

$$= \left( 1 + i\epsilon Q_\mu^{(1)}(x) - \frac{\epsilon^2}{2} (Q_\mu^{(0)}(x))^2 \right) \left( 1 + i\epsilon Q_\mu^{(0)}(x) - \frac{\epsilon^2}{2} (Q_\mu^{(0)}(x))^2 \right) U_\mu^{(0)}(x) \quad (3.95)$$

$$= \left( 1 + i\epsilon Q_\mu^{(0)}(x) + i\epsilon Q_\mu^{(1)}(x) - 2\epsilon^2 (Q_\mu^{(0)}(x))^2 \right) U_\mu^{(0)}(x) + \mathcal{O}(\epsilon^3), \quad (3.96)$$

where we have used that  $Q$  is a functional of  $U$  with  $Q^{(1)} = Q^{(0)} + \mathcal{O}(\epsilon)$ . We compare this to the flowed field at  $t = 2\epsilon$

$$U_\mu(x, 2\epsilon) = \left( 1 + i\epsilon Q_\mu(x, \epsilon) \right) U_\mu(x, \epsilon) \quad (3.97)$$

$$= \left( 1 + i\epsilon Q_\mu(x, 0) + i\epsilon Q_\mu(x, \epsilon) - \epsilon^2 Q_\mu(x, 0)^2 \right) U_\mu(x, 0) + \mathcal{O}(\epsilon^3) \quad (3.98)$$

We see that we have to set  $t = 2\varrho$  for the leading order to remain the same and the difference between smearing and flow is of order  $t^2/4$ . For more stout iterations we see that we have to set  $\varrho = t/n$ , in order to follow the Wilson flow to order  $t$ . Then, in the limit  $\varrho \rightarrow 0$ ,  $n \rightarrow \infty$ ,  $t = n \cdot \varrho = \text{const.}$  stout smearing converges to the Wilson flow while the error is always of order  $t^2/(2n)$ .

Performing many stout smearing steps with small smearing parameters is therefore akin to integrating the Wilson flow equation by Newton's method. This is one way to implement the Wilson flow in numerical simulations, others use higher order integration procedures like Runge-Kutta etc. [8].

## 4 Lattice Perturbation Theory

Lattice perturbation theory is an integral part of many calculations using the lattice as a regularisation. Even though the lattice is primarily used to access the non-perturbative regime of large coupling strengths, knowledge of the small coupling regime is often crucial to perform the continuum limit and match lattice results to their physical continuum counterparts.

A comprehensive introduction and review of the field is given in [49]. A less recent introduction to the topic can be found in [50].

Some important applications of lattice perturbation theory include:

- The computation and matching of renormalization factors [51–60].
- The calculation of improvement coefficients such as  $c_{\text{SW}}$  from (3.52) [6, 30, 61–64],  $(c_0, c_1, c_2, c_3)$  from (3.56) [38, 65–68] or coefficients of improved currents [69–73].
- Calculation of the energy-momentum-tensor [74, 75]
- Renormalization of moments of parton distribution functions [76–80]
- The Schrödinger functional [57, 81]
- Position space methods for two-loop calculations [82, 83]
- And many more.

The fundamental starting point of lattice perturbation theory is to expand the link variables according to

$$U_\mu(x) = e^{ig_0 T^a A_\mu^a(x)} \tag{4.1}$$

Inserting this expansion up to the desired order in  $g_0$  into the action, then lets one read off the Feynman rules from the interaction terms of the fields. Because (4.1) is an infinite series in  $g_0$ , there are additional Feynman rules for each order of  $g_0$  one includes. This is what makes lattice perturbation theory much more involved compared to the continuum and calculations beyond one loop extremely difficult. Additionally each lattice action generates different Feynman rules and especially adding higher dimensional terms to the action for improvement etc. quickly leads to very large expressions. Therefore for all but the most basic examples, computer algebra systems or other automated methods [84–90] are needed.

**Fourier transforms for lattice perturbation theory.** As mentioned before, in lattice perturbation theory an infinite lattice is assumed. The lattice momenta then become continuous but are confined to the Brillouin zone  $\{p = (p_1, p_2, p_3, p_4) | p_i \in [-\pi/a, \pi/a]\}$  by the lattice spacing  $a$ . Thus we have integrals to evaluate in momentum space rather than sums.

Additionally, it is very convenient to define the Fourier transforms of the gluon fields  $A_\mu(x)$  at the half-way-point  $x + \hat{\mu}/2$  rather than at  $x$ . In this way results turn out in terms of trigonometric functions of the momenta and remaining phase factors always cancel [49].

Thus, the Fourier transforms we will be using for all perturbative calculations are (in lattice units):

$$A_\mu^a(x) = \int_{-\pi}^{\pi} \frac{d^4 k}{(2\pi)^4} e^{i(x+\hat{\mu}/2)k} A_\mu^a(k) , \quad A_\mu^a(k) = \sum_x e^{-i(x+\hat{\mu}/2)k} A_\mu^a(x) \quad (4.2)$$

$$\psi(x) = \int_{-\pi}^{\pi} \frac{d^4 p}{(2\pi)^4} e^{ixp} \psi(p) , \quad \psi(p) = \sum_x e^{-ixp} \psi(p) \quad (4.3)$$

$$\bar{\psi}(x) = \int_{-\pi}^{\pi} \frac{d^4 p}{(2\pi)^4} e^{-ixp} \bar{\psi}(p) , \quad \bar{\psi}(p) = \sum_x e^{ixp} \bar{\psi}(p) \quad (4.4)$$

$$\delta(x, y) = \int_{-\pi}^{\pi} \frac{d^4 p}{(2\pi)^4} e^{i(x-y)p} , \quad \delta(p - q) = \frac{1}{(2\pi)^4} \sum_x e^{-ix(p-q)} . \quad (4.5)$$

## 4.1 The Gauge Action

Before deriving the gluon propagator and other Feynman rules from the lattice gauge action

$$\mathcal{S}_G = \frac{2}{g_0^2} \sum_x \sum_{\mu < \nu} \text{ReTr} [1 - P_{\mu\nu}(x)] , \quad (4.6)$$

two additions need to be made. One concerns the gauge freedom leading to over-counting in the path integral. Thus, gauge-fixing and the Faddeev-Popov procedure will lead, very similar to the continuum, to the inclusion of ghosts (see section 4.1). The other addition stems from the Haar measure  $\mathcal{D}U$  on the group  $SU(N_c)$  and its relation to the measure  $\mathcal{D}A$  on the algebra  $\mathfrak{su}(N_c)$ . The Haar measure for a single link variable is

$$dU_\mu(x) = \sqrt{\det(g(A_\mu(x)))} \prod_a dA_\mu^a(x) , \quad (4.7)$$

where the metric  $g$  is given by [91]

$$g(A_\mu(x)) = \frac{1 - \cos(g_0 t^a A_\mu^a(x))}{(g_0 t^a A_\mu^a(x))^2} , \quad (4.8)$$

with  $t^a A_\mu^a(x)$  the gauge field in the adjoint representation ( $(t^a)^{bc} = -if^{abc}$ ,  $\text{Tr}[t^a t^b] = N_c \delta^{ab}$ ). By using  $\det(g) = \exp(\text{Tr} \ln(g))$ , we get an addition to the action coming from the switch of integration variables

$$\mathcal{D}U = e^{-\mathcal{S}_{\text{meas}}} \mathcal{D}A \quad (4.9)$$

with

$$\mathcal{S}_{\text{meas}} = \frac{1}{2} \sum_{x,\mu} \text{Tr} \ln \left[ \frac{2 - 2 \cos(g_0 t^a A_\mu^a(x))}{(g_0 t^a A_\mu^a(x))^2} \right] \quad (4.10)$$

$$= -\frac{1}{2} \sum_{x,\mu} \text{Tr} \ln \left[ 1 + 2 \sum_{n=1}^{\infty} \frac{(-1)^n (g_0 t^a A_\mu^a(x))^{2n}}{(2n+2)!} \right] \quad (4.11)$$

$$= -\frac{1}{2} \sum_{x,\mu} \text{Tr} \ln \left[ 1 - 2 \frac{(g_0 t^a A_\mu^a(x))^2}{24} + \mathcal{O}(g_0^4) \right] \quad (4.12)$$

$$= \sum_{x,\mu} \text{Tr} \left[ \frac{(g_0 t^a A_\mu^a(x))^2}{24} \right] + \mathcal{O}(g_0^4) \quad (4.13)$$

$$= \sum_{x,\mu} \frac{g_0^2 N_c}{24} A_\mu^a(x) A_\mu^a(x) + \mathcal{O}(g_0^4) . \quad (4.14)$$

The extra factor of 2 in the logarithm in (4.10) is chosen such that the series in (4.11) starts with a unit matrix.

Thus, the measure contributes a mass counter term at one-loop order. Higher orders are only relevant at two loops and beyond.

The gauge fixing and Faddeev-Popov procedure is similar to the continuum [49]. The gauge fixing term for a covariant gauge is

$$\mathcal{S}_{\text{gf}} = -\frac{1}{2\xi} \sum_{\mu\nu} A_\mu(x) \vec{\nabla}_\mu \vec{\nabla}_\nu A_\nu(x) \quad (4.15)$$

with the forward and backward derivatives

$$\vec{\nabla}_\mu f(x) = f(x + \hat{\mu}) - f(x) \quad (4.16)$$

$$\vec{\nabla}_\mu f(x) = f(x) - f(x - \hat{\mu}) . \quad (4.17)$$

The ghost action is (see for example [49] for derivations)

$$\mathcal{S}_{\text{gh}} = - \sum_x \bar{c}^a(x) \vec{\nabla}_\mu \hat{D}_\mu^{ab} c^b(x) . \quad (4.18)$$

The main difference to the continuum is in the covariant derivative for the ghost fields

$$\hat{D}_\mu = (M^\dagger)^{-1} \vec{\nabla}_\mu + i g_0 t^a A_\mu^a(x) \quad (4.19)$$

with

$$M = \frac{e^{ig_0 t^a A_\mu^a(x)} - 1}{ig_0 t^a A_\mu^a(x)} \quad (4.20)$$

With the expansion

$$(M^\dagger)^{-1} = 1 + \frac{i}{2} g_0 A_\mu(x) - \frac{1}{12} g_0^2 A_\mu(x)^2 + \mathcal{O}(g_0^3) , \quad (4.21)$$

it becomes apparent, that there are also an infinite amount of ghost-gluon interaction terms at increasing order of  $g_0$ .

Altogether, the pure lattice gauge action for perturbation theory looks like

$$\mathcal{S}_G + \mathcal{S}_{\text{meas}} + \mathcal{S}_{\text{gf}} + \mathcal{S}_{\text{gh}} . \quad (4.22)$$

With gauge fixing in place, the free kinetic part for the gauge fields can be inverted, giving us the gluon propagator

$$G_{\mu\nu}^{ab}(k) = \delta^{ab} \frac{1}{\hat{k}^2} \left( \delta_{\mu\nu} - (1 - \xi) \frac{\hat{k}_\mu \hat{k}_\nu}{\hat{k}^2} \right) \quad (4.23)$$

and the ghost propagator

$$G_{\text{gh}}^{ab}(k) = \frac{\delta^{ab}}{\hat{k}^2} . \quad (4.24)$$

**Notation** The hat notation is used for functions of momenta, which become regular momenta in the limit  $a \rightarrow 0$ , i.e. with explicit factors of  $a$ :

$$\hat{k}_\mu = \frac{2}{a} \sin \left( \frac{a}{2} k_\mu \right) \quad \hat{k}^2 = \sum_\mu \hat{k}_\mu^2 \quad (4.25)$$

Other abbreviations for trigonometric functions we will use often are (in lattice units)

$$s(k_\mu) = \sin \left( \frac{1}{2} k_\mu \right) \quad c(k_\mu) = \cos \left( \frac{1}{2} k_\mu \right) \quad (4.26)$$

$$\bar{s}(k_\mu) = \sin(k_\mu) \quad \bar{c}(k_\mu) = \cos(k_\mu) \quad (4.27)$$

$$s^2(k) = \sum_\mu s(k_\mu)^2 \quad \bar{s}^2(k) = \sum_\mu \bar{s}(k_\mu)^2 \quad (4.28)$$

**Derivation of gluon propagator** The expansion of the plaquette gauge action in  $g_0$  works very similarly to what we have already seen in the expansion for  $a \rightarrow 0$  in Eqn. (3.19). Here we have

$$S_G = \frac{1}{2} \sum_x \sum_{\mu\nu} \text{Tr}[(F_{\mu\nu}^{\text{lat}})^2] + \mathcal{O}(g_0) = \frac{1}{4} \delta^{ab} \sum_x \sum_{\mu\nu} F_{\mu\nu}^{a\text{lat}} F_{\mu\nu}^{b\text{lat}} + \mathcal{O}(g_0) . \quad (4.29)$$

The free part ( $g_0 = 0$ ) of  $(F_{\mu\nu}^{\text{lat}})^2$  together with the gauge fixing term gives

$$\sum_{\mu\nu} \left( \frac{\delta^{ab}}{4} (\vec{\nabla}_\mu A_\nu^a(x) - \vec{\nabla}_\nu A_\mu^a(x))^2 + \frac{1}{2\xi} (\bar{\nabla}_\mu A_\mu^a(x)) (\bar{\nabla}_\nu A_\nu^a(x)) \right) \quad (4.30)$$

$$= \sum_{\mu\nu} \left( \frac{\delta^{ab}}{2} (\vec{\nabla}_\mu A_\nu^a(x) \vec{\nabla}_\mu A_\nu^a(x) - \vec{\nabla}_\mu A_\nu^a(x) \vec{\nabla}_\nu A_\mu^a(x)) + \frac{1}{2\xi} (\vec{\nabla}_\mu A_\mu^a(x)) (\vec{\nabla}_\nu A_\nu^a(x)) \right). \quad (4.31)$$

In momentum space this becomes

$$\sum_{\mu\nu} \delta^{ab} \left( -\delta_{\mu\nu} \hat{k}^2 + \hat{k}_\mu \hat{k}_\nu + \frac{1}{\xi} \hat{k}_\mu \hat{k}_\nu \right) A_\mu^a(k) A_\nu^b(k) = \sum_{\mu\nu} G_{\mu\nu}^{ab}(k)^{-1} A_\mu^a(k) A_\nu^b(k). \quad (4.32)$$

Finally we notice that

$$\sum_\nu \left( -\delta_{\mu\nu} \hat{k}^2 + \hat{k}_\mu \hat{k}_\nu + \frac{1}{\xi} \hat{k}_\mu \hat{k}_\nu \right) \frac{\delta_{\nu\rho} \hat{k}^2 - (1-\xi) \hat{k}_\nu \hat{k}_\rho}{(\hat{k}^2)^2} = \delta_{\mu\rho}, \quad (4.33)$$

giving us the propagator (4.23) as the inverse of  $G_{\mu\nu}^{ab}(k)^{-1}$ .

All the vertices relevant to one-loop calculations of the pure gauge lattice action are [49]:  
The three-gluon vertex:

$$V_{3g,\mu\nu\rho}^{abc}(k_1, k_2, k_3) = -\frac{ig_0}{3} f^{abc} \left[ \delta_{\mu\nu} s(k_{1\rho} - k_{2\rho}) c(k_{3\mu}) + 2 \text{ cyclic perms} \right], \quad (4.34)$$

the ghost-ghost-gluon vertex:

$$V_{1gh,\mu}^{abc}(p, q) = ig_0 f^{abc} 2c(p_\mu) s(q_\mu), \quad (4.35)$$

the four-gluon vertex:

$$\begin{aligned} V_{4g,\mu\nu\rho\sigma}^{abcd}(k_1, k_2, k_3, k_4) &= g_0^2 (v_{4g,\mu\nu\rho\sigma}^{abcd}(k_1, k_2, k_3, k_4) \\ &\quad + v_{4g,\mu\rho\nu\sigma}^{acbd}(k_1, k_3, k_2, k_4) \\ &\quad + v_{4g,\mu\sigma\rho\nu}^{adcb}(k_1, k_4, k_3, k_2) \\ &\quad + w_{4g,\mu\nu\rho\sigma}^{abcd}(k_1, k_2, k_3, k_4)) \end{aligned} \quad (4.36)$$

with

$$\begin{aligned} v_{4g,\mu\nu\rho\sigma}^{abcd}(k_1, k_2, k_3, k_4) &= -f^{abe} f^{cde} \\ &\times \left[ \delta_{\mu\rho} \delta_{\nu\sigma} \left( c(k_{2\mu} - k_{4\mu}) c(k_{1\nu} - k_{3\nu}) - \frac{4}{3} s(k_{1\nu}) s(k_{2\mu}) s(k_{3\nu}) s(k_{4\mu}) \right) \right. \\ &- \delta_{\mu\sigma} \delta_{\nu\rho} \left( c(k_{2\mu} - k_{3\mu}) c(k_{1\nu} - k_{4\nu}) - \frac{4}{3} s(k_{1\nu}) s(k_{2\mu}) s(k_{3\mu}) s(k_{4\nu}) \right) \\ &+ \frac{2}{3} \left( \delta_{\nu\rho} \delta_{\nu\sigma} s(k_{4\mu} - k_{3\mu}) s(k_{1\nu}) c(k_{2\mu}) - \delta_{\mu\rho} \delta_{\mu\sigma} s(k_{4\nu} - k_{3\nu}) s(k_{2\mu}) c(k_{1\nu}) \right. \\ &\left. + \delta_{\mu\nu} \delta_{\mu\sigma} s(k_{2\rho} - k_{1\rho}) s(k_{3\sigma}) c(k_{4\rho}) - \delta_{\mu\nu} \delta_{\mu\rho} s(k_{2\sigma} - k_{1\sigma}) s(k_{4\rho}) c(k_{3\sigma}) \right) \\ &\left. + \frac{1}{3} \delta_{\mu\nu} \delta_{\mu\rho} \delta_{\mu\sigma} \sum_\lambda s(k_{2\lambda} - k_{1\lambda}) s(k_{4\lambda} - k_{3\lambda}) \right] \end{aligned} \quad (4.37)$$

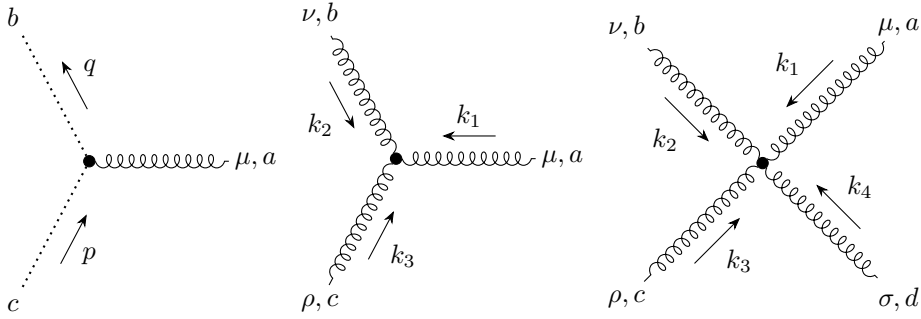


**Figure 4.1:** Gauge vertices for one-loop lattice perturbation theory.

and

$$\begin{aligned}
 w_{4g,\mu\nu\rho\sigma}^{abcd}(k_1, k_2, k_3, k_4) = & \frac{4}{3} \left( \delta^{abe} \delta^{cde} + \delta^{ace} \delta^{bde} + \delta^{ade} \delta^{cbe} \right. \\
 & + \frac{2}{3} (\delta^{ab} \delta^{cd} + \delta^{ac} \delta^{bd} + \delta^{ad} \delta^{cb}) \left. \right) \left( \delta_{\mu\nu} \delta_{\mu\rho} \delta_{\mu\sigma} \sum_{\lambda} s(k_{1\lambda}) s(k_{2\lambda}) s(k_{3\lambda}) s(k_{4\lambda}) \right. \\
 & - \delta_{\mu\nu} \delta_{\mu\rho} s(k_{1\sigma}) s(k_{2\sigma}) s(k_{3\sigma}) s(k_{4\mu}) - \delta_{\mu\nu} \delta_{\mu\sigma} s(k_{1\rho}) s(k_{2\rho}) s(k_{3\rho}) s(k_{4\mu}) \\
 & - \delta_{\mu\rho} \delta_{\mu\sigma} s(k_{1\nu}) s(k_{2\nu}) s(k_{3\nu}) s(k_{4\mu}) - \delta_{\nu\rho} \delta_{\nu\sigma} s(k_{1\mu}) s(k_{2\mu}) s(k_{3\mu}) s(k_{4\nu}) \\
 & + \delta_{\mu\nu} \delta_{\rho\sigma} s(k_{1\rho}) s(k_{2\rho}) s(k_{3\mu}) s(k_{4\mu}) + \delta_{\mu\rho} \delta_{\nu\sigma} s(k_{1\nu}) s(k_{2\nu}) s(k_{3\mu}) s(k_{4\mu}) \\
 & \left. + \delta_{\mu\rho} \delta_{\nu\sigma} s(k_{1\nu}) s(k_{2\rho}) s(k_{3\mu}) s(k_{4\mu}) \right), \tag{4.38}
 \end{aligned}$$

the ghost-ghost-gluon-gluon vertex

$$V_{2gh,\mu\nu}^{abcd}(p, q) = \frac{g_0^2}{3} (\{t^a, t^b\})^{cd} \delta_{\mu\nu} s(p_\mu) s(q_\mu), \tag{4.39}$$

and the measure counter term:

$$C_{\text{meas},\mu\nu}^{ab} = -\frac{g_0^2}{4} \delta^{ab} \delta_{\mu\nu}. \tag{4.40}$$

For the one-loop calculations presented in this thesis namely the fermion self energy and the improvement coefficient  $c_{\text{SW}}$ , the measure and ghost Feynman rules are not needed. They only contribute whenever internal gluon lines begin and end at purely gluonic vertices.

### 4.1.1 Improvement

Here we give the versions of the later needed Feynman rules of the tree-level Symanzik improved gauge action (3.59).

The following gluon propagator and three-gluon vertex have been derived in Refs. [66, 67]. The gluon propagator in a general covariant gauge is

$$G_{\mu\nu}^{ab}(k) = \frac{\delta^{ab}}{4(s^2(k))^2} \left( \xi s(k_\mu) s(k_\nu) + \sum_{\rho} (\delta_{\mu\nu} s(k_\rho) - \delta_{\mu\rho} s(k_\rho)) s(k_\rho) A_{\rho\nu}(k) \right). \tag{4.41}$$

The symmetric matrix  $A$  is given by

$$A_{\mu\nu}(k) = \frac{(1 - \delta_{\mu\nu})}{\Delta(k)} \left[ (s^2(k))^2 - 4c_1 s^2(k) \left( 2 \sum_{\rho} s(k_{\rho})^4 + s^2(k) \sum_{\rho \neq \mu, \nu} s(k_{\rho})^2 \right) \right. \\ \left. + 16c_1^2 \left( \left( \sum_{\rho} s(k_{\rho})^4 \right)^2 + s^2(k) \sum_{\rho} s(k_{\rho})^4 \sum_{\tau \neq \mu\nu} s(k_{\tau})^2 + (s^2(k))^2 \prod_{\rho \neq \mu, \nu} s(k_{\rho})^2 \right) \right] \quad (4.42)$$

with the denominator taking the form

$$\Delta(k) = \left( s^2(k) - 4c_1 \sum_{\rho} s(k_{\rho})^4 \right) \left[ s^2(k) - 4c_1 \left( (s^2(k))^2 + \sum_{\tau} s(k_{\tau})^4 \right) \right. \\ \left. + 8c_1^2 \left( (s^2(k))^3 + 2 \sum_{\tau} s(k_{\tau})^6 - s^2(k) \sum_{\tau} s(k_{\tau})^4 \right) \right] \\ - 16c_1^3 \sum_{\rho} s(k_{\rho})^4 \prod_{\tau \neq \rho} s(k_{\tau})^2. \quad (4.43)$$

Similarly, the three-gluon vertex is found to be

$$V_{g3\mu\nu\rho}^{abc}(k_1, k_2, k_3) = -\frac{ig_0}{6} f^{abc} \left( c_0 V_{g3\mu\nu\rho}^{(0)}(k_1, k_2, k_3) + c_1 V_{g3\mu\nu\rho}^{(1)}(k_1, k_2, k_3) \right) \quad (4.44)$$

with

$$V_{g3\mu\nu\rho}^{(0)}(k_1, k_2, k_3) = 2 \left[ \delta_{\mu\nu} s(k_{1\rho} - k_{2\rho}) c(k_{3\mu}) + 2 \text{cyclic perms} \right] \quad (4.45)$$

$$V_{g3\mu\nu\rho}^{(1)}(k_1, k_2, k_3) = 8V_{g3\mu\nu\rho}^{(0)}(k_1, k_2, k_3) \\ + 8 \left[ \delta_{\mu\nu} \left( c(k_{3\mu}) \left[ s(k_{1\mu} - k_{2\mu})(\delta_{\mu\rho} s^2(k_3) - s(k_{3\mu})s(k_{3\rho})) \right. \right. \right. \\ \left. \left. \left. - s(k_{1\rho} - k_{2\rho})(s(k_{1\rho})^2 + s(k_{2\rho})^2) \right] \right. \right. \\ \left. \left. + s(k_{1\rho} - k_{2\rho})(s(k_{1\mu})s(k_{2\mu}) - c(k_{1\mu})c(k_{2\mu})s(k_{3\mu})^2) \right) \right. \\ \left. + 2 \text{cyclic perms} \right]. \quad (4.46)$$

## 4.2 The Fermion Action

We know the propagator

$$S_W^{ab}(p) = \delta^{ab} \frac{-i\cancel{s}(p) + 2rs^2(p)}{\bar{s}^2(p) + (2rs^2(p))^2} \quad (4.47)$$

of the massless Wilson fermion from (3.39). Most relevant for later calculations are the three vertices of one, two, and three gluons coupling to a quark anti-quark pair shown

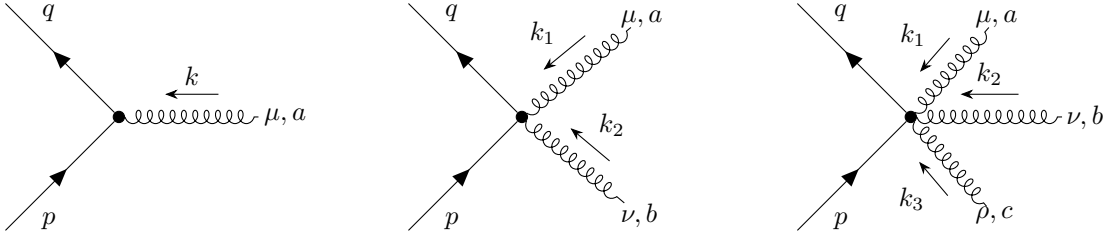


**Figure 4.2:** Momentum assignments for the vertices with one, two and three gluons.

in Fig. 4.2. They are (for the Wilson fermion action):

$$V_{1W\mu}^a(p, q) = -g_0 T^a \left( i\gamma_\mu c(p_\mu + q_\mu) + rs(p_\mu + q_\mu) \right) \quad (4.48)$$

$$V_{2W\mu\nu}^{ab}(p, q) = \frac{g_0^2}{2} T^a T^b \delta_{\mu\nu} \left( i\gamma_\mu s(p_\mu + q_\mu) - rc(p_\mu + q_\mu) \right) \quad (4.49)$$

$$V_{3W\mu\nu\rho}^{abc}(p, q) = \frac{g_0^3}{6} T^a T^b T^c \delta_{\mu\nu} \delta_{\mu\rho} \left( i\gamma_\mu c(p_\mu + q_\mu) + rs(p_\mu + q_\mu) \right) \quad (4.50)$$

### 4.2.1 Clover Improvement

By adding the clover improvement term to a fermion action, the following contributions have to be added to the vertices, which have been given in Ref. [63]

$$V_{1c\mu}(p, q) = i \frac{g_0}{2} c_{\text{SW}} \sum_\nu \sigma_{\mu\nu} c(p_\mu - q_\mu) \bar{s}(p_\nu - q_\nu) \quad (4.51)$$

$$\begin{aligned} V_{2c\mu\nu}(p, q, k_1, k_2) &= ig_0^2 c_{\text{SW}} \left( \frac{1}{4} \delta_{\mu\nu} \sum_\rho \sigma_{\mu\rho} s(q_\mu - p_\mu) (\bar{s}(k_{2\rho}) - \bar{s}(k_{1\rho})) \right. \\ &\quad \left. + \sigma_{\mu\nu} \left( c(k_{1\nu}) c(k_{2\mu}) c(q_\mu - p_\mu) c(p_\nu - p_\nu) - \frac{1}{2} c(k_{1\mu}) c(k_{2\nu}) \right) \right) \end{aligned} \quad (4.52)$$

$$\begin{aligned} V_{3c\mu\nu\rho}(p, q, k_1, k_2, k_3) &= ig_0^3 c_{\text{SW}} T^a T^b T^c \left( \delta_{\mu\nu} \delta_{\mu\rho} \sum_\alpha \sigma_{\mu\alpha} \left[ -\frac{1}{12} c(q_\mu - p_\mu) \bar{s}(q_\alpha - p_\alpha) \right. \right. \\ &\quad \left. \left. - \frac{1}{2} c(q_\mu - p_\mu) c(q_\alpha - p_\alpha) c(k_{3\alpha} - k_{1\alpha}) s(k_{2\alpha}) \right] \right. \\ &\quad \left. + \delta_{\mu\nu} \sigma_{\mu\rho} \left[ -\frac{1}{2} c(q_\mu - p_\mu) c(q_\rho - p_\rho) c(k_{1\rho} + k_{2\rho}) s(k_{3\mu}) + \frac{1}{4} s(k_{1\mu} + k_{2\mu}) c(2k_{2\rho} + k_{3\rho}) \right] \right. \\ &\quad \left. + \delta_{\nu\rho} \sigma_{\mu\nu} \left[ -\frac{1}{2} c(q_\mu - p_\mu) c(q_\nu - p_\nu) c(k_{2\mu} + k_{3\mu}) s(k_{1\nu}) + \frac{1}{4} s(k_{2\nu} + k_{3\nu}) c(k_{1\mu} + 2k_{2\mu}) \right] \right. \\ &\quad \left. + \delta_{\mu\rho} \sigma_{\mu\nu} \left[ \frac{1}{2} c(q_\nu - p_\nu) c(k_{3\nu} - k_{1\nu}) s(k_{1\mu} + 2k_{2\mu} + k_{3\mu}) \right] \right) \end{aligned} \quad (4.53)$$

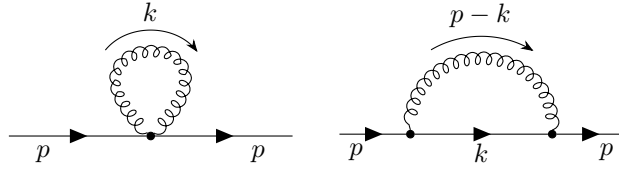


**Figure 4.3:** Tadpole (left) and sunset (right) diagrams of the quark self energy.

### 4.3 Fermion Self-Energy

Due to the Wilson term, even if one sets the bare fermion mass  $m$  to zero in the lattice action, the quarks and consequently the hadronic bound states will effectively not be massless. In other words, the bare quark mass does not only receive multiplicative but also additive renormalisation

$$am_R = Z_m(am + am_{\text{shift}}), \quad (4.54)$$

where  $am_{\text{shift}}$  is called the *additive mass shift*. Conversely the *critical mass*  $am_{\text{crit}} = -am_{\text{shift}} < 0$  is defined as the bare mass one would have to choose to get massless quarks/a massless pion. Often this is also expressed through the *critical hopping parameter*<sup>1</sup>

$$\kappa_{\text{crit}} = \frac{1}{2(am_{\text{crit}} + 4)}. \quad (4.55)$$

Perturbatively, the critical mass is given by the divergent term in the  $a$ -expansion of the fermion self energy, i.e. quantum corrections to the fermion propagator.

At the one-loop order the fermion self-energy  $\Sigma$  receives contributions from the “tadpole” and the “sunset” diagrams shown in Fig. 4.3. We define  $\Sigma_0$  through the linearly divergent part and  $\Sigma_1$  as the finite piece in an expansion in the lattice spacing [49, 92, 93]

$$\Sigma = \frac{g_0^2 C_F}{16\pi^2} \left( \frac{\Sigma_0}{a} + \Sigma_1 i \not{p} + \mathcal{O}(a) \right), \quad (4.56)$$

where  $p_\mu$  is the momentum of the external fermion (see Fig. 4.3), and the relation to the critical mass is [2]

$$am_{\text{crit}} = \frac{g_0^2 C_F}{16\pi^2} \Sigma_0. \quad (4.57)$$

The contributions to  $\Sigma$  from the two diagrams read

$$\Sigma^{(\text{tadpole})} = \int_{-\pi}^{\pi} \frac{d^4 k}{(2\pi)^4} \sum_{\mu, \nu, a} G_{\mu\nu}(k) V_{2\mu\nu}^{aa}(p, p, k, -k) \quad (4.58)$$

$$\Sigma^{(\text{sunset})} = \int_{-\pi}^{\pi} \frac{d^4 k}{(2\pi)^4} \sum_{\mu, \nu, a} V_{1\mu}^a(p, k) G_{\mu\nu}(p - k) S(k) V_{1\nu}^a(k, p) \quad (4.59)$$

<sup>1</sup>The *hopping expansion* is an expansion of the inverse of the Dirac operator  $D^{-1} = (1 - \kappa H)^{-1}$  with the hopping parameter  $\kappa = (2am + 8)^{-1}$  and  $H(x, y) = \sum_{\pm\mu} (1 - \gamma_\mu) U_\mu(x) \delta(x + \hat{\mu}, y)$  the hopping matrix. For large quark masses, i.e.  $\kappa < 1/8$ , the inverse is then a series in  $\kappa$ :  $D^{-1} = \sum_n \kappa^n H^n$  [1].

respectively, and from the sum we obtain  $\Sigma_0$  and  $\Sigma_1$  by

$$\frac{g_0^2 C_F}{16\pi^2} \frac{\Sigma_0}{a} = \Sigma|_{p=0} \quad (4.60)$$

$$\frac{g_0^2 C_F}{16\pi^2} \Sigma_1 = \frac{1}{4} \text{Tr} \left[ \frac{\partial}{\partial p_\mu} \Sigma \cdot \gamma_\mu \right]_{p=0}, \quad (4.61)$$

where  $\mu$  is kept fixed, i.e. not summed over. In most gauge choices (like Feynman gauge  $\xi = 0$ , which we are using here),  $\Sigma_1$  diverges logarithmically for  $p \rightarrow 0$  (more specifically the contribution from the “sunset” diagram to  $\Sigma_1$  diverges). To deal with such divergent integrals the *Kawai method* can be used [91] (also see [49]). From the original lattice integral with finite external momenta  $p, q$

$$I = \int_{-\pi}^{\pi} \frac{d^4 k}{(2\pi)^4} \mathcal{I}(k, p, q), \quad (4.62)$$

the divergence is split off into an analytically solvable continuum-like integral

$$I - J = \lim_{a \rightarrow 0} \int_{-\frac{\pi}{a}}^{\frac{\pi}{a}} \frac{dk}{(2\pi)^4} \mathcal{I}(ak, ap, aq) - \mathcal{J}(ak, ap, aq) \quad (4.63)$$

and a lattice integral at  $p, q = 0$

$$\begin{aligned} J &= \int_{-\pi}^{\pi} \frac{d^4 k}{(2\pi)^4} \mathcal{I}(k, 0, 0) + \sum_{\mu\nu} p_\mu q_\nu \int_{-\pi}^{\pi} \frac{d^4 k}{(2\pi)^4} \frac{\partial^2 \mathcal{I}(k, p, q)}{\partial p_\mu \partial q_\nu} \Big|_{p,q=0} \\ &\quad + \sum_{\mu\nu} \frac{p_\mu p_\nu}{2} \int_{-\pi}^{\pi} \frac{d^4 k}{(2\pi)^4} \frac{\partial^2 \mathcal{I}(k, p, 0)}{\partial p_\mu \partial p_\nu} \Big|_{p=0} + \sum_{\mu\nu} \frac{q_\mu q_\nu}{2} \int_{-\pi}^{\pi} \frac{d^4 k}{(2\pi)^4} \frac{\partial^2 \mathcal{I}(k, 0, q)}{\partial q_\mu \partial q_\nu} \Big|_{q=0}. \end{aligned} \quad (4.64)$$

While the split  $I = (I - J) + J$  takes care of the divergence for  $p, q \rightarrow 0$ , the two integrals  $J$  and  $I - J$  individually might still be divergent. This divergence needs to be regularized in intermediate steps and vanishes once the sum of the two integrals is taken.

In the case of  $\Sigma_1^{(\text{sunset})}$ , the continuum-like integral is [49]

$$(I - J)^{(\text{sunset})} \cdot i\psi = -g_0^2 C_F \int_{-\infty}^{\infty} \frac{dk}{(2\pi)^4} \frac{1}{(p-k)^2} \sum_{\mu} \gamma_\mu \frac{-ik}{k^2} \gamma_\mu \quad (4.65)$$

$$= \frac{g_0^2 C_F}{16\pi^2} i\psi (\ln(p^2) - \ln(\mu^2) - 2), \quad (4.66)$$

regularized by a small mass  $\mu$ . The divergent lattice integral with the same regularisation is then of the form

$$J^{(\text{sunset})} = \frac{g_0^2 C_F}{16\pi^2} (\ln(\mu^2) + \text{const.}) . \quad (4.67)$$

One way of evaluating a divergent lattice integral is by subtracting a known lattice integral with the same divergence. In this case we use the integral

$$\mathcal{B}_2 = \int_{-\pi}^{\pi} \frac{d^4 k}{(2\pi)^4} \frac{1}{(4s^2(k))^2}. \quad (4.68)$$

Its regularized version gives

$$\mathcal{B}_2(\mu) = \frac{1}{16\pi^2} (-\ln(\mu^2) + F_0 - \gamma_E) + \mathcal{O}(\mu^2), \quad (4.69)$$

where  $\gamma_E = 0.57721566490153(1)$  is the Euler-Mascheroni constant and  $F_0$  a lattice constant given in Ref. [94] as  $F_0 = 4.369225233874758(1)$ . We define the constant part of  $\Sigma_1$  as  $\Sigma_{10}$

$$\Sigma_1 = \log(p^2) + \Sigma_{10} \quad (4.70)$$

which we can calculate numerically as

$$\Sigma_{10}^{(\text{sunset})} = \int_{-\pi}^{\pi} \frac{d^4 k}{(2\pi)^4} \left[ \frac{16\pi^2}{g_0^2 C_F} J^{(\text{sunset})} + 16\pi^2 \mathcal{B}_2 \right] + 16\pi^2 (-2 - F_0 + \gamma_E). \quad (4.71)$$

We use *Mathematica* [95] to carry out the analytic derivations as well as the numerical integrations.

The procedure outlined so far for the calculation of  $\Sigma_1$  does not depend on which lattice Feynman rules were used as long as they have the correct continuum limit (4.65). In Chapter 7 we will present results for  $\Sigma_0$  and  $\Sigma_{10}$  for all combinations of the Wilson and Brillouin fermion actions and plaquette and Lüscher-Weisz gluon actions. For any of these no new divergencies are introduced; only the zero momentum lattice integral  $J$  changes.

The integrals for  $\Sigma_0^{(\text{sunset})}$ ,  $\Sigma_0^{(\text{tadpole})}$ , and  $\Sigma_1^{(\text{tadpole})}$  are finite and can be directly evaluated at  $p = 0$ .

## 4.4 Perturbative Determination of $c_{\text{SW}}$

The Sheikholeslami-Wohlert improvement coefficient  $c_{\text{SW}}$  in Eq. (3.52) has a perturbative expansion

$$c_{\text{SW}} = c_{\text{SW}}^{(0)} + g_0^2 c_{\text{SW}}^{(1)} + \mathcal{O}(g_0^4) \quad (4.72)$$

in powers of the bare coupling  $g_0^2$ . It can be calculated via the quark-quark-gluon-vertex function

$$\Lambda_\mu^a(p, q) = \sum_{L=0}^{\infty} g_0^{2L+1} \Lambda_\mu^{a(L)}(p, q), \quad (4.73)$$

where the number of loops  $L$  matches the enumeration of the expansion coefficients  $c_{\text{SW}}^{(L)}$ .

## Tree Level

We present the following derivation for a general Wilson-like fermion action parametrised through the  $\lambda_i$  and  $\rho_i$  from Eqn. 3.42 which includes Brillouin and Wilson fermions.

At the tree level the vertex (4.73) is given by the lattice version of the  $q\bar{q}g$ -vertex (5.13), which we expand to first order in  $a$

$$\begin{aligned}\Lambda_\mu^{a(0)}(p, q) &= V_{1\mu}^a(ap, aq) = -g_0 T^a \left( i\gamma_\mu (2\rho_1 + 12\rho_2 + 24\rho_3 + 16\rho_4) \right. \\ &\quad + a \left[ \frac{r}{2}(p_\mu + q_\mu)(\lambda_1 + 6\lambda_2 + 12\lambda_3 + 8\lambda_4) + \frac{i}{2}c_{\text{SW}}^{(0)} \sum_\nu \sigma_{\mu\nu}(p_\nu - q_\nu) \right] \\ &\quad \left. + \mathcal{O}(a^2) \right). \end{aligned}\quad (4.74)$$

Sandwiching it with on-shell spinors  $u$  and  $\bar{u}$  one finds

$$\bar{u}(q)\Lambda_\mu^{a(0)}(p, q)u(p) = -g_0 T^a \bar{u}(q) \left( i\gamma_\mu (2\rho_1 + 12\rho_2 + 24\rho_3 + 16\rho_4) \right. \quad (4.75)$$

$$\begin{aligned}&\quad + \frac{a}{2} \left[ r(\lambda_1 + 6\lambda_2 + 12\lambda_3 + 8\lambda_4) - c_{\text{SW}}^{(0)} \right] (p_\mu + q_\mu) \Big) u(p) \\ &\quad + \mathcal{O}(a^2), \end{aligned}\quad (4.76)$$

and hence the condition  $c_{\text{SW}}^{(0)} = r(\lambda_1 + 6\lambda_2 + 12\lambda_3 + 8\lambda_4)$  to eliminate  $\mathcal{O}(a)$  contributions. From Eqs. (3.48) and (3.50) we see that both actions fulfil  $(\lambda_1 + 6\lambda_2 + 12\lambda_3 + 8\lambda_4) = 1$  as they must in order to have a correct continuum limit. Thus, the tree-level improvement coefficient is equal<sup>2</sup> to the Wilson parameter  $r$  for both Wilson and Brillouin fermions.

## One-Loop Level

At the one-loop level the general form of the vertex function is

$$g_0^3 \Lambda_\mu^{a(1)} = -g_0^3 T^a \left( \gamma_\mu F_1 + a\cancel{q}\gamma_\mu F_2 + a\gamma_\mu \cancel{p}F_3 + a(p_\mu + q_\mu)G_1 + a(p_\mu - q_\mu)H_1 \right), \quad (4.77)$$

where the  $F_2$  and  $F_3$  terms do not contribute to on-shell quantities, and  $H_1$  vanishes due to symmetry arguments [63]. Sandwiching this equation with on-shell spinors thus gives

$$\begin{aligned}g_0^3 \bar{u}(q) &\left( \frac{a}{2}c_{\text{SW}}^{(1)}(p_\mu + q_\mu)T^a + \Lambda_\mu^{a(1)}(p, q) \right) u(p) \\ &= g_0^3 \bar{u}(q) \left( i\gamma_\mu F_1 + \frac{a}{2}(p_\mu + q_\mu)(c_{\text{SW}}^{(1)} - 2G_1)T^a + \mathcal{O}(a^2) \right) u(p). \end{aligned}\quad (4.78)$$

This results in the condition

$$c_{\text{SW}}^{(1)} = 2G_1. \quad (4.79)$$

---

<sup>2</sup>Some authors write  $rc_{\text{SW}}$  instead of  $c_{\text{SW}}$  in Eq. (3.52), such that  $c_{\text{SW}}^{(0)}$  always equals one. However, the one-loop value  $c_{\text{SW}}^{(1)}$  does not naturally factorise in this way, and has a complicated, non-polynomial  $r$ -dependence.

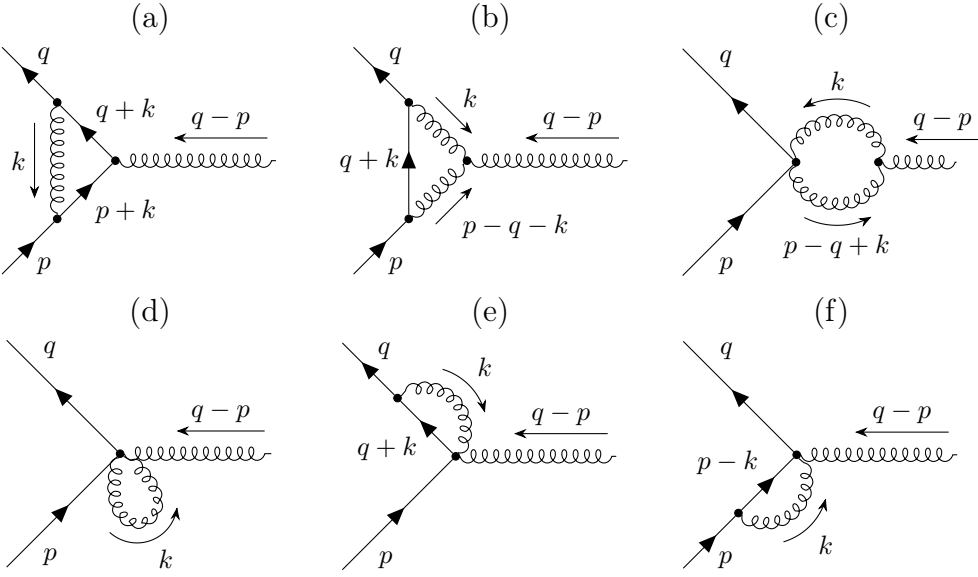


**Figure 4.4:** The six one-loop diagrams contributing to the vertex function.

We use the following equation (given in Ref. [63]) to extract  $G_1$  from the vertex function

$$g_0^3 T^a G_1 = -\frac{1}{8} \text{Tr} \left[ \left( \frac{\partial}{\partial p_\mu} + \frac{\partial}{\partial q_\mu} \right) \Lambda_\mu^{a(1)} - \left( \frac{\partial}{\partial p_\nu} - \frac{\partial}{\partial q_\nu} \right) \Lambda_\mu^{a(1)} \gamma_\nu \gamma_\mu \right]_{p,q \rightarrow 0}^{\mu \neq \nu}. \quad (4.80)$$

The six diagrams that contribute at the one-loop level are shown in Figure 4.4. We use Mathematica notebooks that take the previously generated Feynman rules as input and construct from them the relevant integrals corresponding to the six diagrams. Next, Eq. (4.80) gets applied to each integral, and the resulting expressions are added and numerically integrated over the four-dimensional Brillouin zone. For individual diagrams, the integrals (with one exception) are divergent and need to be regularized, which is explained below.

## Regularization

The sum of all diagrams is finite and can be numerically integrated without further ado (“all in one approach”). As a check and to compare results with other calculations, it is very helpful to calculate the contribution from each diagram separately. Five of the six diagrams are logarithmically IR-divergent. Therefore, we need to regularize these integrals and extract the divergent part before we can evaluate them numerically. To this end we subtract from each divergent lattice integral the simplest logarithmically divergent lattice integral  $\mathcal{B}_2$  (see Eqns. (4.68) and (4.69)) multiplied with an appropriate pre-factor.

These pre-factors can be determined by taking the limit  $a \rightarrow 0$  in the divergent integral, which leaves a simple continuum-like integral. From it the pre-factor can be read off (see box with sample calculation below).

**Example calculation of diagram (c)** *The integral corresponding to diagram (c) is*

$$\Lambda_{\mu}^{a(1)(c)} = 6 \int_{-\pi}^{\pi} \frac{d^4 k}{(2\pi)^4} \sum_{\nu, \rho, \sigma, \tau} \sum_{b,c} V_{2\nu\rho}^{b,c}(p, q, k, q - p - k) G_{\nu\sigma}(k) G_{\rho\tau}(p - q + k) \\ \times V_{3g\mu\sigma\tau}^{abc}(q - p, -k, p - q + k). \quad (4.81)$$

The pre-factor  $6 = 2 \cdot 3$  is due to the possible permutations of the internal gluon lines. The simplest form of this integral is the case of the Wilson fermion action and the plaquette gluon action. In order to compute  $G_1^{(c)}$  by Eq. (4.80), we need the derivatives

$$\frac{\partial}{\partial p_{\nu}} \Lambda_{\mu}^{a(1)(c)} \Big|_{p,q=0}^{\mu \neq \nu} = g_0^3 N_c T^a \int_{-\pi}^{\pi} \frac{d^4 k}{(2\pi)^4} \left\{ \frac{-3\bar{s}(k_{\mu})\bar{s}(k_{\nu}) + is^2(k)\bar{s}(k_{\mu})\gamma_{\nu}}{64(s^2(k))^3} \right. \\ \left. - ic_{\text{SW}}^{(0)} \cdot \frac{3c(k_{\mu})^2\bar{c}(k_{\nu})\sigma_{\mu\nu} + \bar{s}(k_{\mu})\sum_{\rho}\sigma_{\nu\rho}\bar{s}(k_{\rho})}{64(s^2(k))^2} \right\} \quad (4.82)$$

$$\frac{\partial}{\partial q_{\nu}} \Lambda_{\mu}^{a(1)(c)} \Big|_{p,q=0}^{\mu \neq \nu} = g_0^3 N_c T^a \int_{-\pi}^{\pi} \frac{d^4 k}{(2\pi)^4} \left\{ \frac{3\bar{s}(k_{\mu})\bar{s}(k_{\nu}) + is^2(k)\bar{s}(k_{\mu})\gamma_{\nu}}{64(s^2(k))^3} \right. \\ \left. + ic_{\text{SW}}^{(0)} \cdot \frac{3c(k_{\mu})^2\bar{c}(k_{\nu})\sigma_{\mu\nu} + \bar{s}(k_{\mu})\sum_{\rho}\sigma_{\nu\rho}\bar{s}(k_{\rho})}{64(s^2(k))^2} \right\} \quad (4.83)$$

$$\frac{\partial}{\partial p_{\mu}} \Lambda_{\mu}^{a(1)(c)} \Big|_{p,q=0} = g_0^3 N_c T^a \int_{-\pi}^{\pi} \frac{d^4 k}{(2\pi)^4} \left\{ \frac{3\bar{s}(k_{\mu})^2 - 3\bar{c}(k_{\mu})s^2}{64(s^2(k))^3} \right. \\ \left. - ic_{\text{SW}}^{(0)} \frac{\bar{s}(k_{\mu})\sum_{\rho}\sigma_{\mu\rho}\bar{s}(k_{\rho})}{64(s^2(k))^2} \right\} \quad (4.84)$$

$$\frac{\partial}{\partial q_{\mu}} \Lambda_{\mu}^{a(1)(c)} \Big|_{p,q=0} = - \frac{\partial}{\partial p_{\mu}} \Lambda_{\mu}^{a(1)(c)} \Big|_{p,q=0}. \quad (4.85)$$

Here we may use that under the integral only even functions will survive, therefore terms of the form  $s(k_{\mu})s(k_{\nu})$  and  $\bar{s}(k_{\mu})\bar{s}(k_{\nu})$  with  $\mu \neq \nu$  do not contribute. This yields

$$g_0^3 T^a G_1^{(c)} = -\frac{1}{8} \text{Tr} \left[ - \left( \frac{\partial}{\partial p_{\nu}} - \frac{\partial}{\partial q_{\nu}} \right) \Lambda_{\mu}^{a(1)} \gamma_{\nu} \gamma_{\mu} \right]_{p,q \rightarrow 0}^{\mu \neq \nu} \quad (4.86)$$

$$= -\frac{1}{8} g_0^3 N_c T^a \int_{-\pi}^{\pi} \frac{d^4 k}{(2\pi)^4} \text{Tr} \left[ \left( \frac{3\bar{s}(k_{\mu})\bar{s}(k_{\nu})}{32(s^2(k))^3} \right. \right. \\ \left. \left. + ic_{\text{SW}}^{(0)} \frac{(3c(k_{\mu})^2\bar{c}(k_{\nu}) - \bar{s}(k_{\mu})^2)\sigma_{\mu\nu}}{32(s^2(k))^2} \right) \gamma_{\nu} \gamma_{\mu} \right] \quad (4.87)$$

$$= g_0^3 N_c c_{\text{SW}}^{(0)} T^a \int_{-\pi}^{\pi} \frac{d^4 k}{(2\pi)^4} \frac{3c(k_{\mu})^2\bar{c}(k_{\nu}) - \bar{s}(k_{\mu})^2}{64(s^2(k))^2}; \quad (4.88)$$

This integral is divergent and cannot be directly calculated numerically. In order to regularize it we subtract the simple lattice integral  $\mathcal{B}_2$

$$\int_{-\pi}^{\pi} \frac{d^4 k}{(2\pi)^4} \left( \frac{3c(k_\mu)^2 \bar{c}(k_\nu) - \bar{s}(k_\mu)^2}{64(s^2(k))^2} - c \cdot \frac{1}{(4s^2(k))^2} \right) = \text{finite} \quad (4.89)$$

where all we need to know is the appropriate coefficient  $c$ . We can determine it easily by restoring factors of the lattice spacing  $k \rightarrow ak$ , expanding the first term to lowest order in  $a$

$$\int_{-\pi}^{\pi} \frac{d^4 k}{(2\pi)^4} \frac{3}{4} \frac{1}{(k_1^2 + k_2^2 + k_3^2 + k_4^2)^2} + \mathcal{O}(a^2) \quad (4.90)$$

and reading off  $c = 3/4$ . Thus, the contribution to  $c_{\text{SW}}^{(1)}$  coming from diagram (c) is

$$c_{\text{SW}}^{(1)(c)} = 2G_1^{(c)} = c_{\text{SW}}^{(0)} N_c \left( \frac{3}{2} \mathcal{B}_2(\mu) - 0.041375026(1) \right) \quad (4.91)$$

$$= \frac{9}{2} \mathcal{B}_2(\mu) - 0.124125079(1), \quad (4.92)$$

where we have set  $c_{\text{SW}}^{(0)} = r = 1$  and  $N_c = 3$  in the last step.

Because in the sum of all diagrams the divergencies cancel, we can add arbitrary constants to  $\mathcal{B}_2$ . Thus, the results we give in Section A.1 for the individual diagrams depend on our choice of regularizing integral and care must be taken when comparing to results obtained with other methods.

**Comparing our results to those in Ref. [63]** We like to compare our results to those by Aoki and Kuramashi in Ref. [63], who calculated  $c_{\text{SW}}^{(1)}$  for the Wilson action and for various improved gauge actions. They used a slightly different method of regularization and encoded the divergence in

$$L = \frac{1}{16\pi^2} \ln \left( \frac{\pi^2}{\mu^2} \right). \quad (4.93)$$

In essence they used the following two divergent continuum-like integrals

$$\mathcal{L}_1 = \int_{-\pi}^{\pi} \frac{d^4 k}{(2\pi)^4} \frac{1}{k^2(k^2 + \mu^2)} = L + \mathcal{O}(\mu^2) \quad (4.94)$$

$$\mathcal{L}_2 = \int_{-\pi}^{\pi} \frac{d^4 k}{(2\pi)^4} \frac{1}{(k^2 + \mu^2)^2} = L - \frac{1}{16\pi^2} + \mathcal{O}(\mu^2) \quad (4.95)$$

coming from the expansion of the lattice Feynman rules to  $\mathcal{O}(a)$ . The integral  $\mathcal{L}_1$  appears in diagrams (a),(e) and (f), whereas  $\mathcal{L}_2$  appears in diagrams (b) and (c).

Hence, the relations

$$\mathcal{L}_1 = \mathcal{B}_2(\mu) + \frac{1}{16\pi^2} (\ln(\pi^2) - F_0 + \gamma_E) \quad (4.96)$$

$$\mathcal{L}_2 = \mathcal{B}_2(\mu) + \frac{1}{16\pi^2} (\ln(\pi^2) - F_0 + \gamma_E - 1) \quad (4.97)$$

will convert our results to those in the formalism of Ref. [63] (see Table 5.4 and Table 5.5 below).

# 5 Perturbation Theory of Brillouin Fermions

In this section, we present the Feynman rules for the Brillouin fermion action and use them to calculate the self-energy  $\Sigma_0$  and one-loop improvement coefficient  $c_{\text{SW}}$ . These results have been published in [9, 96].

Due to the large number of points involved in the Brillouin action, the expressions for the quark-gluon vertices become very large. We have defined functions (5.5)-(5.12) to describe reoccurring patterns of trigonometric functions, but still the expressions are quite lengthy. This also leads the relatively long run-times of the analytical and numerical calculations performed by *Mathematica*.

In Sections 9 and A.1 we give a short comparison of  $\Sigma_0$  and  $c_{\text{SW}}^{(1)}$  between Wilson and Brillouin fermions. More results including both actions and stout smearing/Wilson flow are presented in Chapters 7 and 8.

## 5.1 Feynman Rules

We start by calculating the propagator of the Brillouin fermion

$$S_B(k) = \left( \sum_\mu \gamma_\mu \nabla_\mu^{\text{iso}}(k) - \frac{r}{2} \Delta^{\text{bri}}(k) \right)^{-1} = \frac{-\sum_\mu \gamma_\mu \nabla_\mu^{\text{iso}}(k) - \frac{r}{2} \Delta^{\text{bri}}(k)}{\frac{r^2}{4} \Delta^{\text{bri}}(k)^2 - \left( \sum_\mu \nabla_\mu^{\text{iso}}(k)^2 \right)} \quad (5.1)$$

with the Fourier transforms of the “free” derivative  $\nabla_\mu^{\text{iso}}$  and Laplace operator  $\Delta^{\text{bri}}$

$$\nabla_\mu^{\text{iso}}(k) = \frac{i}{27} \bar{s}(k_\mu) \prod_{\nu \neq \mu} (\bar{c}(k_\nu) + 2) \quad (5.2)$$

$$\Delta^{\text{bri}}(k) = 4 \left( c(k_1)^2 c(k_2)^2 c(k_3)^2 c(k_4)^2 - 1 \right). \quad (5.3)$$

The propagator then takes the form

$$S_B(k) = \frac{-\frac{i}{27} \sum_\mu (\gamma_\mu \bar{s}(k_\mu) \prod_{\nu \neq \mu} (\bar{c}(k_\nu) + 2)) - 2r(c(k_1)^2 c(k_2)^2 c(k_3)^2 c(k_4)^2 - 1)}{4r^2(c(k_1)^2 c(k_2)^2 c(k_3)^2 c(k_4)^2 - 1)^2 + \frac{1}{729} \sum_\mu (\bar{s}(k_\mu)^2 \prod_{\nu \neq \mu} (\bar{c}(k_\nu) + 2)^2)}. \quad (5.4)$$

The following combinations of sine and cosine functions are very convenient to shorten the lengthy expressions for the vertices

$$K_{\mu\nu}^{(fg)}(p, q) = f(p_\mu + q_\mu) [\bar{g}(p_\nu) + \bar{g}(q_\nu)] \quad (5.5)$$

$$K_{\mu\nu\rho}^{(fgh)}(p, q) = f(p_\mu + q_\mu) \left\{ \bar{g}(p_\nu) \bar{h}(p_\rho) + \bar{g}(q_\nu) \bar{h}(q_\rho) + [\bar{g}(p_\nu) + \bar{g}(q_\nu)] [\bar{h}(p_\rho) + \bar{h}(q_\rho)] \right\} \quad (5.6)$$

$$K_{\mu\nu\rho\sigma}^{(fghj)}(p, q) = f(p_\mu + q_\mu) \left\{ 2[\bar{g}(p_\nu) \bar{h}(p_\rho) \bar{j}(p_\sigma) + \bar{g}(q_\nu) \bar{h}(q_\rho) \bar{j}(q_\sigma)] + [\bar{g}(p_\nu) + \bar{g}(q_\nu)] [\bar{h}(p_\rho) + \bar{h}(q_\rho)] [\bar{j}(p_\sigma) + \bar{j}(q_\sigma)] \right\} \quad (5.7)$$

$$L_{\mu\nu}^{(fg)}(p, q, k) = f(p_\mu + q_\mu + k_\mu)g(2p_\nu + k_\nu) \quad (5.8)$$

$$L_{\mu\nu\rho}^{(fgh)}(p, q, k) = f(p_\mu + q_\mu + k_\mu)g(2p_\nu + k_\nu)[\bar{h}(p_\rho) + \bar{h}(p_\rho + k_\rho) + \bar{h}(q_\rho)] \quad (5.9)$$

$$\begin{aligned} L_{\mu\nu\rho\sigma}^{(fghj)}(p, q, k) &= f(p_\mu + q_\mu + k_\mu)g(2p_\nu + k_\nu) \\ &\times \left\{ \bar{h}(p_\rho)\bar{j}(p_\sigma) + \bar{h}(p_\rho + k_\rho)\bar{j}(p_\sigma + k_\sigma) + \bar{h}(q_\rho)\bar{j}(q_\sigma) \right. \\ &\left. + [\bar{h}(p_\rho) + \bar{h}(p_\rho + k_\rho) + \bar{h}(q_\rho)][\bar{j}(p_\sigma) + \bar{j}(p_\sigma + k_\sigma) + \bar{j}(q_\sigma)] \right\} \end{aligned} \quad (5.10)$$

$$M_{\mu\nu\rho}^{(fgh)}(p, q, k_1, k_2) = f(p_\mu + q_\mu + k_{1\mu} + k_{2\mu})g(2p_\nu + k_{1\nu} + 2k_{2\nu})h(2p_\rho + k_{2\rho}) \quad (5.11)$$

$$\begin{aligned} M_{\mu\nu\rho\sigma}^{(fghj)}(p, q, k_1, k_2) &= f(p_\mu + q_\mu + k_{1\mu} + k_{2\mu})g(2p_\nu + k_{1\nu} + 2k_{2\nu})h(2p_\rho + k_{2\rho}) \\ &\times \left\{ \bar{j}(p_\sigma) + \bar{j}(p_\sigma + k_{2\sigma}) + \bar{j}(p_\sigma + k_{1\sigma} + k_{2\sigma}) + \bar{j}(q_\sigma) \right\} \end{aligned} \quad (5.12)$$

with  $f, g, h, j \in \{s, c\}$  and the abbreviations  $s$ ,  $\bar{s}$ ,  $c$ , and  $\bar{c}$  given in (4.26)-(4.28).

With this the  $\bar{q}qg$ -vertex is given by:

$$\begin{aligned} V_{1B\mu}^a(p, q) &= -g_0 T^a \left[ r\lambda_1 s(p_\mu + q_\mu) + 2i\rho_1 c(p_\mu + q_\mu)\gamma_\mu \right. \\ &+ \sum_{\substack{\nu=1 \\ \nu \neq \mu}}^4 \left\{ r\lambda_2 K_{\mu\nu}^{(sc)}(p, q) + 2i\rho_2 (K_{\mu\nu}^{(cc)}(p, q)\gamma_\mu - K_{\mu\nu}^{(ss)}(p, q)\gamma_\nu) \right\} \\ &+ \frac{1}{3} \sum_{\substack{\nu, \rho=1 \\ \neq (\nu, \rho; \mu)}}^4 \left\{ r\lambda_3 K_{\mu\nu\rho}^{(scc)}(p, q) + 2i\rho_3 (K_{\mu\nu\rho}^{(ccc)}(p, q)\gamma_\mu - 2K_{\mu\nu\rho}^{(ssc)}(p, q)\gamma_\nu) \right\} \\ &\left. + \frac{1}{9} \sum_{\substack{\nu, \rho, \sigma=1 \\ \neq (\nu, \rho, \sigma; \mu)}}^4 \left\{ r\lambda_4 K_{\mu\nu\rho\sigma}^{(sccc)}(p, q) + 2i\rho_4 (K_{\mu\nu\rho\sigma}^{(cccc)}(p, q)\gamma_\mu - 3K_{\mu\nu\rho\sigma}^{(sscc)}(p, q)\gamma_\nu) \right\} \right] \end{aligned} \quad (5.13)$$

**Sample calculation of  $V_{1B\mu}^a(p, q)$ .** As a short example we show in some detail how to derive the part of the  $\bar{q}qg$ -vertex  $V_{1\mu}^a(p, q)$  proportional to  $\lambda_2$  and  $\rho_2$ , i.e. we start with the following term of the Brillouin action

$$\sum_{x,y} \bar{\psi}(x) \left( \sum_{\substack{\mu, \nu = \pm 1 \\ |\mu| \neq |\nu|}}^{\pm 4} \left( \rho_2 \gamma_\mu - r \frac{\lambda_2}{4} \right) W_{\mu\nu}(x) \delta(x + \hat{\mu} + \hat{\nu}, y) \right) \psi(y). \quad (5.14)$$

First we rewrite the sum, such that it is over positive indices only

$$\begin{aligned} \sum_{x,y} \sum_{\substack{\mu, \nu = 1 \\ \mu \neq \nu}}^4 \bar{\psi}(x) &\left[ \left( \rho_2 \gamma_\mu - r \frac{\lambda_2}{4} \right) \right. \\ &\times \left. \left( W_{\mu\nu}(x) \delta(x + \hat{\mu} + \hat{\nu}, y) + W_{\mu-\nu}(x) \delta(x + \hat{\mu} - \hat{\nu}, y) \right) \right] \end{aligned}$$

$$\left. + \left( -\rho_2 \gamma_\mu - r \frac{\lambda_2}{4} \right) \times \left( W_{-\mu\nu}(x) \delta(x - \hat{\mu} + \hat{\nu}, y) + W_{-\mu-\nu}(x) \delta(x - \hat{\mu} - \hat{\nu}, y) \right) \right] \psi(y) \quad (5.15)$$

where  $\gamma_{-\mu} = -\gamma_\mu$  has been used. We insert

$$W_{\mu\nu}(x) = \frac{1}{2} (U_\mu(x) U_\nu(x + \hat{\mu}) + U_\nu(x) U_\mu(x + \hat{\nu})) \quad (5.16)$$

expanded to order  $g_0$ , hence we replace

$$W_{\mu\nu}(x) \rightarrow i g_0 T^a \frac{1}{2} (A_\mu^a(x) + A_\nu^a(x + \hat{\mu}) + A_\nu^a(x) + A_\mu^a(x + \hat{\nu})) \quad (5.17)$$

$$W_{\mu-\nu}(x) \rightarrow i g_0 T^a \frac{1}{2} (A_\mu^a(x) - A_\nu^a(x + \hat{\mu} - \hat{\nu}) - A_\nu^a(x - \hat{\nu}) + A_\mu^a(x - \hat{\nu})) \quad (5.18)$$

$$W_{-\mu\nu}(x) \rightarrow i g_0 T^a \frac{1}{2} (-A_\mu^a(x - \hat{\mu}) + A_\nu^a(x - \hat{\mu}) + A_\nu^a(x) - A_\mu^a(x - \hat{\mu} + \hat{\nu})) \quad (5.19)$$

$$\begin{aligned} W_{-\mu-\nu}(x) \rightarrow i g_0 T^a \frac{1}{2} & (-A_\mu^a(x - \hat{\mu}) - A_\nu^a(x - \hat{\mu} - \hat{\nu}) - A_\nu^a(x - \hat{\nu}) \\ & - A_\mu^a(x - \hat{\mu} - \hat{\nu})) \end{aligned} \quad (5.20)$$

where we have used

$$U_{-\mu}(x) = U_\mu^\dagger(x - \hat{\mu}) = 1 - i g_0 T^a A_\mu^a(x - \hat{\mu}) + \mathcal{O}(g_0^2). \quad (5.21)$$

Next we insert the Fourier transforms of  $\bar{\psi}$ ,  $\psi$ ,  $A$  and  $\delta$ . One example term reads

$$\begin{aligned} & \sum_{x,y} \sum_{\substack{\mu,\nu=1 \\ \mu \neq \nu}}^4 \bar{\psi}(x) \left( \rho_2 \gamma_\mu - r \frac{\lambda_2}{4} \right) A_\mu^a(x) \delta(x + \hat{\mu} + \hat{\nu}, y) \psi(y) \\ &= \sum_{x,y} \sum_{\substack{\mu,\nu=1 \\ \mu \neq \nu}}^4 \int_{-\pi}^{\pi} \frac{d^4 q}{(2\pi)^4} \int_{-\pi}^{\pi} \frac{d^4 k}{(2\pi)^4} \int_{-\pi}^{\pi} \frac{d^4 r}{(2\pi)^4} \int_{-\pi}^{\pi} \frac{d^4 p}{(2\pi)^4} \end{aligned} \quad (5.22)$$

$$\times e^{-ixq} \bar{\psi}(q) \left( \rho_2 \gamma_\mu - r \frac{\lambda_2}{4} \right) e^{i(x+\hat{\mu}/2)k} A_\mu^a(k) e^{i(x+\hat{\mu}+\hat{\nu}-y)r} e^{ipy} \psi(p). \quad (5.23)$$

The sum over  $y$  introduces  $(2\pi)^4 \delta(r - p)$ , which lets us perform the  $r$ -integral. Then the sum over  $x$  introduces  $(2\pi)^4 \delta(q - p - k)$ , which enforces momentum conservation at the vertex and allows us to perform the  $k$ -integral. As a result we are left with

$$\sum_{\substack{\mu,\nu=1 \\ \mu \neq \nu}}^4 \int_{-\pi}^{\pi} \frac{d^4 q}{(2\pi)^4} \int_{-\pi}^{\pi} \frac{d^4 p}{(2\pi)^4} \bar{\psi}(q) \left( \rho_2 \gamma_\mu - r \frac{\lambda_2}{4} \right) \psi(p) A_\mu^a(q - p) e^{\frac{i}{2}(q_\mu + p_\mu)} e^{ip_\nu}. \quad (5.24)$$

Together with the term  $-\left(-\rho_2\gamma_\mu - r\frac{\lambda_2}{4}\right)A_\mu^a(x - \hat{\mu})\delta(x - \hat{\mu} - \hat{\nu}, y)$  this yields the contribution

$$\rho_2\gamma_\mu \cos\left(\frac{1}{2}(p_\mu + q_\mu) + p_\nu\right) - \frac{r\lambda_2}{4} \sin\left(\frac{1}{2}(p_\mu + q_\mu) + p_\nu\right) \quad (5.25)$$

to the  $q\bar{q}g$  vertex. Adding all the other terms and some more trigonometric manipulations will finally result in what is shown in Eq. (5.13).

The procedure for the  $q\bar{q}gg$ - and  $q\bar{q}ggg$ -vertices is basically the same. After Fourier transforming the fields, we integrate out the gluon momentum  $k_1$  and find ourselves left with expressions containing  $p, q, k_2$  and  $p, q, k_2, k_3$  respectively. At this point some diligence is needed to rename the indices in terms containing for example  $A_\nu^a(k_1)A_\mu^b(k_2)$  or  $A_\rho^a(k_1)A_\nu^b(k_2)A_\mu^c(k_3)$  such that everything is proportional to  $A_\mu^a(k_1)A_\nu^b(k_2)$  and  $A_\mu^a(k_1)A_\nu^b(k_2)A_\rho^c(k_3)$ , respectively.

The  $q\bar{q}gg$  vertex for the Brillouin action takes the form

$$\begin{aligned} V_{2B\,\mu\nu}^{ab}(p, q, k_1, k_2) = & ag_0^2 T^a T^b \left\{ -\frac{1}{2}r\lambda_1\delta_{\mu\nu}c(p_\mu + q_\mu) + i\rho_1\delta_{\mu\nu}s(p_\mu + q_\mu)\gamma_\mu \right. \\ & + r\lambda_2 \left( (1 - \delta_{\mu\nu})L_{\mu\nu}^{(ss)}(p, q, k_2) - \frac{1}{2}\delta_{\mu\nu} \sum_{\substack{\alpha=1 \\ \alpha \neq \mu}}^4 K_{\mu\alpha}^{(cc)}(p, q) \right) \\ & + r\lambda_3 \left( \frac{2}{3}(1 - \delta_{\mu\nu}) \sum_{\substack{\rho=1 \\ \neq (\rho, \mu, \nu)}}^4 L_{\mu\nu\rho}^{(ssc)}(p, q, k_2) - \frac{1}{6}\delta_{\mu\nu} \sum_{\substack{\alpha, \rho=1 \\ \neq (\alpha, \rho, \mu)}}^4 K_{\mu\alpha\rho}^{(ccc)}(p, q) \right) \\ & + r\lambda_4 \left( \frac{1}{6}(1 - \delta_{\mu\nu}) \sum_{\substack{\rho, \sigma=1 \\ \neq (\rho, \sigma, \mu, \nu)}}^4 L_{\mu\nu\rho\sigma}^{(sscc)}(p, q, k_2) - \frac{1}{18}\delta_{\mu\nu} \sum_{\substack{\alpha, \rho, \sigma=1 \\ \neq (\alpha, \rho, \sigma, \mu)}}^4 K_{\mu\alpha\rho\sigma}^{(cccc)}(p, q) \right) \\ & + i\rho_2 \left( 2(1 - \delta_{\mu\nu}) \left[ L_{\mu\nu}^{(cs)}(p, q, k_2)\gamma_\mu + L_{\mu\nu}^{(sc)}(p, q, k_2)\gamma_\nu \right] \right. \\ & \left. + \delta_{\mu\nu} \sum_{\substack{\alpha=1 \\ \alpha \neq \mu}}^4 \left[ K_{\mu\alpha}^{(sc)}(p, q)\gamma_\mu + K_{\mu\alpha}^{(cs)}(p, q)\gamma_\nu \right] \right) \\ & + i\rho_3 \left( \frac{4}{3}(1 - \delta_{\mu\nu}) \sum_{\substack{\rho=1 \\ \neq (\rho; \mu, \nu)}}^4 \left[ L_{\mu\nu\rho}^{(csc)}(p, q, k_2)\gamma_\mu + L_{\mu\nu\rho}^{(sc)}(p, q, k_2)\gamma_\nu - L_{\mu\nu\rho}^{(sss)}(p, q, k_2)\gamma_\rho \right] \right. \\ & \left. + \frac{1}{3}\delta_{\mu\nu} \sum_{\substack{\alpha, \rho=1 \\ \neq (\alpha, \rho; \mu)}}^4 \left[ K_{\mu\alpha\rho}^{(scc)}(p, q)\gamma_\mu + 2K_{\mu\alpha\rho}^{(ccs)}(p, q)\gamma_\rho \right] \right) \\ & + i\rho_4 \left( \frac{1}{3}(1 - \delta_{\mu\nu}) \sum_{\substack{\rho, \sigma=1 \\ \neq (\rho, \sigma, \mu, \nu)}}^4 \left[ L_{\mu\nu\rho\sigma}^{(cscc)}(p, q, k_2)\gamma_\mu + L_{\mu\nu\rho\sigma}^{(sccc)}(p, q, k_2)\gamma_\nu - 2L_{\mu\nu\rho\sigma}^{(sssc)}(p, q, k_2)\gamma_\rho \right] \right) \end{aligned}$$

$$+ \frac{1}{9} \delta_{\mu\nu} \sum_{\substack{\alpha,\rho,\sigma=1 \\ \neq(\alpha,\rho,\sigma,\mu)}}^4 \left[ K_{\mu\alpha\rho\sigma}^{(scce)}(p,q) \gamma_\mu + 3K_{\mu\alpha\rho\sigma}^{(ccsc)}(p,q) \gamma_\rho \right] \right\} . \quad (5.26)$$

And finally, the  $q\bar{q}ggg$  vertex for the Brillouin action takes the form

$$\begin{aligned} V_{3B\mu\nu\rho}^{abc}(p,q,k_1,k_2,k_3) = & a^2 g_0^3 T^a T^b T^c \left\{ \frac{1}{6} \delta_{\mu\nu} \delta_{\mu\rho} (r\lambda_1 s(p_\mu + q_\mu) + 2i\rho_1 c(p_\mu + q_\mu) \gamma_\mu) \right. \\ & + r\lambda_2 \left( \frac{1}{2} (1 - \delta_{\mu\rho}) [\delta_{\mu\nu} L_{\mu\rho}^{(cs)}(p,q,k_3) + \delta_{\nu\rho} L_{\mu\rho}^{(sc)}(p,q,k_2+k_3)] + \frac{1}{6} \delta_{\mu\nu} \delta_{\mu\rho} \sum_{\substack{\alpha=1 \\ \alpha \neq \mu}}^4 K_{\mu\alpha}^{(sc)}(p,q) \right) \\ & + r\lambda_3 \left( -\frac{2}{3} (1 - \delta_{\mu\nu})(1 - \delta_{\mu\rho})(1 - \delta_{\nu\rho}) M_{\mu\nu\rho}^{(sss)}(p,q,k_2,k_3) + \frac{1}{18} \delta_{\mu\nu} \delta_{\mu\rho} \sum_{\substack{\alpha,\beta=1 \\ \neq(\alpha,\beta,\mu)}}^4 K_{\mu\alpha\beta}^{(sc)}(p,q) \right. \\ & \left. + \frac{1}{3} (1 - \delta_{\mu\rho}) \sum_{\substack{\alpha=1 \\ \neq(\alpha,\mu,\rho)}}^4 [\delta_{\mu\nu} L_{\mu\rho\alpha}^{(csc)}(p,q,k_3) + \delta_{\nu\rho} L_{\mu\rho\alpha}^{(sc)}(p,q,k_2+k_3)] \right) \\ & + r\lambda_4 \left( -\frac{1}{3} (1 - \delta_{\mu\nu})(1 - \delta_{\mu\rho})(1 - \delta_{\nu\rho}) \sum_{\substack{\sigma=1 \\ \neq(\sigma,\mu,\nu,\rho)}}^4 M_{\mu\nu\rho\sigma}^{(sssc)}(p,q,k_2,k_3) \right. \\ & \left. + \frac{1}{12} (1 - \delta_{\mu\rho}) \sum_{\substack{\alpha,\sigma=1 \\ \neq(\alpha,\sigma;\mu,\rho)}}^4 [\delta_{\mu\nu} L_{\mu\rho\alpha\sigma}^{(cscc)}(p,q,k_3) + \delta_{\nu\rho} L_{\mu\rho\alpha\sigma}^{(scce)}(p,q,k_2+k_3)] \right. \\ & \left. + \frac{1}{54} \delta_{\mu\nu} \delta_{\mu\rho} \sum_{\substack{\alpha,\beta,\sigma=1 \\ \neq(\alpha,\beta,\sigma,\mu)}}^4 K_{\mu\alpha\beta\sigma}^{(scce)}(p,q) \right) \\ & + i\rho_2 \left( \frac{1}{3} \delta_{\mu\nu} \delta_{\mu\rho} \sum_{\substack{\alpha=1 \\ \alpha \neq \mu}}^4 [K_{\mu\alpha}^{(cc)}(p,q) \gamma_\mu - K_{\mu\alpha}^{(ss)}(p,q) \gamma_\alpha] \right. \\ & \left. + \delta_{\mu\nu} (1 - \delta_{\mu\rho}) [L_{\mu\rho}^{(cc)}(p,q,k_3) \gamma_\rho - L_{\mu\rho}^{(ss)}(p,q,k_3) \gamma_\mu] \right. \\ & \left. + \delta_{\nu\rho} (1 - \delta_{\mu\nu}) [L_{\mu\rho}^{(cc)}(p,q,k_2+k_3) \gamma_\mu - L_{\mu\rho}^{(ss)}(p,q,k_2+k_3) \gamma_\nu] \right) \\ & + i\rho_3 \left( -\frac{4}{3} (1 - \delta_{\mu\nu})(1 - \delta_{\mu\rho})(1 - \delta_{\nu\rho}) \right. \\ & \times \left[ M_{\mu\nu\rho}^{(css)}(p,q,k_2,k_3) \gamma_\mu + M_{\mu\nu\rho}^{(scs)}(p,q,k_2,k_3) \gamma_\nu + M_{\mu\nu\rho}^{(ssc)}(p,q,k_2,k_3) \gamma_\rho \right] \\ & \left. + \frac{1}{9} \delta_{\mu\nu} \delta_{\mu\rho} \sum_{\substack{\alpha,\beta=1 \\ \neq(\alpha,\beta,\mu)}}^4 [K_{\mu\alpha\beta}^{(ccc)}(p,q) \gamma_\mu - K_{\mu\alpha\beta}^{(ssc)}(p,q) \gamma_\alpha - K_{\mu\alpha\beta}^{(scs)}(p,q) \gamma_\beta] \right) \end{aligned}$$

$$\begin{aligned}
& -\frac{2}{3}\delta_{\mu\nu}(1-\delta_{\mu\rho}) \sum_{\substack{\alpha=1 \\ \neq(\alpha,\mu,\rho)}}^4 \left[ L_{\mu\rho\alpha}^{(ssc)}(p,q,k_3)\gamma_\mu - L_{\mu\rho\alpha}^{(ccc)}(p,q,k_3)\gamma_\rho \right. \\
& + L_{\mu\rho\alpha}^{(css)}(p,q,k_3)\gamma_\alpha \Big] - \frac{2}{3}\delta_{\nu\rho}(1-\delta_{\mu\nu}) \sum_{\substack{\alpha=1 \\ \neq(\alpha,\mu,\nu)}}^4 \left[ -L_{\mu\nu\alpha}^{(ccc)}(p,q,k_2+k_3)\gamma_\mu \right. \\
& \left. + L_{\mu\nu\alpha}^{(ssc)}(p,q,k_2+k_3)\gamma_\nu + L_{\mu\nu\alpha}^{(scs)}(p,q,k_2+k_3)\gamma_\alpha \right] \Big) \\
& + i\rho_4 \left( -\frac{2}{3}(1-\delta_{\mu\nu})(1-\delta_{\mu\rho})(1-\delta_{\nu\rho}) \sum_{\substack{\sigma=1 \\ \neq(\sigma,\mu,\nu,\rho)}}^4 \left[ M_{\mu\nu\rho\sigma}^{(cssc)}(p,q,k_2,k_3)\gamma_\mu \right. \right. \\
& + M_{\mu\nu\rho\sigma}^{(scsc)}(p,q,k_2,k_3)\gamma_\nu + M_{\mu\nu\rho\sigma}^{(sscc)}(p,q,k_2,k_3)\gamma_\rho - M_{\mu\nu\rho\sigma}^{(ssss)}(p,q,k_2,k_3)\gamma_\sigma \Big] \\
& + \frac{1}{27}\delta_{\mu\nu}\delta_{\mu\rho} \sum_{\substack{\alpha,\beta,\sigma=1 \\ \neq(\alpha,\beta,\sigma,\mu)}}^4 \left[ K_{\mu\alpha\beta\sigma}^{(cccc)}(p,q)\gamma_\mu - K_{\mu\alpha\beta\sigma}^{(sscc)}(p,q)\gamma_\alpha \right. \\
& \left. - K_{\mu\alpha\beta\sigma}^{(scsc)}(p,q)\gamma_\beta - K_{\mu\alpha\beta\sigma}^{(scs)}(p,q)\gamma_\sigma \right] \\
& - \frac{1}{6}\delta_{\mu\nu}(1-\delta_{\mu\rho}) \sum_{\substack{\alpha,\sigma=1 \\ \neq(\alpha,\sigma,\mu,\rho)}}^4 \left[ L_{\mu\rho\alpha\sigma}^{(ssc)}(p,q,k_3)\gamma_\mu - L_{\mu\rho\alpha\sigma}^{(cccc)}(p,q,k_3)\gamma_\rho \right. \\
& \left. + L_{\mu\rho\alpha\sigma}^{(cssc)}(p,q,k_3)\gamma_\alpha + L_{\mu\rho\alpha\sigma}^{(cscs)}(p,q,k_3)\gamma_\sigma \right] \\
& + \frac{1}{6}\delta_{\nu\rho}(1-\delta_{\mu\nu}) \sum_{\substack{\alpha,\sigma=1 \\ \neq(\alpha,\sigma,\mu,\nu)}}^4 \left[ L_{\mu\nu\alpha\sigma}^{(cccc)}(p,q,k_2+k_3)\gamma_\mu - L_{\mu\nu\alpha\sigma}^{(sscc)}(p,q,k_2+k_3)\gamma_\nu \right. \\
& \left. + L_{\mu\nu\alpha\sigma}^{(scsc)}(p,q,k_2+k_3)\gamma_\alpha + L_{\mu\nu\alpha\sigma}^{(scs)}(p,q,k_2+k_3)\gamma_\sigma \right] \Big) \Bigg\}. \tag{5.27}
\end{aligned}$$

## 5.2 Self-Energy of the Brillouin Clover Fermion

Here we give some one-loop results for the self energy  $\Sigma_0$  (as explained in Section A.3) of the Brillouin clover fermion using the Feynman rules from Sections 9 and 8.

Table 5.1 gives the values of  $\Sigma_0$  and the contributions from the two diagrams for all four combinations of fermion and gluon actions. Only the ‘‘sunset’’ diagram receives contributions from the clover term Feynman rules (linear and quadratic in  $c_{\text{SW}}$ ). We define

$$\Sigma_0^{(\text{sunset})} = \Sigma_0^{(0)(\text{sunset})} + c_{\text{SW}}\Sigma_0^{(1)(\text{sunset})} + c_{\text{SW}}^2\Sigma_0^{(2)(\text{sunset})}. \tag{5.28}$$

They are given in Table 5.2 for  $r = 1$  and  $N_c = 3$ . Figure 5.1 shows  $\Sigma_0$  plotted against eleven values of the Wilson parameter  $r$  between 0.5 and 1.5. Table 5.3 gives the same

Action	$\Sigma_0^{(\text{tadpole})}$	$\Sigma_0^{(\text{sunset})}$	$\Sigma_0$
Wilson/Plaq.	-48.9322(1)	16.9458(1)	-31.9864(1)
Brillouin/Plaq.	-48.9322(1)	17.7727(1)	-31.1595(1)
Wilson/Sym.	-40.5177(1)	16.6854(1)	-23.8323(1)
Brillouin/Sym.	-39.0998(1)	16.3742(1)	-22.7256(1)

**Table 5.1:** Contributions to the self energy  $\Sigma_0$  for  $c_{\text{SW}} = r = 1$  coming from the tadpole and sunset diagrams, along with the sum.

Action	$\Sigma_{00}^{(\text{sunset})}$	$\Sigma_{01}^{(\text{sunset})}$	$\Sigma_{02}^{(\text{sunset})}$
Wilson/Plaq.	-2.5025(1)	13.7331(1)	5.7151(1)
Brillouin/ Plaq.	-5.0086(1)	12.9489(1)	9.8325(1)
Wilson/ Sym.	0.0745(1)	11.9482(1)	4.6627(1)
Brillouin/ Sym.	-2.8534(1)	11.3450(1)	7.8826(1)

**Table 5.2:** Contributions to the self energy  $\Sigma_0^{(\text{sunset})}$  of the sunset diagram at different orders of  $c_{\text{SW}}$  (for  $r = 1$ ).

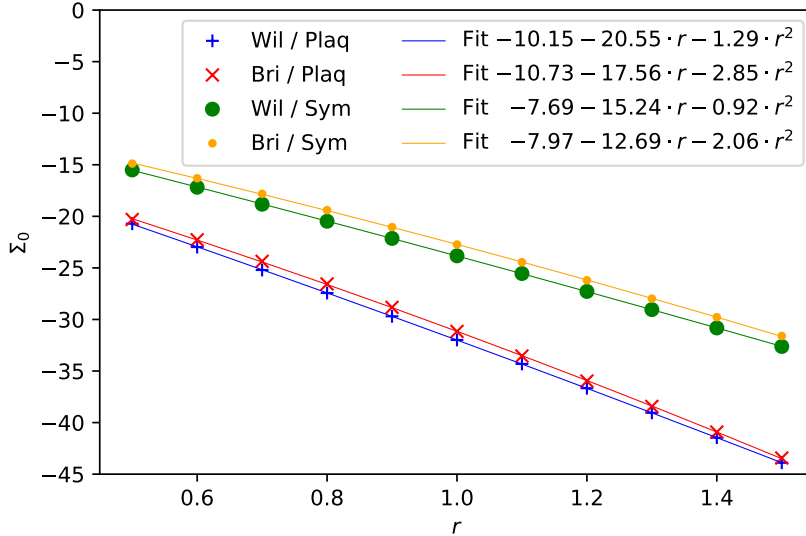


**Figure 5.1:** Self energy  $\Sigma_0$  of Wilson and Brillouin fermions as a function of  $r$ .

data including the split-up between the two diagrams. We see that for  $\Sigma_0$ , and thereby the additive mass shift, the difference between the Brillouin and Wilson fermion actions is very small compared to the impact the inclusion of the Symanzik improved gauge action has. This is largely due to the “tadpole” part being dominant. There is no difference in the plaquette case and only a minimal one in the “sym” case (see Tab. 5.1). Additionally, for the “sunset” diagram a larger difference between Wilson and Brillouin for  $c_{\text{SW}} = 0$  gets damped by the inclusion of the clover term (see Tab. 5.2).

	$\Sigma_0^{(\text{tadpole})}$		$\Sigma_0^{(\text{subset})}$		$\Sigma_0$	
$r$	Wil./Plaq.	Bri./Plaq.	Wil./Plaq.	Bri./Plaq.	Wil./Plaq.	Bri./Plaq.
0.5	-24.4661(1)	-24.4661(1)	3.7505(1)	4.1566(1)	-20.7156(1)	-20.3094(1)
0.6	-29.3593(1)	-29.3593(1)	6.3797(1)	7.0854(1)	-22.9797(1)	-22.2739(1)
0.7	-34.2525(1)	-34.2525(1)	9.0474(1)	9.8887(1)	-25.2052(1)	-24.3638(1)
0.8	-39.1458(1)	-39.1458(1)	11.7083(1)	12.5913(1)	-27.4375(1)	-26.5545(1)
0.9	-44.0390(1)	-44.0390(1)	14.3433(1)	15.2139(1)	-29.6956(1)	-28.8251(1)
1.0	-48.9322(1)	-48.9322(1)	16.9458(1)	17.7727(1)	-31.9864(1)	-31.1595(1)
1.1	-53.8254(1)	-53.8254(1)	19.5147(1)	20.2804(1)	-34.3108(1)	-33.5450(1)
1.2	-58.7186(1)	-58.7186(1)	22.0517(1)	22.7465(1)	-36.6669(1)	-35.9721(1)
1.3	-63.6119(1)	-63.6119(1)	24.5597(1)	25.1785(1)	-39.0522(1)	-38.4333(1)
1.4	-68.5051(1)	-68.5051(1)	27.0415(1)	27.5823(1)	-41.4636(1)	-40.9227(1)
1.5	-73.3983(1)	-73.3983(1)	29.5000(1)	29.9625(1)	-43.8983(1)	-43.4358(1)
$r$	Wil./Sym.	Bri./Sym.	Wil./Sym.	Bri./Sym.	Wil./Sym.	Bri./Sym.
0.5	-20.2588(1)	-19.5499(1)	4.7572(1)	4.6636(1)	-15.5016(1)	-14.8863(1)
0.6	-24.3106(1)	-23.4599(1)	7.1298(1)	7.1531(1)	-17.1808(1)	-16.3068(1)
0.7	-28.3624(1)	-27.3699(1)	9.5352(1)	9.5532(1)	-18.8272(1)	-17.817(1)
0.8	-32.4142(1)	-31.2799(1)	11.9382(1)	11.8810(1)	-20.4760(1)	-19.399(1)
0.9	-36.4659(1)	-35.1898(1)	14.3235(1)	14.151(1)	-22.1425(1)	-21.04(1)
1.0	-40.5178(1)	-39.0998(1)	16.6854(1)	16.374(1)	-23.8323(1)	-22.73(1)
1.1	-44.5695(1)	-43.0098(1)	19.0229(1)	18.560(1)	-25.5467(1)	-24.45(1)
1.2	-48.6213(1)	-46.9198(1)	21.3369(1)	20.716(1)	-27.2844(1)	-26.20(1)
1.3	-52.6731(1)	-50.8298(1)	23.6293(1)	22.846(1)	-29.0438(1)	-27.98(1)
1.4	-56.7248(1)	-54.7397(1)	25.9021(1)	24.956(1)	-30.8228(1)	-29.78(1)
1.5	-60.7766(1)	-58.6497(1)	28.1575(1)	27.048(1)	-32.6191(1)	-31.60(1)

**Table 5.3:** Self energy  $\Sigma_0$  of Wilson and Brillouin fermions with plaquette and tree-level Symanzik improved (“Lüscher-Weisz”) gauge action as a function of  $r$ .

### 5.3 $c_{\text{SW}}^{(1)}$ for Brillouin Fermions

Here we give results for the one-loop value  $c_{\text{SW}}^{(1)}$  (see Sec. A.6) with Brillouin (and Wilson) fermions using the Feynman rules given in 9 and 8.

The numerical results for each diagram and their sum is given in Table 5.4 for Wilson and Brillouin fermions, with plaquette and Lüscher-Weisz glue. Table 5.5 contains the same results converted into the formalism of Ref. [63] (see Section A.6 for details on the conversion). Our numbers in the “Wilson” columns agree with (and improve on) the numbers given there. Throughout the “sum” (which results from adding the six regulated single-diagram contributions) agrees with the result of the direct numerical integration of the un-regularised (finite) “all in one” approach.

A closer look at Table 5.4 reveals interesting features. The second column indicates that not only the divergent parts of all diagrams would cancel each other, but also that that of diagram (a) would cancel the combined (e,f) divergence, and that (b) cancels (c). This allows us to split the sum of all diagrams into two finite parts, one proportional to  $N_c$  [diagrams (a),(d),(e),(f)] and one proportional to  $1/N_c$  [diagrams (b),(c),(d)]. The

Diag.	$\mathcal{B}_2$	Wilson/Plaq.	Brillouin/Plaq.	Wilson/Sym.	Brillouin/Sym.
(a)	-1/3	0.009852153(1)	0.0100402212(1)	0.01048401(1)	0.0108335(1)
(b)	-9/2	0.125895883(1)	0.098371668(1)	0.1285594(1)	0.102829(1)
(c)	+9/2	-0.124125079(1)	-0.100558858(1)	-0.1337781(1)	-0.1098254(1)
(d)	0	0.297394534(1)	0.142461144(1)	0.2354388(1)	0.1120815(1)
(e)	+1/6	-0.020214623(1)	-0.013344189(1)	-0.022229808(1)	-0.013659(1)
(f)	+1/6	-0.020214623(1)	-0.013344189(1)	-0.022229808(1)	-0.013659(1)
Sum	0	0.26858825(1)	0.12362580(1)	0.1962445(1)	0.088601(1)

**Table 5.4:** Divergent and constant contributions to  $c_{\text{SW}}^{(1)}$  from each diagram for  $N_c = 3$  and  $r = 1$ . The second column gives the coefficient of the logarithmic divergence encoded in  $\mathcal{B}_2(\mu) = \frac{1}{16\pi^2}(-\ln(\mu^2) + F_0 - \gamma_E)$ .

Diag.	$L$	Wilson/Plaq.	Brillouin/Plaq.	Wilson/Sym.	Brillouin/Sym.
(a)	-1/3	0.004569626(1)	0.0047576939(1)	0.00520148(1)	0.0055510(1)
(b)	-9/2	0.083078349(1)	0.055554134(1)	0.1142384(1)	0.088508(1)
(c)	+9/2	-0.081307544(1)	-0.057741323(1)	-0.1194571(1)	-0.0955044(1)
(d)	0	0.297394534(1)	0.142461144(1)	0.2354388(1)	0.1120815(1)
(e)	+1/6	-0.017573359(1)	-0.010702925(1)	-0.019588545(1)	-0.011018(1)
(f)	+1/6	-0.017573359(1)	-0.010702925(1)	-0.019588545(1)	-0.011018(1)
Sum	0	0.26858825(1)	0.12362580(1)	0.1962445(1)	0.088601(1)

**Table 5.5:** Divergent and constant contributions to  $c_{\text{SW}}^{(1)}$  from each diagram for  $N_c = 3$  and  $r = 1$ . The second column gives the coefficient of the logarithmic divergence encoded in  $L := \frac{1}{16\pi^2} \ln(\pi^2/\mu^2)$ . This corresponds to the formalism used in Ref. [63]

corresponding coefficients are given in Table 5.6 for  $r = 1$ , and setting  $N_c = 3$  is found to reproduce the previous results for  $c_{\text{SW}}^{(1)}$ .

Action	$N_c$	$1/N_c$	$c_{\text{SW}}^{(1)}$ for $N_c = 3$
Wilson/Plaq.	0.098842471(1)	-0.08381750(1)	0.26858825(1)
Wilson/Sym.	0.0718695(1)	-0.05809245(1)	0.1962445(1)
Brillouin/Plaq.	0.04578552(1)	-0.04119226(1)	0.12362580(1)
Brillouin/Sym.	0.032600(1)	-0.0275974(1)	0.088601(1)

**Table 5.6:** Coefficients of  $N_c$  and  $1/N_c$  in  $c_{\text{SW}}^{(1)}$  and the full result for  $N_c = 3$  for  $r = 1$ .

For any  $N_c$ , the value of  $c_{\text{SW}}^{(1)}$  for Brillouin fermions is about half the value for Wilson fermions. This holds with plaquette glue and with Lüscher-Weisz glue. In addition, we have performed the same calculations for several values of the Wilson parameter  $r$  in the range 0.5, 0.6, ..., 1.5. The results are shown in Figure 5.2 and listed in Table 5.7. More data is given in Appendix A.1.

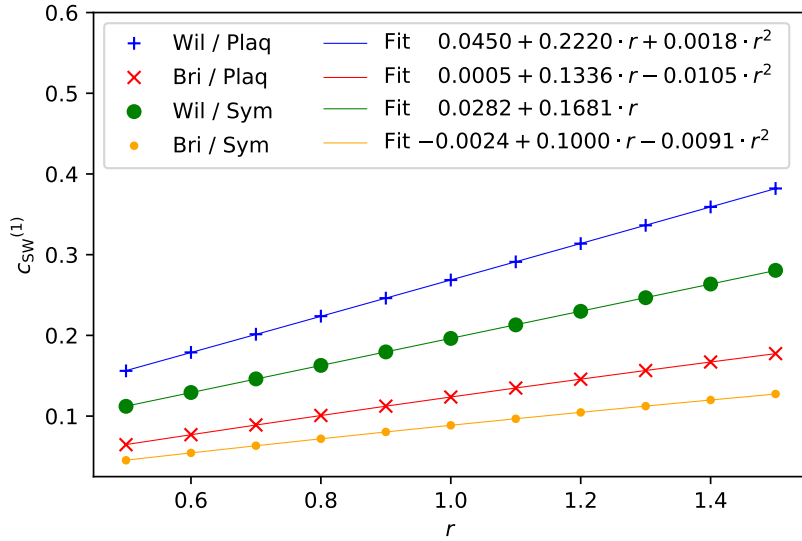


**Figure 5.2:** The one-loop values of  $c_{\text{SW}}^{(1)}$  for Wilson and Brillouin fermions with  $N_c = 3$  as a function of  $r$ .

$r$	$c_{\text{SW}}^{(1)} (N_c = 3)$			
	Wilson/Plaq.	Brillouin/Plaq.	Wilson/Sym.	Brillouin/Sym.
0.5	0.15603501(1)	0.064568(1)	0.1121103(1)	0.045279(1)
0.6	0.17891256(1)	0.076957(1)	0.1292256(1)	0.054428(1)
0.7	0.20141780(1)	0.089006(1)	0.14607072(1)	0.063298(1)
0.8	0.2237942(1)	0.100777(1)	0.1628066(1)	0.071932(1)
0.9	0.2461643(1)	0.123626(1)	0.1795168(1)	0.080360(1)
1.0	0.26858825(1)	0.12362580(1)	0.1962445(1)	0.088601(1)
1.1	0.29109341(1)	0.13474599(1)	0.21301078(1)	0.096670(1)
1.2	0.31369009(1)	0.14568094(1)	0.22982530(1)	0.104577(1)
1.3	0.33637959(1)	0.15643861(1)	0.2466912(1)	0.112330(1)
1.4	0.35915870(1)	0.16702454(1)	0.2636083(1)	0.119934(1)
1.5	0.35915870(1)	0.17744258(1)	0.2805746(1)	0.127392(1)

**Table 5.7:** Coefficient  $c_{\text{SW}}^{(1)}$  for Wilson and Brillouin fermions for  $N_c = 3$  as a function of  $r$ .

# 6 Lattice Perturbation Theory of Stout Smearing and the Wilson Flow

In this chapter we look at stout smearing and the Wilson flow as introduced in Section 7.3 from the point of view of lattice perturbation theory. Rather than investigating a specific fermion action with stout or flowed links and perturbatively expanding it to gain the Feynman rules, we expand the stout or flowed links on their own. Then we figure out how to connect the “form factors” that transition the original gluon fields to the smeared or flowed ones, to the Feynman rules of an arbitrary fermion action.

As the stout transformation and the Wilson flow are related, the main piece of work that is required for their perturbative expansion, is the expansion of  $Q_\mu(x)$  (see Eqauation 3.78). Hence, after having expanded  $e^{i\varrho Q_\mu(x)}$  in Section 6.1.3 for the stout link variable, the expansion of the flowed link variable in Section 6.2.4 requires much less work, as we will be able to reuse a lot of the results. Section 9 then explains how to obtain the Feynman rules.

## 6.1 Perturbative Stout Smearing

In lattice perturbation theory, the group element  $U_\mu(x) \in SU(N_c)$  is written as the exponential of a linear combination of generators  $T^a$  and gluon fields  $A_\mu^a(x)$

$$U_\mu(x) = e^{ig_0 T^a A_\mu^a(x)} . \quad (6.1)$$

Expanding the action to the desired order in the bare coupling  $g_0$  then gives the Feynman rules. For one-loop calculations we need to expand up to third order in  $g_0$

$$\begin{aligned} U_\mu(x) = 1 + ig_0 T^a A_\mu^a(x) - \frac{g_0^2}{2} T^a T^b A_\mu^a(x) A_\mu^b(x) \\ - i \frac{g_0^3}{6} T^a T^b T^c A_\mu^a(x) A_\mu^b(x) A_\mu^c(x) + \mathcal{O}(g_0^4). \end{aligned} \quad (6.2)$$

In order for  $U_\mu(x)$  to be unitary, the exponent  $ig_0 T^a A_\mu^a(x)$  has to be anti-hermitian. This means the gluon fields  $A_\mu^a(x)$  are real (because the generators are hermitian). This implies that the momentum space field  $A_\mu^a(k)$  fulfils

$$A_\mu^a(k) = A_\mu^a(-k) . \quad (6.3)$$

As we are going to be working in momentum space, it is helpful to keep in mind that taking the hermitian conjugate in position space involves the transformation  $k \rightarrow -k$  in momentum space.

For a link variable after stout smearing, things are more complicated. As the smeared link variable  $U_\mu^{(n)}(x)$  is again a group element of  $SU(N_c)$  [7], we expect it to have an exponential representation similar to the un-smeared one

$$U_\mu^{(n)}(x) = e^{ig_0 T^a \tilde{A}_\mu^{(n)a}(g_0, x)} \quad (6.4)$$

$$\begin{aligned} &= 1 + ig_0 T^a \tilde{A}_\mu^{(n)a}(g_0, x) - \frac{g_0^2}{2} T^a T^b \tilde{A}_\mu^{(n)a}(g_0, x) \tilde{A}_\mu^{(n)b}(g_0, x) \\ &\quad - i \frac{g_0^3}{6} T^a T^b T^c \tilde{A}_\mu^{(n)a}(g_0, x) \tilde{A}_\mu^{(n)b}(g_0, x) \tilde{A}_\mu^{(n)c}(g_0, x) + \mathcal{O}(T^4). \end{aligned} \quad (6.5)$$

This expansion in terms of generators  $T$  does, however, no longer coincide with the expansion in the bare coupling  $g_0$ . The new fields  $\tilde{A}_\mu^{(n)a}(g_0, x)$  are themselves functions of  $g_0$ . By expanding  $\tilde{A}_\mu^{(n)a}(g_0, x)$  in powers of  $g_0$  we will be able to determine its coefficients by comparison with the perturbative expansion of the right hand side of Eq. (3.76). This also means that, as we will see below, we will be able to infer the general structure of the coefficients of  $\tilde{A}_\mu^{(n)a}(g_0, x)$  from the perturbative expansion of only the first smearing step

$$U_\mu^{(1)}(x) = \exp \{i\varrho Q_\mu^{(0)}(x)\} U_\mu^{(0)}(x), \quad (6.6)$$

which in turn allows us to use the following strategy: Expand Eq. (6.6) to the desired order in  $g_0$  and replace  $A_\mu^{(0)}(x)$  by the expansion of  $\tilde{A}_\mu^{(n)a}(g_0, x)$ . This will generate new contributions to higher orders in  $g_0$  and give the results for a general smearing step  $n+1 > 1$ .

We start by defining expansions of  $S_\mu(x)$  and  $Q_\mu(x)$  in  $g_0$  (we drop the superscript (0) for now):

$$S_\mu(x) = 6 + ig_0 T^a S_{1\mu}^a(x) - g_0^2 T^a T^b S_{2\mu}^{ab}(x) - ig_0^3 T^a T^b T^c S_{3\mu}^{abc}(x) + \mathcal{O}(g_0^4) \quad (6.7)$$

$$\begin{aligned} Q_\mu(x) &= g_0 T^a Q_{1\mu}^a(x) + ig_0^2 \left( T^a T^b - T^b T^a \right) Q_{2\mu}^{ab}(x) \\ &\quad + g_0^3 \left( T^a T^b T^c + T^c T^b T^a - \frac{1}{N_c} \text{Tr} [T^a T^b T^c + T^c T^b T^a] \right) Q_{3\mu}^{abc}(x) + \mathcal{O}(g_0^4). \end{aligned} \quad (6.8)$$

Using the Baker-Campbell-Hausdorff-formula

$$e^X e^Y = e^{X+Y+\frac{1}{2}[X,Y]+\frac{1}{12}([X,[X,Y]]+[Y,[Y,X]])+\dots}, \quad (6.9)$$

we therefore get

$$\begin{aligned} &\exp \{i\varrho Q_\mu(x)\} \exp \{ig_0 T^a A_\mu^a(x)\} = \\ &\exp \left\{ ig_0 T^a A_\mu^a(x) + i\varrho g_0 T^a Q_{1\mu}^a(x) - \varrho g_0^2 [T^a, T^b] Q_{2\mu}^{[ab]}(x) \right. \\ &\quad \left. + i\varrho g_0^3 \left( T^a T^b T^c + T^c T^b T^a - \frac{1}{N_c} \text{Tr} [T^a T^b T^c + T^c T^b T^a] \right) Q_{3\mu}^{abc}(x) \right. \\ &\quad \left. + \frac{1}{2} \left( -\varrho g_0^2 [T^a, T^b] Q_{1\mu}^a(x) A_\mu^b(x) - i\varrho g_0^3 [[T^a, T^b], T^c] Q_{2\mu}^{[ab]}(x) A_\mu^c(x) \right) \right\} \end{aligned}$$

$$\begin{aligned} & + \frac{1}{12} \left( -i\varrho^2 g_0^3 [T^a, [T^b, T^c]] Q_{1\mu}^a(x) Q_{1\mu}^b(x) A_\mu^c(x) \right. \\ & \left. - i\varrho g_0^3 [T^a, [T^b, T^c]] A_\mu^a(x) A_\mu^b(x) Q_{1\mu}^c(x) \right) + \mathcal{O}(g_0^4) \end{aligned} \quad (6.10)$$

$$\begin{aligned} & = 1 + ig_0 T^a (A_\mu^a(x) + \varrho Q_{1\mu}^a(x)) \\ & - \frac{1}{2} g_0^2 T^a T^b (A_\mu^a(x) + \varrho Q_{1\mu}^a(x)) (A_\mu^b(x) + \varrho Q_{1\mu}^b(x)) \\ & - \varrho g_0^2 [T^a, T^b] \left( \frac{1}{2} Q_{1\mu}^a(x) A_\mu^b(x) + Q_{2\mu}^{ab}(x) \right) \\ & - i \frac{g_0^3}{6} T^a T^b T^c (A_\mu^a(x) + \varrho Q_{1\mu}^a(x)) (A_\mu^b(x) + \varrho Q_{1\mu}^b(x)) (A_\mu^c(x) + \varrho Q_{1\mu}^c(x)) \\ & - i \frac{g_0^3}{2} \{T^a, [T^b, T^c]\} (A_\mu^a(x) + \varrho Q_{1\mu}^a(x)) \left( \frac{1}{2} \varrho Q_{1\mu}^b(x) A_\mu^c(x) + \varrho Q_{2\mu}^{bc}(x) \right) \\ & + i \frac{g_0^3}{2} [T^a, [T^b, T^c]] A_\mu^a(x) \varrho Q_{2\mu}^{[bc]}(x) \\ & + \frac{1}{12} \left( -i\varrho^2 g_0^3 [T^a, [T^b, T^c]] Q_{1\mu}^a(x) Q_{1\mu}^b(x) A_\mu^c(x) \right. \\ & \left. - i\varrho g_0^3 [T^a, [T^b, T^c]] A_\mu^a(x) A_\mu^b(x) Q_{1\mu}^c(x) \right) \\ & + i\varrho g_0^3 \left( T^a T^b T^c + T^c T^b T^a - \frac{1}{N_c} \text{Tr}[T^a T^b T^c + T^c T^b T^a] \right) Q_{3\mu}^{abc}(x) + \mathcal{O}(g_0^4) \end{aligned} \quad (6.11)$$

where we have used

$$e^{ax+bx^2+cx^3} = 1 + ax + (\tfrac{1}{2}a^2 + b)x^2 + (\tfrac{1}{6}a^3 + \tfrac{1}{2}(ab + ba) + c)x^3 + \mathcal{O}(x^4) \quad (6.12)$$

in the second step. Based on this, it is convenient to define fields  $A^{(n)a}$ ,  $A^{(n)ab}$ ,  $\bar{A}^{(n)abc}$ , and  $\hat{A}^{(n)abc}$  at each order in  $g_0$  for a general  $n$  such that

$$\begin{aligned} U_\mu^{(n)}(x) & = 1 + ig_0 T^a A_\mu^{(n)a}(x) - \frac{g_0^2}{2} \left( T^a T^b A_\mu^{(n)a}(x) A_\mu^{(n)b}(x) + [T^a, T^b] A_\mu^{(n)ab}(x) \right) \\ & - i \frac{g_0^3}{6} \left( T^a T^b T^c A_\mu^{(n)a}(x) A_\mu^{(n)b}(x) A_\mu^{(n)c}(x) + \frac{3}{2} \{T^a, [T^b, T^c]\} A_\mu^{(n)a}(x) A_\mu^{(n)bc}(x) \right. \\ & \left. + [T^a, [T^b, T^c]] \bar{A}_\mu^{(n)abc}(x) \right. \\ & \left. + \left( T^a T^b T^c + T^c T^b T^a - \frac{1}{N_c} \text{Tr}[T^a T^b T^c + T^c T^b T^a] \right) \hat{A}_\mu^{(n)abc}(x) \right) + \mathcal{O}(g_0^4). \end{aligned} \quad (6.13)$$

We can now also incorporate  $\bar{A}$  into  $\hat{A}$  because

$$\begin{aligned} [T^a, [T^b, T^c]] \bar{A}_\mu^{(n)abc}(x) & = 2[T^a, T^b T^c] \bar{A}_\mu^{(n)a[b]}(x) \\ & = 2(T^a T^b T^c + T^c T^b T^a) \bar{A}_\mu^{(n)a[b]}(x) \end{aligned} \quad (6.14)$$

and

$$\text{Tr}[T^a T^b T^c + T^c T^b T^a] \bar{A}_\mu^{(n)a[b]}(x) = \text{Tr}[T^a T^b T^c - T^b T^c T^a] \bar{A}_\mu^{(n)a[b]}(x) = 0. \quad (6.15)$$

Thus we can write

$$\begin{aligned}
U_\mu^{(n)}(x) = & 1 + ig_0 T^a A_\mu^{(n)a}(x) - \frac{g_0^2}{2} \left( T^a T^b A_\mu^{(n)a}(x) A_\mu^{(n)b}(x) + [T^a, T^b] A_\mu^{(n)ab}(x) \right) \\
& - i \frac{g_0^3}{6} \left( T^a T^b T^c A_\mu^{(n)a}(x) A_\mu^{(n)b}(x) A_\mu^{(n)c}(x) + \frac{3}{2} \{T^a, [T^b, T^c]\} A_\mu^{(n)a}(x) A_\mu^{(n)bc}(x) \right. \\
& \left. + \left( T^a T^b T^c + T^c T^b T^a - \frac{1}{N_c} \text{Tr}[T^a T^b T^c + T^c T^b T^a] \right) A_\mu^{(n)abc}(x) \right) \\
& + \mathcal{O}(g_0^4)
\end{aligned} \tag{6.16}$$

with

$$A_\mu^{(n)abc}(x) = \hat{A}_\mu^{(n)abc}(x) + 2\bar{A}_\mu^{(n)a[bc]}(x). \tag{6.17}$$

We define their Fourier transforms as

$$A_\mu^{(n)a}(x) = \int_{-\pi}^{\pi} \frac{d^4 k}{(2\pi)^4} e^{i(x+\hat{\mu}/2)k} A_\mu^{(n)a}(k) \tag{6.18}$$

$$A_\mu^{(n)ab}(x) = \int_{-\pi}^{\pi} \frac{d^4 k_1}{(2\pi)^4} \int_{-\pi}^{\pi} \frac{d^4 k_2}{(2\pi)^4} e^{i(x+\hat{\mu}/2)(k_1+k_2)} A_\mu^{(n)ab}(k_1, k_2) \tag{6.19}$$

$$A_\mu^{(n)abc}(x) = \int_{-\pi}^{\pi} \frac{d^4 k_1}{(2\pi)^4} \int_{-\pi}^{\pi} \frac{d^4 k_2}{(2\pi)^4} \int_{-\pi}^{\pi} \frac{d^4 k_3}{(2\pi)^4} e^{i(x+\hat{\mu}/2)(k_1+k_2+k_3)} A_\mu^{(n)abc}(k_1, k_2, k_3). \tag{6.20}$$

These fields are ultimately functions of the original gluon fields

$$A_\mu^{(n)a}(x) = \sum_\nu \sum_y \tilde{g}_{\mu\nu}^{(n)}(\varrho, y) A_\nu^{(0)a}(x+y) \tag{6.21}$$

$$A_\mu^{(n)ab}(x) = \sum_{\nu\rho} \sum_{yz} \tilde{g}_{\mu\nu\rho}^{(n)}(\varrho, y, z) A_\nu^{(0)a}(x+y) A_\rho^{(0)b}(x+z) \tag{6.22}$$

$$A_\mu^{(n)abc}(x) = \sum_{\nu\rho\sigma} \sum_{yzr} \tilde{g}_{\mu\nu\rho\sigma}^{(n)}(\varrho, y, z, r) A_\nu^{(0)a}(x+y) A_\rho^{(0)b}(x+z) A_\sigma^{(0)c}(x+r) \tag{6.23}$$

$$A_\mu^{(n)a}(k) = \sum_\nu \tilde{g}_{\mu\nu}^{(n)}(\varrho, k) A_\nu^{(0)a}(k) \tag{6.24}$$

$$A_\mu^{(n)ab}(k_1, k_2) = \sum_{\nu\rho} \tilde{g}_{\mu\nu\rho}^{(n)}(\varrho, k_1, k_2) A_\nu^{(0)a}(k_1) A_\rho^{(0)b}(k_2) \tag{6.25}$$

$$A_\mu^{(n)abc}(k_1, k_2, k_3) = \sum_{\nu\rho\sigma} \tilde{g}_{\mu\nu\rho\sigma}^{(n)}(\varrho, k_1, k_2, k_3) A_\nu^{(0)a}(k_1) A_\rho^{(0)b}(k_2) A_\sigma^{(0)c}(k_3) \tag{6.26}$$

with some complicated functions simply denoted by  $\tilde{g}$  here. Sections 9, 9, and 9 will be largely concerned with determining the momentum space  $\tilde{g}$  explicitly.

### Connecting the perturbative and $SU(N_c)$ -expansions

In order to relate the smeared gluon field  $\tilde{A}_\mu^{(n)a}(g_0, x)$  to the perturbative functions  $A_\mu^{(n)a}(x)$ ,  $A_\mu^{(n)ab}(x)$ , and  $A_\mu^{(n)abc}(x)$ , we need to expand the products of color matrices such that only terms with a single  $T^a$  remain. We use

$$[T^a, T^b] = if^{abc}T^c, \quad f^{abc} = -2i\text{Tr}(T^a[T^b, T^c]) \quad (6.27)$$

$$\{T^a, T^b\} = \frac{1}{N_c}\delta^{ab} + d^{abc}T^c, \quad d^{abc} = 2\text{Tr}(T^a\{T^b, T^c\}) \quad (6.28)$$

and

$$T^aT^b = \frac{1}{2N_c}\delta^{ab} + \frac{1}{2}(d^{abc} + if^{abc})T^c \quad (6.29)$$

$$\text{Tr}[T^aT^bT^c] = \frac{1}{2}\text{Tr}[T^a\{T^b, T^c\} + T^a[T^b, T^c]] = \frac{1}{4}(d^{abc} + if^{abc}). \quad (6.30)$$

With the above color identities we can now rewrite the following expressions in a way that only one generator  $T$  remains:

$$[T^a, T^b]A_\mu^{(n)[ab]}(x) = if^{abc}T^aA_\mu^{(n)[bc]}(x) \quad (6.31)$$

$$\begin{aligned} & \left( T^aT^bT^c + T^cT^bT^a - \frac{1}{N_c}\text{Tr}[T^aT^bT^c + T^cT^bT^a] \right) A_\mu^{(n)abc}(x) \\ &= \left( \frac{1}{2}(\{T^a, \{T^b, T^c\}\} + [T^a, [T^b, T^c]]) - \frac{1}{N_c}\text{Tr}[T^aT^bT^c + T^cT^bT^a] \right) A_\mu^{(n)abc}(x) \end{aligned} \quad (6.32)$$

$$= T^a \left[ \frac{1}{N_c}\delta^{ae}\delta^{bc} + \frac{1}{2}(d^{bcd}d^{eda} - f^{bcd}f^{eda}) \right] A_\mu^{(n)ebc}(x). \quad (6.33)$$

Thus we can rearrange our perturbative expansion (6.13) to look like

$$\begin{aligned} U_\mu^{(n)}(x) = & 1 + ig_0T^a \left\{ A_\mu^{(n)a}(x) - \frac{g_0}{2}f^{abc}A_\mu^{(n)[bc]}(x) \right. \\ & - \frac{g_0^2}{6} \left[ \frac{1}{N_c}\delta^{ae}\delta^{bc} + \frac{1}{2}(d^{bcd}d^{eda} - f^{bcd}f^{eda}) \right] A_\mu^{(n)ebc}(x) + \mathcal{O}(g_0^3) \Big\} \\ & - \frac{g_0^2}{2}T^aT^b \left\{ A_\mu^{(n)a}(x)A_\mu^{(n)a}(x) - \frac{g_0}{2} \left( A_\mu^{(n)a}(x)f^{bcd} + f^{acd}A_\mu^{(n)b}(x) \right) A_\mu^{(n)[cd]}(x) + \mathcal{O}(g_0^2) \right\} \\ & - i\frac{g_0^3}{6}T^aT^bT^c \left\{ A_\mu^{(n)a}(x)A_\mu^{(n)b}(x)A_\mu^{(n)c}(x) + \mathcal{O}(g_0) \right\} + \mathcal{O}(T^4). \end{aligned} \quad (6.34)$$

We can see that the expressions in the large braces correspond to the first, second, and third order of an expansion of the exponential function, each cut off to give an overall highest order of  $g_0^3$ . Hence we can give the first few orders of the smeared gluon field as

$$\begin{aligned} \tilde{A}_\mu^{(n)a}(g_0, x) = & A_\mu^{(n)a}(x) - \frac{g_0}{2}f^{abc}A_\mu^{(n)[bc]}(x) \\ & - \frac{g_0^2}{6} \left[ \frac{1}{N_c}\delta^{ae}\delta^{bc} + \frac{1}{2}(d^{bcd}d^{eda} - f^{bcd}f^{eda}) \right] A_\mu^{(n)ebc}(x) + \mathcal{O}(g_0^3). \end{aligned} \quad (6.35)$$

Thus, we have expressed the new gluon field in terms of the perturbative fields.

### 6.1.1 Leading Order

As we have seen, at leading order the perturbative and  $SU(N_c)$  expansions are identical:  $\tilde{A}_\mu^{(n)a}(g_0, x) = A_\mu^{(n)a}(x) + \mathcal{O}(g_0)$ . The sum of staples at leading order is:

$$\begin{aligned} S_\mu^{(n)}(x) &= 6+ \\ &ig_0 T^a \left( \sum_{\nu=1}^4 \left[ A_\nu^{(n)a}(x) + A_\mu^{(n)a}(x + \hat{\nu}) - A_\nu^{(n)a}(x + \hat{\mu}) - A_\nu^{(n)a}(x - \hat{\nu}) \right. \right. \\ &\quad \left. \left. + A_\mu^{(n)a}(x - \hat{\nu}) + A_\nu^{(n)a}(x + \hat{\mu} - \hat{\nu}) \right] - 2A_\mu^{(n)a}(x) \right) + \mathcal{O}(g_0^2) \end{aligned} \quad (6.36)$$

where the sum now includes the  $\nu = \mu$  term, which is compensated by the subtraction of  $2A_\mu^{(n)a}(x)$ . Therefore

$$\begin{aligned} Q_{1\mu}^{(n)a}(x) &= \sum_{\nu=1}^4 \left[ A_\nu^{(n)a}(x) + A_\mu^{(n)a}(x + \hat{\nu}) - A_\nu^{(n)a}(x + \hat{\mu}) - A_\nu^{(n)a}(x - \hat{\nu}) \right. \\ &\quad \left. + A_\mu^{(n)a}(x - \hat{\nu}) + A_\nu^{(n)a}(x + \hat{\mu} - \hat{\nu}) - 2A_\mu^{(n)a}(x) \right] \end{aligned} \quad (6.37)$$

$$= -6A_\mu^{(n)a}(x) + S_{1\mu}^{(n)a}(x). \quad (6.38)$$

The smeared gluon field in position space can then be written as a convolution [97]:

$$A_\mu^{(n+1)a}(x) = A_\mu^{(n)a}(x) + \varrho Q_{1\mu}^{(n)a}(x) \quad (6.39)$$

$$= A_\mu^{(n)a}(x) + \varrho \sum_{\nu=1}^4 \sum_y g_{\mu\nu}(y) A_\nu^{(n)a}(x+y) \quad (6.40)$$

$$=: \sum_{\nu} \sum_y \tilde{g}_{\mu\nu}(\varrho, y) A_\nu^{(n)a}(x+y) \quad (6.41)$$

with  $\tilde{g}_{\mu\nu}(\varrho, y) = \delta_{\mu\nu} + \varrho g_{\mu\nu}(y)$  and

$$\begin{aligned} g_{\mu\nu}(y) &= \delta(y, 0) - \delta(y, \hat{\mu}) - \delta(y, -\hat{\nu}) + \delta(y, \hat{\mu} - \hat{\nu}) \\ &+ \delta_{\mu\nu} \left[ \sum_{\tau=1}^4 (\delta(y, \hat{\tau}) + \delta(y, -\hat{\tau})) - 8\delta(y, 0) \right]. \end{aligned} \quad (6.42)$$

Performing a Fourier-transformation using  $\delta(x, y) = \int_{-\pi}^{\pi} \frac{d^4 p}{(2\pi)^4} e^{i(x-y)p}$  we get:

$$\begin{aligned} &e^{ipy} \left( 1 - e^{-ip_\mu} - e^{ip_\nu} + e^{-i(p_\mu - p_\nu)} + \delta_{\mu\nu} \left[ -8 + \sum_{\tau=1}^4 (e^{-ip_\tau} + e^{ip_\tau}) \right] \right) \\ &= e^{ipy} e^{-\frac{i}{2}(p_\mu - p_\nu)} \left( -\delta_{\mu\nu} \hat{p}^2 + \hat{p}_\mu \hat{p}_\nu \right). \end{aligned} \quad (6.43)$$

Now we can express the Fourier transform of the first order smeared gluon field as

$$\begin{aligned} A_\mu^{(n+1)a}(x) &= \sum_{\nu,y} \int_{-\pi}^{\pi} \frac{d^4 k}{(2\pi)^4} \int_{-\pi}^{\pi} \frac{d^4 p}{(2\pi)^4} e^{iy p} e^{-\frac{i}{2}(p_\mu - p_\nu)} \left( \delta_{\mu\nu} + \varrho \left( -\delta_{\mu\nu} \hat{p}^2 + \hat{p}_\mu \hat{p}_\nu \right) \right) \\ &\times e^{i(x+y+\hat{\nu}/2)k} A_\nu^{(n)a}(k) \end{aligned} \quad (6.44)$$

$$= \sum_\nu \int_{-\pi}^{\pi} \frac{d^4 k}{(2\pi)^4} e^{i(x+\hat{\mu}/2)k} \left( \delta_{\mu\nu} + \varrho \left( -\delta_{\mu\nu} \hat{k}^2 + \hat{k}_\mu \hat{k}_\nu \right) \right) A_\nu^{(n)a}(k), \quad (6.45)$$

where we have used  $\sum_x e^{-ix(p-q)} = (2\pi)^4 \delta(p-q)$  and performed the integration over  $p$ . Thus at leading order the result in momentum space is

$$A_\mu^{(n+1)a}(k) = A_\mu^{(n)a}(k) + \varrho \sum_\nu g_{\mu\nu}(k) A_\nu^{(n)a}(k) \quad (6.46)$$

with

$$g_{\mu\nu}(k) = -\delta_{\mu\nu} \hat{k}^2 + \hat{k}_\mu \hat{k}_\nu. \quad (6.47)$$

Expressing it in terms of the function  $f(k) = 1 - \varrho \hat{k}^2$ , it becomes easier to iterate

$$A_\mu^{(n+1)a}(k) = \sum_\nu \left( f(k) \delta_{\mu\nu} - (f(k) - 1) \frac{\hat{k}_\mu \hat{k}_\nu}{\hat{k}^2} \right) A_\nu^{(n)a}(k). \quad (6.48)$$

In this form, the form factor retains the same structure after multiple iterations, only the powers of  $f$  increase [97, 98]:

$$A_\mu^{(n)a}(k) = \sum_\nu \left( f^n(k) \delta_{\mu\nu} - (f^n(k) - 1) \frac{\hat{k}_\mu \hat{k}_\nu}{\hat{k}^2} \right) A_\nu^{(0)a}(k) \quad (6.49)$$

$$=: \sum_\nu \tilde{g}_{\mu\nu}^n(\varrho, k) A_\nu^{(0)a}(k) \quad (6.50)$$

We note that  $\tilde{g}_{\mu\nu}^n(\varrho, k)$  is not exactly the Fourier transform of  $\tilde{g}_{\mu\nu}^n(\varrho, y)$  but rather fulfills the same purpose in momentum space of relating the newly smeared field to the one of the previous smearing step.

### 6.1.2 Next-to-Leading Order

At higher orders the expansions deviate and Eqs. (6.10) and (6.11) would need to be modified for a general smearing step  $n \rightarrow n + 1$  to include the higher order perturbative fields  $A_\mu^{(n)[ab]}(x)$ ,  $\bar{A}_\mu^{(n)abc}(x)$  and  $\hat{A}_\mu^{(n)abc}(x)$ . This is why we start again by considering the

first smearing step. At order  $g_0^2$ , the sum of staples  $S_\mu^{(0)}(x)$  is given by:

$$\begin{aligned} S_{2\mu}^{(0)ab}(x) = & \sum_{\nu \neq \mu} \left[ A_\nu^a(x) A_\mu^b(x + \hat{\nu}) - A_\nu^a(x) A_\nu^b(x + \hat{\mu}) - A_\mu^a(x + \hat{\nu}) A_\nu^b(x + \hat{\mu}) \right. \\ & - A_\nu^a(x - \hat{\nu}) A_\mu^b(x - \hat{\nu}) - A_\nu^a(x - \hat{\nu}) A_\nu^b(x + \hat{\mu} - \hat{\nu}) \\ & + A_\mu^a(x - \hat{\nu}) A_\nu^b(x + \hat{\mu} - \hat{\nu}) + \frac{1}{2} \left\{ A_\nu^a(x) A_\nu^b(x) + A_\mu^a(x + \hat{\nu}) A_\mu^b(x + \hat{\nu}) \right. \\ & + A_\nu^a(x + \hat{\mu}) A_\nu^b(x + \hat{\mu}) + A_\nu^a(x - \hat{\nu}) A_\nu^b(x - \hat{\nu}) + A_\mu^a(x - \hat{\nu}) A_\mu^b(x - \hat{\nu}) \\ & \left. \left. + A_\nu^a(x + \hat{\mu} - \hat{\nu}) A_\nu^b(x + \hat{\mu} - \hat{\nu}) \right\} \right]. \end{aligned} \quad (6.51)$$

The part in braces  $\{\dots\}$  is symmetric in  $a \leftrightarrow b$  and will therefore disappear in  $A_\mu^{(1)[ab]}(x)$ .<sup>1</sup> We get

$$Q_{2\mu}^{(0)ab}(x) = \frac{1}{2} \left( -S_{1\mu}^{(0)a}(x) A_\mu^{(0)b}(x) + S_{2\mu}^{(0)ab}(x) \right) \quad (6.52)$$

which leaves

$$A_\mu^{(1)[ab]}(x) = 2\varrho \left( \frac{1}{2} Q_{1\mu}^{(0)[a}(x) A_\mu^{(0)b]}(x) + Q_{2\mu}^{(0)[ab]}(x) \right) = \varrho S_{2\mu}^{(0)[ab]}(x), \quad (6.53)$$

which we can write as a double convolution:

$$S_{2\mu}^{(0)[ab]}(x) = \sum_{y,z} \sum_{\nu,\rho=1}^4 g_{\mu\nu\rho}(y,z) \cdot A_\nu^{[a}(x+y) A_\rho^{b]}(x+z) \quad (6.54)$$

$$= \sum_{y,z} \sum_{\nu,\rho=1}^4 \frac{1}{2} (g_{\mu\nu\rho}(y,z) - g_{\mu\rho\nu}(z,y)) \cdot A_\nu^a(x+y) A_\rho^b(x+z) \quad (6.55)$$

with

$$\begin{aligned} g_{\mu\nu\rho}(y,z) = & \delta_{\mu\nu} [\delta(y, -\hat{\rho}) \delta(z, \hat{\mu} - \hat{\rho}) - \delta(y, \hat{\rho}) \delta(z, \hat{\mu})] \\ & + \delta_{\mu\rho} [\delta(y, 0) \delta(z, \hat{\nu}) - \delta(y, -\hat{\nu}) \delta(z, -\hat{\nu})] \\ & - \delta_{\nu\rho} [\delta(y, 0) \delta(z, \hat{\mu}) + \delta(y, -\hat{\nu}) \delta(z, \hat{\mu} - \hat{\nu})]. \end{aligned} \quad (6.56)$$

Fourier transforming gives us

$$A_\mu^{(1)[ab]}(k_1, k_2) = \varrho \sum_{\nu,\rho} g_{\mu\nu\rho}(k_1, k_2) A_\nu^a(k_1) A_\rho^b(k_2), \quad (6.57)$$

where

$$\begin{aligned} g_{\mu\nu\rho}(k_1, k_2) = & 2i \left( \delta_{\mu\rho} c(k_{1\mu}) s(2k_{2\nu} + k_{1\nu}) - \delta_{\mu\nu} c(k_{2\mu}) s(2k_{1\rho} + k_{2\rho}) \right. \\ & \left. + \delta_{\nu\rho} s(k_{1\mu} - k_{2\mu}) c(k_{1\nu} + k_{2\nu}) \right). \end{aligned} \quad (6.58)$$

---

<sup>1</sup>We use the following shorthand notation for symmetrised and anti-symmetrised expressions:  $A^{\{ab\}} = \frac{1}{2}(A^{ab} + A^{ba})$  and  $A^{[ab]} = \frac{1}{2}(A^{ab} - A^{ba})$ .

Although  $g_{\mu\nu\rho}(k_1, k_2)$  is imaginary (and therefore so is  $A_\mu^{(1)[ab]}(k_1, k_2)$ ), it also fulfills  $g_{\mu\nu\rho}(-k_1, -k_2) = -g_{\mu\nu\rho}(k_1, k_2)$ , which means that  $A_\mu^{(1)[ab]}(x)$  is real.

If we were to repeat the previous calculation for a smearing step  $n \rightarrow n+1$ , we would not only have to replace the  $A_\mu^{(0)a}(x)$  by  $A_\mu^{(n)a}(x)$  but the expansion of  $S_{2\mu}^{(n)ab}(x)$  would also contain terms linear in  $A_\mu^{(n)[ab]}(x)$ . Instead, it is easier to realize that we can get the same contribution by replacing

$$T^a A_\mu^{(0)a}(x) \rightarrow T^a \tilde{A}_\mu^{(n)a}(g_0, x) = T^a A_\mu^{(n)a}(x) - \frac{g_0}{2i} [T^a, T^b] A_\mu^{(n)[ab]}(x) + \mathcal{O}(g_0^2) \quad (6.59)$$

in the *leading order* calculation. Then we get for a general smearing step

$$\begin{aligned} A_\mu^{(n+1)[ab]}(k_1, k_2) &= \sum_\nu \tilde{g}_{\mu\nu}(\varrho, k_1 + k_2) A_\nu^{(n)[ab]}(k_1, k_2) \\ &\quad + \varrho \sum_{\nu, \rho} g_{\mu\nu\rho}(k_1, k_2) A_\nu^{(n)a}(k_1) A_\rho^{(n)b}(k_2) . \end{aligned} \quad (6.60)$$

By iterating once

$$\begin{aligned} A_\mu^{(2)[ab]}(k_1, k_2) &= \sum_\nu \tilde{g}_{\mu\nu}(\varrho, k_1 + k_2) \varrho \sum_{\rho\sigma} g_{\nu\rho\sigma}(k_1, k_2) A_\rho^{(0)a}(k_1) A_\sigma^{(0)b}(k_2) \\ &\quad + \varrho \sum_{\nu, \rho} g_{\mu\nu\rho}(k_1, k_2) A_\nu^{(1)a}(k_1) A_\rho^{(1)b}(k_2) \end{aligned} \quad (6.61)$$

and twice

$$\begin{aligned} A_\mu^{(3)[ab]}(k_1, k_2) &= \sum_\nu \tilde{g}_{\mu\nu}^2(\varrho, k_1 + k_2) \varrho \sum_{\rho\sigma} g_{\nu\rho\sigma}(k_1, k_2) A_\rho^{(0)a}(k_1) A_\sigma^{(0)b}(k_2) \\ &\quad + \sum_\nu \tilde{g}_{\mu\nu}(\varrho, k_1 + k_2) \varrho \sum_{\rho\sigma} g_{\nu\rho\sigma}(k_1, k_2) A_\rho^{(1)a}(k_1) A_\sigma^{(1)b}(k_2) \\ &\quad + \varrho \sum_{\nu, \rho} g_{\mu\nu\rho}(k_1, k_2) A_\nu^{(2)a}(k_1) A_\rho^{(2)b}(k_2) , \end{aligned} \quad (6.62)$$

we can infer the general form

$$A_\mu^{(n)[ab]}(k_1, k_2) = \sum_{\nu\rho\sigma} \varrho g_{\nu\rho\sigma}(k_1, k_2) \sum_{m=0}^{n-1} \tilde{g}_{\mu\nu}^{n-m-1}(\varrho, k_1 + k_2) A_\rho^{(m)a}(k_1) A_\sigma^{(m)b}(k_2) . \quad (6.63)$$

Finally we can also express the first order fields in the sum in terms of the original un-smeared ones

$$\begin{aligned} A_\mu^{(n)[ab]}(k_1, k_2) &= \sum_{\alpha\beta\gamma\nu\rho} \varrho g_{\alpha\beta\gamma} \left[ \sum_{m=0}^{n-1} \tilde{g}_{\mu\alpha}^{n-m-1}(\varrho, k_1 + k_2) \tilde{g}_{\beta\nu}^m(\varrho, k_1) \tilde{g}_{\gamma\rho}^m(\varrho, k_2) \right] A_\nu^{(0)a}(k_1) A_\rho^{(0)b}(k_2) \\ &=: \sum_{\nu\rho} \tilde{g}_{\mu\nu\rho}^{(n)}(\varrho, k_1, k_2) A_\nu^{(0)a}(k_1) A_\rho^{(0)b}(k_2) . \end{aligned} \quad (6.64)$$

### 6.1.3 Next-to-Next-to-Leading Order

As before, we start again by considering the first smearing step and generalise later to an arbitrary number of smearing steps. At third order we have defined two perturbative fields  $\bar{A}$  and  $\hat{A}$  in Eq. (6.13), where the former can be read off of Eq. (6.11) to be

$$\bar{A}_\mu^{(1)abc}(x) = -3\varrho A_\mu^a(x)Q_{2\mu}^{[bc]}(x) + \frac{1}{2}\varrho^2 Q_{1\mu}^a(x)Q_{1\mu}^b(x)A_\mu^c(x) + \frac{1}{2}\varrho A_\mu^a(x)A_\mu^b(x)Q_{1\mu}^c(x) \quad (6.65)$$

$$\begin{aligned} &= -\frac{3}{2}A_\mu^a(x)A_\mu^{(1)[bc]}(x) + \frac{3}{2}\varrho A_\mu^a(x)Q_{1\mu}^b(x)A_\mu^c(x) + \frac{1}{2}\varrho^2 Q_{1\mu}^a(x)Q_{1\mu}^b(x)A_\mu^c(x) \\ &\quad + \frac{1}{2}\varrho A_\mu^a(x)A_\mu^b(x)Q_{1\mu}^c(x) \end{aligned} \quad (6.66)$$

$$= -\frac{3}{2}A_\mu^a(x)A_\mu^{(1)[bc]}(x) + \frac{1}{2}A_\mu^a(x)A_\mu^{(1)b}(x)A_\mu^c(x) + \frac{1}{2}A_\mu^{(1)a}(x)A_\mu^{(1)b}(x)A_\mu^c(x). \quad (6.67)$$

We have dropped all terms that were symmetric in  $b \leftrightarrow c$  in the last step. Thus  $\bar{A}$  is completely given by already known quantities, which is not surprising as it stems only from the commutator terms of the BCH-formula.

From the third order in the expansion of  $Q_\mu(x)$  we get

$$\hat{A}_\mu^{(1)abc}(x) = -6\varrho Q_{3\mu}^{abc}(x) \quad (6.68)$$

with

$$Q_{3\mu}^{abc}(x) = A_\mu^a(x)A_\mu^b(x)A_\mu^c(x) - \frac{1}{2}V_{1\mu}^a(x)A_\mu^b(x)A_\mu^c(x) + V_{2\mu}^{ab}(x)A_\mu^c(x) - \frac{1}{2}V_{3\mu}^{abc}(x) \quad (6.69)$$

$$\begin{aligned} &= -2A_\mu^a(x)A_\mu^b(x)A_\mu^c(x) - \frac{1}{2}Q_{1\mu}^a(x)A_\mu^b(x)A_\mu^c(x) + V_{2\mu}^{ab}(x)A_\mu^c(x) - V_{3\mu}^{abc}(x). \end{aligned} \quad (6.70)$$

We revisit the sum of staples at second order and define

$$S_{2\mu}^{ab}(x) = s_{1\mu}^{ab}(x) + \frac{1}{2}s_{2\mu}^{ab}(x) \quad (6.71)$$

with

$$\begin{aligned} s_{1\mu\nu}^{ab}(x) &= \sum_\nu \left[ A_\nu^a(x)A_\mu^b(x + \hat{\nu}) - A_\nu^a(x)A_\nu^b(x + \hat{\mu}) - A_\mu^a(x + \hat{\nu})A_\nu^b(x + \hat{\mu}) \right. \\ &\quad \left. - A_\nu^a(x - \hat{\nu})A_\mu^b(x - \hat{\nu}) - A_\nu^a(x - \hat{\nu})A_\nu^b(x + \hat{\mu} - \hat{\nu}) + A_\mu^a(x - \hat{\nu})A_\nu^b(x + \hat{\mu} - \hat{\nu}) \right] \end{aligned} \quad (6.72)$$

$$\begin{aligned} s_{2\mu}^{ab}(x) &= \sum_\nu \left[ A_\nu^a(x)A_\nu^b(x) + A_\mu^a(x + \hat{\nu})A_\mu^b(x + \hat{\nu}) + A_\nu^a(x + \hat{\mu})A_\nu^b(x + \hat{\mu}) \right. \\ &\quad \left. + A_\nu^a(x - \hat{\nu})A_\nu^b(x - \hat{\nu}) + A_\mu^a(x - \hat{\nu})A_\mu^b(x - \hat{\nu}) + A_\nu^a(x + \hat{\mu} - \hat{\nu})A_\nu^b(x + \hat{\mu} - \hat{\nu}) \right. \\ &\quad \left. - 2\delta_{\mu\nu}A_\mu^a(x)A_\mu^b(x) \right] \end{aligned} \quad (6.73)$$

Their Fourier transforms are

$$\begin{aligned} s_{1\mu}^{ab}(x) &= \sum_{yz} \sum_{\nu\rho} a_{1\mu\nu\rho}(y, z) A_\nu^a(x+y) A_\rho^b(x+z) \\ &= \sum_{\nu\rho} \int \frac{d^4 k_1 d^4 k_2}{(2\pi)^8} e^{-i(x+\frac{1}{2}\hat{\mu})(k_1+k_2)} \cdot a_{1\mu\nu\rho}(k_1, k_2) A_\nu^a(k_1) A_\rho^b(k_2) \end{aligned} \quad (6.74)$$

$$\begin{aligned} s_{2\mu}^{ab}(x) &= \sum_y \sum_\nu a_{2\mu\nu}(y) A_\nu^a(x+y) A_\nu^b(x+y) \\ &= \sum_\nu \int \frac{d^4 k_1 d^4 k_2}{(2\pi)^8} e^{-i(x+\frac{1}{2}\hat{\mu})(k_1+k_2)} \cdot a_{2\mu\nu}(k_1, k_2) A_\nu^a(k_1) A_\nu^b(k_2) \end{aligned} \quad (6.75)$$

with

$$\begin{aligned} a_{1\mu\nu\rho}(y, z) &= \delta_{\mu\nu} [\delta(y, -\hat{\rho})\delta(z, \hat{\mu} - \hat{\rho}) - \delta(y, \hat{\rho})\delta(z, \hat{\mu})] \\ &\quad + \delta_{\mu\rho} [\delta(y, 0)\delta(z, \hat{\nu}) - \delta(y, -\hat{\nu})\delta(z, -\hat{\nu})] \\ &\quad - \delta_{\nu\rho} [\delta(y, 0)\delta(z, \hat{\mu}) + \delta(y, -\hat{\nu})\delta(z, \hat{\mu} - \hat{\nu})] \end{aligned} \quad (6.76)$$

$$\begin{aligned} a_{2\mu\nu}(y) &= \delta_{\mu\nu} \sum_{\alpha=1}^4 [\delta(y, \hat{\alpha}) + \delta(y, -\hat{\alpha}) - 2\delta(y, 0)] + 6\delta_{\mu\nu}\delta(y, 0) \\ &\quad + \delta(y, 0) + \delta(y, \hat{\mu}) + \delta(y, -\hat{\nu}) + \delta(y, \hat{\mu} - \hat{\nu}) \end{aligned} \quad (6.77)$$

and

$$\begin{aligned} a_{1\mu\nu\rho}(k_1, k_2) &= -\delta_{\mu\nu} [2i \sin(k_{1\rho} + \frac{1}{2}k_{2\rho}) e^{\frac{i}{2}k_{2\mu}}] + \delta_{\mu\rho} [2i \sin(k_{2\nu} + \frac{1}{2}k_{1\nu}) e^{-\frac{i}{2}k_{1\mu}}] \\ &\quad - \delta_{\nu\rho} [2 \cos(\frac{1}{2}k_{1\nu} + \frac{1}{2}k_{2\nu}) e^{-\frac{i}{2}(k_{1\mu} - k_{2\mu})}] \end{aligned} \quad (6.78)$$

$$= -h_{\mu\nu\rho}(k_1, k_2) + g_{\mu\nu\rho}(k_1, k_2). \quad (6.79)$$

Here  $h_{\mu\nu\rho}$  and  $g_{\mu\nu\rho}$  are essentially the real and imaginary parts of  $a_{1\mu\nu\rho}$ , i.e.

$$\begin{aligned} g_{\mu\nu\rho}(k_1, k_2) &= 2i \left( -\delta_{\mu\nu} c(k_{2\mu}) s(2k_{1\rho} + k_{2\rho}) + \delta_{\mu\rho} c(k_{1\mu}) s(2k_{2\nu} + k_{1\nu}) \right. \\ &\quad \left. + \delta_{\nu\rho} s(k_{1\mu} - k_{2\mu}) c(k_{1\nu} + k_{2\nu}) \right) \end{aligned} \quad (6.80)$$

$$\begin{aligned} h_{\mu\nu\rho}(k_1, k_2) &= 2 \left( -\delta_{\mu\nu} s(k_{2\mu}) s(2k_{1\rho} + k_{2\rho}) - \delta_{\mu\rho} s(k_{1\mu}) s(2k_{2\nu} + k_{1\nu}) \right. \\ &\quad \left. + \delta_{\nu\rho} c(k_{1\mu} - k_{2\mu}) c(k_{1\nu} + k_{2\nu}) \right). \end{aligned} \quad (6.81)$$

We know the anti-symmetric  $g_{\mu\nu\rho}$  already from the second order.

Furthermore,

$$\begin{aligned} a_{2\mu\nu}(k_1, k_2) &= 6\delta_{\mu\nu} + \delta_{\mu\nu} \sum_{\alpha=1}^4 [2 \cos(k_{1\alpha} + k_{2\alpha}) - 2] \\ &\quad + 4 \cos(\frac{1}{2}(k_{1\mu} + k_{2\mu})) \cos(\frac{1}{2}(k_{1\nu} + k_{2\nu})) \end{aligned} \quad (6.82)$$

$$= 6\delta_{\mu\nu} - \delta_{\mu\nu} 4s^2(k_1 + k_2) + 4c(k_{1\mu} + k_{2\mu})c(k_{1\nu} + k_{2\nu}) \quad (6.83)$$

where we have defined  $g_{\mu\nu}^{(i)}(k)$  which is a variation of  $g_{\mu\nu}(k)$  with cosines in the second term instead of sines.

For the sum of staples at third order we define

$$S_{3\mu}^{abc}(x) = s_{1\mu}^{abc}(x) + \frac{1}{2}s_{2\mu}^{abc}(x) + \frac{1}{6}s_{3\mu}^{abc}(x) \quad (6.84)$$

with

$$s_{1\mu}^{abc}(x) = \sum_{\nu} \left[ -A_{\nu}^a(x)A_{\mu}^b(x + \hat{\nu})A_{\nu}^c(x + \hat{\mu}) - A_{\nu}^a(x - \hat{\nu})A_{\mu}^b(x - \hat{\nu})A_{\nu}^c(x + \hat{\mu} - \hat{\nu}) \right] \quad (6.85)$$

$$\begin{aligned} s_{2\mu}^{abc}(x) = & \sum_{\nu} \left[ \{ A_{\nu}^a(x)A_{\mu}^b(x + \hat{\nu})A_{\nu}^c(x + \hat{\mu}) + A_{\nu}^a(x)A_{\nu}^b(x + \hat{\mu})A_{\nu}^c(x + \hat{\mu}) \right. \\ & + A_{\mu}^a(x + \hat{\nu})A_{\nu}^b(x + \hat{\mu})A_{\nu}^c(x + \hat{\mu}) - A_{\nu}^a(x - \hat{\nu})A_{\mu}^b(x - \hat{\nu})A_{\mu}^c(x - \hat{\nu}) \\ & - A_{\nu}^a(x - \hat{\nu})A_{\nu}^b(x + \hat{\mu} - \hat{\nu})A_{\nu}^c(x + \hat{\mu} - \hat{\nu}) + A_{\mu}^a(x - \hat{\nu})A_{\nu}^b(x + \hat{\mu} - \hat{\nu})A_{\nu}^c(x + \hat{\mu} - \hat{\nu}) \} \\ & + \{ -A_{\mu}^a(x + \hat{\nu})A_{\mu}^b(x + \hat{\nu})A_{\nu}^c(x + \hat{\mu}) + A_{\nu}^a(x)A_{\nu}^b(x)A_{\mu}^c(x + \hat{\nu}) - A_{\nu}^a(x)A_{\nu}^b(x)A_{\nu}^c(x + \hat{\mu}) \\ & + A_{\mu}^a(x - \hat{\nu})A_{\mu}^b(x - \hat{\nu})A_{\nu}^c(x + \hat{\mu} - \hat{\nu}) + A_{\nu}^a(x - \hat{\nu})A_{\nu}^b(x - \hat{\nu})A_{\mu}^c(x - \hat{\nu}) \\ & \left. + A_{\nu}^a(x - \hat{\nu})A_{\nu}^b(x - \hat{\nu})A_{\nu}^c(x + \hat{\mu} - \hat{\nu}) \right] \end{aligned} \quad (6.86)$$

$$\begin{aligned} s_{3\mu}^{abc}(x) = & \sum_{\nu} \left[ -2\delta_{\mu\nu}A_{\mu}^a(x)A_{\mu}^b(x)A_{\mu}^c(x) + A_{\nu}^a(x)A_{\nu}^b(x)A_{\nu}^c(x) + A_{\mu}^a(x + \hat{\nu})A_{\mu}^b(x + \hat{\nu})A_{\mu}^c(x + \hat{\nu}) \right. \\ & - A_{\nu}^a(x + \hat{\mu})A_{\nu}^b(x + \hat{\mu})A_{\nu}^c(x + \hat{\mu}) - A_{\nu}^a(x - \hat{\nu})A_{\nu}^b(x - \hat{\nu})A_{\nu}^c(x - \hat{\nu}) \\ & \left. + A_{\mu}^a(x - \hat{\nu})A_{\mu}^b(x - \hat{\nu})A_{\mu}^c(x - \hat{\nu}) + A_{\nu}^a(x + \hat{\mu} - \hat{\nu})A_{\nu}^b(x + \hat{\mu} - \hat{\nu})A_{\nu}^c(x + \hat{\mu} - \hat{\nu}) \right]. \end{aligned} \quad (6.87)$$

They can be written as

$$s_{1\mu}^{abc}(x) = \sum_{y,z,r} \sum_{\nu\rho\sigma} b_{1\mu\nu\rho\sigma}(y, z, r) A_{\nu}^a(x + y) A_{\rho}^b(x + z) A_{\sigma}^c(x + r) \quad (6.88)$$

$$\begin{aligned} s_{2\mu}^{abc}(x) = & \sum_{y,z} \sum_{\nu\rho} b_{21\mu\nu\rho}(y, z) A_{\nu}^a(x + y) A_{\rho}^b(x + z) A_{\rho}^c(x + z) \\ & + \sum_{y,z} \sum_{\nu\rho} b_{22\mu\nu\rho}(y, z) A_{\nu}^a(x + y) A_{\nu}^b(x + y) A_{\rho}^c(x + z) \end{aligned} \quad (6.89)$$

$$s_{3\mu}^{abc}(x) = \sum_y \sum_{\nu} b_{3\mu\nu}(y) A_{\nu}^a(x + y) A_{\nu}^b(x + y) A_{\nu}^c(x + y) \quad (6.90)$$

with

$$b_{1\mu\nu\rho\sigma}(y, z, r) = -\delta_{\mu\rho}\delta_{\nu\sigma} \left( \delta(y, 0)\delta(z, \hat{\nu})\delta(r, \hat{\mu}) + \delta(y, -\hat{\nu})\delta(z, -\hat{\nu})\delta(r, \hat{\mu} - \hat{\nu}) \right) \quad (6.91)$$

$$b_{21\mu\nu\rho}(y, z) = \delta_{\mu\nu} \left( \delta(y, \hat{\rho})\delta(z, \hat{\mu}) + \delta(y, -\hat{\rho})\delta(z, \hat{\mu} - \hat{\rho}) \right)$$

$$\begin{aligned}
& + \delta_{\mu\rho} \left( \delta(y, 0) \delta(z, \hat{\nu}) - \delta(y, -\hat{\nu}) \delta(z, -\hat{\nu}) \right) \\
& + \delta_{\nu\rho} \left( \delta(y, 0) \delta(z, \hat{\mu}) - \delta(y, -\hat{\mu}) \delta(z, \hat{\mu} - \hat{\nu}) \right)
\end{aligned} \tag{6.92}$$

$$\begin{aligned}
b_{22\mu\nu\rho}(y, z) = & \delta_{\mu\nu} \left( -\delta(y, \hat{\rho}) \delta(z, \hat{\mu}) + \delta(y, -\hat{\rho}) \delta(z, \hat{\mu} - \hat{\rho}) \right) \\
& + \delta_{\mu\rho} \left( \delta(y, 0) \delta(z, \hat{\nu}) + \delta(y, -\hat{\nu}) \delta(z, -\hat{\nu}) \right) \\
& + \delta_{\nu\rho} \left( -\delta(y, 0) \delta(z, \hat{\mu}) + \delta(y, -\hat{\mu}) \delta(z, \hat{\mu} - \hat{\nu}) \right)
\end{aligned} \tag{6.93}$$

$$b_{3\mu\nu}(y) = 6\delta_{\mu\nu}\delta(y, 0) + g_{\mu\nu}(y) . \tag{6.94}$$

Fourier transforming the  $s_{i\mu}^{abc}(x)$  leads to

$$s_{1\mu}^{abc}(x) = \sum_{\nu\rho\sigma} \int \frac{d^4k_1 d^4k_2 d^4k_3}{(2\pi)^{12}} e^{-i(x + \frac{1}{2}\hat{\mu})(k_1 + k_2 + k_3)} b_{1\mu\nu\rho\sigma}(k_1, k_2, k_3) A_\nu^a(k_1) A_\rho^b(k_2) A_\sigma^c(k_3) \tag{6.95}$$

$$\begin{aligned}
s_{2\mu}^{abc}(x) = & \sum_{\nu\rho} \int \frac{d^4k_1 d^4k_2 d^4k_3}{(2\pi)^{12}} e^{-i(x + \frac{1}{2}\hat{\mu})(k_1 + k_2 + k_3)} b_{21\mu\nu\rho}(k_1, k_2 + k_3) A_\nu^a(k_1) A_\rho^b(k_2) A_\rho^c(k_3) \\
& + \sum_{\nu\rho} \int \frac{d^4k_1 d^4k_2 d^4k_3}{(2\pi)^{12}} e^{-i(x + \frac{1}{2}\hat{\mu})(k_1 + k_2 + k_3)} b_{22\mu\nu\rho}(k_1 + k_2, k_3) A_\nu^a(k_1) A_\nu^b(k_2) A_\rho^c(k_3)
\end{aligned} \tag{6.96}$$

$$s_{3\mu}^{abc}(x) = \sum_{\nu} \int \frac{d^4k_1 d^4k_2 d^4k_3}{(2\pi)^{12}} e^{-i(x + \frac{1}{2}\hat{\mu})(k_1 + k_2 + k_3)} g_{\mu\nu}(k_1 + k_2 + k_3) A_\nu^a(k_1) A_\nu^b(k_2) A_\nu^c(k_3) \tag{6.97}$$

with

$$b_{1\mu\nu\rho\sigma}(k_1, k_2, k_3) = -2\delta_{\mu\rho}\delta_{\nu\sigma} \cos\left(\frac{1}{2}k_{1\nu} + k_{2\nu} + \frac{1}{2}k_{3\nu}\right) e^{\frac{i}{2}(k_{1\mu} - k_{3\mu})} \tag{6.98}$$

$$\begin{aligned}
b_{21\mu\nu\rho}(k_1, k_2 + k_3) = & \delta_{\mu\nu} 2 \cos\left(k_{1\rho} + \frac{1}{2}(k_{2\rho} + k_{3\rho})\right) e^{-\frac{i}{2}(k_{2\mu} + k_{3\mu})} \\
& + \delta_{\mu\rho} (-2i) \sin\left(\frac{1}{2}k_{1\nu} + k_{2\nu} + k_{3\nu}\right) e^{\frac{i}{2}k_{1\mu}} \\
& + \delta_{\nu\rho} (-2i) \sin\left(\frac{1}{2}(k_{1\nu} + k_{2\nu} + k_{3\nu})\right) e^{\frac{i}{2}(k_{1\mu} - k_{2\mu} - k_{3\mu})}
\end{aligned} \tag{6.99}$$

$$\begin{aligned}
b_{22\mu\nu\rho}(k_1 + k_2, k_3) = & \delta_{\mu\nu} 2i \sin\left(k_{1\rho} + k_{2\rho} + \frac{1}{2}k_{3\rho}\right) e^{-\frac{i}{2}k_{3\mu}} \\
& + \delta_{\mu\rho} 2 \cos\left(\frac{1}{2}(k_{1\nu} + k_{2\nu}) + k_{3\nu}\right) e^{\frac{i}{2}(k_{1\mu} + k_{2\mu})} \\
& + \delta_{\nu\rho} 2i \sin\left(\frac{1}{2}(k_{1\nu} + k_{2\nu} + k_{3\nu})\right) e^{\frac{i}{2}(k_{1\mu} + k_{2\mu} - k_{3\mu})}
\end{aligned} \tag{6.100}$$

$$b_{3\mu\nu}(k_1 + k_2 + k_3) = 6\delta_{\mu\nu} + g_{\mu\nu}(k_1 + k_2 + k_3) . \tag{6.101}$$

We can symmetrise these expressions according to

$$(T^a T^b T^c + T^c T^b T^a) v_{i\mu}^{abc} = (T^a T^b T^c + T^c T^b T^a) \frac{1}{2} (v_{i\mu}^{abc} + v_{i\mu}^{cba}) \tag{6.102}$$

and observe that under the integrals

$$b_{1\mu\nu\rho\sigma}(k_1, k_2, k_3) A_\nu^c(k_1) A_\rho^b(k_2) A_\sigma^a(k_3) = b_{1\mu\sigma\rho\nu}(k_3, k_2, k_1) A_\nu^a(k_1) A_\rho^b(k_2) A_\sigma^c(k_3) \quad (6.103)$$

$$b_{21\mu\nu\rho}(k_1, k_2 + k_3) A_\nu^c(k_1) A_\rho^b(k_2) A_\sigma^a(k_3) = b_{21\mu\rho\nu}(k_3, k_1 + k_2) A_\nu^a(k_1) A_\rho^b(k_2) A_\sigma^c(k_3) \quad (6.104)$$

$$b_{22\mu\nu\rho}(k_1 + k_2, k_3) A_\nu^c(k_1) A_\rho^b(k_2) A_\sigma^a(k_3) = b_{22\mu\rho\nu}(k_2 + k_3, k_1) A_\nu^a(k_1) A_\rho^b(k_2) A_\sigma^c(k_3). \quad (6.105)$$

Thus we need

$$b_{1\mu\nu\rho\sigma}(k_1, k_2, k_3) + b_{1\mu\sigma\rho\nu}(k_3, k_2, k_1) = -4\delta_{\mu\rho}\delta_{\nu\sigma}c(k_{1\nu} + 2k_{2\nu} + k_{3\nu})c(k_{1\mu} - k_{3\mu}) \quad (6.106)$$

$$=: g_{\mu\nu\rho\sigma}^{(iii)}(k_1, k_2, k_3) \quad (6.107)$$

$$\begin{aligned} b_{21\mu\nu\rho}(k_1, k_2 + k_3) + b_{22\mu\rho\nu}(k_2 + k_3, k_1) &= 4\delta_{\mu\nu}c(2k_{1\rho} + k_{2\rho} + k_{3\rho})c(k_{2\mu} + k_{3\mu}) \\ &\quad + 4\delta_{\mu\rho}s(k_{1\mu})s(k_{1\nu} + 2(k_{2\nu} + k_{3\nu})) \\ &\quad + 4\delta_{\nu\rho}s(k_{1\mu} - k_{2\mu} - k_{3\mu})s(k_{1\nu} + k_{2\nu} + k_{3\nu}) \end{aligned} \quad (6.108)$$

$$=: g_{\mu\nu\rho}^{(ii)}(k_1, k_2 + k_3) \quad (6.109)$$

$$b_{22\mu\nu\rho}(k_1 + k_2, k_3) + b_{21\mu\rho\nu}(k_3, k_1 + k_2) = g_{\mu\rho\nu}^{(ii)}(k_3, k_1 + k_2). \quad (6.110)$$

Now we can write

$$\begin{aligned} \hat{A}_\mu^{(1)abc}(k_1, k_2, k_3) &= \rho \sum_{\nu\rho\sigma} \left( 3(h_{\mu\nu\rho}(k_1, k_2) - g_{\mu\nu\rho}(k_1, k_2))\delta_{\mu\sigma} + \frac{3}{2}g_{\mu\nu}(k_1)\delta_{\mu\rho}\delta_{\mu\sigma} \right. \\ &\quad \left. + \frac{3}{2}(g_{\mu\nu}^{(i)}(k_1, k_2)\delta_{\nu\rho}\delta_{\mu\sigma} + g_{\mu\nu\rho}^{(ii)}(k_1, k_2 + k_3)\delta_{\rho\sigma} + g_{\mu\nu\rho\sigma}^{(iii)}(k_1, k_2, k_3)) \right. \\ &\quad \left. + \frac{1}{2}g_{\mu\nu}(k_1 + k_2 + k_3)\delta_{\nu\rho}\delta_{\nu\sigma} \right) A_\nu^a(k_1) A_\rho^b(k_2) A_\sigma^c(k_3) \end{aligned} \quad (6.111)$$

For a general smearing step  $n > 1$  we have to take into account that in the previous step  $A_\mu^{(n-1)[ab]} \neq 0$ ,  $\bar{A}_\mu^{(n-1)abc} \neq 0$ , and  $\hat{A}_\mu^{(n-1)abc} \neq 0$ . Again we replace the un-smeared gluon field  $A^{(0)}$  in the previous orders by the smeared one  $\tilde{A}^{(n)}$  and collect all terms of order  $g_0^3$ :

$$\begin{aligned} U_\mu^{(n+1)}(k) &= 1 + ig_0 \sum_\nu \tilde{g}_{\mu\nu}(\varrho, k) \left( T^a A_\nu^{(n)a}(k) - \frac{g_0}{2i}[T^a, T^b] A_\nu^{(n)[ab]}(k_1, k_2) \right. \\ &\quad \left. - \frac{g_0^2}{6} \left( T^a T^b T^c + T^c T^b T^a - \frac{1}{N_c} \text{Tr}[T^a T^b T^c + T^c T^b T^a] \right) A_\nu^{(n)abc}(k_3, k_4, k_5) \right) \\ &\quad - \frac{g_0^2}{2} \sum_{\nu\rho} \left( \tilde{g}_{\mu\nu}(\varrho, k_1) \tilde{g}_{\mu\rho}(\varrho, k_2) + 2g_{\mu\nu\rho}(k_1, k_2) \right) \left( T^a A_\nu^{(n)a}(k_1) - \frac{g_0}{2i}[T^a, T^b] A_\nu^{(n)[ab]}(k_{11}, k_{12}) \right) \\ &\quad \times \left( T^a A_\rho^{(n)a}(k_2) - \frac{g_0}{2i}[T^a, T^b] A_\rho^{(n)[ab]}(k_{21}, k_{22}) \right) \\ &\quad - i \frac{g_0^3}{6} \sum_{\nu\rho\sigma} \left( T^a T^b T^c \tilde{g}_{\mu\nu}(\varrho, k_1) \tilde{g}_{\mu\rho}(\varrho, k_2) \tilde{g}_{\mu\sigma}(\varrho, k_3) + \frac{3}{2}\{T^a, [T^b, T^c]\} \tilde{g}_{\mu\nu}(\varrho, k_1) \rho g_{\mu\rho\sigma}(k_2, k_3) \right) \end{aligned}$$

$$\begin{aligned}
& + [T^a, [T^b, T^c]] \left( -\frac{3}{2} \delta_{\mu\nu} \varrho g_{\mu\rho\sigma}(k_2, k_3) + \frac{1}{2} \delta_{\mu\nu} \tilde{g}_{\mu\rho}(\varrho, k_2) \delta_{\mu\sigma} + \frac{1}{2} \tilde{g}_{\mu\nu}(\varrho, k_1) \tilde{g}_{\mu\rho}(\varrho, k_2) \delta_{\mu\sigma} \right) \\
& + \left( T^a T^b T^c + T^c T^b T^a - \frac{1}{N_c} \text{Tr}[T^a T^b T^c + T^c T^b T^a] \right) \hat{G}_{\mu\nu\rho\sigma}(k_1, k_2, k_3) \\
& \times A_\nu^{(n)a}(k_1) A_\rho^{(n)b}(k_2) A_\sigma^{(n)c}(k_3)
\end{aligned} \tag{6.112}$$

with  $k = k_1 + k_2 = k_3 + k_4 + k_5$ ,  $k_1 = k_{11} + k_{12}$ , and  $k_2 = k_{21} + k_{22}$ . From the third term involving the product  $\tilde{A}_\nu \tilde{A}_\rho$  the following terms appear at order  $g_0^3$ :

$$\begin{aligned}
& -i \frac{g_0^3}{4} \sum_{\nu\rho} \left( (\tilde{g}_{\mu\nu}(\varrho, k_1) \tilde{g}_{\mu\rho}(\varrho, k_2 + k_3) + 2g_{\mu\nu\rho}(k_1, k_2 + k_3)) T^a [T^b, T^c] A_\nu^{(n)a}(k_1) A_\rho^{(n)[bc]}(k_2, k_3) \right. \\
& + (\tilde{g}_{\mu\nu}(\varrho, k_1 + k_2) \tilde{g}_{\mu\rho}(\varrho, k_3) + 2g_{\mu\nu\rho}(k_1 + k_2, k_3)) [T^a, T^b] T^c A_\nu^{(n)[ab]}(k_1, k_2) A_\rho^{(n)c}(k_3) \Big) \\
& = -i \frac{g_0^3}{6} \left( \frac{3}{2} \{T^a, [T^b, T^c]\} \sum_{\nu\rho} \tilde{g}_{\mu\nu}(\varrho, k_1) \tilde{g}_{\mu\rho}(\varrho, k_2 + k_3) A_\nu^{(n)a}(k_1) A_\rho^{(n)[bc]}(k_2, k_3) \right. \\
& \left. + 3[T^a, [T^b, T^c]] \sum_{\nu\rho} g_{\mu\nu\rho}(k_1, k_2 + k_3) A_\nu^{(n)a}(k_1) A_\rho^{(n)[bc]}(k_2, k_3) \right) .
\end{aligned} \tag{6.113}$$

Then we have for our two third-order fields:

$$\begin{aligned}
\bar{A}_\mu^{(n+1)abc}(k_1, k_2, k_3) &= \sum_\nu \tilde{g}_{\mu\nu}(\varrho, k_1 + k_2 + k_3) \bar{A}_\nu^{(n)abc}(k_1, k_2, k_3) \\
& + 3\varrho \sum_{\nu\rho} g_{\mu\nu\rho}(k_1, k_2 + k_3) A_\nu^{(n)a}(k_1) A_\rho^{(n)[bc]}(k_2, k_3) \\
& - \frac{3}{2}\varrho \sum_{\nu\rho\sigma} \delta_{\mu\nu} g_{\mu\rho\sigma}(k_2, k_3) A_\nu^{(n)a}(k_1) A_\rho^{(n)b}(k_2) A_\sigma^{(n)c}(k_3) \\
& + \frac{1}{2} A_\mu^{(n)a}(k_1) A_\mu^{(n+1)b}(k_2) A_\mu^{(n)c}(k_3) + \frac{1}{2} A_\mu^{(n+1)a}(k_1) A_\mu^{(n+1)b}(k_2) A_\mu^{(n)c}(k_3)
\end{aligned} \tag{6.114}$$

$$\begin{aligned}
\hat{A}_\mu^{(n+1)abc}(k_1, k_2, k_3) &= \sum_\nu \tilde{g}_{\mu\nu}(\varrho, k_1 + k_2 + k_3) \hat{A}_\nu^{(n)abc}(k_1, k_2, k_3) \\
& + \varrho \sum_{\nu\rho\sigma} \left( 3(h_{\mu\nu\rho}(k_1, k_2) + g_{\mu\nu\rho}(k_1, k_2)) \delta_{\mu\sigma} + \frac{3}{2} g_{\mu\nu}(k_1) \delta_{\mu\rho} \delta_{\mu\sigma} \right. \\
& + \frac{3}{2} \left( g_{\mu\nu}^{(i)}(k_1, k_2) \delta_{\nu\rho} \delta_{\mu\sigma} + g_{\mu\nu\rho}^{(ii)}(k_1, k_2 + k_3) \delta_{\rho\sigma} + g_{\mu\nu\rho\sigma}^{(iii)}(k_1, k_2, k_3) \right) \\
& \left. + \frac{1}{2} g_{\mu\nu}(k_1 + k_2 + k_3) \delta_{\nu\rho} \delta_{\nu\sigma} \right) A_\nu^{(n)a}(k_1) A_\rho^{(n)b}(k_2) A_\sigma^{(n)c}(k_3) ,
\end{aligned} \tag{6.115}$$

and finally

$$\begin{aligned}
A_\mu^{(n+1)abc}(k_1, k_2, k_3) &= \hat{A}_\mu^{(n+1)abc}(k_1, k_2, k_3) + 2\bar{A}_\mu^{(n+1)a[bc]}(k_1, k_2, k_3) \\
& = \sum_\nu \tilde{g}_{\mu\nu}(\varrho, k_1 + k_2 + k_3) A_\nu^{(n)abc}(k_1, k_2, k_3)
\end{aligned} \tag{6.116}$$

$$\begin{aligned}
& + 6\varrho \sum_{\nu\rho} g_{\mu\nu\rho}(k_1, k_2 + k_3) A_\nu^{(n)a}(k_1) A_\rho^{(n)[bc]}(k_2, k_3) \\
& + \sum_{\nu\rho\sigma} \left( \frac{1}{2} \varrho^2 \left( g_{\mu\nu}(k_1) g_{\mu\rho}(k_2) \delta_{\mu\sigma} - g_{\mu\nu}(k_1) \delta_{\mu\rho} g_{\mu\sigma}(k_3) \right) + \varrho G_{\mu\nu\rho\sigma}(k_1, k_2, k_3) \right) \\
& \times A_\nu^{(n)a}(k_1) A_\rho^{(n)b}(k_2) A_\sigma^{(n)c}(k_3)
\end{aligned} \tag{6.117}$$

with

$$\begin{aligned}
G_{\mu\nu\rho\sigma}(k_1, k_2, k_3) = & \frac{1}{2} g_{\mu\nu}(k_1) \delta_{\mu\rho} \delta_{\mu\sigma} + \delta_{\mu\nu} g_{\mu\rho}(k_2) \delta_{\mu\sigma} + 3h_{\mu\nu\rho}(k_1, k_2) \delta_{\mu\sigma} \\
& + \frac{3}{2} \left( g_{\mu\nu}^{(i)}(k_1, k_2) \delta_{\nu\rho} \delta_{\mu\sigma} + g_{\mu\nu\rho}^{(ii)}(k_1, k_2 + k_3) \delta_{\rho\sigma} + g_{\mu\nu\rho\sigma}^{(iii)}(k_1, k_2, k_3) \right) \\
& + \frac{1}{2} g_{\mu\nu}(k_1 + k_2 + k_3) \delta_{\nu\rho} \delta_{\nu\sigma} .
\end{aligned} \tag{6.118}$$

After two smearing steps:

$$\begin{aligned}
A_\mu^{(2)abc}(k_1, k_2, k_3) = & \sum_{\alpha} \tilde{g}_{\mu\alpha}(\varrho, k_1 + k_2 + k_3) \sum_{\nu\rho\sigma} G_{\alpha\nu\rho\sigma}(\varrho, k_1, k_2, k_3) A_\nu^{(0)a}(k_1) A_\rho^{(0)b}(k_2) A_\sigma^{(0)c}(k_3) \\
& + 6\varrho \sum_{\nu\rho} g_{\mu\nu\rho}(k_1, k_2 + k_3) A_\nu^{(1)a}(k_1) A_\rho^{(1)[bc]}(k_2, k_3) \\
& + \sum_{\nu\rho\sigma} \tilde{G}_{\mu\nu\rho}(\varrho, k_1, k_2, k_3) A_\nu^{(1)a}(k_1) A_\rho^{(1)b}(k_2) A_\sigma^{(1)c}(k_3) .
\end{aligned} \tag{6.119}$$

After three smearing steps:

$$\begin{aligned}
A_\mu^{(3)abc}(k_1, k_2, k_3) = & \sum_{\alpha} \tilde{g}_{\mu\alpha}^2(\varrho, k_1 + k_2 + k_3) \sum_{\nu\rho\sigma} \tilde{G}_{\alpha\nu\rho\sigma}(\varrho, k_1, k_2, k_3) A_\nu^{(0)a}(k_1) A_\rho^{(0)b}(k_2) A_\sigma^{(0)c}(k_3) \\
& + \sum_{\alpha} \tilde{g}_{\mu\alpha}(\varrho, k_1 + k_2 + k_3) \sum_{\nu\rho\sigma} \tilde{G}_{\alpha\nu\rho\sigma}(\varrho, k_1, k_2, k_3) A_\nu^{(1)a}(k_1) A_\rho^{(1)b}(k_2) A_\sigma^{(1)c}(k_3) \\
& + \tilde{G}_{\mu\nu\rho}(\varrho, k_1, k_2, k_3) A_\nu^{(2)a}(k_1) A_\rho^{(2)b}(k_2) A_\sigma^{(2)c}(k_3) \\
& + 6\varrho \sum_{\alpha} \tilde{g}_{\mu\alpha}(\varrho, k_1 + k_2 + k_3) \sum_{\nu\rho} g_{\alpha\nu\rho}(k_1, k_2 + k_3) A_\nu^{(1)a}(k_1) A_\rho^{(1)[bc]}(k_2, k_3) \\
& + 6\varrho \sum_{\nu\rho} g_{\mu\nu\rho}(k_1, k_2 + k_3) A_\nu^{(2)a}(k_1) A_\rho^{(2)[bc]}(k_2, k_3) .
\end{aligned} \tag{6.120}$$

After  $n$  smearing steps:

$$\begin{aligned}
A_\mu^{(n)abc}(k_1, k_2, k_3) = & 6\varrho \sum_{\alpha\nu\rho} g_{\alpha\nu\rho}(k_1, k_2 + k_3) \sum_{m=1}^{n-1} \tilde{g}_{\mu\alpha}^{n-m-1}(\varrho, k_1 + k_2 + k_3) A_\nu^{(m)a}(k_1) A_\rho^{(m)[bc]}(k_2, k_3) \\
& + \sum_{\alpha\nu\rho\sigma} \left( \frac{1}{2} \varrho^2 \left( g_{\alpha\nu}(k_1) g_{\mu\rho}(k_2) \delta_{\mu\sigma} - g_{\mu\nu}(k_1) \delta_{\mu\rho} g_{\mu\sigma}(k_3) \right) + \varrho G_{\alpha\nu\rho\sigma}(k_1, k_2, k_3) \right)
\end{aligned}$$

$$\times \sum_{m=0}^{n-1} \tilde{g}_{\mu\alpha}^{n-m-1}(\varrho, k_1 + k_2 + k_3) A_\nu^{(m)a}(k_1) A_\rho^{(m)b}(k_2) A_\sigma^{(m)c}(k_3). \quad (6.121)$$

Plugging in the relations from leading order and next-to-leading order, we express the end result as a function of the unsmeared fields:

$$\begin{aligned} A_\mu^{(n)abc}(k_1, k_2, k_3) &= \\ &\sum_{\nu\rho\sigma} \left( \sum_{\alpha\beta\gamma} 6\varrho g_{\alpha\beta\gamma}(k_1, k_2 + k_3) \sum_{m=1}^{n-1} \tilde{g}_{\mu\alpha}^{n-m-1}(\varrho, k_1 + k_2 + k_3) \tilde{g}_{\beta\nu}^m(\varrho, k_1) \tilde{g}_{\gamma\rho\sigma}^{(m)}(\varrho, k_2, k_3) \right. \\ &+ \sum_{\alpha\beta\gamma\delta} \left( \frac{1}{2} \varrho^2 \left( g_{\alpha\beta}(k_1) g_{\alpha\gamma}(k_2) \delta_{\alpha\delta} - g_{\alpha\beta}(k_1) \delta_{\alpha\gamma} g_{\alpha\delta}(k_3) \right) + \varrho G_{\alpha\beta\gamma\delta}(k_1, k_2, k_3) \right) \\ &\times \left. \sum_{m=0}^{n-1} \tilde{g}_{\mu\alpha}^{n-m-1}(\varrho, k_1 + k_2 + k_3) \tilde{g}_{\beta\nu}^m(\varrho, k_1) \tilde{g}_{\gamma\rho}^m(\varrho, k_2) \tilde{g}_{\delta\sigma}^m(\varrho, k_3) \right) A_\nu^{(0)a}(k_1) A_\rho^{(0)b}(k_2) A_\sigma^{(0)c}(k_3) \\ &=: \sum_{\nu\rho\sigma} \tilde{g}_{\mu\nu\rho\sigma}^{(n)}(k_1, k_2, k_3) A_\nu^{(0)a}(k_1) A_\rho^{(0)b}(k_2) A_\sigma^{(0)c}(k_3). \end{aligned} \quad (6.122)$$

and we have found the last of the three  $\tilde{g}$ -functions from Eq. (6.26).

## 6.2 Perturbative Wilson Flow

The Wilson flow is defined through

$$\partial_t U_\mu(x, t) = iQ_\mu(x, t)U_\mu(x, t) \quad (6.123)$$

$$U_\mu(x, 0) = U_\mu(x) \quad (6.124)$$

with the same  $Q_\mu$  as in the definition of stout smearing but made up from the “flowed” fields  $U_\mu(x, t)$  instead of the smeared fields. We already know the perturbative expansion of  $Q_\mu$

$$\begin{aligned} Q_\mu(x, t) &= g_0 T^a Q_{1\mu}^a(x, t) + ig_0^2 [T^a, T^b] Q_{2\mu}^{ab}(x, t) \\ &+ g_0^3 \left( T^a T^b T^c + T^c T^b T^a - \frac{1}{N_c} \text{Tr} [T^a T^b T^c + T^c T^b T^a] \right) Q_{3\mu}^{abc}(x, t) \end{aligned} \quad (6.125)$$

We define the expansion of the flowed link variable in terms of fields  $A_\mu^a(x, t)$ ,  $A_\mu^{[ab]}(x, t)$ , and  $A_\mu^{abc}(x, t)$  such that similarly to the smeared case

$$\begin{aligned} U_\mu(x, t) &= 1 + ig_0 T^a A_\mu^a(x, t) - \frac{g_0^2}{2} \left( T^a T^b A_\mu^a(x, t) A_\mu^b(x, t) + [T^a, T^b] A_\mu^{[ab]}(x, t) \right) \\ &- i \frac{g_0^3}{6} \left( T^a T^b T^c A_\mu^a(x, t) A_\mu^b(x, t) A_\mu^c(x, t) + \frac{3}{2} \{T^a, [T^b, T^c]\} A_\mu^a(x, t) A_\mu^{[ab]}(x, t) \right. \\ &\left. + \left( T^a T^b T^c + T^c T^b T^a - \frac{1}{N_c} \text{Tr} [T^a T^b T^c + T^c T^b T^a] \right) A_\mu^{abc}(x, t) \right) + \mathcal{O}(g_0^4). \end{aligned} \quad (6.126)$$

They fulfil the initial conditions

$$A_\mu^a(x, 0) = A_\mu^a(x), \quad A_\mu^{[ab]}(x, 0) = 0, \quad A_\mu^{abc}(x, 0) = 0 \quad (6.127)$$

and we define their Fourier transforms consistently:

$$A_\mu^a(x, t) = \int_{-\pi}^{\pi} \frac{d^4 k}{(2\pi)^4} e^{i(x+\hat{\mu}/2)k} A_\mu^a(k, t) \quad (6.128)$$

$$A_\mu^{ab}(x, t) = \int_{-\pi}^{\pi} \frac{d^4 k_1}{(2\pi)^4} \int_{-\pi}^{\pi} \frac{d^4 k_2}{(2\pi)^4} e^{i(x+\hat{\mu}/2)(k_1+k_2)} A_\mu^{ab}(k_1, k_2, t) \quad (6.129)$$

$$A_\mu^{abc}(x, t) = \int_{-\pi}^{\pi} \frac{d^4 k_1}{(2\pi)^4} \int_{-\pi}^{\pi} \frac{d^4 k_2}{(2\pi)^4} \int_{-\pi}^{\pi} \frac{d^4 k_3}{(2\pi)^4} e^{i(x+\hat{\mu}/2)(k_1+k_2+k_3)} A_\mu^{abc}(k_1, k_2, k_3, t) \quad (6.130)$$

As in the stout smearing case, we can connect the perturbative fields to the flowed gluon field  $\tilde{A}_\mu^a(g_0, x, t)$  in the  $SU(N_c)$  expansion such that

$$U_\mu(x, t) = e^{ig_0 T^a \tilde{A}_\mu^a(g_0, x, t)} \quad (6.131)$$

and

$$\begin{aligned} \tilde{A}_\mu^a(g_0, x, t) &= A_\mu^a(x, t) - \frac{g_0}{2} f^{abc} A_\mu^{[bc]}(x, t) \\ &\quad - \frac{g_0^2}{6} \left[ \frac{1}{N_c} \delta^{ae} \delta^{bc} + \frac{1}{2} (d^{bcd} d^{eda} - f^{bcd} f^{eda}) \right] A_\mu^{ebc}(x, t) + \mathcal{O}(g_0^3). \end{aligned} \quad (6.132)$$

### 6.2.1 Leading Order

At leading order the differential equation is

$$\partial_t A_\mu^a(x, t) = Q_{1\mu}^a(x, t) = \sum_{\nu, y} g_{\mu\nu}(y) A_\nu^a(x+y, t) \quad (6.133)$$

which in momentum space becomes

$$\partial_t A_\mu^a(k, t) = \sum_{\nu} g_{\mu\nu}(k) A_\nu^a(k, t) \quad (6.134)$$

with the same  $g_{\mu\nu}$  as defined at leading order of the stout smearing. With

$$g_{\mu\nu}^2(k) = \sum_{\alpha} g_{\mu\alpha}(k) g_{\alpha\nu}(k) = -\hat{k}^2 g_{\mu\nu}(k), \quad (6.135)$$

the matrix exponential of  $g$  is

$$\begin{aligned} \exp(g(k)t)_{\mu\nu} &= \delta_{\mu\nu} + g_{\mu\nu} t + \frac{1}{2} g_{\mu\nu}^2 t^2 + \dots \\ &= \delta_{\mu\nu} - \frac{1}{\hat{k}^2} (e^{-\hat{k}^2 t} - 1) g_{\mu\nu}(k). \end{aligned} \quad (6.136)$$

With the initial condition for  $t = 0$ , we arrive at:

$$A_\mu^a(k, t) = \sum_\nu \left( e^{-\hat{k}^2 t} \delta_{\mu\nu} - \left( e^{-\hat{k}^2 t} - 1 \right) \frac{\hat{k}_\mu \hat{k}_\nu}{\hat{k}^2} \right) A_\nu^a(k, 0) \quad (6.137)$$

$$=: \sum_\nu B_{\mu\nu}(k, t) A_\nu^a(k, 0) \quad (6.138)$$

It is easy to see that for an infinitesimal flow-time  $t = \epsilon$ , the exponentials become  $e^{-\hat{k}^2 \epsilon} = 1 - \epsilon \hat{k}^2 + \mathcal{O}(\epsilon^2)$  and the flow transformation becomes the same as a stout smearing with smearing parameter  $\varrho = \epsilon$ , reiterating the fact that the Wilson flow is generated by infinitesimal stout smearing.

The same result is obtained by starting from  $n$  stout smearings and taking the limit  $n \rightarrow \infty$  while keeping the product  $n\varrho =: t$  constant. Then  $f(k)^n = (1 - \frac{t}{n} \hat{k}^2)^n \rightarrow e^{-\hat{k}^2 t}$  [99]. Moreover, this means for a small flow time  $t < 1$ :

$$B_{\mu\nu}(k, t) = \tilde{g}_{\mu\nu}(t, k) + \frac{t^2}{2} (\hat{k}^2)^2 g_{\mu\nu}(k) + \mathcal{O}(t^3) \quad (6.139)$$

$$= \tilde{g}_{\mu\nu}^2(t/2, k) + \frac{t^2}{4} (\hat{k}^2)^2 g_{\mu\nu}(k) + \mathcal{O}(t^3) \quad (6.140)$$

$$= \tilde{g}_{\mu\nu}^n(t/n, k) + \frac{t^2}{2n} (\hat{k}^2)^2 g_{\mu\nu}(k) + \mathcal{O}(t^3). \quad (6.141)$$

Thus the error we get by approximating the flowed field by the field which has been smeared  $n$  times with smearing parameter  $\varrho = t/n$  is always of the order  $t^2$  but decreases with  $1/n$ .

### 6.2.2 Next-to-Leading Order

At order  $g_0^2$ , the differential equation is

$$T^a T^b \partial_t (A_\mu^a(x, t) A_\mu^b(x, t)) + [T^a, T^b] \partial_t A_\mu^{[ab]}(x) = 2T^a T^b Q_{1\mu}^a(x, t) A_\mu^b(x, t) + 2[T^a, T^b] Q_{2\mu}^{ab}(x, t) \quad (6.142)$$

With

$$Q_{2\mu}^{ab}(x, t) = \frac{1}{2} \left( -S_{1\mu}^a(x, t) A_\mu^b(x, t) + S_{2\mu}^{ab}(x, t) - 6A_\mu^{[ab]}(x, t) \right) \quad (6.143)$$

and the result from the leading order we arrive at

$$\partial_t A_\mu^{[ab]}(x) = S_{2\mu}^{[ab]}(x, t) - 6A_\mu^{[ab]}(x, t) \quad (6.144)$$

$$= \sum_{\nu, y} g_{\mu\nu}(y) A_\nu^{[ab]}(x+y, t) + \sum_{\nu\rho, yz} g_{\mu\nu\rho}(y, z) A_\nu^a(x+y, t) A_\rho^b(x+z, t). \quad (6.145)$$

In momentum space, we have

$$\partial_t A_\mu^{ab}(k_1, k_2, t) = \sum_\nu g_{\mu\nu}(k_1 + k_2) A_\nu^{[ab]}(k_1, k_2, t) + \sum_{\nu\rho} g_{\mu\nu\rho}(k_1, k_2) A_\nu^a(k_1, t) A_\rho^b(k_2, t) \quad (6.146)$$

with the same  $g_{\mu\nu\rho}$  we know from stout smearing. Now we have an inhomogenous differential equation and make the ansatz

$$A_\mu^{[ab]}(k_1, k_2, t) = \sum_\alpha B_{\mu\alpha}(k_1 + k_2, t) C_\alpha^{[ab]}(k_1, k_2, t) \quad (6.147)$$

as we know that  $B_{\mu\nu}$  solves the homogeneous part. For the inhomogeneous part we need to solve

$$\sum_\alpha B_{\mu\alpha}(k_1 + k_2, t) \partial_t C_\alpha^{[ab]}(k_1, k_2, t) = \sum_{\nu\rho} g_{\mu\nu\rho}(k_1, k_2) A_\nu^a(k_1, t) A_\rho^b(k_2, t) \quad (6.148)$$

or equivalently

$$\partial_t C_\mu^{[ab]}(k_1, k_2, t) = \sum_\alpha B_{\mu\alpha}(k_1 + k_2, -t) \sum_{\nu\rho} g_{\alpha\nu\rho}(k_1, k_2) A_\nu^a(k_1, t) A_\rho^b(k_2, t) , \quad (6.149)$$

because  $(B_{\mu\nu}(k, t))^{-1} = B_{\mu\nu}(k, -t)$ . Thus

$$C_\mu^{[ab]}(k_1, k_2, t) = \sum_{\alpha\nu\rho} g_{\alpha\nu\rho}(k_1, k_2) \int_0^t B_{\mu\alpha}(k_1 + k_2, -t') A_\nu^a(k_1, t') A_\rho^b(k_2, t') dt' \quad (6.150)$$

and

$$\begin{aligned} A_\mu^{[ab]}(k_1, k_2, t) &= \sum_{\alpha\beta\nu\rho} B_{\mu\alpha}(k_1 + k_2, t) \int_0^t B_{\alpha\beta}(k_1 + k_2, -t') g_{\beta\nu\rho}(k_1, k_2) A_\nu^a(k_1, t') A_\rho^b(k_2, t') dt' \\ &= \sum_{\alpha\nu\rho} g_{\alpha\nu\rho}(k_1, k_2) \int_0^t B_{\mu\alpha}(k_1 + k_2, t - t') A_\nu^a(k_1, t') A_\rho^b(k_2, t') dt' , \end{aligned} \quad (6.151)$$

where we have used  $\sum_\alpha B_{\mu\alpha}(k, t_1) B_{\alpha\nu}(k, t_2) = B_{\mu\nu}(k, t_1 + t_2)$ . We can also go further and express  $A_\mu^{[ab]}$  in terms of the original gluon fields

$$\begin{aligned} A_\mu^{[ab]}(k_1, k_2, t) &= \sum_{\alpha\beta\gamma\nu\rho} g_{\alpha\beta\gamma}(k_1, k_2) \left[ \int_0^t B_{\mu\alpha}(k_1 + k_2, t - t') B_{\beta\nu}(k_1, t') B_{\gamma\rho}(k_2, t') dt' \right] \\ &\quad \times A_\nu^a(k_1, 0) A_\rho^b(k_2, 0) \\ &=: \sum_{\nu\rho} B_{\mu\nu\rho}(k_1, k_2, t) A_\nu^a(k_1, 0) A_\rho^b(k_2, 0) . \end{aligned} \quad (6.152)$$

Again we can check that we recover  $A_\mu^{(1)[ab]}(k_1, k_2)$  for an infinitesimal flow time  $t = \epsilon$

$$\begin{aligned} A_\mu^{[ab]}(k_1, k_2, \epsilon) &= \sum_{\alpha\beta\gamma\nu\rho} g_{\alpha\beta\gamma\delta}(k_1, k_2) \left[ \epsilon B_{\mu\alpha}(k_1 + k_2, 0) B_{\beta\nu}(k_1, 0) B_{\gamma\rho}(k_2, 0) \right] \\ &\quad \times A_\nu^a(k_1, 0) A_\rho^b(k_2, 0) \end{aligned} \quad (6.153)$$

$$= \sum_{\nu\rho} \epsilon g_{\mu\nu\rho}(k_1, k_2) A_\nu^a(k_1, 0) A_\rho^b(k_2, 0) = A_\mu^{(1)[ab]}(k_1, k_2) \Big|_{\rho=\epsilon} . \quad (6.154)$$

If we expand further (for small  $t < 1$ ) we get

$$\begin{aligned} B_{\mu\nu\rho}(k_1, k_2, t) &= \sum_{\alpha\beta\gamma} g_{\alpha\beta\gamma}(k_1, k_2) \left( \delta_{\mu\alpha}\delta_{\beta\nu}\delta_{\gamma\rho}t + \frac{1}{2}(g_{\mu\alpha}(k_1+k_2)\delta_{\beta\nu}\delta_{\gamma\rho} + \delta_{\mu\alpha}g_{\beta\nu}(k_1)\delta_{\gamma\rho} \right. \\ &\quad \left. + \delta_{\mu\alpha}\delta_{\beta\nu}g_{\gamma\rho}(k_2))t^2 + \mathcal{O}(t^3) \right) \end{aligned} \quad (6.155)$$

$$= \tilde{g}_{\mu\nu\rho}^{(1)}(t, k_1, k_2) + \frac{t^2}{2}(\dots) + \mathcal{O}(t^3) \quad (6.156)$$

$$= \tilde{g}_{\mu\nu\rho}^{(n)}(t/n, k_1, k_2) + \frac{t^2}{2n}(\dots) + \mathcal{O}(t^3) \quad (6.157)$$

which shows the same behaviour as the first order fields.

### 6.2.3 Next-to-Next-to-Leading Order

The differential equation at third order is

$$\begin{aligned} &-i\frac{g_0^3}{6} \left[ T^a T^b T^c \partial_t (A_\mu^a(x, t) A_\mu^b(x, t) A_\mu^c(x, t)) + \frac{3}{2} \{T^a, [T^b, T^c]\} \partial_t (A_\mu^a(x, t) A_\mu^{[bc]}(x, t)) \right. \\ &+ \left( T^a T^b T^c + T^c T^b T^a - \frac{1}{N_c} \text{Tr}(T^a T^b T^c + T^c T^b T^a) \right) \partial_t A_\mu^{abc}(x, t) \Big] \\ &= -ig_0^3 \left[ \frac{1}{2} T^a T^b T^c Q_{1\mu}^a(x, t) A_\mu^b(x, t) A_\mu^c(x, t) + \frac{1}{2} T^a [T^b, T^c] Q_{1\mu}^a(x, t) A_\mu^{[bc]}(x, t) \right. \\ &+ [T^a, T^b] T^c Q_{2\mu}^{ab}(x, t) A_\mu^c(x, t) \\ &\quad \left. - \left( T^a T^b T^c + T^c T^b T^a - \frac{1}{N_c} \text{Tr}(T^a T^b T^c + T^c T^b T^a) \right) Q_{3\mu}^{abc}(x, t) \right]. \end{aligned} \quad (6.158)$$

The right hand side can be rewritten to look like

$$\begin{aligned} &-i\frac{g_0^3}{6} \left( T^a T^b T^c \partial_t (A_\mu^a(x, t) A_\mu^b(x, t) A_\mu^c(x, t)) + \frac{3}{2} \{T^a [T^b, T^c]\} \partial_t (A_\mu^a(x, t) A_\mu^{[bc]}(x, t)) \right. \\ &- \left( T^a T^b T^c + T^c T^b T^a - \frac{1}{N_c} \text{Tr}(T^a T^b T^c + T^c T^b T^a) \right) \left( -\frac{1}{2} Q_{1\mu}^a(x, t) A_\mu^b(x, t) A_\mu^c(x, t) \right. \\ &- A^a Q_{1\mu}^b A_\mu^c(x, t) + 3V_{2\mu}^{\{ab\}}(x, t) A_\mu^c(x, t) - 3V_{3\mu}^{abc}(x, t) - 6A_\mu^a(x, t) A_\mu^b(x, t) A_\mu^c(x, t) \\ &\quad \left. \left. + 6A_\mu^{abc}(x, t) \right) \right). \end{aligned} \quad (6.159)$$

Thus

$$\begin{aligned} \partial_t A_\mu^{abc}(x, t) &= \frac{1}{2} Q_{1\mu}^a(x, t) A_\mu^b(x, t) A_\mu^c(x, t) + A^a Q_{1\mu}^b A_\mu^c(x, t) - 3V_{2\mu}^{\{ab\}}(x, t) A_\mu^c(x, t) \\ &\quad + 3V_{3\mu}^{abc}(x, t) + 6A_\mu^a(x, t) A_\mu^b(x, t) A_\mu^c(x, t) - 6A_\mu^{abc}(x, t). \end{aligned} \quad (6.160)$$

In momentum space we get

$$\begin{aligned} \partial_t A_\mu^{abc}(k_1, k_2, k_3, t) &= \sum_\nu g_{\mu\nu}(k_1 + k_2 + k_3) A_\nu^{abc}(k_1, k_2, k_3, t) \\ &+ 6 \sum_{\nu\rho} g_{\mu\nu\rho}(k_1, k_2 + k_3) A_\nu^a(k_1, t) A_\rho^{[bc]}(k_2, k_3, t) \\ &+ \sum_{\nu\rho\sigma} G_{\mu\nu\rho\sigma}(k_1, k_2, k_3) A_\nu^a(k_1, t) A_\rho^b(k_2, t) A_\sigma^c(k_3, t) . \end{aligned} \quad (6.161)$$

We make again the following ansatz

$$A_\mu^{abc}(k_1, k_2, k_3, t) = \sum_\alpha B_{\mu\alpha}(k_1 + k_2 + k_3, t) C_\alpha^{abc}(k_1, k_2, k_3, t) , \quad (6.162)$$

as we know from the leading order that  $B_{\mu\nu}(k_1 + k_2 + k_3, t)$  satisfies the homogeneous part of the differential equation. Then we are left with the inhomogeneous part

$$\begin{aligned} \sum_\alpha B_{\mu\alpha}(k_1 + k_2 + k_3, t) \partial_t C_\alpha^{abc}(k_1, k_2, k_3, t) &= \\ 6 \sum_{\nu\rho} g_{\mu\nu\rho}(k_1, k_2 + k_3) A_\nu^a(k_1, t) A_\rho^{[bc]}(k_2, k_3, t) \\ + \sum_{\nu\rho\sigma} G_{\mu\nu\rho\sigma}(k_1, k_2, k_3) A_\nu^a(k_1, t) A_\rho^b(k_2, t) A_\sigma^c(k_3, t) , \end{aligned} \quad (6.163)$$

or equivalently

$$\begin{aligned} \partial_t C_\alpha^{abc}(k_1, k_2, k_3, t) &= \\ 6 \sum_{\alpha\nu\rho} B_{\mu\alpha}(k_1 + k_2 + k_3, -t) g_{\alpha\nu\rho}(k_1, k_2 + k_3) A_\nu^a(k_1, t) A_\rho^{[bc]}(k_2, k_3, t) \\ + \sum_{\alpha\nu\rho\sigma} B_{\mu\alpha}(k_1 + k_2 + k_3, -t) G_{\alpha\nu\rho\sigma}(k_1, k_2, k_3) A_\nu^a(k_1, t) A_\rho^b(k_2, t) A_\sigma^c(k_3, t) . \end{aligned} \quad (6.164)$$

Integrating this and putting everything together, we get

$$\begin{aligned} A_\mu^{abc}(k_1, k_2, k_3, t) &= \\ \sum_{\alpha\nu\rho} g_{\alpha\nu\rho}(k_1, k_2 + k_3) \int_0^t B_{\mu\alpha}(k_1 + k_2 + k_3, t - t') A_\nu^a(k_1, t') A_\rho^{[bc]}(k_2, k_3, t') dt' \\ + \sum_{\alpha\nu\rho\sigma} G_{\alpha\nu\rho\sigma}(k_1, k_2, k_3) \int_0^t B_{\mu\alpha}(k_1 + k_2 + k_3, t - t') A_\nu^a(k_1, t') A_\rho^b(k_2, t') A_\sigma^c(k_3, t') dt' , \end{aligned} \quad (6.165)$$

which we further relate to the unflowed fields by use of the previous orders' results:

$$\begin{aligned}
A_\mu^{abc}(k_1, k_2, k_3, t) &= \\
&\sum_{\nu\rho\sigma} \left( \sum_{\alpha\beta\gamma} g_{\alpha\beta\gamma}(k_1, k_2 + k_3) \int_0^t B_{\mu\alpha}(k_1 + k_2 + k_3, t - t') B_{\beta\nu}(k_1, t') B_{\gamma\rho\sigma}(k_2, k_3, t') dt' \right. \\
&+ \sum_{\alpha\beta\gamma\delta} G_{\alpha\beta\gamma\delta}(k_1, k_2, k_3) \int_0^t B_{\mu\alpha}(k_1 + k_2 + k_3, t - t') B_{\beta\nu}(k_1, t') B_{\gamma\rho}(k_2, t') B_{\delta\sigma}(k_3, t') dt' \left. \right) \\
&\times A_\nu^a(k_1, 0) A_\rho^b(k_2, 0) A_\sigma^c(k_3, 0) \\
&=: \sum_{\nu\rho\sigma} B_{\mu\nu\rho\sigma}(k_1, k_2, k_3, t) A_\nu^a(k_1, 0) A_\rho^b(k_2, 0) A_\sigma^c(k_3, 0). \tag{6.166}
\end{aligned}$$

Again, we can check that the error one makes by approximating the Wilson flow by stout smearing is of the order  $t^2/(2n)$ :

$$B_{\mu\nu\rho\sigma}(k_1, k_2, k_3, t) = \tilde{g}_{\mu\nu\rho\sigma}^{(n)}(t/n, k_1, k_2, k_3) + \frac{t^2}{2n}(\dots). \tag{6.167}$$

Thus we have found three  $B$ -functions that are the Wilson flow equivalent to the  $\tilde{g}$ -functions from the expansion of stout smearing.

### 6.2.4 Continuum Limit

In the continuum limit  $a \rightarrow 0$ , we replace  $\cos(k_\mu) \rightarrow 1$  and  $\sin(k_\mu) \rightarrow k_\mu$ , and expand to first order in the momenta. We get

$$B_{\mu\nu}(k, t) \rightarrow \sum_\nu \left( e^{-k^2 t} \delta_{\mu\nu} - \left( e^{-k^2 t} - 1 \right) \frac{k_\mu k_\nu}{k^2} \right) \tag{6.168}$$

$$g_{\mu\nu\rho}(k_1, k_2) \rightarrow i \left( -\delta_{\beta\nu} (2k_{1\rho} + k_{2\rho}) + \delta_{\beta\rho} (2k_{2\nu} + k_{1\nu}) + \delta_{\nu\rho} (k_{1\mu} - k_{2\mu}) \right) \tag{6.169}$$

$$G_{\mu\nu\rho\sigma}(k_1, k_2, k_3) \rightarrow 6 (\delta_{\mu\nu} \delta_{\rho\sigma} - \delta_{\mu\rho} \delta_{\nu\sigma}), \tag{6.170}$$

and the flowed field  $\tilde{A}_\mu$  from Eq. (6.132) in this limit fulfils the differential equation of the continuum gradient flow

$$\partial_t \tilde{A}_\mu(x, t) = \sum_\nu \tilde{D}_\nu \tilde{F}_{\nu\mu}, \quad \tilde{A}_\mu(x, 0) = A_\mu(x) \tag{6.171}$$

with

$$\tilde{D}_\mu = \partial_\mu + [\tilde{A}_\mu(x, t), \cdot], \quad \tilde{F}_{\mu\nu} = \partial_\mu \tilde{A}_\nu(x, t) - \partial_\nu \tilde{A}_\mu(x, t) + [\tilde{A}_\mu(x, t), \tilde{A}_\nu(x, t)]. \tag{6.172}$$

These results agree with the ones given in Refs. [8, 41] (see also Section 7.3).

## 6.3 Feynman Rules

The Feynman rules are obtained by inserting the expansion of the link variables (6.173) into the Fermion action. This results in expressions for anti-quark-quark- $n$ -gluon vertices at each order  $g_0^n$ . These vertices are proportional to  $a^{n-1}$  such that only the  $\bar{q}qg$  vertex survives in the continuum limit  $a \rightarrow 0$ , as is expected from continuum perturbation theory. For the purpose of one-loop calculations, we will need the  $\bar{q}qg$ -,  $\bar{q}qgg$ - and  $\bar{q}qggg$ -vertex, i.e. anything up to order  $g_0^3$ .

For deriving the Feynman rules of the fermion action including stout smearing or Wilson flow, there are two possible strategies. One is to simply insert the perturbative expansion of the smeared or flowed link variable into the action and expand to the needed order in  $g_0$ . This "brute force" approach leads to very large intermediate expressions and involves many steps where indices have to be renamed etc. This is not feasible beyond one step of stout smearing. The second much more effective method is based on the  $SU(N_c)$ -expansion of the link variable. One simply derives the Feynman rules for generic link variables of the form

$$U_\mu(x) = 1 + ig_0 T^a A_\mu^a(x) - \frac{g_0^2}{2} T^a T^b A_\mu^a(x) A_\mu^b(x) - i \frac{g_0^3}{6} T^a T^b T^c A_\mu^a(x) A_\mu^b(x) A_\mu^c(x) \quad (6.173)$$

which results in fairly simple expressions. One then couples the stout or flow "form factors" to these generic Feynman rules to obtain the complete results. This also practically allows us to easily split lengthy expressions into smaller parts for Mathematica to work on. The following sections show the derivations of the generic Feynman rules and how to couple them to stout smearing or the Wilson flow.

We start with the Wilson quark action

$$S_W = \sum_{x,y} \sum_{\mu=\pm 1}^{\pm 4} \bar{\psi}(x) \frac{1}{2} \left[ U_\mu(x) \delta_{x+\hat{\mu},y} \gamma_\mu - r \left( U_\mu(x) \delta_{x+\hat{\mu},y} - \delta_{x,y} \right) \right] \psi(y) . \quad (6.174)$$

Links with negative indices are given by  $U_{-\mu}(x) = U_\mu^\dagger(x - \hat{\mu})$  and  $\gamma_{-\mu} = -\gamma_\mu$ . Up to order  $g_0^3$  we get the well known three vertices of a quark anti-quark pair coupling to one, two, and three gluons respectively.

$$V_{1W\mu}^a(p, q) = -g_0 T^a \left( i \gamma_\mu c(p_\mu + q_\mu) + rs(p_\mu + q_\mu) \right) \quad (6.175)$$

$$V_{2W\mu\nu}^{ab}(p, q) = \frac{g_0^2}{2} T^a T^b \delta_{\mu\nu} \left( i \gamma_\mu s(p_\mu + q_\mu) - rc(p_\mu + q_\mu) \right) \quad (6.176)$$

$$V_{3W\mu\nu\rho}^{abc}(p, q) = \frac{g_0^3}{6} T^a T^b T^c \delta_{\mu\nu} \delta_{\mu\rho} \left( i \gamma_\mu c(p_\mu + q_\mu) + rs(p_\mu + q_\mu) \right) \quad (6.177)$$

These appear in the expansion of the action contracted with the (original) gluon fields

$$\begin{aligned} S_W \sim & \sum_\mu \bar{\psi}(q) T^a V_{1\mu}(p, q) A_\mu^a(q-p) \psi(p) \\ & + \sum_{\mu\nu} \bar{\psi}(q) T^a T^b V_{2\mu\nu}(p, q) A_\mu^a(k_1) A_\nu^b(k_2) \delta(q-p-k_1-k_2) \psi(p) \end{aligned}$$

$$+ \sum_{\mu\nu\rho} \bar{\psi}(q) T^a T^b T^c V_{3\mu\nu\rho}(p, q) A_\mu^a(k_1) A_\nu^b(k_2) A_\rho^c(k_3) \delta(q - p - k_1 - k_2 - k_3) \psi(p) \quad (6.178)$$

In order to derive the Feynman rules with smearing or gradient flow, we replace the gluon fields  $A_\mu^a$  by  $\tilde{A}_\mu^{(n)a}$  or  $\tilde{A}_\mu^a(t)$  respectively. Thereby new terms are added at higher orders of  $g_0$ . For example, replacing the  $A_\mu^a$  which couples to  $V_{1\mu}^a$  by a smeared or flowed field, provides the new  $\bar{q}qg$  vertex with a form factor and adds terms to the  $\bar{q}qgg$  and  $\bar{q}qggg$  vertices proportional to  $A_\mu^{[ab]}$  and  $A_\mu^{abc}$  respectively. Specifically the new stout smeared vertices look like

$$V_{1\mu}^{(n)a}(p, q) = T^a \sum_\nu \tilde{g}_{\mu\nu}^n(\varrho, q - p) V_{1\nu}(p, q) \quad (6.179)$$

$$\begin{aligned} V_{2\mu\nu}^{(n)ab}(p, q, k_1, k_2) &= T^a T^b \sum_{\rho\sigma} \tilde{g}_{\mu\rho}^n(\varrho, k_1) \tilde{g}_{\nu\sigma}^n(\varrho, k_2) V_{2\rho\sigma}(p, q, k_1, k_2) \\ &\quad - \frac{g_0}{2i} [T^a, T^b] \sum_\rho \tilde{g}_{\rho\mu\nu}^{(n)}(k_1, k_2) V_{1\rho}(p, q) \end{aligned} \quad (6.180)$$

$$\begin{aligned} V_{3\mu\nu\rho}^{(n)abc}(p, q, k_1, k_2, k_3) &= T^a T^b T^c \sum_{\alpha\beta\gamma} \tilde{g}_{\mu\alpha}^n(\varrho, k_1) \tilde{g}_{\nu\beta}^n(\varrho, k_2) \tilde{g}_{\rho\gamma}^n(\varrho, k_3) V_{3\alpha\beta\gamma}(p, q, k_1, k_2, k_3) \\ &\quad - \frac{g_0}{2i} \{T^a, [T^b, T^c]\} \sum_{\alpha\beta} \tilde{g}_{\mu\alpha}^n(\varrho, k_1) \tilde{g}_{\beta\nu\rho}^{(n)}(\varrho, k_2, k_3) V_{2\alpha\beta}(p, q, k_1, k_2 + k_3) \\ &\quad - \frac{g_0^2}{6} \left[ T^a T^b T^c + T^c T^b T^a - \frac{1}{N_c} \text{Tr}(T^a T^b T^c + T^c T^b T^a) \right] \sum_\alpha \tilde{g}_{\alpha\mu\nu\rho}^{(n)}(\varrho, k_1, k_2, k_3) V_{1\alpha}(p, q) \end{aligned} \quad (6.181)$$

with the  $\tilde{g}$  given in Eqs. (6.50), (6.64), and (6.122). The vertices with Wilson flow are analogously

$$V_{1\mu}^a(p, q, t) = T^a \sum_\nu B_{\mu\nu}(q - p, t) V_{1\nu}(p, q) \quad (6.182)$$

$$\begin{aligned} V_{2\mu\nu}^{ab}(p, q, k_1, k_2, t) &= T^a T^b \sum_{\rho\sigma} B_{\mu\rho}(k_1, t) B_{\nu\sigma}(k_2, t) V_{2\rho\sigma}(p, q, k_1, k_2) \\ &\quad - \frac{g_0}{2i} [T^a, T^b] \sum_\rho B_{\rho\mu\nu}(k_1, k_2, t) V_{1\rho}(p, q) \end{aligned} \quad (6.183)$$

$$\begin{aligned} V_{3\mu\nu\rho}^{abc}(p, q, k_1, k_2, k_3, t) &= T^a T^b T^c \sum_{\alpha\beta\gamma} B_{\mu\alpha}(k_1, t) B_{\nu\beta}(k_2, t) B_{\rho\gamma}(k_3, t) V_{3\alpha\beta\gamma}(p, q, k_1, k_2, k_3) \\ &\quad - \frac{g_0}{2i} \{T^a, [T^b, T^c]\} \sum_{\alpha\beta} B_{\mu\alpha}(k_1, t) B_{\beta\nu\rho}(k_2, k_3, t) V_{2\alpha\beta}(p, q, k_1, k_2 + k_3) \\ &\quad - \frac{g_0^2}{6} \left[ T^a T^b T^c + T^c T^b T^a - \frac{1}{N_c} \text{Tr}(T^a T^b T^c + T^c T^b T^a) \right] \sum_\alpha B_{\alpha\mu\nu\rho}(k_1, k_2, k_3, t) V_{1\alpha}(p, q) \end{aligned} \quad (6.184)$$

with the  $B$  given in Eqs. (6.138), (6.152), and (6.166).

# 7 Fermion Self-Energy with Stout Smearing and Wilson Flow

In this section we present the results of our calculations for the fermion self-energy. The methods to perturbatively determine  $\Sigma_0$  and  $\Sigma_1$  have been described in Section A.3. We present our results for the four combinations of two fermion and two gluon actions. The Feynman rules for the Wilson, Brillouin and clover fermion actions are given in Sections 8 and 9. Both fermion actions included the clover improvement term with the tree-level value  $c_{\text{sw}} = r$ , but we give additional results for the self-energy for the unimproved actions ( $c_{\text{sw}} = 0$ ) and for arbitrary values of  $c_{\text{sw}}$  in Appendices A.3 and A.3.

Smearing or Wilson flow form factors are coupled to the vertex Feynman rules as explained in Section 9.

The gluon actions are the standard Wilson plaquette action (denoted by “plaq”) and the tree-level improved Lüscher-Weisz action (denoted by “sym”), see Section 8.

We calculated all results for six different values of the Wilson parameter

$$r \in \{0.6, 0.8, 1.0, 1.2, 1.4\}. \quad (7.1)$$

While most data is shown for  $r = 1$ , as it is the preferred value, we show the dependence on  $r$  in some places, where it is instructive.

Following the structure of Chapter 6, we first present the results with up to four steps of stout smearing in Sections 7.1 and 7.2. Then we show the Wilson flow results in Sections 7.3 and 7.4. By plotting the data of both sections side by side we can illustrate how stout smearing approximates the Wilson flow.

## 7.1 $\Sigma_0$ with Stout Smearing

The linearly divergent part of the self-energy  $\Sigma_0/a$  gives the additive renormalisation of the Wilson (or Brillouin) fermion

$$-am_{\text{crit}} = -\frac{g_0^2 C_F}{16\pi^2} \Sigma_0. \quad (7.2)$$

At one-loop order on the lattice there are two Feynman diagrams contributing to the self-energy, the “tadpole” and the “sunset” (see Section A.3). Figures 7.1 and 7.2 show the contributions of these two diagrams. Figure 7.3 then gives their sum  $\Sigma_0$ .

In Ref. [98], results for  $\Sigma_0$  with up to three steps of stout smearing at the specific value  $\varrho = 0.1$  (labelled there as  $\alpha = 0.6$ , due to the perturbative matching between stout and APE smearing) were given, which agree with our results (see Appendix A.3 for details). In addition, results for  $\Sigma_0$  and  $\Sigma_1$  with one step of SLINC smearing for plaquette and Lüscher-Weisz gluons were given in Ref. [64]. In the SLINC action only the links entering the Wilson part of the fermion action are subject to one step of stout smearing, while

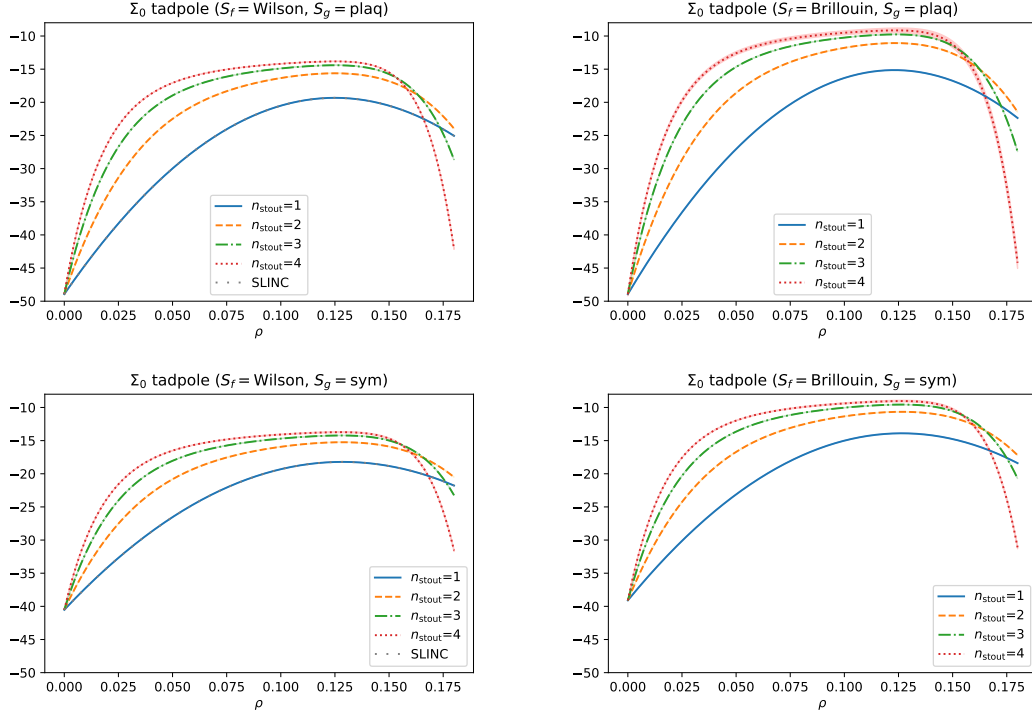


**Figure 7.1:** Contributions from the “tadpole” diagram to the self energy  $\Sigma_0$  with up to four stout smearing steps as a function of the smearing parameter  $\rho$ . Four combinations of fermion and gluon actions are shown. The SLINC results in the left hand panels coincide with the  $n_{\text{stout}} = 1$  results. All results for  $c_{\text{SW}} = r = 1$ .

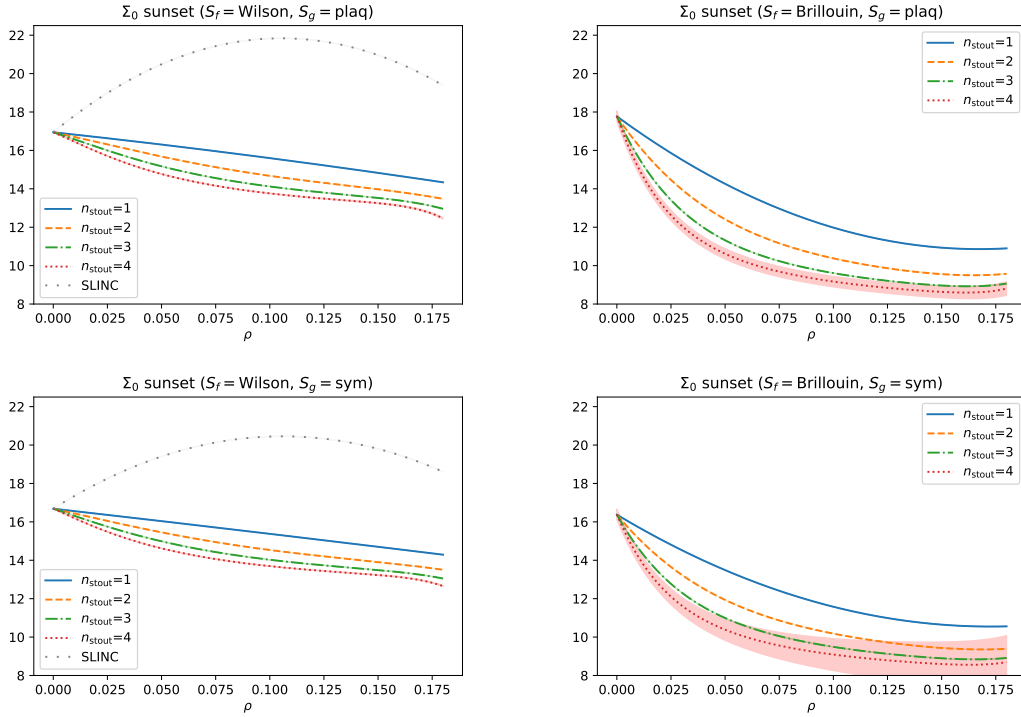


**Figure 7.2:** The same as Figure 7.1 but for the contribution of the “sunset” diagram.

the clover part stays unsmeared. Reproducing these results<sup>1</sup> served as a cross-check for our code. We have included the SLiNC results in our Wilson/plaq and Wilson/sym plots.

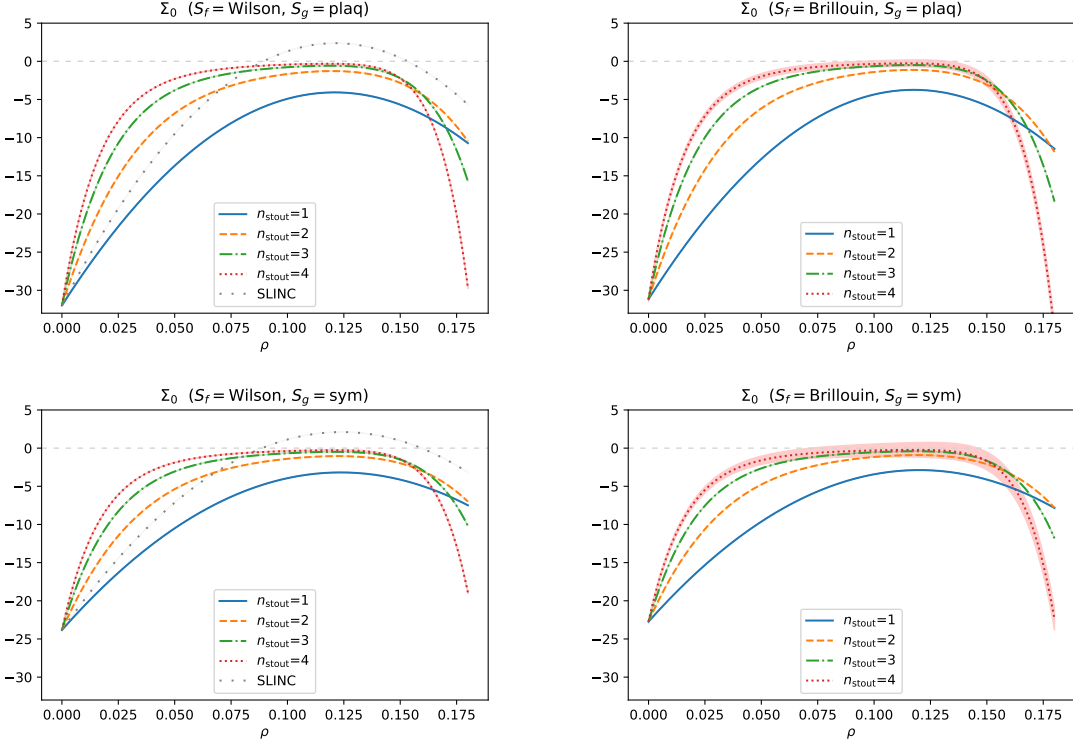


**Figure 7.3:** The same as Figures 7.1 and 7.2 but for the physical  $\Sigma_0 = \Sigma_0^{(\text{tadpole})} + \Sigma_0^{(\text{subset})}$ .

As we have noted before in Section 9 about the unsmeared  $\Sigma_0$ , the difference between the Wilson and Brillouin fermions is rather small compared to the difference the improved gauge action makes. The same stays true with stout smearing (see Figure 7.3 and Table 7.1), even though the deviations are more pronounced in the individual diagrams (see Figures 7.1 and 7.2).

In Table 7.1, we give  $\Sigma_0$  for six values of  $\rho$ . This data can be used to quickly and efficiently perform for example a spline interpolation to find  $\Sigma_0$  at a specific  $\rho$ .

The full result consists of polynomials in  $\rho$  with degree  $2n_{\text{stout}}$ , and the coefficients are the estimated values of lattice integrals. These coefficients are given in Table A.4 in Appendix A.3.

All four combinations of fermions and gluons, depicted in Figure 7.3 show that choosing a reasonable  $\rho$  reduces the additive mass shift quite drastically. The initial slope is proportional to  $n_{\text{stout}}$  (see Table A.4).

Compared to the full curve, the SLiNC curve (wide-spaced dots) seems to be an improvement for small values of  $\rho$ , but for a value  $\rho \sim 0.08$ , the critical mass of SLiNC

<sup>1</sup>There is a typo in Eqn. (53) of Ref. [64], the number 2235.407087 should read 2335.407087.

	$\varrho$	$n = 1$	$n = 2$	$n = 3$	$n = 4$
$\Sigma_0$ (Wil./plaq)	0.05	-13.67830(4)	-6.81841(4)	-3.79814(4)	-2.30(1)
	0.09	-5.89958(4)	-2.12071(5)	-1.00136(6)	-0.56(2)
	0.11	-4.29949(4)	-1.37888(5)	-0.62450(6)	-0.34(2)
	0.12	-4.07175(4)	-1.27800(6)	-0.57513(6)	-0.32(3)
	0.125	-4.10097(4)	-1.31229(6)	-0.60582(7)	-0.34(3)
	0.13	-4.22557(4)	-1.41647(6)	-0.69334(7)	-0.42(3)
$\Sigma_0$ (Wil./sym)	0.05	-10.50283(3)	-5.36991(3)	-3.05827(4)	-1.89(4)
	0.09	-4.70711(3)	-1.76141(5)	-0.85802(8)	-0.49(6)
	0.11	-3.43187(3)	-1.15565(5)	-0.5431(2)	-0.31(7)
	0.12	-3.19992(3)	-1.04722(6)	-0.4871(2)	-0.28(8)
	0.125	-3.18535(3)	-1.05160(6)	-0.4966(2)	-0.29(8)
	0.13	-3.23840(3)	-1.10355(6)	-0.5435(3)	-0.33(9)
$\Sigma_0$ (Bri./plaq)	0.05	-12.79494(4)	-6.172(5)	-3.346(5)	-2.0(4)
	0.09	-5.24477(5)	-1.800(5)	-0.824(5)	-0.4(5)
	0.11	-3.85017(5)	-1.171(5)	-0.512(6)	-0.3(5)
	0.12	-3.74800(6)	-1.133(5)	-0.497(6)	-0.3(5)
	0.125	-3.84569(6)	-1.206(5)	-0.551(6)	-0.3(5)
	0.13	-4.04257(6)	-1.356(5)	-0.670(7)	-0.4(5)
$\Sigma_0$ (Bri./sym)	0.05	-9.629(5)	-4.772(1)	-2.650(2)	-1.6(6)
	0.09	-4.115(5)	-1.475(2)	-0.699(2)	-0.4(8)
	0.11	-3.013(5)	-0.965(2)	-0.440(3)	0(1)
	0.12	-2.875(5)	-0.905(2)	-0.411(3)	0(1)
	0.125	-2.910(5)	-0.937(2)	-0.437(3)	0(1)
	0.13	-3.014(5)	-1.021(2)	-0.506(4)	0(2)

**Table 7.1:**  $\Sigma_0$  for six different values of the smearing parameter  $\varrho$  and stout steps  $n = 1, 2, 3, 4$ , with  $c_{\text{SW}} = r = 1$ .

fermions changes sign. On the other hand, the ‘‘overall smearing’’ advocated in Ref. [98] seems to be rather benevolent; the more smearing steps (with  $0 < \varrho < 0.12$ ) are taken, the faster  $\Sigma_0$  tends to zero. Moreover, regardless of  $n_{\text{stout}}$  and the chosen fermion or gluon background, the maximum of  $\Sigma_0$  is always near  $\varrho \sim 0.12$ , see Tab. 7.2 for details. This is consistent with the observation made in Ref. [98] that  $\varrho$  in the stout recipe should be kept below 0.125 in order to have a (first order) smearing form factor smaller than one throughout the Brillouin zone.

	$n = 1$	$n = 2$	$n = 3$	$n = 4$
$\varrho_{\max}$ of $\Sigma_0$ (Wil./plaq)	0.12096871(3)	0.11973422(9)	0.1189366(3)	0.1187(4)
$\varrho_{\max}$ of $\Sigma_0$ (Wil./sym)	0.12357712(3)	0.1220287(3)	0.120999(5)	0.1204(9)
$\varrho_{\max}$ of $\Sigma_0$ (Bri./plaq)	0.11757534(6)	0.116809(3)	0.11640(3)	0.116(3)
$\varrho_{\max}$ of $\Sigma_0$ (Bri./sym)	0.119987(2)	0.118926(3)	0.11831(5)	0.118(7)

**Table 7.2:** Position of the extreme points in Figure 7.3.

Finally, Figures 7.4 and 7.5 show the dependence of  $\Sigma_0$  on the Wilson parameter  $r$ . Even though the one-loop self-energy is not a linear function in  $r$ , due to the enumerator of the fermion propagator containing it,  $\Sigma_0$  behaves almost linear over the range shown. Again, no qualitative difference can be discerned between the Wilson fermion of Figure 7.4 and the Brillouin fermion of Figure 7.5. For increasing  $\rho$  the behaviour approaches a constant line, more quickly so, the more stout steps have been taken.

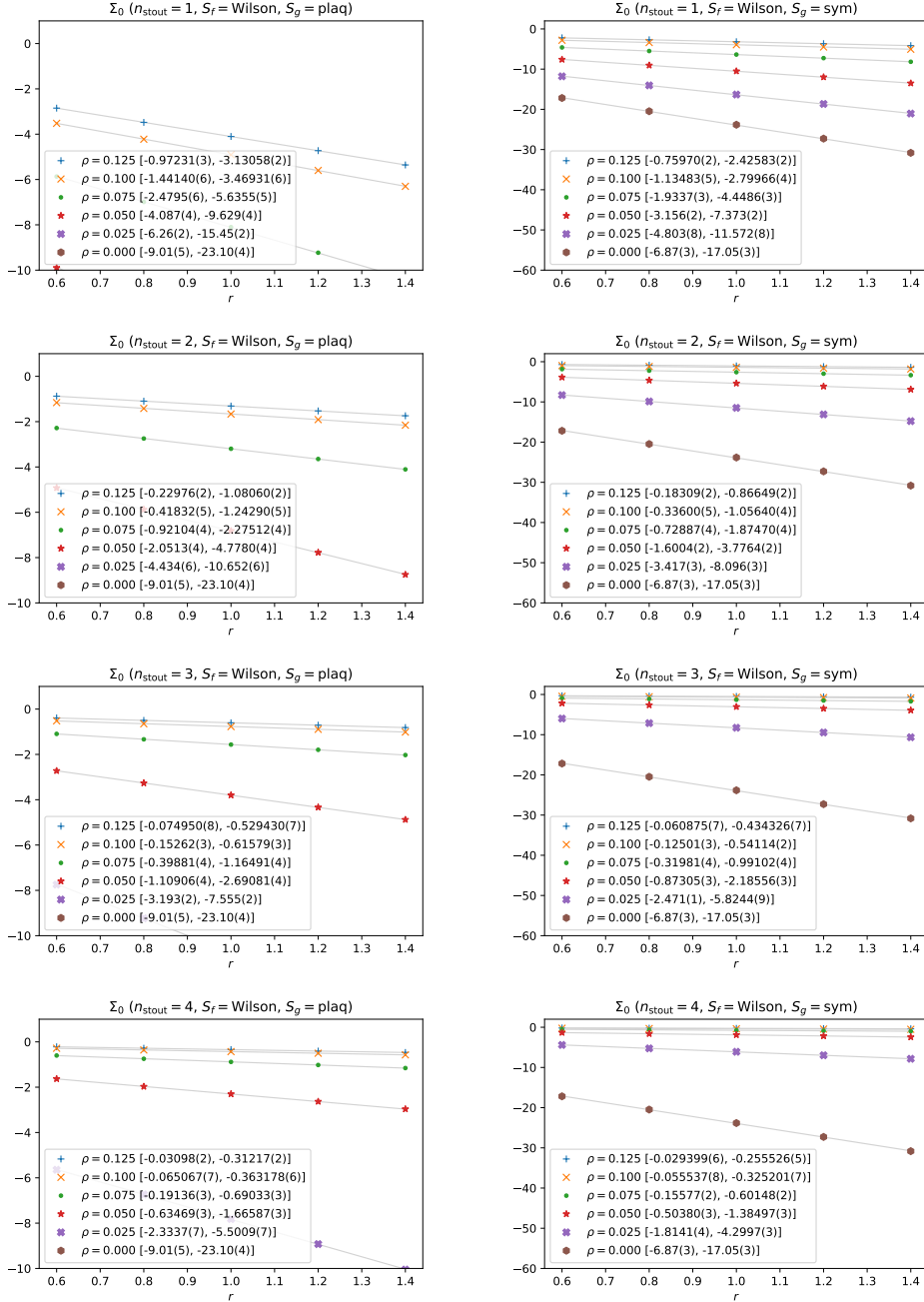


**Figure 7.4:**  $\Sigma_0$  of the Wilson clover fermion (with  $c_{\text{SW}} = r$ ) as a function of the Wilson parameter  $r$  for six values of  $\rho$ . Linear fits of the form  $c_0 + c_1 \cdot r$  are also shown and the fit coefficients  $[c_0, c_1]$  given in brackets.

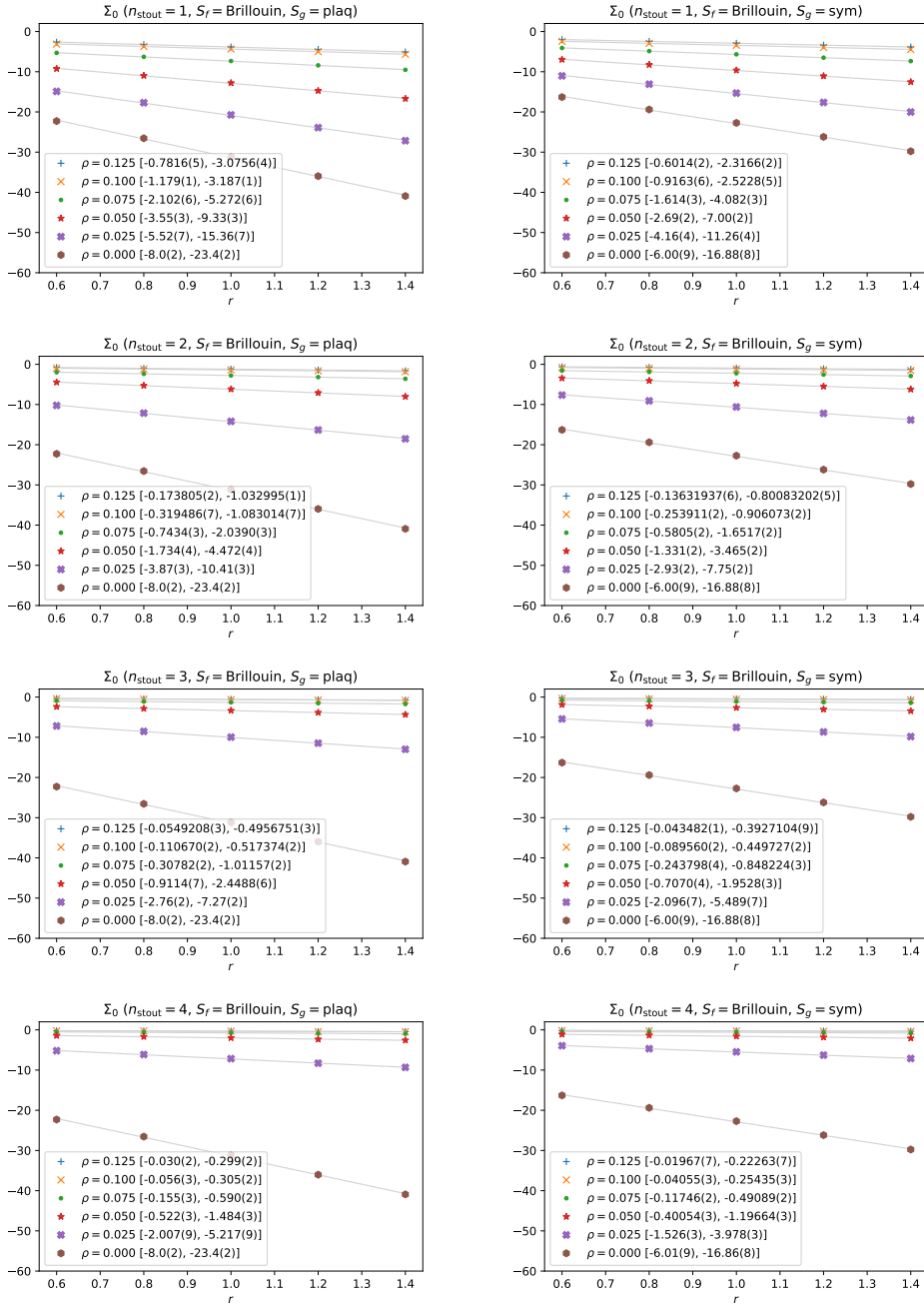


Figure 7.5: The same as Figure 7.4 but for the Brillouin clover fermion.

## 7.2 $\Sigma_1$ with Stout Smearing

The part of the fermion self energy at  $\mathcal{O}(1)$  is  $\Sigma_1$ . It is proportional to  $i\psi$  and in Feynman gauge it is logarithmically divergent for  $p \rightarrow 0$  (see Section A.3). We write

$$\Sigma_1 = \ln(p^2) + \Sigma_{10} , \quad (7.3)$$

and quote and plot the constant part  $\Sigma_{10}$ . Figures 7.6, 7.7, and 7.8 are the equivalent to Figures 7.1, 7.2, and 7.3 but for  $\Sigma_{10}$ .

The differences between the Wilson and Brillouin actions is much more pronounced here, than they were for  $\Sigma_0$ . The tadpole diagram with the Brillouin action gives a contribution about twice that of the Wilson action. For the sunset diagram the situation is reversed. In the sum (Figure 7.8), the Brillouin curves start at about twice the value of the Wilson curves but then seem to converge towards a very similar value close to  $-6$ . The positions of the minima of Figure 7.8 are given in Table 7.3.

Figures 7.9 and 7.10 show the  $r$ -dependence of  $\Sigma_{10}$ . Like for  $\Sigma_0$ , the dependence is linear over the range shown and flattens out for increasing  $\varrho$  and  $n_{\text{stout}}$ .

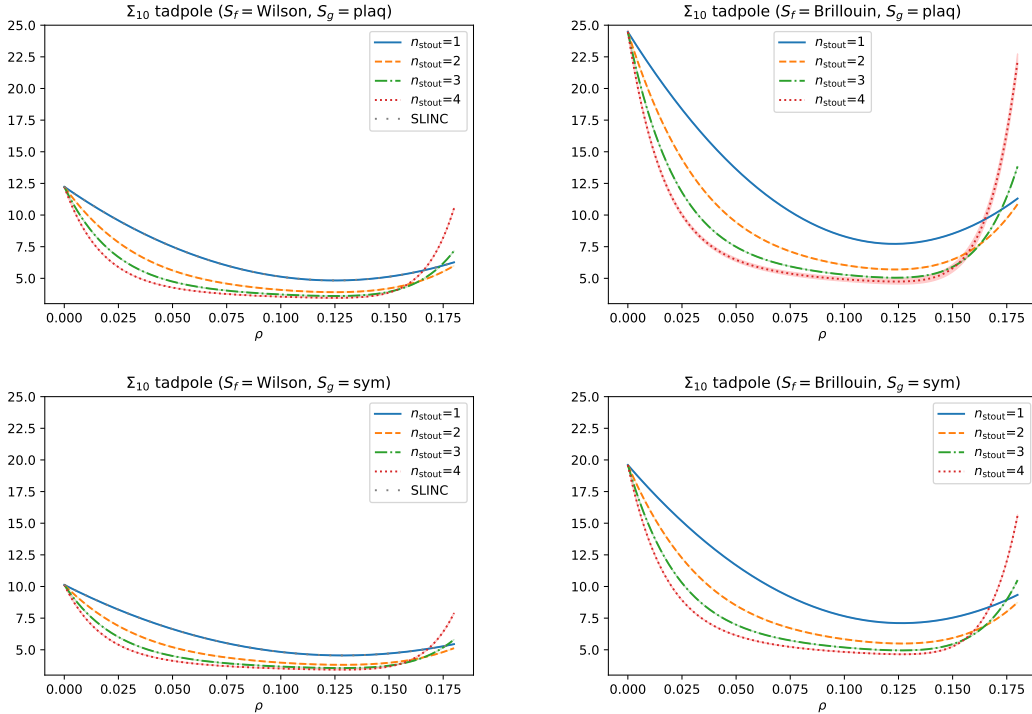


**Figure 7.6:** Contributions from the “tadpole” diagram to  $\Sigma_{10}$  with up to four stout smearing steps as a function of the smearing parameter  $\varrho$ . Four combinations of fermion and gluon actions are shown. The SLINC results in the left hand panels coincide with the  $n_{\text{stout}} = 1$  results. All results for  $c_{\text{SW}} = r = 1$  and in Feynman gauge.

	$n = 1$	$n = 2$	$n = 3$	$n = 4$
$\varrho_{\min}$ of $\Sigma_{10}$ (Wil./plaq)	0.13078397(5)	0.1285409(2)	0.1271189(9)	0.1263(6)
$\varrho_{\min}$ of $\Sigma_{10}$ (Wil./sym)	0.13417728(6)	0.1315944(2)	0.129866(6)	0.1287(6)
$\varrho_{\min}$ of $\Sigma_{10}$ (Bri./plaq)	0.12399691(3)	0.123425(5)	0.12317(4)	0.124(5)
$\varrho_{\min}$ of $\Sigma_{10}$ (Bri./sym)	0.12725(6)	0.12637(2)	0.12583(5)	0.1287(6)

**Table 7.3:** Position of the extreme points in Figure 7.8.

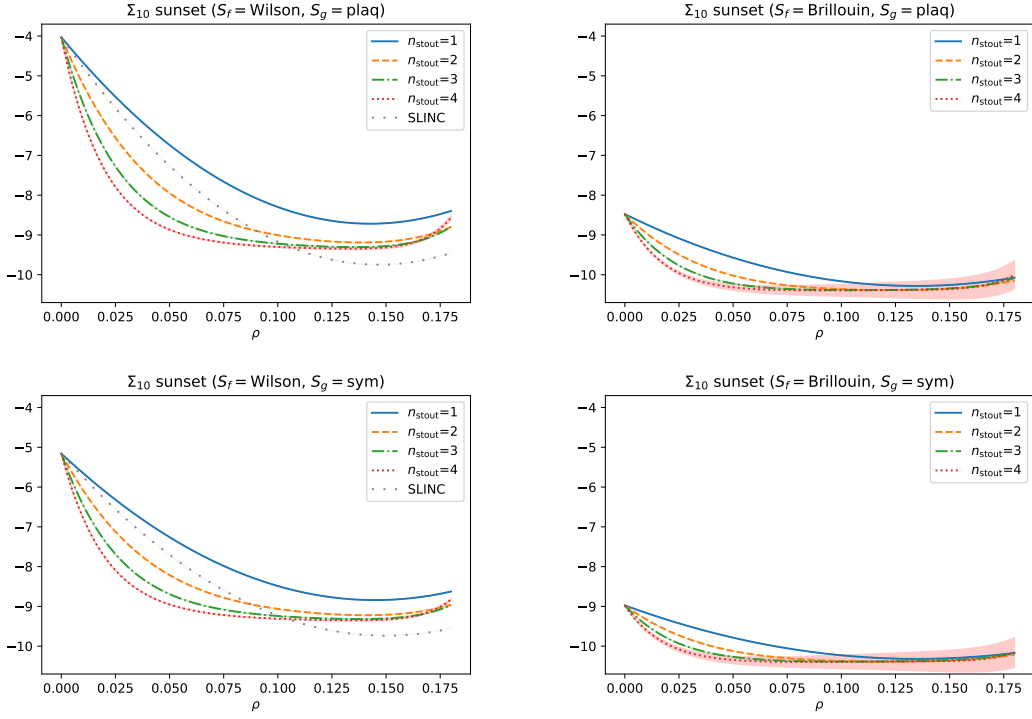


**Figure 7.7:** The same as Figure 7.6 but for the contribution of the “sunset” diagram.

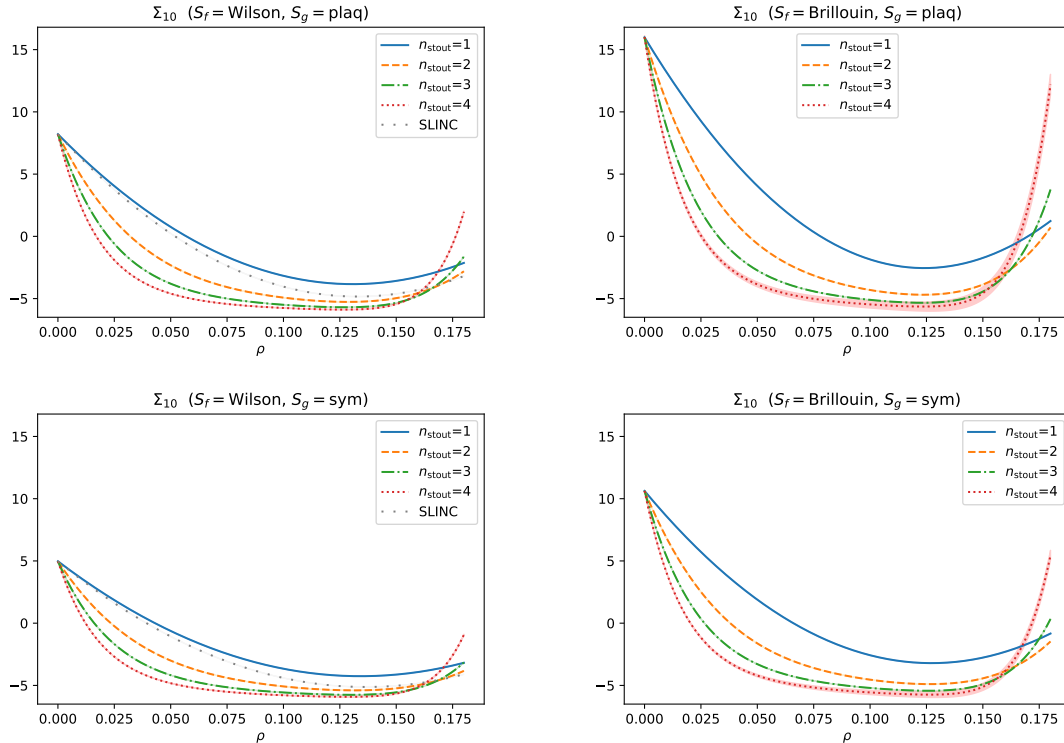


**Figure 7.8:** The same as Figures 7.6 and 7.7 but for their sum  $\Sigma_{10}$ .

	$\varrho$	$n = 1$	$n = 2$	$n = 3$	$n = 4$
$\Sigma_{10}$ (Wil./plaq)	0.05	0.75710(4)	-2.32322(4)	-3.80405(4)	-4.599(7)
	0.09	-2.66716(4)	-4.65582(5)	-5.34360(5)	-5.66(2)
	0.11	-3.53426(4)	-5.11323(5)	-5.60877(5)	-5.83(2)
	0.12	-3.75656(4)	-5.23165(5)	-5.67941(6)	-5.88(2)
	0.125	-3.81490(4)	-5.26045(5)	-5.69546(6)	-5.89(2)
	0.13	-3.83802(4)	-5.26563(5)	-5.69366(7)	-5.88(3)
$\Sigma_{10}$ (Wil./sym)	0.05	-0.625159(8)	-3.00765(1)	-4.18067(2)	-4.824(9)
	0.09	-3.25805(1)	-4.86118(2)	-5.43657(5)	-5.71(2)
	0.11	-3.95912(2)	-5.24318(2)	-5.66454(9)	-5.86(2)
	0.12	-4.15581(2)	-5.35110(2)	-5.7305(2)	-5.90(3)
	0.125	-4.21569(2)	-5.38307(2)	-5.7497(2)	-5.92(3)
	0.13	-4.24993(2)	-5.39832(2)	-5.7566(2)	-5.92(3)
$\Sigma_{10}$ (Bri./plaq)	0.05	4.05350(2)	-0.594(3)	-2.738(4)	-3.9(2)
	0.09	-1.15508(2)	-3.949(3)	-4.892(5)	-5.3(3)
	0.11	-2.31246(2)	-4.556(3)	-5.250(5)	-5.6(4)
	0.12	-2.52943(2)	-4.681(3)	-5.331(6)	-5.6(4)
	0.125	-2.54748(2)	-4.688(3)	-5.335(6)	-5.6(4)
	0.13	-2.50524(3)	-4.651(3)	-5.302(6)	-5.6(4)
$\Sigma_{10}$ (Bri./sym)	0.05	1.889(7)	-1.624(2)	-3.292(3)	-4.2(1)
	0.09	-2.02(2)	-4.243(2)	-5.027(4)	-5.4(2)
	0.11	-2.96(2)	-4.750(2)	-5.335(5)	-5.7(2)
	0.12	-3.16(2)	-4.872(2)	-5.415(5)	-5.7(3)
	0.125	-3.21(2)	-4.895(2)	-5.430(5)	-5.7(3)
	0.13	-3.20(2)	-4.888(3)	-5.421(6)	-5.7(3)

**Table 7.4:**  $\Sigma_{10}$  for six different values of the smearing parameter  $\varrho$  and stout steps  $n = 1, 2, 3, 4$ , with  $c_{\text{SW}} = r = 1$  in Feynman gauge.

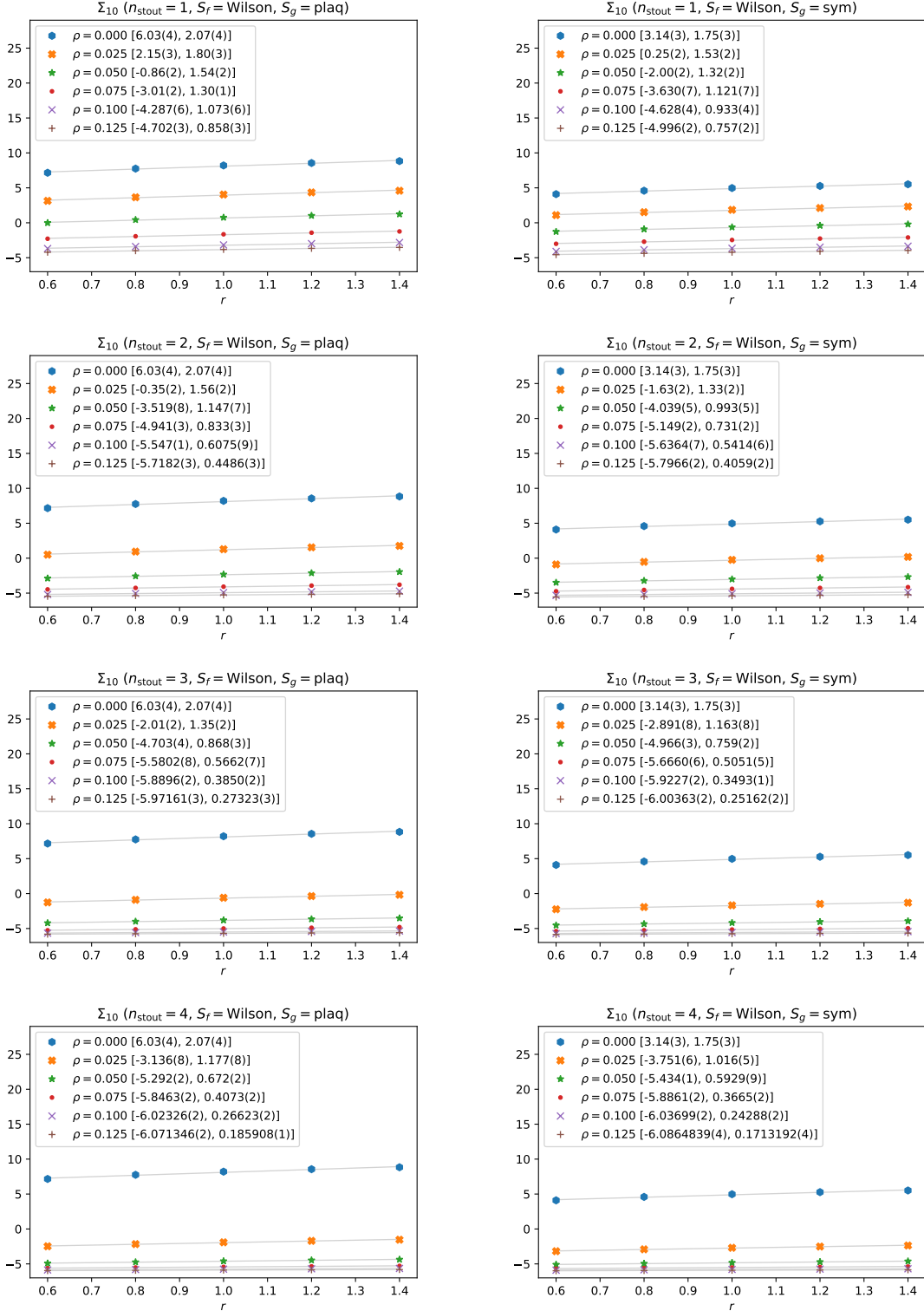


**Figure 7.9:**  $\Sigma_{10}$  of the Wilson clover fermion (with  $c_{\text{SW}} = r$ ) as a function of the Wilson parameter  $r$  for six values of  $\rho$ . Linear fits of the form  $c_0 + c_1 \cdot r$  are also shown and the fit coefficients  $[c_0, c_1]$  given in brackets.

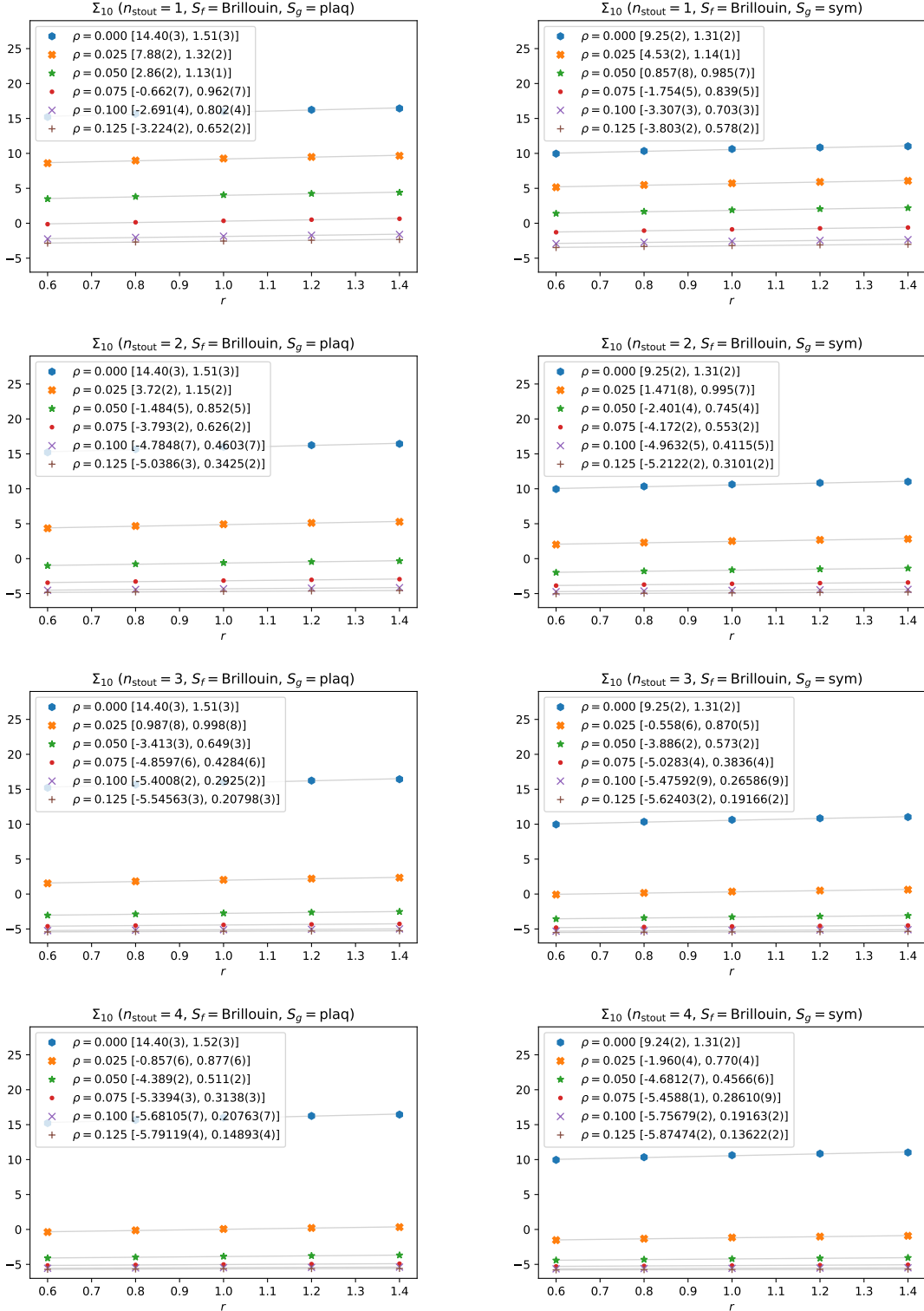


**Figure 7.10:** The same as Figure 7.9 but for the Brillouin clover fermion.

## 7.3 $\Sigma_0$ with Wilson Flow

The relationship between the (dimensionless) flow time and the cumulative smearing parameter is

$$t/a^2 = n_{\text{stout}} \cdot \varrho, \quad (7.4)$$

with errors of order  $t^2/(a^4 n_{\text{stout}})$  (see 7.3 and Equations (6.141), (6.157), and (6.167)). A nice illustration of this correspondence is shown in Figures 7.11, 7.12, and 7.13, where the stout results from Section 7.1 have been plotted again, but against  $\varrho \cdot n_{\text{stout}}$  instead of  $\varrho$  together with the Wilson flow results for  $t \in [0, 1]$ . One can see how for increasing  $n_{\text{stout}}$  the stout curves converge towards the Wilson flow curve (black crosses).

The dotted vertical lines in Figures 7.11, 7.12, and 7.13 indicate integer multiples of 0.125. They are meant to separate each curve into a part where it gives a reasonable approximation to the gradient flow (to the left) and a part where it does not (to the right). For instance the mark at  $3 \cdot 0.125 = 0.375$  separates the dash-dotted line ( $n_{\text{stout}} = 3$ ) into an ascending part (where it approximates the crosses quite well), and a descending part (where it does not). In the terminology of numerical mathematics one would say that multiple stout smearings implement a simple integration scheme (with an integration error in the flow time  $t/a^2$  which scales like  $1/n_{\text{stout}}$ ), and the caveat  $\varrho < 0.125$  of Ref. [98] is meant to limit the integration error.

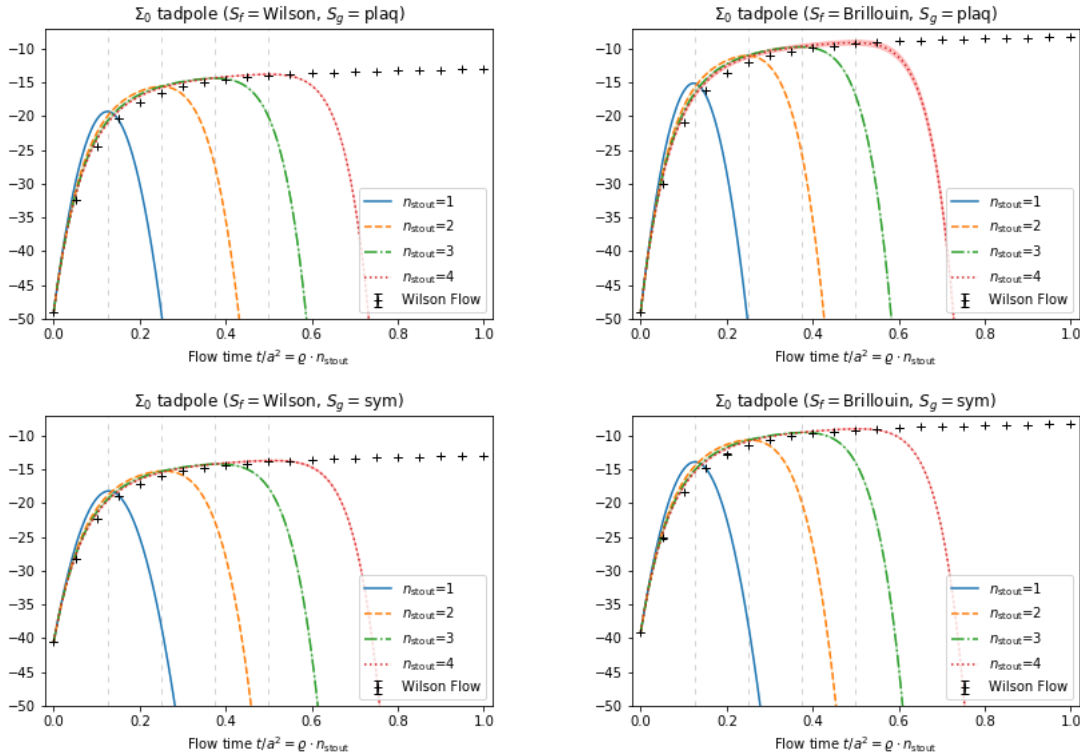


**Figure 7.11:** Contributions from the “tadpole” diagram to the self energy  $\Sigma_0$  with Wilson flow and up to four stout smearing steps as a function of the flow time  $t$  or  $\varrho \cdot n_{\text{stout}}$  respectively. Four combinations of fermion and gluon actions are shown. All results for  $c_{\text{SW}} = r = 1$ .

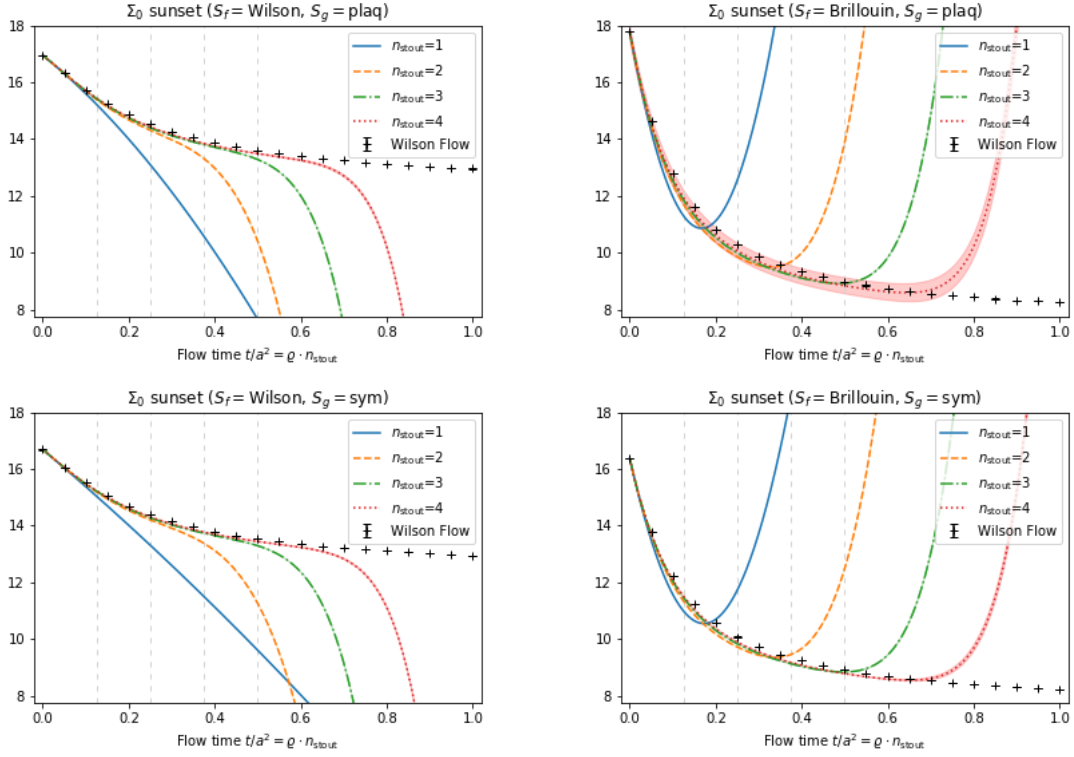


**Figure 7.12:** The same as Figure 7.11 but for the Contribution of the “sunset” diagram.

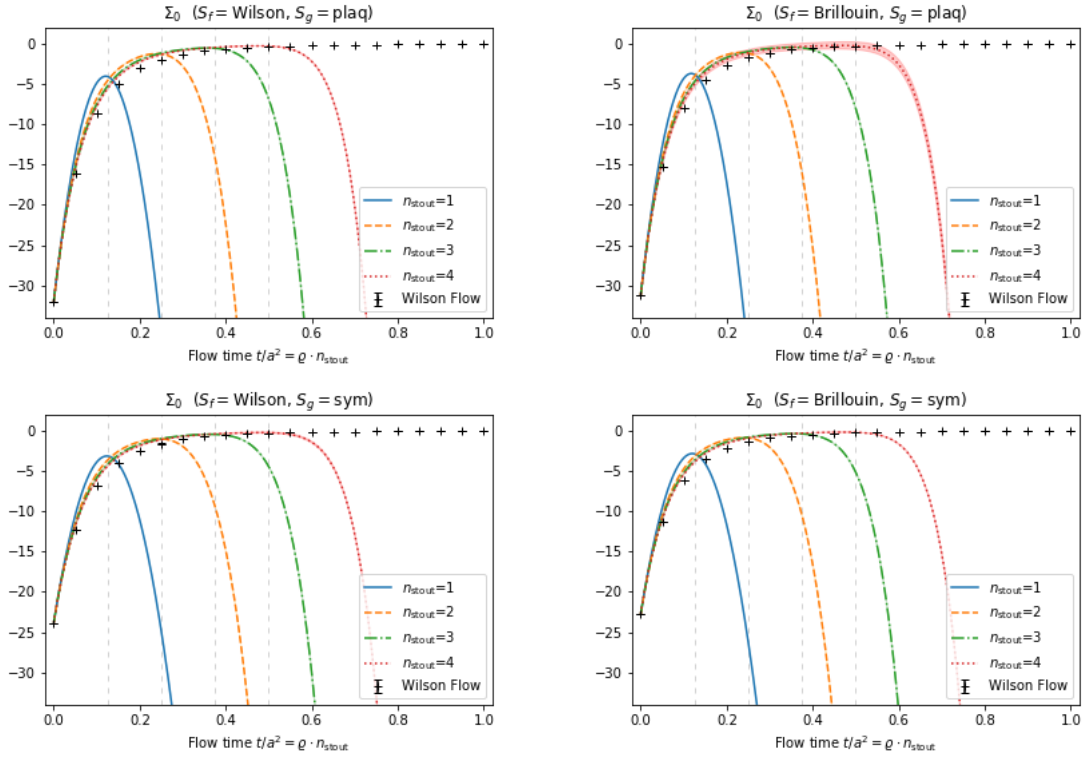


**Figure 7.13:** The same as Figures 7.11 and 7.12 but for the sum  $\Sigma_0$ .

The Wilson flow results for  $\Sigma_0$  themselves appear to have an exponential-like form approaching zero for increasing flow time. On closer inspection, the sum of at least two exponential functions is required to describe their behaviour adequately. This becomes apparent in Figure 7.14, which shows the Wilson flow curves for all five values of  $r$  on a logarithmic y-axis. Each curve exhibits a kind of kink between  $t = 0.2$  and  $t = 0.4$ . Considering the two-exponential fit functions, this is the point where the second of the exponentials becomes dominant.

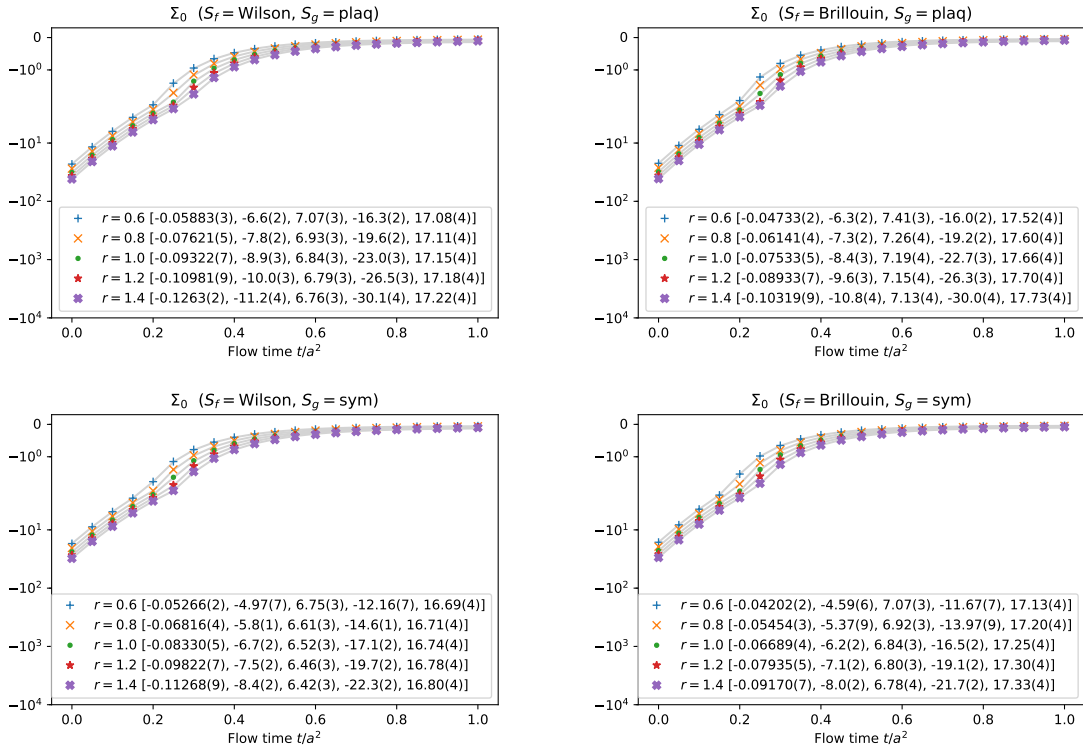


**Figure 7.14:** Logarithmic plot of  $\Sigma_0$  with Wilson flow as a function of the flow time  $t$  for five different values of  $r$  (and  $c_{\text{SW}} = r$ ). Two-exponential fits of the form  $c_0 + c_1 e^{-c_2 t} + c_3 e^{-c_4 t}$  are also shown and the coefficients  $[c_0, c_1, c_2, c_3, c_4]$  given in brackets.

The dependence of the Wilson flow results on  $r$  is unsurprisingly very similar to that of stout smearing. Figure 7.15 shows  $\Sigma_0$  for our five  $r$  values and five flow times  $t \in \{0.1, 0.2, 0.3, 0.4, 1.0\}$ . Note that we have not included the data for  $t = 0$  here (which can be found in Figures 7.4 and 7.5 for  $\varrho = 0$ ), because it would have made it impossible to resolve the data for  $t \geq 0.1$ .

We see again, as for the results with higher  $n_{\text{stout}}$ , that the  $r$  dependence quickly approaches a constant for  $t > 0.2$ .

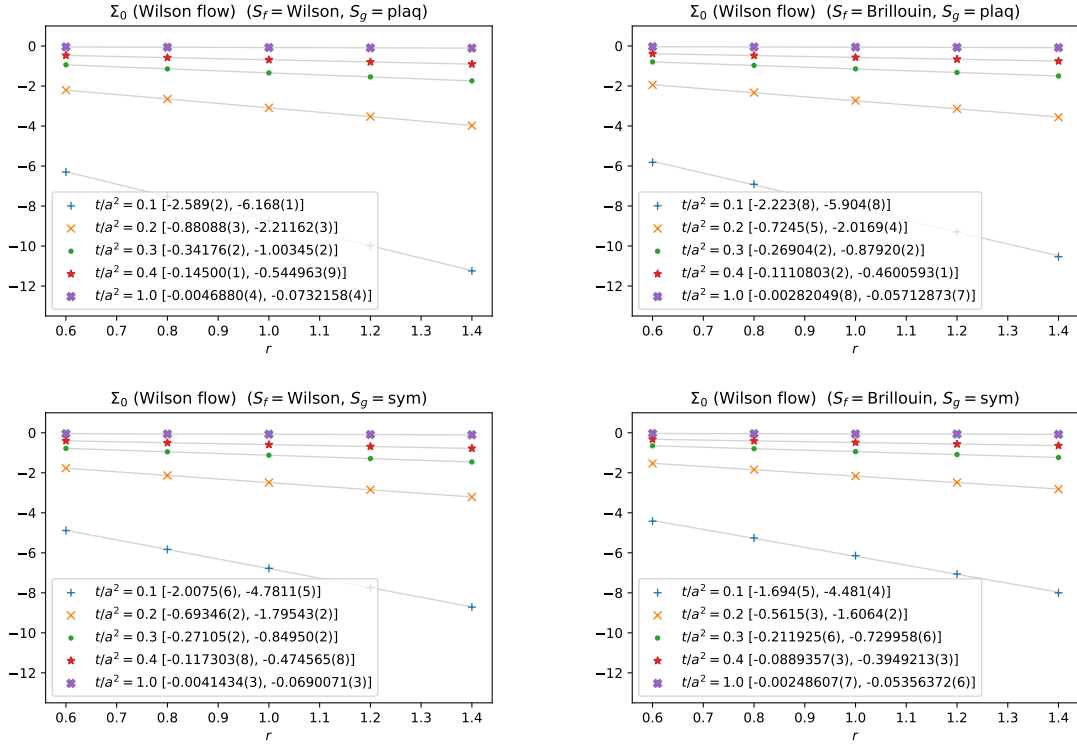


**Figure 7.15:**  $\Sigma_0$  as a function of the Wilson parameter  $r$  (with  $c_{\text{SW}} = r$ ) for five values of the flow time  $t$ . Linear fits of the form  $c_0 + c_1 \cdot r$  are also shown and the fit coefficients  $[c_0, c_1]$  given in brackets.

## 7.4 $\Sigma_1$ with Wilson Flow

For the constant part  $\Sigma_{10}$  we see again (Figures 7.16, 7.17 and 7.18) how the stout smearing results approximate the Wilson flow increasingly well the more steps are taken.

Figure 7.19 shows that again (at least) two exponentials are needed to describe the flowed results with some accuracy.

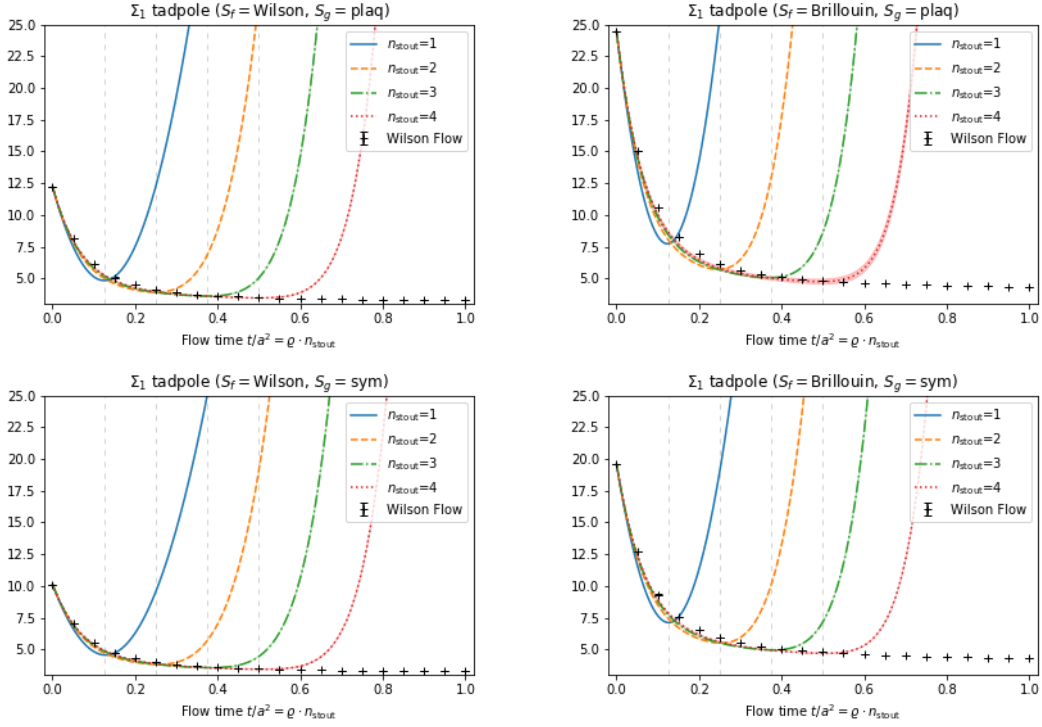


**Figure 7.16:** Contributions from the “tadpole” diagram to the self energy  $\Sigma_{10}$  with Wilson flow and up to four stout smearing steps as a function of the flow time  $t$  or  $\rho \cdot n_{\text{stout}}$  respectively. Four combinations of fermion and gluon actions are shown. All results for  $c_{\text{SW}} = r = 1$  and in Feynman gauge.

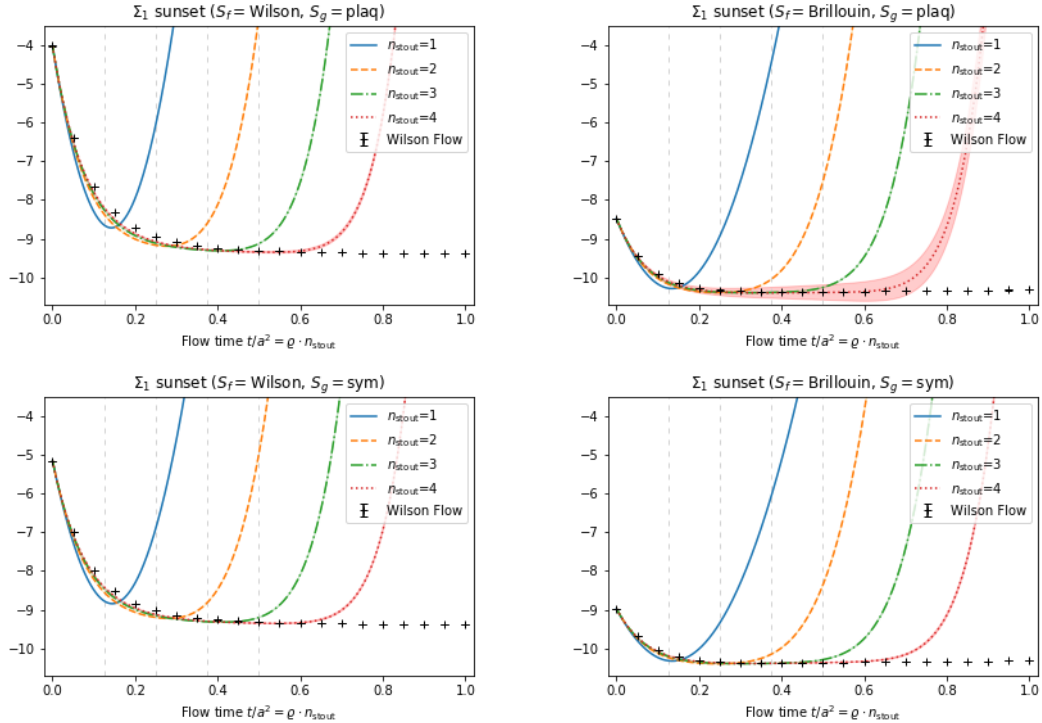


**Figure 7.17:** The same as Figure 7.16 but for the Contribution of the “sunset” diagram.

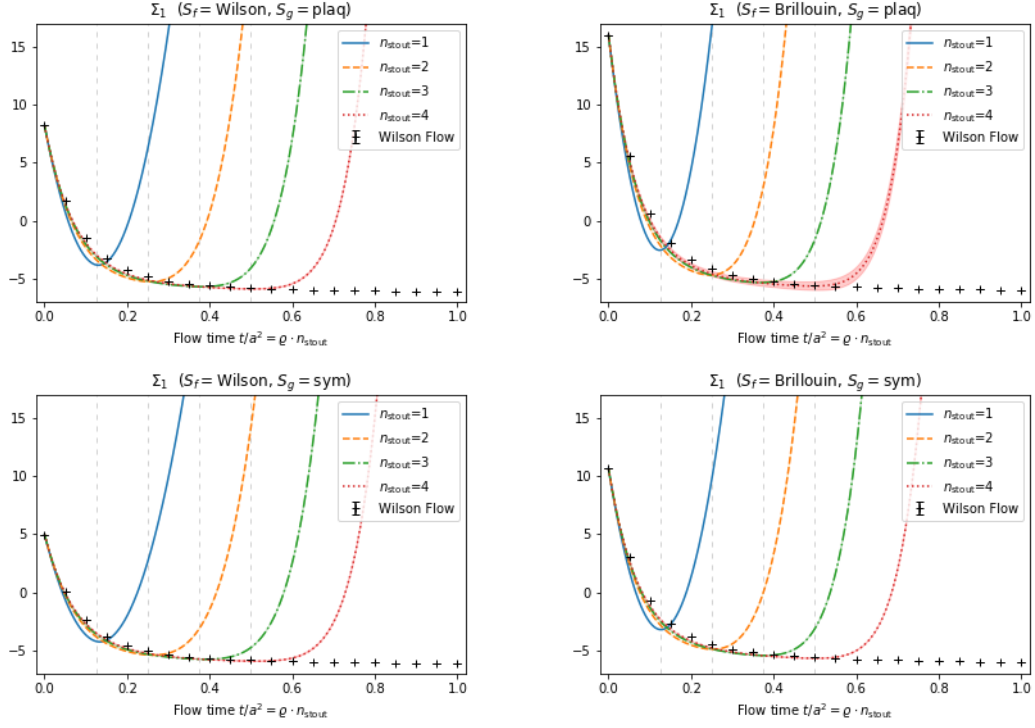


**Figure 7.18:** The same as Figures 7.16 and 7.12 but for the sum  $\Sigma_{10}$ .

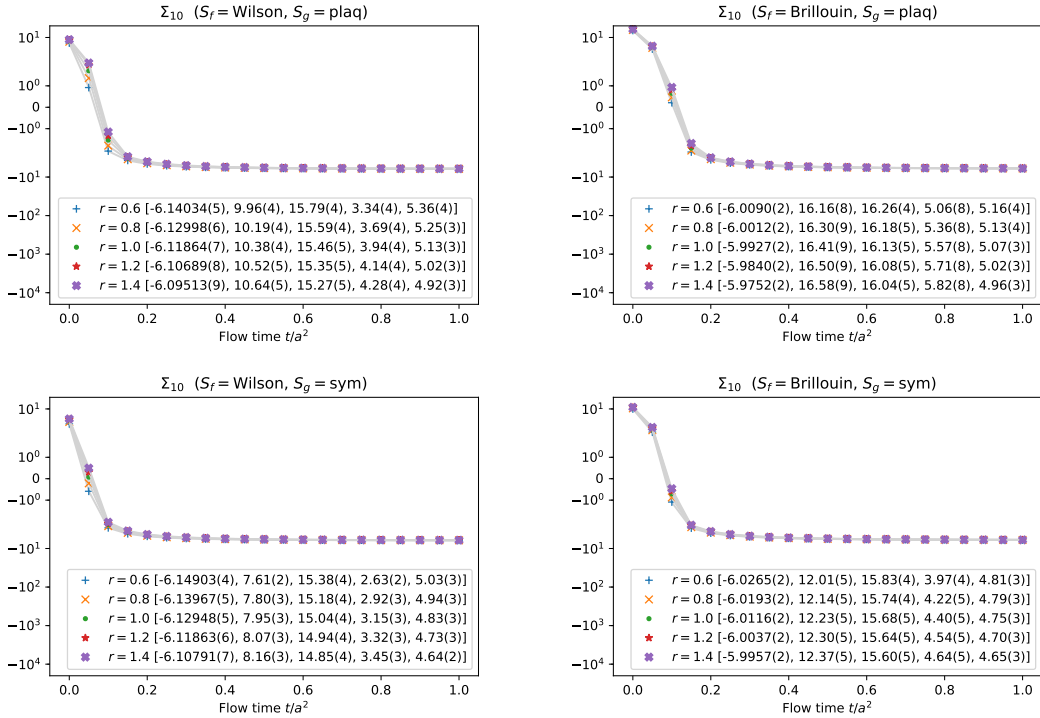


**Figure 7.19:** Logarithmic plot of  $\Sigma_{10}$  with Wilson flow as a function of the flow time  $t$  for five different values of  $r$  (and  $c_{\text{SW}} = r$ ). Two-exponential fits of the form  $c_0 + c_1 e^{-c_2 t} + c_3 e^{-c_4 t}$  are also shown and the coefficients  $[c_0, c_1, c_2, c_3, c_4]$  given in brackets.

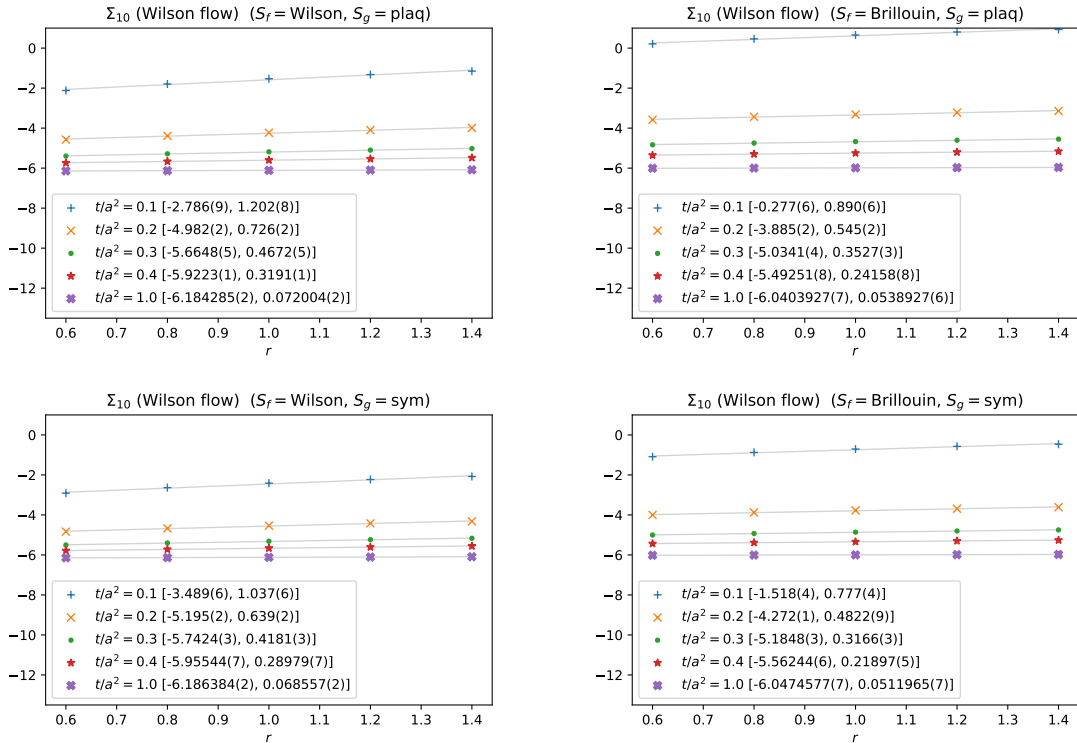


**Figure 7.20:**  $\Sigma_{10}$  as a function of the Wilson parameter  $r$  (with  $c_{\text{SW}} = r$ ) for five values of the flow time  $t$ . Linear fits of the form  $c_0 + c_1 \cdot r$  are also shown and the fit coefficients  $[c_0, c_1]$  given in brackets.

## 8 One-Loop $c_{\text{SW}}$ with Stout Smearing and Wilson Flow

In this chapter we present the results of our one-loop determination of the Sheikholeslami-Wohlert coefficient with stout smearing or Wilson flow and four combinations of fermion (Wilson or Brillouin) and gluon (plaquette or Lüscher-Weisz) actions.

How the one-loop value  $c_{\text{SW}}^{(1)}$  is calculated is explained in Section A.6. The required Feynman rules can be found in Sections 8 and 8 and for how smearing or flowing is incorporated see Section 9.

As mentioned before in A.1, even though the individual one-loop diagrams are almost all divergent, the final result can be split up into two parts proportional to  $N_c$  and  $1/N_c$  respectively (or equivalently into one part proportional to  $N_c$  and one to  $C_F$  etc.). Hence we give results for the full  $c_{\text{SW}}^{(1)}$  with  $N_c = 3$ , but also the coefficients of  $N_c$  and  $1/N_c$  to allow for other values of  $N_c$ .

For the self energy of the clover fermion it was possible and reasonable to not necessarily set  $c_{\text{SW}}$  to its tree-level value  $c_{\text{SW}}^{(0)} = r$  and give results for a general  $c_{\text{SW}}$  (see Appendix A.3). Here, in the determination of  $c_{\text{SW}}^{(1)}$ , however, we have to of course follow the perturbative expansion of  $c_{\text{SW}}$  and need to set  $c_{\text{SW}}^{(0)} = r$  to cancel all the divergencies in the sum of all diagrams.

There is an interesting feature of the Wilson and Brillouin fermion actions we are using here, that make the computation of  $c_{\text{SW}}^{(1)}$  much easier. The finite tadpole diagram (d) (see Figure 4.4) is the only place, where the  $\bar{q}qggg$ -vertex is needed. This vertex is of order  $g_0^3$  and in turn the only place the third order of the perturbative expansion of stout smearing or Wilson flow appears. Due to a cancellation between the Wilson/Brillouin part and the clover part in the vertex, the expression which the third order form factor couples to, vanishes. Thus stout smearing or Wilson flow of order  $g_0^3$ , i.e. the form factors  $\tilde{g}_{\mu\nu\rho\sigma}^{(n)}(\varrho, k_1, k_2, k_3)$  from Equation (6.122) and  $B_{\mu\nu\rho\sigma}(k_1, k_2, k_3, t)$  from Equation (6.166), is not needed to compute  $c_{\text{SW}}^{(1)}$  for Wilson-like fermions. This is true as long as the same smearing/flowing is applied to the covariant derivative and Laplacian part of the action as well as the clover term. For the determination of  $c_{\text{SW}}^{(1)}$  with SLiNC fermions in Ref. [64] for example, this is not the case.

**Proof:** *Without knowing the particular form of  $\tilde{g}_{\mu\nu\rho\sigma}^{(n)}$  (or  $B_{\mu\nu\rho\sigma}$ ) we can show, that they are not needed in the computation of  $c_{\text{SW}}^{(1)}$ . The only place, where the third order could contribute is in the tadpole diagram (d). It is given by*

$$\Lambda_\mu^{a(1)(d)}(p, q) = \sum_{b,\nu\rho} V_{3\mu\nu\rho}^{abb}(p, q, q-p, k, -k) G_{\nu\rho}(k) + 2 \text{ perms .} \quad (8.1)$$

The term in question (ignoring pre-factors and permutations) is

$$\sum_{\nu\rho\alpha} \tilde{g}_{\alpha\mu\nu\rho}^{(n)}(\varrho, q - p, k, -k) V_{1\alpha}(p, q) G_{\nu\rho}(k) . \quad (8.2)$$

For  $V_{1\mu}(p, q)$  we insert the sum of Wilson and clover Feynman rules. They are the only parts that have a Dirac structure, thus they determine the structure after taking the trace in (4.80)

$$\text{Tr}[V_{1W\alpha}(p, q) + V_{1c\alpha}(p, q)] = -4g_0rs(p_\alpha + q_\alpha) \quad (8.3)$$

$$\begin{aligned} \text{Tr}[(V_{1W\alpha}(p, q) + V_{1c\alpha}(p, q))\gamma_\nu\gamma_\mu] &= -2g_0c_{\text{SW}}^{(0)}(\delta_{\mu\alpha}c(p_\mu - q_\mu)\bar{s}(p_\nu - q_\nu) \\ &\quad - \delta_{\nu\alpha}c(p_\nu - q_\nu)\bar{s}(p_\mu - q_\mu)) . \end{aligned} \quad (8.4)$$

All of these terms involve sine functions. Thus terms involving the derivative of  $\tilde{g}_{\alpha\mu\nu\rho}^{(n)}$  will vanish when we set  $p, q$  to zero. The only derivatives that survive are (with  $\mu \neq \nu$ )

$$\left( \frac{\partial}{\partial p_\mu} + \frac{\partial}{\partial q_\mu} \right) \text{Tr}[V_{1W\alpha}(p, q) + V_{1c\alpha}(p, q)] = -4g_0r\delta_{\mu\alpha}c(p_\alpha + q_\alpha) \quad (8.5)$$

$$\left( \frac{\partial}{\partial p_\nu} - \frac{\partial}{\partial q_\nu} \right) \text{Tr}[(V_{1W\alpha}(p, q) + V_{1c\alpha}(p, q))\gamma_\nu\gamma_\mu] = -4g_0c_{\text{SW}}^{(0)}\delta_{\mu\alpha}c(q_\mu - p_\mu)\bar{c}(q_\nu - p_\nu) . \quad (8.6)$$

Setting  $p$  and  $q$  to zero and plugging in the tree-level value  $c_{\text{SW}}^{(0)} = r$  makes both terms identical and they cancel each other in  $G_1$ .

The whole argument above did not depend on the particular form of the form factor  $\tilde{g}$  (or  $B$ ) nor on the number of smearing steps or whether it was the stout smearing or Wilson flow form factor.

The same happens for any Wilson-like fermion action which fulfills the condition  $\lambda_1 + 6\lambda_2 + 12\lambda_3 + 8\lambda_4 = 1$ .

This does not mean, that there is no contribution at all coming from diagram (d). There are still terms coupling to the first and second order form factors in the  $\bar{q}qggg$ -vertex (see Equations 6.181 and 6.184).

Similar to the previous chapter, we present the  $c_{\text{SW}}^{(1)}$  results with up to four stout steps first (Section 8.1). Then we can illustrate again how the stout curves converge towards the Wilson flow curves in Section 8.2.

## 8.1 $c_{\text{SW}}^{(1)}$ with Stout Smearing

In this section we give results for  $c_{\text{SW}}^{(1)}$  with up to four steps of stout smearing for the Wilson fermion action with plaquette (plaq) and Lüscher-Weisz (sym) gluon background as well as for the Brillouin fermion action with plaquette gluons. The combination of Brillouin fermions and the Symanzik improved gauge action produces especially large expressions, which can become very time and memory intensive to integrate. For this

reason we give only results for one and two stout steps for this particular combination.

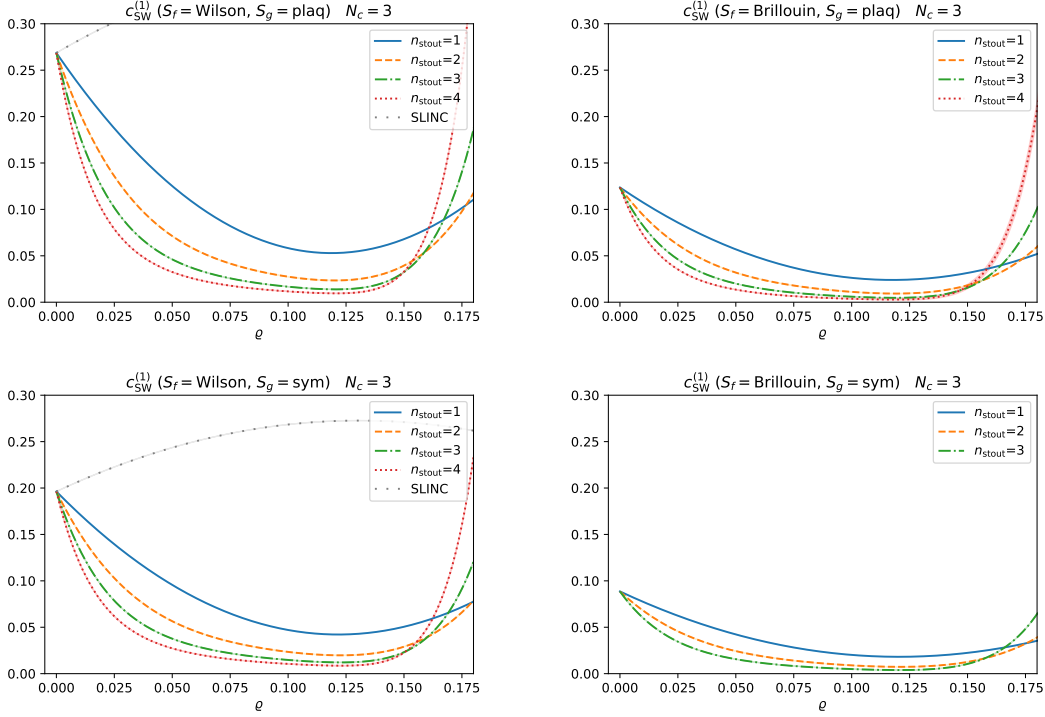


**Figure 8.1:** The one-loop improvement coefficient  $c_{\text{SW}}^{(1)}$  with  $N_c = 3$  up to four steps of stout smearing as a function of the smearing parameter  $\varrho$ . The four panels corepond to the four combinations of the Wilson (left) and Brillouin (right) fermion actions and the plaquette (top) and Lüscher-Weisz (bottom) gauge actions.

In Figure 8.1,  $c_{\text{SW}}^{(1)}$  is plotted against the smearing parameter  $\varrho$  for  $N_c = 3$ . The curves descend from the unsmeared value with an initial slope proportional to  $n_{\text{stout}}$  and approach zero. They reach their minima around  $\varrho = 0.12$  (see Table A.10 for details) before rising again for values larger than 0.125. All in all the picture looks very similar to the ones we have seen for the two parts of the self-energy in Sections 7.1 and 7.2. For increasing  $n_{\text{stout}}$  the curves approach zero faster and are starting to create a plateau closer and closer to the  $x$ -axis. As we have seen in Section A.1 for the unsmeared value of  $c_{\text{SW}}^{(1)}$ , switching to the Brillouin action approximately halves the value. This continues to be true for  $\varrho > 0$  and the improved gluon action reduces the value further by another 30%.

In the panels showing results with the Wilson action we have also included SLiNC results, where only the kinetic part of the action undergoes one step of stout smearing but not the link variables in the clover term. Our numbers in this case show some discrepancies to those given by *Horsley et al.* in Ref. [64], which we were unfortunately unable to resolve. In Table 8.2 we show our results next to those of Ref. [64] in the representation used there, i.e. coefficients of  $C_F$  and  $N_c$ . In the plaquette case there is a difference in the coefficient of  $C_F \varrho^2$ , while in the Symanzik case there are differences for both coefficients of  $\varrho$  and  $\varrho^2$ . The absolute differences in the coefficients of  $C_F$  are four

		$n = 1$	$n = 2$	$n = 3$	$n = 4$
Wil./plaq	$\varrho_{\min}$	0.1186789(3)	0.12009(3)	0.1205(3)	0.1207(3)
	$c_{\text{SW min}}^{(1)}$	0.052915(2)	0.0234(1)	0.0138(1)	0.0095(2)
Wil./sym	$\varrho_{\min}$	0.12166(2)	0.12268(4)	0.1228(1)	0.123(1)
	$c_{\text{SW min}}^{(1)}$	0.0422(1)	0.0197(1)	0.0121(1)	0.0086(3)
Bri./plaq	$\varrho_{\min}$	0.117679(1)	0.1188(1)	0.1186(1)	0.118(3)
	$c_{\text{SW min}}^{(1)}$	0.02399(2)	0.0093(1)	0.0047(1)	0.003(1)
Bri./sym	$\varrho_{\min}$	0.12046(2)	0.121(1)		
	$c_{\text{SW min}}^{(1)}$	0.0182(1)	0.0073(1)		

**Table 8.1:** Position and values of the minima in Figure 8.1

times <sup>1</sup> the absolute differences in the coefficients of  $N_c$ .

This suggests that they might stem from the same place, which is most likely the (d) or (e) and (f) diagrams as their colour factors are the only ones including both  $C_F$  and  $N_c$ . We were however unable to reproduce the numbers of Ref. [64], even when using the exact expressions for the Feynman rules given in the appendix of Ref. [64] and the methods described there, as far as possible. Hence, we are unable to settle this issue definitively, but have performed many error searches and cross-checks in our Mathematica code to be reasonably confident in our methods and results.

	$C_F \cdot \varrho^0$	$C_F \cdot \varrho^1$	$C_F \cdot \varrho^2$
This work (plaq)	0.167635	1.079148	-3.68668
Ref. [64] (plaq)	0.167635	1.079148	-3.697285
	$N_c \cdot \varrho^0$	$N_c \cdot \varrho^1$	$N_c \cdot \varrho^2$
This work (plaq)	0.015025	0.009618	-0.284785
Ref. [64] (plaq)	0.015025	0.009617	-0.284786
	$C_F \cdot \varrho^0$	$C_F \cdot \varrho^1$	$C_F \cdot \varrho^2$
This work (sym)	0.116185	0.857670	-2.85147
Ref. [64] (sym)	0.116185	0.828129	-2.455080
	$N_c \cdot \varrho^0$	$N_c \cdot \varrho^1$	$N_c \cdot \varrho^2$
This work (sym)	0.013777	0.008520	-0.2228016
Ref. [64] (sym)	0.013777	0.015905	-0.321899

**Table 8.2:** Comparison of our result for SLiNC fermions (one step of stout smearing in the Wilson action but not in the clover term) to those of Horsley et al. [64]. Coefficients of  $C_F = (N_c^2 - 1)/(2N_c)$  and  $N_c$  in combination with three orders of the smearing parameter  $\varrho$  (called  $\omega$  in [64]) are shown. Uncertainties are of the order of the last digit printed.

In Table 8.3 we give values of  $c_{\text{SW}}^{(1)}$  for a select number of  $\varrho$ , in order to allow for a quick way to interpolate to any desired value of  $\varrho$ .

Figures 8.4 and 8.5 show the behaviour of  $c_{\text{SW}}^{(1)}$  as a function of  $r$ . Although  $c_{\text{SW}}^{(1)}$  is not a linear function of  $r$ , it shows linear behaviour over the range  $r \in [0.6, 1.4]$  shown

<sup>1</sup>Explicitely  $\frac{0.8576704 - 0.828129}{0.015905 - 0.00852} \approx 4.00002$  and  $\frac{2.85147 - 2.455080}{0.321899 - 0.2228016} \approx 4.000004$ .

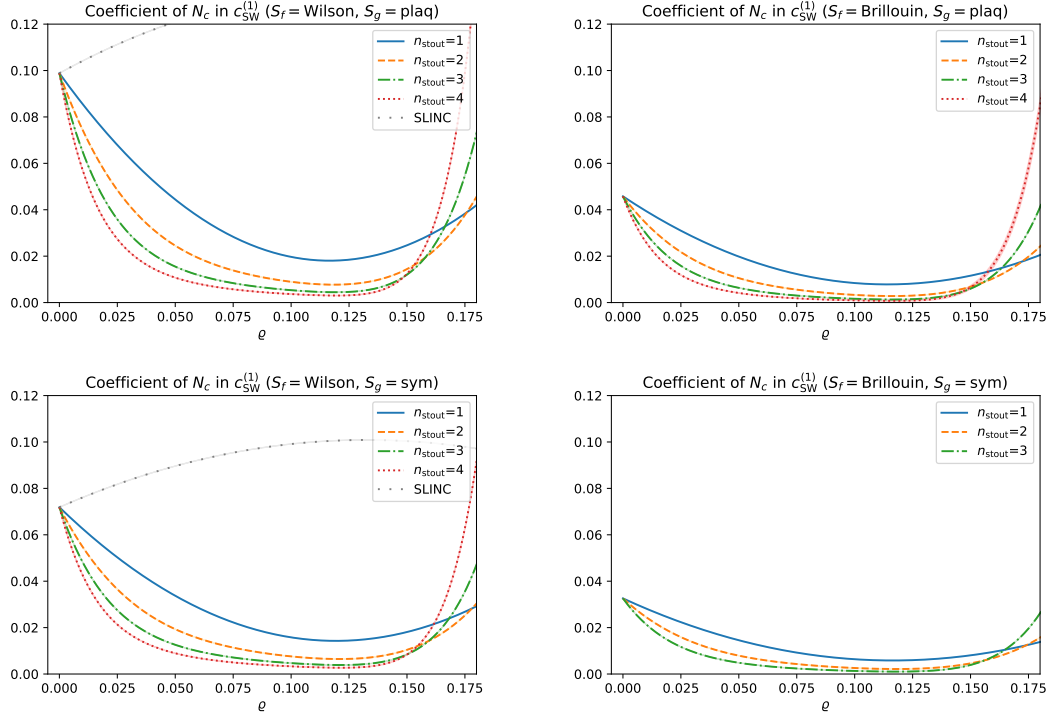


**Figure 8.2:** The same as Figure 8.1 but for the coefficient of  $N_c$  in  $c_{\text{SW}}^{(1)}$ .

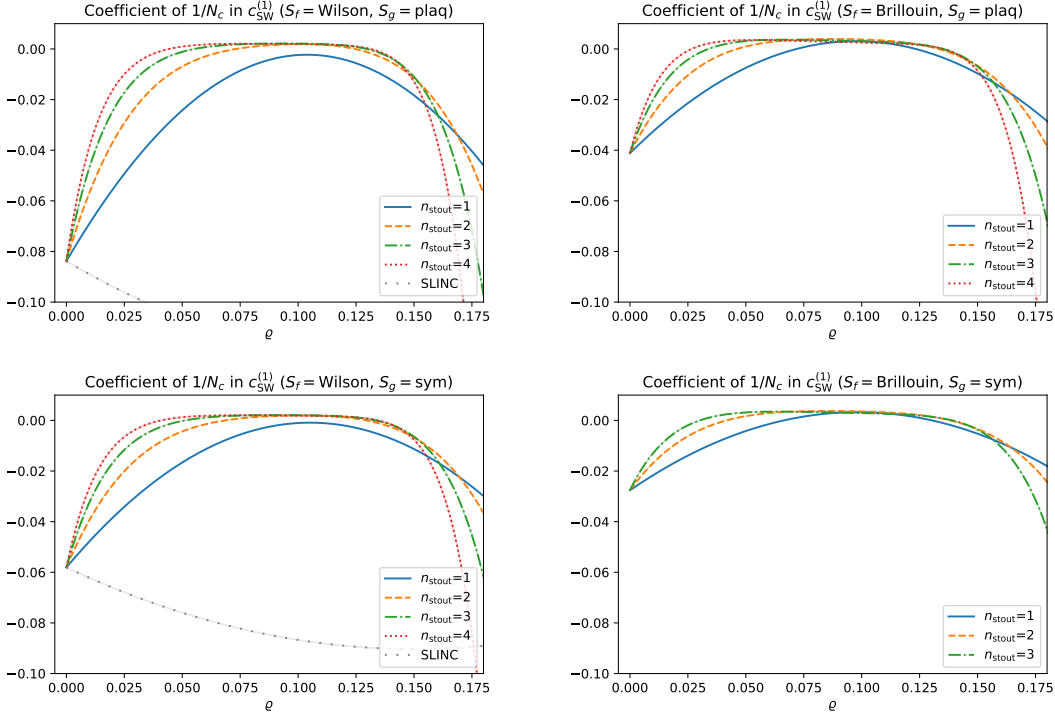


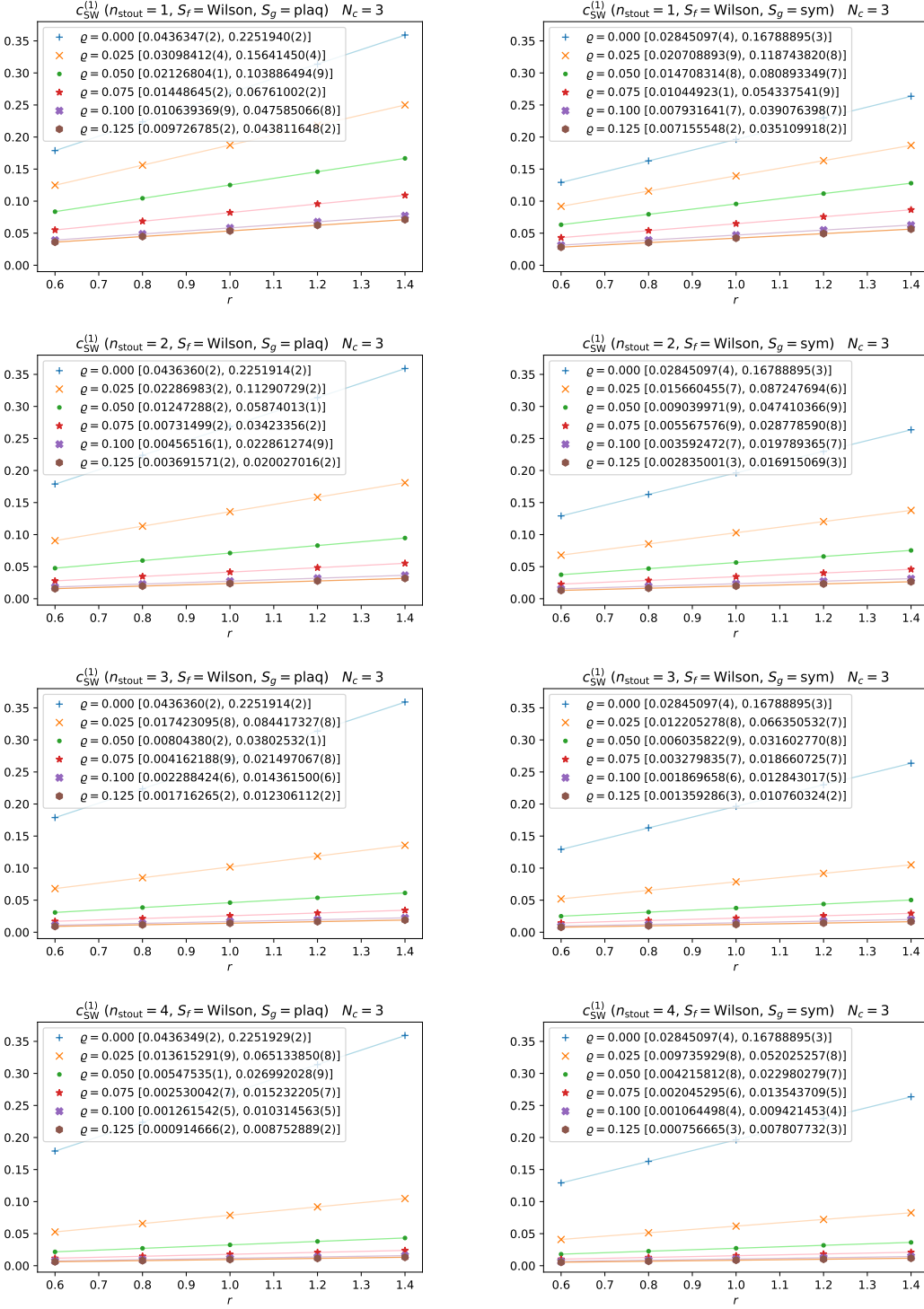
**Figure 8.3:** The same as Figures 8.1 and 8.2 but for the coefficient of  $1/N_c$  in  $c_{\text{SW}}^{(1)}$ .

there. Again, as for the fermion self energy, we see the lines approaching a constant for

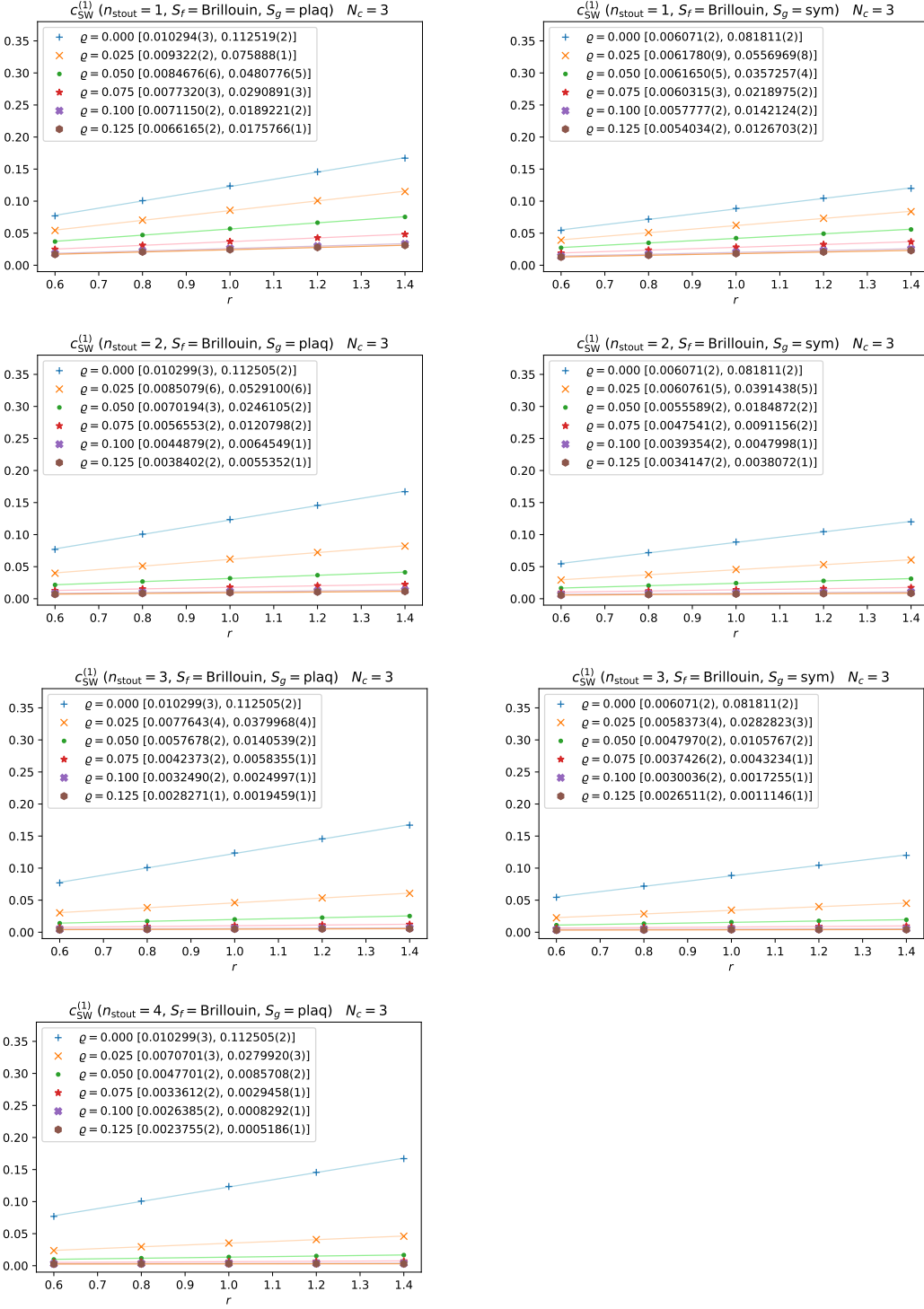
increasing  $\varrho$ , which happens faster and faster, the more stout steps are performed. The effect of the Brillouin and Lüscher-Weisz actions not just lowers the values overall but also decreases the slopes.

	$\varrho$	$n = 1$	$n = 2$	$n = 3$	$n = 4$
$c_{\text{SW}}^{(1)}$ (Wil./plaq))	0.05	0.1251411(9)	0.07125(5)	0.04611(4)	0.03251(5)
	0.09	0.065509(2)	0.03191(7)	0.01953(5)	0.0136(1)
	0.11	0.054068(2)	0.02455(8)	0.01470(6)	0.0102(2)
	0.12	0.052941(2)	0.02343(9)	0.01382(7)	0.0095(2)
	0.125	0.053526(2)	0.02374(9)	0.01404(7)	0.0097(2)
	0.13	0.054877(2)	0.02478(9)	0.01495(7)	0.0105(3)
$c_{\text{SW}}^{(1)}$ (Wil./sym))	0.05	0.09562(4)	0.05649(5)	0.03768(4)	0.02724(8)
	0.09	0.05259(5)	0.02693(7)	0.01706(6)	0.0121(2)
	0.11	0.04357(5)	0.02098(9)	0.01307(7)	0.0093(2)
	0.12	0.04219(6)	0.01979(9)	0.01216(8)	0.0086(3)
	0.125	0.04227(6)	0.01977(9)	0.01214(8)	0.0086(3)
	0.13	0.04288(6)	0.0202(1)	0.01257(9)	0.0090(3)
$c_{\text{SW}}^{(1)}$ (Bri./plaq))	0.05	0.056945(2)	0.03189(4)	0.02003(4)	0.01353(6)
	0.09	0.029502(2)	0.01327(5)	0.00728(5)	0.0045(2)
	0.11	0.024414(2)	0.00974(6)	0.00503(6)	0.0031(4)
	0.12	0.024028(2)	0.00931(6)	0.00473(7)	0.0029(5)
	0.125	0.024375(2)	0.00956(7)	0.00495(7)	0.0031(7)
	0.13	0.025082(2)	0.01019(7)	0.00555(8)	0.0037(9)
$c_{\text{SW}}^{(1)}$ (Bri./sym))	0.05	0.04226(3)	0.02429(4)	0.01558(4)	
	0.09	0.02266(4)	0.01056(5)	0.00596(6)	
	0.11	0.01869(4)	0.00781(6)	0.00418(7)	
	0.12	0.01816(4)	0.00734(6)	0.00386(8)	
	0.125	0.01826(4)	0.00741(6)	0.00395(8)	
	0.13	0.01860(5)	0.00773(6)	0.00427(8)	

**Table 8.3:** Values of  $c_{\text{SW}}^{(1)}$  for  $N_c = 3$  with up to four steps of stout smearing at six values of the smearing parameter  $\varrho$ .



**Figure 8.4:** Dependence of  $c_{\text{SW}}^{(1)}$  on the Wilson parameter  $r$  for Wilson fermions and  $N_c = 3$ . The number of stout smearing steps increases from top to bottom, the left column showing results with the plaquette gauge action, the right column those with the Lüscher-Weisz action. Linear least-square fits of the form  $c_0 + c_1 \cdot r$  are also shown and the coefficients  $[c_0, c_1]$  given in brackets.

**Figure 8.5:** The same as Figure 8.4 but for Brillouin fermions.

## 8.2 $c_{SW}^{(1)}$ with Wilson Flow

We begin the discussion of the Wilson flow results, like we did for the self energy in Section 7.3, by illustrating the approximation of the gradient flow by smearing. We plot

in Figures 8.6, 8.7, and 8.8 the stout curves against the cumulative smearing parameter  $\varrho n_{\text{stout}}$  together with the Wilson flow results.

It appears the discussion from Sections 7.3 and 7.4 is equally applicable here. The stout data follows the flow data increasingly well the more stout steps are used, up until  $t \approx 0.125 \cdot n_{\text{stout}}$  (indicated by vertical dotted lines). There, they diverge quite abruptly away from the flow results.

Similar plots to Figures 8.6-8.8 for each of the six diagrams contributing to  $c_{\text{SW}}^{(1)}$  are given in Figures A.9-A.13 in Appendix A.6.

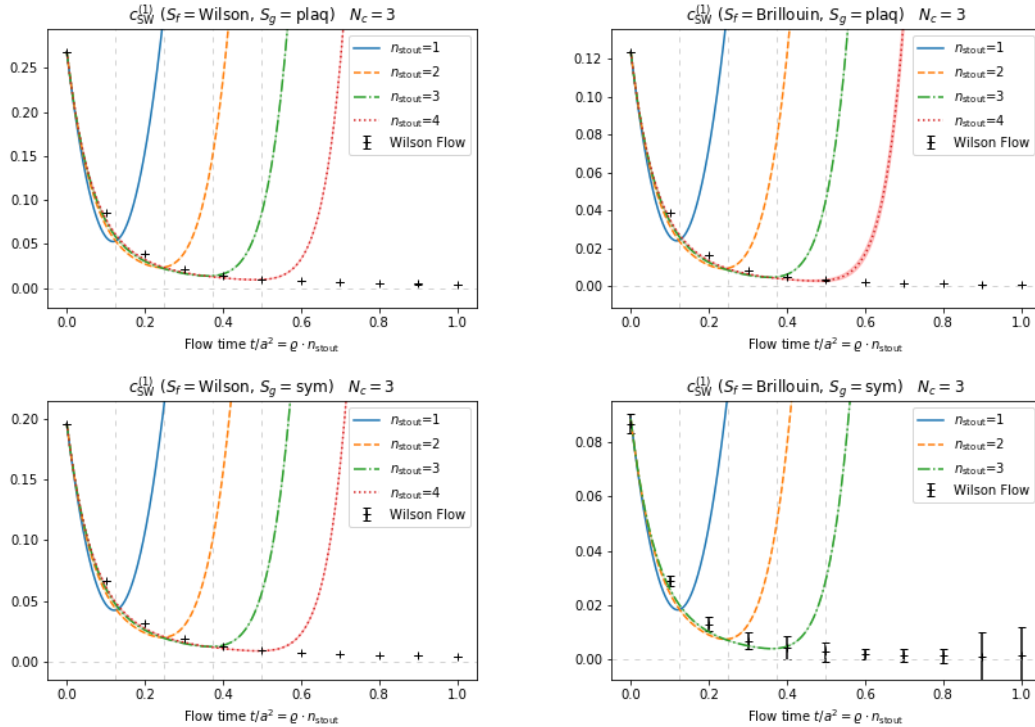


**Figure 8.6:** The one-loop improvement coefficient  $c_{\text{SW}}^{(1)}$  for  $N_c = 3$  with both Wilson flow and up to four stout smearing steps. Results are plotted against the flow time  $t$  or  $\varrho \cdot n_{\text{stout}}$  respectively. The four combinations of fermion (Wilson or Brillouin) and gluon (plaquette or Symanzik) actions are shown.

All Wilson flow results with  $r \in \{0.6, 0.8, 1.0, 1.2, 1.4\}$  are shown in Figure 8.9. They can be reasonably well described by a fit function with the sum of two exponentials. The fit coefficients are given in the legends of the plots. See Appendix A.6 for similar plots for general  $N_c$ . Finally we show the dependence of  $c_{\text{SW}}^{(1)}$  with Wilson flow on  $r$ . Again we see a linear behaviour over the range shown. Note that we do not show the data for  $t = 0$  (it is given in Figures 8.4 and 8.5 for  $\varrho = 0$ ) as it would create a large gap to the results at  $t \geq 0.1$ .

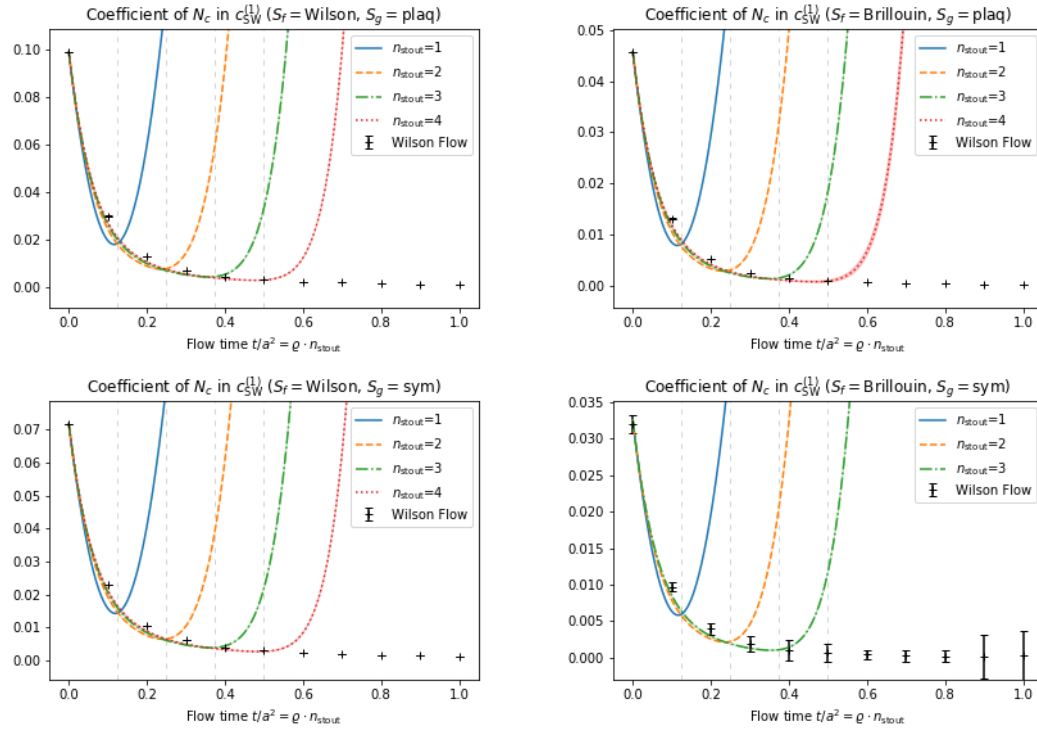


**Figure 8.7:** The same as Figure 8.6 but for the coefficient of  $N_c$  in  $c_{SW}^{(1)}$ .

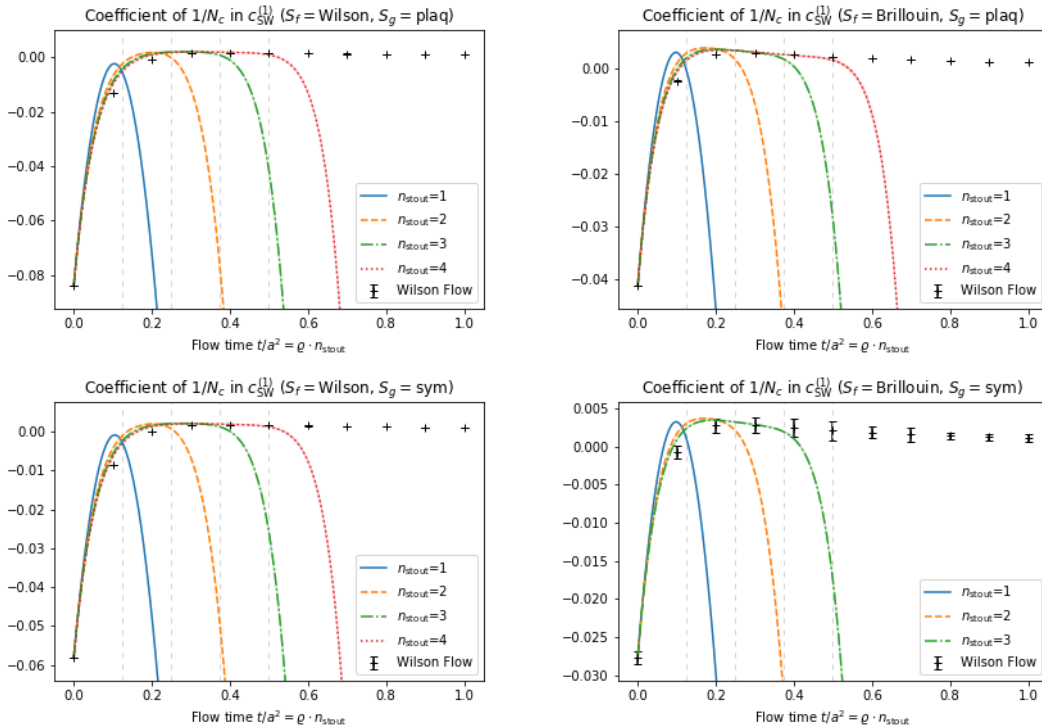


**Figure 8.8:** The same as Figures 8.6 and 8.7 but for the coefficient of  $1/N_c$  in  $c_{SW}^{(1)}$ .

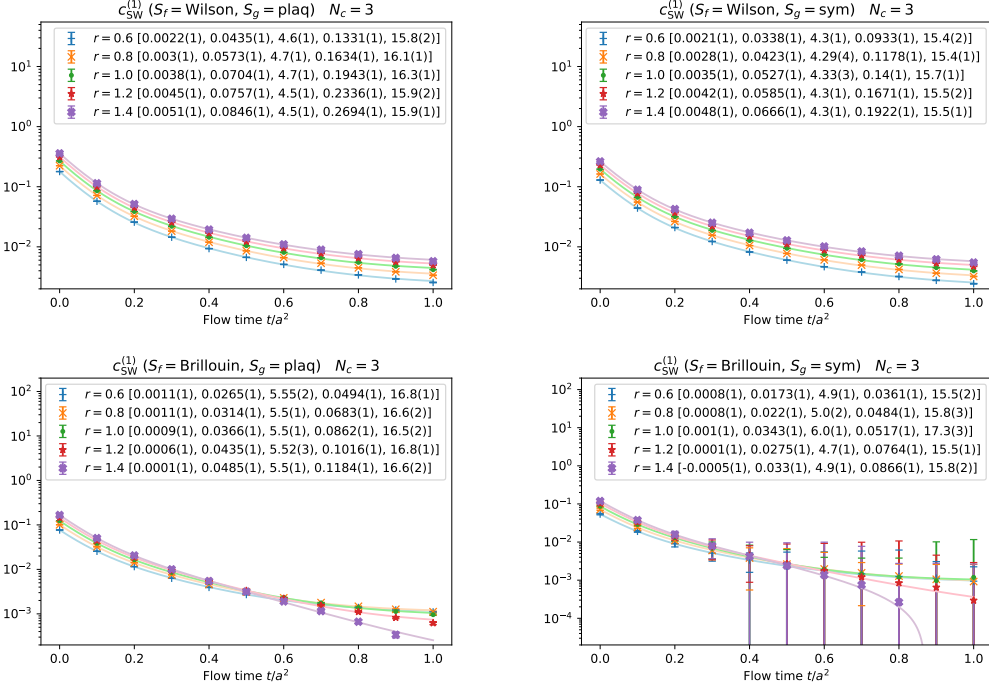


**Figure 8.9:** Logarithmic plot of  $c_{SW}^{(1)}$  with Wilson flow and  $N_c = 3$  as a function of the flow time  $t$  for five different values of  $r$ . Two-exponential fits of the form  $c_0 + c_1 e^{-c_2 t} + c_3 e^{-c_4 t}$  are also shown and the coefficients  $[c_0, c_1, c_2, c_3, c_4]$  given in brackets.

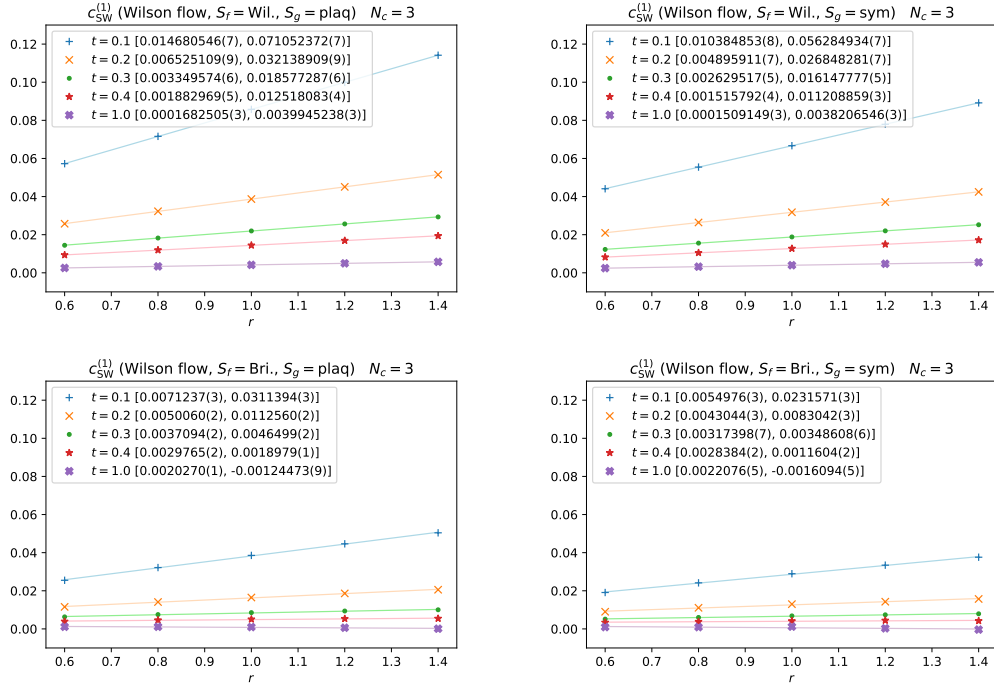


**Figure 8.10:**  $c_{SW}^{(1)}$  for  $N_c = 3$  as a function of  $r$  for a select number of values of the flow time  $t/a^2$ . Linear least-squares fits of the form  $c_0 + c_1 \cdot r$  are also shown and the coefficients  $[c_0, c_1]$  given in brackets.

## 9 Summary and Conclusion

After the introductory Chapters 1 through 4 we began the main part of this thesis by deriving the Feynman rules of the Brillouin action. We found expressions for the  $\bar{q}qg$ ,  $\bar{q}qgg$ , and  $\bar{q}qggg$  vertices, of increasing length and complexity. They displayed, however, some repeating structures and patterns, that allowed us to write them down in a somewhat concise manner (see Section 9). We went on to utilize these Feynman rules to compute the one-loop self energy (Section 9) of the Brillouin fermion as well as the one-loop value for the clover coefficient  $c_{\text{SW}}$  (Section A.1). The former resulted in a critical mass for the Brillouin fermion that is very close to that of the Wilson fermion

$$am_{\text{crit}}^{\text{Wilson/plaq}} = \frac{g_0^2 C_F}{16\pi^2}(-31.9864(1)) \quad am_{\text{crit}}^{\text{Wilson/sym}} = \frac{g_0^2 C_F}{16\pi^2}(-23.8323(1)) \quad (9.1)$$

$$am_{\text{crit}}^{\text{Brillouin/plaq}} = \frac{g_0^2 C_F}{16\pi^2}(-31.1595(1)) \quad am_{\text{crit}}^{\text{Brillouin/sym}} = \frac{g_0^2 C_F}{16\pi^2}(-22.7256(1)), \quad (9.2)$$

while for  $c_{\text{SW}}^{(1)}$  the values are approximately halved in the Brillouin case

$$c_{\text{SW}}^{(1)\text{Wilson/plaq}} = 0.26858825(1) \quad c_{\text{SW}}^{(1)\text{Wilson/sym}} = 0.1962445(1) \quad (9.3)$$

$$c_{\text{SW}}^{(1)\text{Brillouin/plaq}} = 0.12362580(1) \quad c_{\text{SW}}^{(1)\text{Brillouin/sym}} = 0.088601(1). \quad (9.4)$$

Next, in Chapter 6, we took on the perturbative expansion of stout smearing and the Wilson flow order by order, up to  $g_0^3$ . Because stout smearing

$$U_\mu^{(n+1)}(x) = e^{iQ_\mu^{(n)}(x)} U_\mu^{(n)}(x) \quad (9.5)$$

is related to the Wilson flow

$$\partial_t U_\mu(x, t) = iQ_\mu(x, t) U_\mu(x, t) \quad (9.6)$$

the main task of that chapter was the expansion of  $Q_\mu$ . We were able to find the connection between the expansion in  $g_0$  and the new smeared or flowed gluon field  $\tilde{A}_\mu$ , which is again an element of the algebra  $\mathfrak{su}(N_c)$ . We express it as

$$\begin{aligned} \tilde{A}_\mu^{(n)} &= T^a \tilde{A}_\mu^{(n)a} = T^a A_\mu^{(n)a} - \frac{g_0}{2i} [T^a, T^b] A_\mu^{(n)[ab]} \\ &\quad - \frac{g_0^2}{6} \left( T^a T^b T^c + T^c T^b T^a - \frac{1}{N_c} \text{Tr}[T^a T^b T^c + T^c T^b T^a] \right) A_\mu^{(n)abc} + \mathcal{O}(g_0^3) \end{aligned} \quad (9.7)$$

in the stout case and similarly as

$$\begin{aligned} \tilde{A}_\mu(t) &= T^a \tilde{A}_\mu^a(t) = T^a A_\mu^a(t) - \frac{g_0}{2i} [T^a, T^b] A_\mu^{[ab]}(t) \\ &\quad - \frac{g_0^2}{6} \left( T^a T^b T^c + T^c T^b T^a - \frac{1}{N_c} \text{Tr}[T^a T^b T^c + T^c T^b T^a] \right) A_\mu^{abc}(t) + \mathcal{O}(g_0^3) \end{aligned} \quad (9.8)$$

in the flow case. For the perturbative fields  $A^a$ ,  $A^{[ab]}$ , and  $A^{abc}$  we found form factors that depend either on the stout parameters  $(\varrho, n)$  or on the (dimensionless) flow time  $t$  which relate them back to the unsmeared/unflowed fields:

$$A_\mu^{(n)a}(k) = \sum_\nu \tilde{g}_{\mu\nu}^{(n)}(\varrho, k) A_\nu^{(0)a}(k) \quad (9.9)$$

$$A_\mu^{(n)ab}(k_1, k_2) = \sum_{\nu\rho} \tilde{g}_{\mu\nu\rho}^{(n)}(\varrho, k_1, k_2) A_\nu^{(0)a}(k_1) A_\rho^{(0)b}(k_2) \quad (9.10)$$

$$A_\mu^{(n)abc}(k_1, k_2, k_3) = \sum_{\nu\rho\sigma} \tilde{g}_{\mu\nu\rho\sigma}^{(n)}(\varrho, k_1, k_2, k_3) A_\nu^{(0)a}(k_1) A_\rho^{(0)b}(k_2) A_\sigma^{(0)c}(k_3) \quad (9.11)$$

with the  $\tilde{g}$  given in Equations (6.50), (6.64), and (6.122), and

$$A_\mu^a(k, t) = \sum_\nu B_{\mu\nu}(k, t) A_\nu^a(k, 0) \quad (9.12)$$

$$A_\mu^{ab}(k_1, k_2, t) = \sum_{\nu\rho} B_{\mu\nu\rho}(k_1, k_2, t) A_\nu^a(k_1, 0) A_\rho^b(k_2, 0) \quad (9.13)$$

$$A_\mu^{abc}(k_1, k_2, k_3, t) = \sum_{\nu\rho\sigma} B_{\mu\nu\rho\sigma}(k_1, k_2, k_3, t) A_\nu^a(k_1, 0) A_\rho^b(k_2, 0) A_\sigma^c(k_3, 0) \quad (9.14)$$

with the  $B$  functions given in Equations 6.138, 6.152, and 6.166.

In Section 9 we worked out how to couple the  $\tilde{g}$  and  $B$  functions to the vertex Feynman rules of a fermion lattice action. This justifies the laborious analytical derivations that came before, because it greatly simplifies the use of these Feynman rules with stout smearing or Wilson flow for perturbative calculations. A “brute force” approach, where stout smearing is implemented in the action before deriving the Feynman rules, leads in our experience very quickly to expressions that are too long. Even for a computer algebra system, such as Mathematica, they become too large to derive and handle in a reasonable time for anything more than one stout step.

We employed these new tools in the following two chapters (7 and 8) by determining the fermion self energy and the one-loop clover improvement coefficient  $c_{\text{SW}}^{(1)}$ . Due to the relative ease of use of our method for smearing or flowing the Feynman rules, we were able to obtain results with both Wilson and Brillouin clover fermions with up to four steps of stout smearing and could also include the tree-level Symanzik improved (“Lüscher-Weisz”) gluon action in almost all cases.

This allowed us to showcase very nicely how the results obtained with one, two, three and four stout smearing steps approximate the flow results better and better (see Figure 9.1).

For the linearly divergent part of the (clover) fermion self-energy  $\Sigma_0$ , which is proportional to the critical mass, we observed that a smearing parameter close to  $\varrho \approx 0.12$  minimizes the absolute value. One step was able to reduce  $|\Sigma_0|$  by about 85%, two steps by 95%, three steps by 98% and four by over 99%. Parameter values  $\varrho > 0.125$  should be avoided, as the curves for  $\Sigma_0$  no longer approach zero and move away from the Wilson flow results (consistent with observations in Ref. [98]). The behaviour of the  $a^0$  part of the self-energy  $\Sigma_1$  (rather the constant  $\Sigma_{10}$ ) is very similar, except, that it converges towards a value close to  $-6$ .

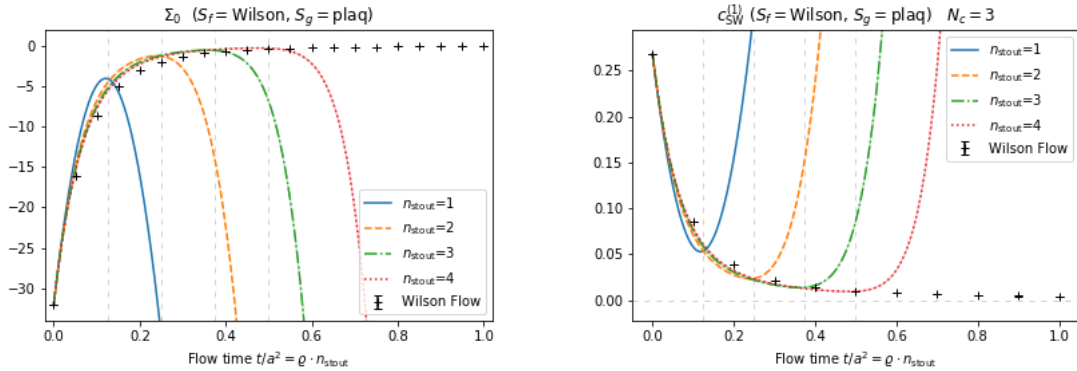


**Figure 9.1:** Plot of one loop  $\Sigma_0 \sim am_{\text{crit}}$  (left) and  $c_{\text{SW}}$  (right) with up to four steps of stout smearing compared to the Wilson flow results at flow time  $t/a^2 = \varrho \cdot n_{\text{stout}}$ .

For  $c_{\text{SW}}^{(1)}$  we saw an approach toward zero, again with minima around  $\varrho \approx 0.12$ . Switching to Brillouin fermions or Lüscher-Weisz gluons brings down the overall values by about 50% and 30% respectively.

The value of  $c_{\text{SW}}$  up to one loop is  $c_{\text{SW}} = r + c_{\text{SW}}^{(1)} g_0^2$ . The value of  $c_{\text{SW}}^{(1)}$  represents the initial slope of a fit function similar to that shown in Figure 3.5. A value of  $c_{\text{SW}}^{(1)}$  close to zero means that the tree-level value  $c_{\text{SW}} = r$  remain a good approximation for a wider range of  $g_0^2$ . The actual length of this range and how steep the behaviour of  $c_{\text{SW}}$  becomes for larger  $g_0^2$ , would require of course a non-perturbative determination of  $c_{\text{SW}}$  or higher order perturbative calculations.

Overall our results suggest that stout smearing and the Wilson flow lead to a fermion action that has improved chiral symmetry ( $am_{\text{crit}} \approx 0$ ) and improved scaling with the lattice constant  $a$ . The former was noted in [98] to be especially true for the combination of smearing and the addition of a clover term. The latter can be expressed as follows: For the unsmeared action adding a clover term and choosing  $c_{\text{SW}} = c_{\text{SW}}^{(0)} = r$  reduces the lattice artifacts from  $\mathcal{O}(a)$  to  $\mathcal{O}(a\alpha_s)$ . For the smeared or flowed action with the same choice for  $c_{\text{SW}}$  (and appropriate  $(\varrho, n)$  and  $t/a^2$ ) the artifacts are already of order  $\mathcal{O}(a\alpha_s^2)$ .

In practical terms we have reiterated the observation from [98] that  $\varrho$  should not be chosen larger than 0.125 but ideally close to 0.12. This also determines the minimal required number of stout steps needed to accurately approximate the Wilson flow for a desired flow time, given by the relation  $t/a^2 = \varrho \cdot n_{\text{stout}} + \mathcal{O}(t^2/(a^4 n_{\text{stout}}))$ .

We hope that our results for the coupling of perturbative smearing and flowing to fermion actions and their Feynman rules will prove useful in future calculations.

Our numerical results may help guide the decision for the use of a specific fermion action with appropriate parameters and hopefully supplement future non-perturbative results.

# A Additional Data

## A.1 $c_{\text{SW}}^{(1)}$ with Brillouin Fermions

To complement the results presented in Section A.1 we give some more detailed data for  $c_{\text{SW}}^{(1)}$  with Brillouin fermions. To enable the reader to adjust the result to arbitrary  $N_c$ , Table A.1 gives the parts  $\sim N_c$  and  $\sim 1/N_c$  separately. Plugging in  $N_c = 3$  reproduces the results listed in Table 5.7. For future reference the splitup into contributions per diagram (for  $N_c = 3$ ) is given in Table A.2 for Wilson fermions and in Table A.3 for Brillouin fermions, respectively.

$r$	$N_c$		$1/N_c$	
	Wilson/Plaq.	Brillouin/Plaq.	Wilson/Plaq.	Brillouin/Plaq.
0.5	0.05715043(1)	0.023738(1)	-0.046248854(1)	-0.0199408(1)
0.6	0.0656271(1)	0.028384(1)	-0.0539062426(2)	-0.0245934(1)
0.7	0.07396653(1)	0.032891(1)	-0.06144543(1)	-0.02900721(1)
0.8	0.08225622(1)	0.037284(1)	-0.0689235(1)	-0.0332272(1)
0.9	0.09054080(1)	0.041578(1)	-0.07637429(1)	-0.037282(1)
1.0	0.09884247(1)	0.04578551(1)	-0.08381749(1)	-0.04119225(1)
1.1	0.10717161(1)	0.049912(1)	-0.09126427(1)	-0.0449695(1)
1.2	0.1155323(1)	0.053963(1)	-0.0987207(1)	-0.04862324(1)
1.3	0.1239253(1)	0.057942(1)	-0.1061899(1)	-0.05215987(1)
1.4	0.1323498(1)	0.061850(1)	-0.1136732(1)	-0.05558402(1)
1.5	0.1408040(1)	0.065691(1)	-0.1211708(2)	-0.05558402(1)
$r$	Wilson/Sym.		Wilson/Sym.	
	Brillouin/Sym.	Brillouin/Sym.	Brillouin/Sym.	Brillouin/Sym.
0.5	0.04087367(1)	0.016533(1)	-0.0315321(1)	-0.0129631(1)
0.6	0.04718026(1)	0.019944(1)	-0.0369456(1)	-0.0162088(1)
0.7	0.05338807(1)	0.023240(1)	-0.04228046(1)	-0.01926933(1)
0.8	0.0595545(1)	0.026441(1)	-0.04757044(1)	-0.02217492(1)
0.9	0.0657097(1)	0.029558(1)	-0.05283676(1)	-0.0249463(1)
1.0	0.0718695(1)	0.032600(1)	-0.05809245(1)	-0.0275974(1)
1.1	0.07804196(1)	0.035572(1)	-0.063345328(1)	-0.03013818(1)
1.2	0.08423066(1)	0.038478(1)	-0.06860003(1)	-0.03257563(1)
1.3	0.09043698(1)	0.041323(1)	-0.0738592(1)	-0.03491483(1)
1.4	0.09666103(1)	0.044107(1)	-0.0791243(1)	-0.0371596(1)
1.5	0.1029022(1)	0.046832(1)	-0.08439603(1)	-0.0393127(1)

**Table A.1:** Parts  $\propto N_c$  and  $\propto 1/N_c$  of  $c_{\text{SW}}^{(1)}$  for Wilson and Brillouin fermions as a function of  $r$ .

Wilson/Plaq.					
$r$	(a)	(b)	(c)		
0.5	$-1/6\mathcal{B}_2 + 0.0048466288(1)$	$-9/4\mathcal{B}_2 + 0.066223184(1)$	$9/4\mathcal{B}_2 - 0.062062540(1)$		
0.6	$-1/5\mathcal{B}_2 + 0.005811036(1)$	$-27/10\mathcal{B}_2 + 0.078124152(1)$	$27/10\mathcal{B}_2 - 0.074475047(1)$		
0.7	$-7/30\mathcal{B}_2 + 0.0068019364(1)$	$-63/20\mathcal{B}_2 + 0.090021110(1)$	$63/20\mathcal{B}_2 - 0.086887555(1)$		
0.8	$-4/15\mathcal{B}_2 + 0.007810019(2)$	$-18/5\mathcal{B}_2 + 0.1019435380(1)$	$18/5\mathcal{B}_2 - 0.099300063(1)$		
0.9	$-3/10\mathcal{B}_2 + 0.00882832(2)$	$-81/20\mathcal{B}_2 + 0.113901379(1)$	$81/20\mathcal{B}_2 - 0.11171257(1)$		
1.0	$-1/3\mathcal{B}_2 + 0.009852153(1)$	$-9/2\mathcal{B}_2 + 0.125895883(1)$	$9/2\mathcal{B}_2 - 0.124125079(1)$		
1.1	$-11/30\mathcal{B}_2 + 0.010878501(1)$	$-99/20\mathcal{B}_2 + 0.13792469(1)$	$99/20\mathcal{B}_2 - 0.136537587(1)$		
1.2	$-2/5\mathcal{B}_2 + 0.011905489(1)$	$-27/5\mathcal{B}_2 + 0.149984155(1)$	$27/5\mathcal{B}_2 - 0.148950095(1)$		
1.3	$-13/30\mathcal{B}_2 + 0.012931987(1)$	$-117/20\mathcal{B}_2 + 0.16207045(1)$	$117/20\mathcal{B}_2 - 0.161362603(1)$		
1.4	$-7/15\mathcal{B}_2 + 0.013957336(1)$	$-63/10\mathcal{B}_2 + 0.174179964(1)$	$63/10\mathcal{B}_2 - 0.17377511(1)$		
1.5	$-1/2\mathcal{B}_2 + 0.014981183(1)$	$-27/4\mathcal{B}_2 + 0.186309485(1)$	$27/4\mathcal{B}_2 - 0.18618762(1)$		
$r$	(d)	(e)	(f)		
0.5	0.148697267(1)	$1/12\mathcal{B}_2 - 0.000834765(1)$	$1/12\mathcal{B}_2 - 0.000834765(1)$		
0.6	0.178436720(1)	$1/10\mathcal{B}_2 - 0.00449215(1)$	$1/10\mathcal{B}_2 - 0.00449215(1)$		
0.7	0.208176174(1)	$7/60\mathcal{B}_2 - 0.00834693(1)$	$7/60\mathcal{B}_2 - 0.00834693(1)$		
0.8	0.237915627(1)	$2/15\mathcal{B}_2 - 0.01228747(1)$	$2/15\mathcal{B}_2 - 0.01228747(1)$		
0.9	0.267655081(1)	$3/20\mathcal{B}_2 - 0.01625395(1)$	$3/20\mathcal{B}_2 - 0.01625395(1)$		
1.0	0.297394534(1)	$1/6\mathcal{B}_2 - 0.020214623(1)$	$1/6\mathcal{B}_2 - 0.020214623(1)$		
1.1	0.327133988(1)	$11/60\mathcal{B}_2 - 0.02415309(1)$	$11/60\mathcal{B}_2 - 0.02415309(1)$		
1.2	0.356873441(2)	$1/5\mathcal{B}_2 - 0.02806145(1)$	$1/5\mathcal{B}_2 - 0.02806145(1)$		
1.3	0.386612895(2)	$13/60\mathcal{B}_2 - 0.03193657(1)$	$13/60\mathcal{B}_2 - 0.03193657(1)$		
1.4	0.416352348(2)	$7/30\mathcal{B}_2 - 0.03577792(1)$	$7/30\mathcal{B}_2 - 0.03577792(1)$		
1.5	0.446091802(2)	$1/4\mathcal{B}_2 - 0.03958640(1)$	$1/4\mathcal{B}_2 - 0.03958640(1)$		
Wilson/Sym.					
$r$	(a)	(b)	(c)		
0.5	$-1/6\mathcal{B}_2 + 0.005143110(1)$	$-9/4\mathcal{B}_2 + 0.065608(1)$	$9/4\mathcal{B}_2 - 0.06688903(1)$		
0.6	$-1/5\mathcal{B}_2 + 0.00618956(1)$	$-27/10\mathcal{B}_2 + 0.0781430(1)$	$27/10\mathcal{B}_2 - 0.08026684(1)$		
0.7	$-7/3\mathcal{B}_2 + 0.00725233(1)$	$-63/20\mathcal{B}_2 + 0.09070162(1)$	$63/20\mathcal{B}_2 - 0.0936446(1)$		
0.8	$-4/15\mathcal{B}_2 + 0.00832513(1)$	$-18/5\mathcal{B}_2 + 0.103291488(1)$	$18/5\mathcal{B}_2 - 0.1070225(1)$		
0.9	$-3/10\mathcal{B}_2 + 0.00940336(1)$	$-81/20\mathcal{B}_2 + 0.11591188(1)$	$81/20\mathcal{B}_2 - 0.12040026(1)$		
1.0	$-1/3\mathcal{B}_2 + 0.01048401(1)$	$-9/2\mathcal{B}_2 + 0.1285594(1)$	$9/2\mathcal{B}_2 - 0.1337781(1)$		
1.1	$-11/30\mathcal{B}_2 + 0.011565172(1)$	$-99/20\mathcal{B}_2 + 0.1412300(1)$	$99/20\mathcal{B}_2 - 0.14715587(1)$		
1.2	$-2/5\mathcal{B}_2 + 0.0126457266(1)$	$-27/5\mathcal{B}_2 + 0.15391985(1)$	$27/5\mathcal{B}_2 - 0.1605337(1)$		
1.3	$-13/30\mathcal{B}_2 + 0.01372504(1)$	$-117/20\mathcal{B}_2 + 0.16662571(1)$	$117/20\mathcal{B}_2 - 0.1739115(1)$		
1.4	$-7/15\mathcal{B}_2 + 0.01480276(1)$	$-63/10\mathcal{B}_2 + 0.17934475(1)$	$63/10\mathcal{B}_2 - 0.1872893(1)$		
1.5	$-1/2\mathcal{B}_2 + 0.0158788(1)$	$-27/4\mathcal{B}_2 + 0.19207465(1)$	$27/4\mathcal{B}_2 - 0.2006671(1)$		
$r$	(d)	(e)	(f)		
0.5	0.11771939(1)	$1/12\mathcal{B}_2 - 0.004735883(1)$	$1/12\mathcal{B}_2 - 0.004735883(1)$		
0.6	0.1412633(1)	$1/10\mathcal{B}_2 - 0.008051702(1)$	$1/10\mathcal{B}_2 - 0.008051702(1)$		
0.7	0.1648071(1)	$7/60\mathcal{B}_2 - 0.011522869(1)$	$7/60\mathcal{B}_2 - 0.011522869(1)$		
0.8	0.18835102(1)	$2/15\mathcal{B}_2 - 0.01506930(1)$	$2/15\mathcal{B}_2 - 0.01506930(1)$		
0.9	0.21189490(1)	$3/20\mathcal{B}_2 - 0.01864652(1)$	$3/20\mathcal{B}_2 - 0.01864652(1)$		
1.0	0.2354388(1)	$1/6\mathcal{B}_2 - 0.022229808(1)$	$1/6\mathcal{B}_2 - 0.022229808(1)$		
1.1	0.25898265(1)	$11/60\mathcal{B}_2 - 0.0258056(1)$	$11/60\mathcal{B}_2 - 0.0258056(1)$		
1.2	0.2825265(1)	$1/5\mathcal{B}_2 - 0.0293666(1)$	$1/5\mathcal{B}_2 - 0.0293666(1)$		
1.3	0.3060704(1)	$13/60\mathcal{B}_2 - 0.032909247(1)$	$13/60\mathcal{B}_2 - 0.032909247(1)$		
1.4	0.3296143(1)	$7/30\mathcal{B}_2 - 0.0364321(1)$	$7/30\mathcal{B}_2 - 0.0364321(1)$		
1.5	0.3531582(1)	$1/4\mathcal{B}_2 - 0.0399350(1)$	$1/4\mathcal{B}_2 - 0.0399350(1)$		

**Table A.2:** Contributions to  $c_{\text{SW}}^{(1)}$  from each diagram as a function of the Wilson parameter  $r$ .

Brillouin/Plaq.					
$r$	(a)	(b)	(c)		
0.5	$-1/6\mathcal{B}_2 + 0.00455393(1)$	$-9/4\mathcal{B}_2 + 0.052949245(1)$	$9/4\mathcal{B}_2 - 0.050279429(1)$		
0.6	$-1/5\mathcal{B}_2 + 0.005634969(1)$	$-27/10\mathcal{B}_2 + 0.061774874(1)$	$27/10\mathcal{B}_2 - 0.06033531(1)$		
0.7	$-7/30\mathcal{B}_2 + 0.00673256(1)$	$-63/20\mathcal{B}_2 + 0.07076411(1)$	$63/20\mathcal{B}_2 - 0.07039120(1)$		
0.8	$-4/15\mathcal{B}_2 + 0.00783569(1)$	$-18/5\mathcal{B}_2 + 0.07987858(1)$	$18/5\mathcal{B}_2 - 0.0804470863(1)$		
0.9	$-3/10\mathcal{B}_2 + 0.00893906(1)$	$-81/20\mathcal{B}_2 + 0.08908850(1)$	$81/20\mathcal{B}_2 - 0.0905029720(1)$		
1.0	$-1/3\mathcal{B}_2 + 0.010040221(1)$	$-9/2\mathcal{B}_2 + 0.098371668(1)$	$9/2\mathcal{B}_2 - 0.100558858(1)$		
1.1	$-11/30\mathcal{B}_2 + 0.01113809(1)$	$-99/20\mathcal{B}_2 + 0.107711629(1)$	$99/20\mathcal{B}_2 - 0.1106147437(1)$		
1.2	$-2/5\mathcal{B}_2 + 0.012232304(1)$	$-27/5\mathcal{B}_2 + 0.117096140(1)$	$27/5\mathcal{B}_2 - 0.12352029(1)$		
1.3	$-13/30\mathcal{B}_2 + 0.013322836(1)$	$-117/20\mathcal{B}_2 + 0.126515999(1)$	$117/20\mathcal{B}_2 - 0.13072652(1)$		
1.4	$-7/15\mathcal{B}_2 + 0.01440984(1)$	$-63/10\mathcal{B}_2 + 0.135964212(1)$	$63/10\mathcal{B}_2 - 0.14078240(1)$		
1.5	$-1/2\mathcal{B}_2 + 0.01549358(1)$	$-27/4\mathcal{B}_2 + 0.145435401(1)$	$27/4\mathcal{B}_2 - 0.150838287(1)$		
$r$	(d)	(e)	(f)		
0.5	$0.073247934(1)$	$1/12\mathcal{B}_2 - 0.007951680(1)$	$1/12\mathcal{B}_2 - 0.007951680(1)$		
0.6	$0.087413353(1)$	$1/10\mathcal{B}_2 - 0.00876542(1)$	$1/10\mathcal{B}_2 - 0.00876542(1)$		
0.7	$0.101417385(1)$	$7/60\mathcal{B}_2 - 0.0097580591(1)$	$7/60\mathcal{B}_2 - 0.0097580591(1)$		
0.8	$0.115260026(1)$	$2/15\mathcal{B}_2 - 0.01087479(1)$	$2/15\mathcal{B}_2 - 0.01087479(1)$		
0.9	$0.12894128(1)$	$3/20\mathcal{B}_2 - 0.01207857(1)$	$3/20\mathcal{B}_2 - 0.01207857(1)$		
1.0	$0.142461144(1)$	$1/6\mathcal{B}_2 - 0.013344189(1)$	$1/6\mathcal{B}_2 - 0.013344189(1)$		
1.1	$0.155819619(1)$	$11/60\mathcal{B}_2 - 0.01465430(1)$	$11/60\mathcal{B}_2 - 0.01465430(1)$		
1.2	$0.169016705(1)$	$1/5\mathcal{B}_2 - 0.01599680(1)$	$1/5\mathcal{B}_2 - 0.01599680(1)$		
1.3	$0.182052403(1)$	$13/60\mathcal{B}_2 - 0.01736306(1)$	$13/60\mathcal{B}_2 - 0.01736306(1)$		
1.4	$0.194926711(1)$	$7/30\mathcal{B}_2 - 0.018746916(1)$	$7/30\mathcal{B}_2 - 0.018746916(1)$		
1.5	$0.207639631(1)$	$1/4\mathcal{B}_2 - 0.02014387(1)$	$1/4\mathcal{B}_2 - 0.02014387(1)$		
Brillouin/Sym.					
$r$	(a)	(b)	(c)		
0.5	$-1/6\mathcal{B}_2 0.0049948(1)$	$-9/4\mathcal{B}_2 0.0535829(1)$	$9/4\mathcal{B}_2 - 0.05491268(1)$		
0.6	$-1/5\mathcal{B}_2 0.0061572(1)$	$-27/10\mathcal{B}_2 0.063236(1)$	$27/10\mathcal{B}_2 - 0.06589522(1)$		
0.7	$-7/30\mathcal{B}_2 0.0073273(1)$	$-63/20\mathcal{B}_2 0.0730149(1)$	$63/20\mathcal{B}_2 - 0.07687776(1)$		
0.8	$-4/15\mathcal{B}_2 0.0084985(1)$	$-18/5\mathcal{B}_2 0.082888(1)$	$18/5\mathcal{B}_2 - 0.0878603(1)$		
0.9	$-3/10\mathcal{B}_2 0.00966762(1)$	$-81/20\mathcal{B}_2 0.092832(1)$	$81/20\mathcal{B}_2 - 0.0988428(1)$		
1.0	$-1/3\mathcal{B}_2 0.0108335(1)$	$-9/2\mathcal{B}_2 0.102829(1)$	$9/2\mathcal{B}_2 - 0.1098254(1)$		
1.1	$-11/30\mathcal{B}_2 0.0119957(1)$	$-99/20\mathcal{B}_2 0.112865(1)$	$99/20\mathcal{B}_2 - 0.1208079(1)$		
1.2	$-2/5\mathcal{B}_2 0.0131542(1)$	$-27/5\mathcal{B}_2 0.122933(1)$	$27/5\mathcal{B}_2 - 0.1317904(1)$		
1.3	$-13/30\mathcal{B}_2 0.0143091(1)$	$-117/20\mathcal{B}_2 0.133025(1)$	$117/20\mathcal{B}_2 - 0.14277298(1)$		
1.4	$-7/15\mathcal{B}_2 0.0154608(1)$	$-63/10\mathcal{B}_2 0.143136(1)$	$63/10\mathcal{B}_2 - 0.1537555(1)$		
1.5	$-1/2\mathcal{B}_2 0.0166094(1)$	$-27/4\mathcal{B}_2 0.153262(1)$	$27/4\mathcal{B}_2 - 0.1647381(1)$		
$r$	(d)	(e)	(f)		
0.5	$0.05771118(1)$	$1/12\mathcal{B}_2 - 0.008049(1)$	$1/12\mathcal{B}_2 - 0.008049(1)$		
0.6	$0.06885251(1)$	$1/10\mathcal{B}_2 - 0.0089611(1)$	$1/10\mathcal{B}_2 - 0.0089611(1)$		
0.7	$0.07986020(1)$	$7/60\mathcal{B}_2 - 0.0100132(1)$	$7/60\mathcal{B}_2 - 0.0100132(1)$		
0.8	$0.09073426(1)$	$2/15\mathcal{B}_2 - 0.0111642(1)$	$2/15\mathcal{B}_2 - 0.0111642(1)$		
0.9	$0.10147468(1)$	$3/20\mathcal{B}_2 - 0.012386(1)$	$3/20\mathcal{B}_2 - 0.012386(1)$		
1.0	$0.1120815(1)$	$1/6\mathcal{B}_2 - 0.013659(1)$	$1/6\mathcal{B}_2 - 0.013659(1)$		
1.1	$0.12255461(1)$	$11/60\mathcal{B}_2 - 0.0149691(1)$	$11/60\mathcal{B}_2 - 0.0149691(1)$		
1.2	$0.13289412(1)$	$1/5\mathcal{B}_2 - 0.016307(1)$	$1/5\mathcal{B}_2 - 0.016307(1)$		
1.3	$0.14309999(1)$	$13/60\mathcal{B}_2 - 0.017666(1)$	$13/60\mathcal{B}_2 - 0.017666(1)$		
1.4	$0.15317223(1)$	$7/30\mathcal{B}_2 - 0.019040(1)$	$7/30\mathcal{B}_2 - 0.019040(1)$		
1.5	$0.1631108(1)$	$1/4\mathcal{B}_2 - 0.020426(1)$	$1/4\mathcal{B}_2 - 0.020426(1)$		

**Table A.3:** Contributions to  $c_{\text{SWBrillouin}}^{(1)}$  for  $N_c = 3$  from each diagram as a function of the Wilson parameter  $r$ .

## A.2 $\Sigma_0$ with Stout Smearing

Here we give the full results for  $\Sigma_0$  with stouts smearing by listing the estimates of the lattice integrals at each order of the smearing parameter  $\varrho$ . Table A.4 gives  $\Sigma_0$  for clover Wilson and clover Brillouin fermions with  $c_{\text{SW}} = 1$ . To enable the reader to use a different value for  $c_{\text{SW}}$ , Tables A.5 and A.6 give the coefficients of  $c_{\text{SW}}^0$ ,  $c_{\text{SW}}^1$ , and  $c_{\text{SW}}^2$  separately (indicated by (0), (1), and (2)).

	Action	$n = 1$	$n = 2$	$n = 3$	$n = 4$
$\varrho^0$	Wil./plaq	-31.98644(3)	-31.98644(3)	-31.98644(3)	-31.986(7)
	Wil./sym	-23.83234(3)	-23.83234(3)	-23.83234(3)	-23.832(6)
	Bri./plaq	-31.15948(3)	-31.160(5)	-31.160(5)	-31.2(4)
	Bri./sym	-22.726(5)	-22.7262(9)	-22.7262(9)	-22.7(3)
$\varrho^1$	Wil./plaq	461.5488(1)	923.0975(2)	1384.6462(3)	1846.19(6)
	Wil./sym	334.19987(5)	668.3997(1)	1002.5996(2)	1336.8(6)
	Bri./plaq	466.4778(2)	932.9567(7)	1399.437(2)	1866.0(2)
	Bri./sym	330.879(5)	661.759(4)	992.639(6)	1323(6)
$\varrho^2$	Wil./plaq	-1907.719658(3)	-11446.31795(2)	-28615.79487(4)	-53416.150(3)
	Wil./sym	-1352.19157(4)	-8113.149(2)	-20282.8736(6)	-37861.370(2)
	Bri./plaq	-1983.73991742(6)	-11902.44(2)	-29756.10(5)	-55544.70(4)
	Bri./sym	-1378.8145(6)	-8272.888(4)	-20682.219(9)	-38606.67(2)
$\varrho^3$	Wil./plaq		69587.70312(7)	347938.5156(4)	974228(2)
	Wil./sym		48476.67898(2)	242383.40(2)	678673.4(2)
	Bri./plaq		74053.1793(9)	370265.894(7)	1036744(30)
	Bri./sym		50653.457(4)	253267.29(2)	709148(5)
$\varrho^4$	Wil./plaq		-171121.8788(3)	-2566828.182(5)	-11978531(7)
	Wil./sym		-117482.6334(5)	-1762239.500(7)	-8223785(5)
	Bri./plaq		-185651.7(2)	-2784775(3)	-12995597(14)
	Bri./sym		-125336.2(2)	-1880044(2)	-8773527(15)
$\varrho^5$	Wil./plaq			10728081.87(2)	100128744(41)
	Wil./sym			7273681(5)	67887689(29)
	Bri./plaq			11831388(7)	110426033(328)
	Bri./sym			7900452(24)	73737147(218)
$\varrho^6$	Wil./plaq			-19627721.69(2)	-549575266(290)
	Wil./sym			-13163619.12(3)	-368581513(347)
	Bri./plaq			-21953363(68)	-614692421(2590)
	Bri./sym			-14523076(11)	-406643350(1494)
$\varrho^7$	Wil./plaq				1795933838(5106)
	Wil./sym				1193026157(2578)
	Bri./plaq				2033345666(27425)
	Bri./sym				1334328214(2111)
$\varrho^8$	Wil./plaq				-2658101497(19216)
	Wil./sym				-1750940862(13091)
	Bri./plaq				-3041513205(92639)
	Bri./sym				-1981884630(9614)

**Table A.4:** Coefficients of powers of  $\varrho$  in  $\Sigma_0$  for Wilson and Brillouin clover fermions with  $c_{\text{SW}} = r = 1$ .

			$\Sigma_0$ (Wilson)			
			$n = 1$	$n = 2$	$n = 3$	$n = 4$
$\varrho^0$	plaq	(0)	-51.43471(4)	-51.43471(4)	-51.43471(4)	-51.435(8)
		(1)	13.73313(4)	13.73313(4)	13.73313(4)	13.732(2)
		(2)	5.7151(3)	5.7151(3)	5.7151(3)	5.7150(5)
	sym	(0)	-40.44323(3)	-40.44323(3)	-40.44323(3)	-40.443(7)
		(1)	11.94822(3)	11.94822(3)	11.94822(3)	11.947(2)
		(2)	4.6627(2)	4.6627(2)	4.6627(2)	4.66255(5)
$\varrho^1$	plaq	(0)	612.3029(1)	1224.6058(2)	1836.9087(3)	2449.21(3)
		(1)	-91.442(4)	-182.884(7)	-274.33(1)	-365.76(3)
		(2)	-59.3118850(8)	-118.623770(2)	-177.935654(4)	-237.248(4)
	sym	(0)	455.5139(1)	911.0278(2)	1366.5417(9)	1822.1(6)
		(1)	-74.603(3)	-149.206(5)	-223.808(8)	-298.403(4)
		(2)	-46.7112574(3)	-93.4225147(6)	-140.1337727(3)	-186.845(1)
$\varrho^2$	plaq	(0)	-2335.4071(3)	-14012.442(2)	-35031.106(4)	-65391.6(2)
		(1)	237.247540(3)	1423.48523(3)	3558.71310(5)	6642.94(9)
		(2)	190.439888(2)	1142.639327(9)	2856.59832(3)	5332.32(7)
	sym	(0)	-1685.5973(3)	-10113.584(3)	-25283.960(4)	-47196.889(4)
		(1)	186.845029(2)	1121.070182(3)	2802.6754(3)	5231.66(3)
		(2)	146.560758(2)	879.36454(1)	2198.41137(2)	4103.70(5)
$\varrho^3$	plaq	(0)		81277.32696(7)	406386.6344(6)	1137883.43(5)
		(1)		-6094.07640(6)	-30470.3820(4)	-85317(2)
		(2)		-5595.54740(2)	-27977.73695(9)	-78337.66(7)
	sym	(0)		57399.24192(3)	286996.21(2)	803589.90(8)
		(1)		-4689.94425(4)	-23449.721432(8)	-65659.2(8)
		(2)		-4232.61867(2)	-21163.09330(3)	-59256.7(2)
$\varrho^4$	plaq	(0)		-193630.40(3)	-2904456.0(4)	-13554132(2)
		(1)		11191.09479(3)	167866.4219(4)	783374(2)
		(2)		11317.4275(3)	169761.412(4)	792220(5)
	sym	(0)		-134388.50(2)	-2015827.5(3)	-9407196.9(4)
		(1)		8465.23735(4)	126978.5602(6)	592567(2)
		(2)		8440.6307(2)	126609.461(2)	590846.979(8)
$\varrho^5$	plaq	(0)			11863189.778(7)	110723094(4)
		(1)			-543236.523(8)	-5070208(26)
		(2)			-591871.37(2)	-5524133(26)
	sym	(0)			8114869(5)	75738794(14)
		(1)			-405150.278(4)	-3781420.66(5)
		(2)			-436037.438(2)	-4069704(48)
$\varrho^6$	plaq	(0)			-21329904.75(2)	-597236493(336)
		(1)			789161.8462(9)	22096532(104)
		(2)			913021.209(7)	25564594(2)
	sym	(0)			-14410242.41(3)	-403487007(319)
		(1)			581383.242(7)	16278817(190)
		(2)			665240.039(6)	18626734(383)
$\varrho^7$	plaq	(0)				1925422531(5277)
		(1)				-58433357(1223)
		(2)				-71058490(163)
	sym	(0)				1286849516(2631)
		(1)				-42575391.8(3)
		(2)				-51248188(2163)
$\varrho^8$	plaq	(0)				-2819282113(19240)
		(1)				71058490(163)
		(2)				90125153(5113)
	sym	(0)				-1866581334(13091)
		(1)				51248188(2163)
		(2)				64387254(3655)

**Table A.5:** Coefficients of powers of  $\varrho$  and powers of  $c_{\text{SW}}$  (indicated by (0),(1),(2) for  $c_{\text{SW}}^0$ ,  $c_{\text{SW}}^1$ , and  $c_{\text{SW}}^2$ ) in  $\Sigma_0$  for Wilson fermions with  $r = 1$ .

$\Sigma_0$  (Brillouin)

			$n = 1$	$n = 2$	$n = 3$	$n = 4$
$\varrho^0$	plaq	(0)	-53.94076(4)	-53.941(4)	-53.941(4)	-54.0(3)
		(1)	12.94885(3)	12.948(2)	12.948(2)	12.97(8)
		(2)	9.83244(2)	9.8323(6)	9.8323(6)	9.833(4)
	sym	(0)	-41.953(4)	-41.9529(5)	-41.9529(5)	-42.0(2)
		(1)	11.344(2)	11.344(2)	11.344(2)	11.37(8)
		(2)	7.88251(4)	7.88251(4)	7.88251(4)	7.88(5)
$\varrho^1$	plaq	(0)	661.0663(8)	1322.137(2)	1983.205(2)	2644.4(5)
		(1)	-79.413155(9)	-158.8299(9)	-238.245(2)	-318(5)
		(2)	-115.1753151(3)	-230.3506(8)	-345.5257(8)	-460.6999(2)
	sym	(0)	485.579(6)	971.157(4)	1456.736(6)	1942(2)
		(1)	-65.2657(2)	-130.5313(4)	-195.7970(6)	-261(7)
		(2)	-89.4351(3)	-178.8702(6)	-268.3053(8)	-357.740(7)
$\varrho^2$	plaq	(0)	-2579.6583169(4)	-15477.948(2)	-38694.870(5)	-72230.432(2)
		(1)	191.492447(2)	1148.94(3)	2872.34(8)	5361.801(6)
		(2)	404.425951(4)	2426.556(2)	6066.389(4)	11323.94(4)
	sym	(0)	-1837.9379(4)	-11027.628(3)	-27569.082(8)	-51462.270(2)
		(1)	151.607(4)	909.64(2)	2274.10(5)	4245.03(1)
		(2)	307.5206(7)	1845.124(4)	4612.81(1)	8610.57(3)
$\varrho^3$	plaq	(0)		91425.349(4)	457126.744(7)	1279955(30)
		(1)		-4621.32585(8)	-23106.4(3)	-64697.4(3)
		(2)		-12750.89(5)	-63754.46(8)	-178513.4(8)
	sym	(0)		63763.842(7)	318819.21(4)	892694(5)
		(1)		-3568.20(6)	-17841.0(2)	-49954.6(2)
		(2)		-9542.184(6)	-47710.92(3)	-133590.9(7)
$\varrho^4$	plaq	(0)		-221010.43(4)	-3315156.5(5)	-15470733(14)
		(1)		8040.4(2)	120606(3)	562823(9)
		(2)		27318.5559(5)	409778(5)	1912312(6)
	sym	(0)		-151604.162(2)	-2274062.43(2)	-10612292(11)
		(1)		6093.4337(2)	91401.506(3)	426533.0(4)
		(2)		20174.58(9)	302619(2)	141232(5)
$\varrho^5$	plaq	(0)			13702606(4)	127890973(274)
		(1)			-372063.47(2)	-3472601(26)
		(2)			-1499149(33)	-13992313(359)
	sym	(0)			9272535(8)	86543590(7013)
		(1)			-277767(11)	-2592501(12)
		(2)			-1094313(24)	-10213737(111)
$\varrho^6$	plaq	(0)			-24880251(34)	-696646561(2635)
		(1)			517689(10)	14495528(440)
		(2)			2409288(8)	67459049(442)
	sym	(0)			-16644843(10)	-466055397(617)
		(1)			381592(9)	10684500(243)
		(2)			1740169(59)	48725863(2153)
$\varrho^7$	plaq	(0)				2264434650(27435)
		(1)				-36856089(668)
		(2)				-194235142(3957)
	sym	(0)				1500125887(3258)
		(1)				-26863447(772)
		(2)				-138932430(107)
$\varrho^8$	plaq	(0)				-3338788918(92715)
		(1)				43231951(1080)
		(2)				254059894(19175)
	sym	(0)				-2193146620(9342)
		(1)				31194907(2858)
		(2)				180072831(7664)

Table A.6: The same as Table A.5 but for Brillouin fermions.

### A.3 $\Sigma_1$ with Stout Smearing

Here we give the same tables as in Appendix A.3 but for  $\Sigma_{10}$  (see Equation 4.70).

	Action	$n = 1$	$n = 2$	$n = 3$	$n = 4$
$\varrho^0$	Wil./plaq	8.20627(3)	8.20627(3)	8.20627(3)	8.206(3)
	Wil./sym	4.973633(5)	4.973633(5)	4.973633(5)	4.974(2)
	Bri./plaq	15.99016(2)	15.990(2)	15.990(2)	16.0(2)
	Bri./sym	10.626(3)	10.626(2)	10.626(2)	10.62(3)
$\varrho^1$	Wil./plaq	-184.19270(6)	-368.3854(2)	-552.57811(7)	-736.77(7)
	Wil./sym	-137.61668(5)	-275.2334(1)	-412.85002(9)	-550.5(2)
	Bri./plaq	-299.02105(4)	-598.044(3)	-897.07(2)	-1196(2)
	Bri./sym	-217.45(9)	-434.907(2)	-652.36(2)	-870(2)
$\varrho^2$	Wil./plaq	704.18682(5)	4225.1209(3)	10562.8023(7)	19717.2(3)
	Wil./sym	512.81660(2)	3076.8996(2)	7692.2490(3)	14358.9(2)
	Bri./plaq	1205.76006(8)	7234.57(2)	18086.42(4)	33761.39(2)
	Bri./sym	854.426(7)	5126.56(4)	12816.4(1)	23924.112(3)
$\varrho^3$	Wil./plaq		-24227.54502(9)	-121137.7249(6)	-339186(1)
	Wil./sym		-17289.6263(2)	-86448.13(4)	-242054.9(4)
	Bri./plaq		-43451.85(4)	-217259.2(2)	-608326(15)
	Bri./sym		-30201.48(8)	-151007.4(2)	-422821(3)
$\varrho^4$	Wil./plaq		56866.2480(2)	852993.719(3)	3980637(6)
	Wil./sym		39893.8762(1)	598408.143(2)	2792571.48(4)
	Bri./plaq		106103.347(7)	1591550.2(1)	7427235(9)
	Bri./sym		72609.223(2)	1089138.34(2)	5082644(6)
$\varrho^5$	Wil./plaq			-3431932.546(6)	-32031358(9)
	Wil./sym			-2372221(1)	-22140728(2)
	Bri./plaq			-6622947.7(5)	-61814175(759)
	Bri./sym			-4473798(2)	-41755504(63)
$\varrho^6$	Wil./plaq			6083762(3)	170345240(173)
	Wil./sym			4150857.326(4)	116224020(336)
	Bri./plaq			12083927(16)	338348326(2297)
	Bri./sym			8072966(12)	226041990(1184)
$\varrho^7$	Wil./plaq				-542124208(1774)
	Wil./sym				-365651055(67)
	Bri./plaq				-1103824050(13784)
	Bri./sym				-730443887(5424)
$\varrho^8$	Wil./plaq				784643279(12269)
	Wil./sym				523847362(2021)
	Bri./plaq				1632177993(46847)
	Bri./sym				1071139558(6746)

**Table A.7:** Coefficients of powers of  $\varrho$  in  $\Sigma_{10}$  for Wilson and Brillouin clover fermions with  $c_{\text{SW}} = r = 1$ .

		$\Sigma_{10}$ (Wilson)				
			$n = 1$	$n = 2$	$n = 3$	$n = 4$
$\varrho^0$	plaq	(0)	11.852396(8)	11.852396(8)	11.852396(8)	11.852(2)
		(1)	-2.248869(6)	-2.248869(6)	-2.248869(6)	-2.249(2)
		(2)	-1.397261(9)	-1.397261(9)	-1.397261(9)	-1.3973(3)
	sym	(0)	8.231254(4)	8.231254(4)	8.231254(4)	8.231(2)
		(1)	-2.015426(5)	-2.015426(5)	-2.015426(5)	-2.01543(5)
		(2)	-1.242203(4)	-1.242203(4)	-1.242203(4)	-1.24223(9)
$\varrho^1$	plaq	(0)	-202.0079(2)	-404.0158(3)	-606.0237(2)	-808.03(4)
		(1)	11.123836(8)	22.24767(2)	33.37151(3)	44.497(3)
		(2)	6.69138(4)	13.38277(7)	20.07415(9)	26.762(8)
	sym	(0)	-152.56416(3)	-305.12832(6)	-457.6925(2)	-610.3(2)
		(1)	9.346879(5)	18.693758(9)	28.040642(8)	37.388(3)
		(2)	5.60061(2)	11.20122(4)	16.80183(6)	22.399(5)
$\varrho^2$	plaq	(0)	739.6836(2)	4438.102(1)	11095.255(3)	20711.14(3)
		(1)	-23.518665(6)	-141.11198(3)	-352.77996(7)	-658.52(8)
		(2)	-11.978147(2)	-71.868869(6)	-179.67220(2)	-335.388(8)
	sym	(0)	541.38051(4)	3248.2831(3)	8120.7077(3)	15158.66(4)
		(1)	-18.958350(2)	-113.75010(2)	-284.37525(2)	-530.83(5)
		(2)	-9.6055598(7)	-57.633356(1)	-144.083397(9)	-268.980(2)
$\varrho^3$	plaq	(0)		-24956.6947(4)	-124783.4729(5)	-349393.7(5)
		(1)		525.716776(9)	2628.58386(7)	7360.035(6)
		(2)		203.43279(2)	1017.16394(6)	2848.1(5)
	sym	(0)		-17858.09191(3)	-89290.4593(2)	-250013.3(2)
		(1)		411.66550(4)	2058.3275(2)	5763.32(2)
		(2)		156.799846(8)	783.99926(3)	2195.2(4)
$\varrho^4$	plaq	(0)		57973.619(4)	869604.29(5)	4058153.0(5)
		(1)		-878.20974(7)	-13173.1458(7)	-61475(3)
		(2)		-229.16130(5)	-3437.4195(4)	-16041.293(2)
	sym	(0)		40735.013(3)	611025.19(5)	2851450.82(9)
		(1)		-672.98584(5)	-10094.788(2)	-47107.302(7)
		(2)		-168.15048(2)	-2522.2572(4)	-11770.532(2)
$\varrho^5$	plaq	(0)			-3477653.965(2)	-32458091(8)
		(1)			39917.11(2)	372559.6(2)
		(2)			5804.3207(6)	54173.62(4)
	sym	(0)			-2406174(1)	-22457620(2)
		(1)			30072.058(6)	280672.57(9)
		(2)			3880.9479(9)	36222.19(2)
$\varrho^6$	plaq	(0)			6141663(3)	171966439(99)
		(1)			-55331.94(5)	-1549295(216)
		(2)			-2569.25(2)	-71939.0(4)
	sym	(0)			4192996.284(4)	117403911(55)
		(1)			-41099.241(6)	-1150778.8(7)
		(2)			-1039.729(6)	-29112.3(3)
$\varrho^7$	plaq	(0)				-545947087(1804)
		(1)				3959099.6(6)
		(2)				-136222(83)
	sym	(0)				-368383101(142)
		(1)				2904907(3)
		(2)				-172862(90)
$\varrho^8$	plaq	(0)				788877857(5503)
		(1)				-4693170(2)
		(2)				458914(149)
	sym	(0)				526824035(1817)
		(1)				-3406008(4)
		(2)				428921(211)

**Table A.8:** Coefficients of powers of  $\varrho$  and powers of  $c_{\text{SW}}$  (indicated by (0),(1),(2) for  $c_{\text{SW}}^0$ ,  $c_{\text{SW}}^1$ , and  $c_{\text{SW}}^2$ ) in  $\Sigma_{10}$  for Wilson fermions with  $r = 1$ .

$\Sigma_{10}$ (Brillouin)						
			$n = 1$	$n = 2$	$n = 3$	$n = 4$
$\varrho^0$	plaq	(0)	20.46155(2)	20.461(3)	20.461(3)	20.5(2)
		(1)	-2.93856(2)	-2.93864(2)	-2.93864(2)	-2.952609(5)
		(2)	-1.532830(6)	-1.53283(8)	-1.53283(8)	-1.54(2)
	sym	(0)	14.572(3)	14.5722(6)	14.5722(6)	14.574(7)
		(1)	-2.58301(7)	-2.58301(7)	-2.58301(7)	-2.58(2)
		(2)	-1.36318(9)	-1.36318(9)	-1.36318(9)	-1.37(2)
$\varrho^1$	plaq	(0)	-324.35103(4)	-648.70(2)	-973.06(2)	-1298(2)
		(1)	17.4217510(5)	34.844(7)	52.27(1)	69.7(5)
		(2)	7.908223(6)	15.8168(2)	23.7248(8)	31.7(9)
	sym	(0)	-238.44(9)	-476.875(2)	-715.31(2)	-954(2)
		(1)	14.324(3)	28.647(5)	42.971(2)	57.913(7)
		(2)	6.65987(7)	13.3197(2)	19.9792(6)	27(1)
$\varrho^2$	plaq	(0)	1262.57585(8)	7575.46(3)	18938.644(2)	35352(6)
		(1)	-41.5552837(3)	-249.33098(8)	-623.3275(2)	-1163.563(9)
		(2)	-15.260512(1)	-91.58(2)	-228.94(3)	-427.30(3)
	sym	(0)	899.6739(2)	5398.0443(7)	13495.106(3)	25191(12)
		(1)	-32.8490(8)	-197.093(4)	-492.73(2)	-919.78(2)
		(2)	-12.400(2)	-74.400(9)	-186.00(2)	-347.23(2)
$\varrho^3$	plaq	(0)		-44737.977(4)	-223689.89(2)	-626332(15)
		(1)		1000.68(2)	5003.42(9)	14009.8(3)
		(2)		285.437498(8)	1427.1875(1)	3995.2(4)
	sym	(0)		-31197.37(2)	-155986.9(2)	-436763(17)
		(1)		770.74(4)	3853.7(2)	10790.48(3)
		(2)		225.15315(2)	1125.76576(8)	3151.5(2)
$\varrho^4$	plaq	(0)		108218.77(2)	1623281.6(3)	7575314(7)
		(1)		-1742.0369(7)	-26131(2)	-121944(13)
		(2)		-373.39763(7)	-5600.965(2)	-26138(9)
	sym	(0)		74211.754(7)	1113176.3(2)	5194823(6)
		(1)		-1316.5626(4)	-19748.440(5)	-92162(6)
		(2)		-285.9756(3)	-4289.634(4)	-20016(5)
$\varrho^5$	plaq	(0)			-6716121(1)	-62683777(758)
		(1)			80671(8)	752905(165)
		(2)			12502(2)	116663(40)
	sym	(0)			-4543113(2)	-42402371(50)
		(1)			60065(3)	560630(21)
		(2)			9250(4)	86313(29)
$\varrho^6$	plaq	(0)			12208037(16)	341824636(1235)
		(1)			-112232.4246(5)	-3142574(475)
		(2)			-11880(7)	-332533(261)
	sym	(0)			8163871(12)	228588075(211)
		(1)			-82529.12(8)	-2310747(77)
		(2)			-8376(4)	-233932(318)
$\varrho^7$	plaq	(0)				-1112322137(13774)
		(1)				7980180(6450)
		(2)				519472(1715)
	sym	(0)				-736579023(493)
		(1)				5804622(1220)
		(2)				336106(1031)
$\varrho^8$	plaq	(0)				1641805450(46407)
		(1)				-9324601(6295)
		(2)				-298231(3615)
	sym	(0)				1078010905(4643)
		(1)				-6719738(2371)
		(2)				-149832(1008)

Table A.9: The same as Table A.8 but for Brillouin fermions.

## A.4 $\Sigma_0$ and $\Sigma_1$ with Wilson Flow

Figures A.1 and A.2 show plots similar to Figure 7.14 but for the coefficients of  $c_{\text{SW}}^0$ ,  $c_{\text{SW}}^1$ , and  $c_{\text{SW}}^2$  of  $\Sigma_0$  called  $\Sigma_0^{(0)}$ ,  $\Sigma_0^{(1)}$ , and  $\Sigma_0^{(2)}$  respectively. Figures A.3 and A.4 show the same for  $\Sigma_{10}$ .

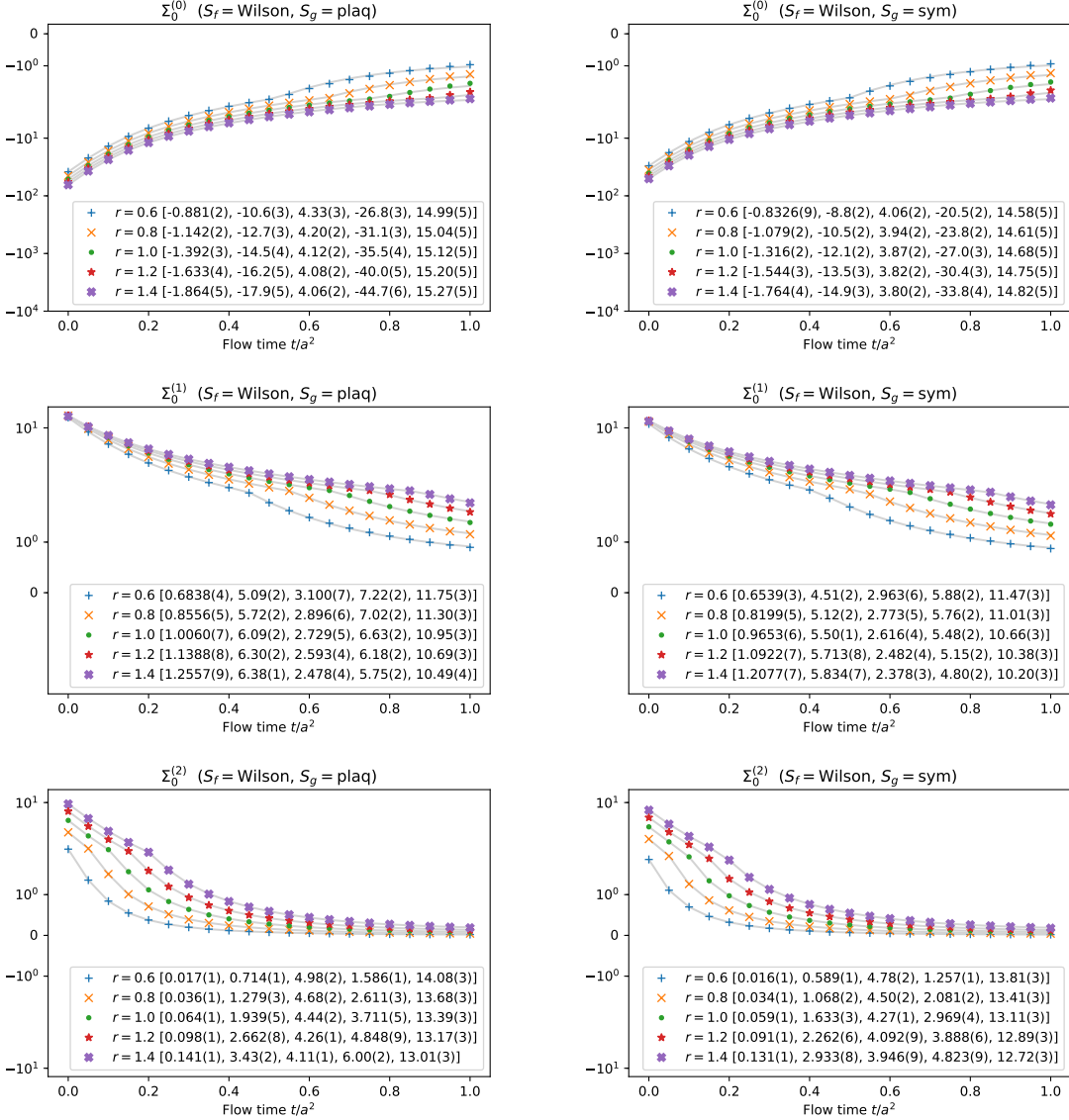


**Figure A.1:** Logarithmic plot of  $\Sigma_0^{(0)}$ ,  $\Sigma_0^{(1)}$ , and  $\Sigma_0^{(2)}$  with Wilson flow as a function of the flow time  $t$  for five different values of  $r$ . Two-exponential fits of the form  $c_0 + c_1 e^{-c_2 t} + c_3 e^{-c_4 t}$  are also shown and the coefficients  $[c_0, c_1, c_2, c_3, c_4]$  given in brackets.

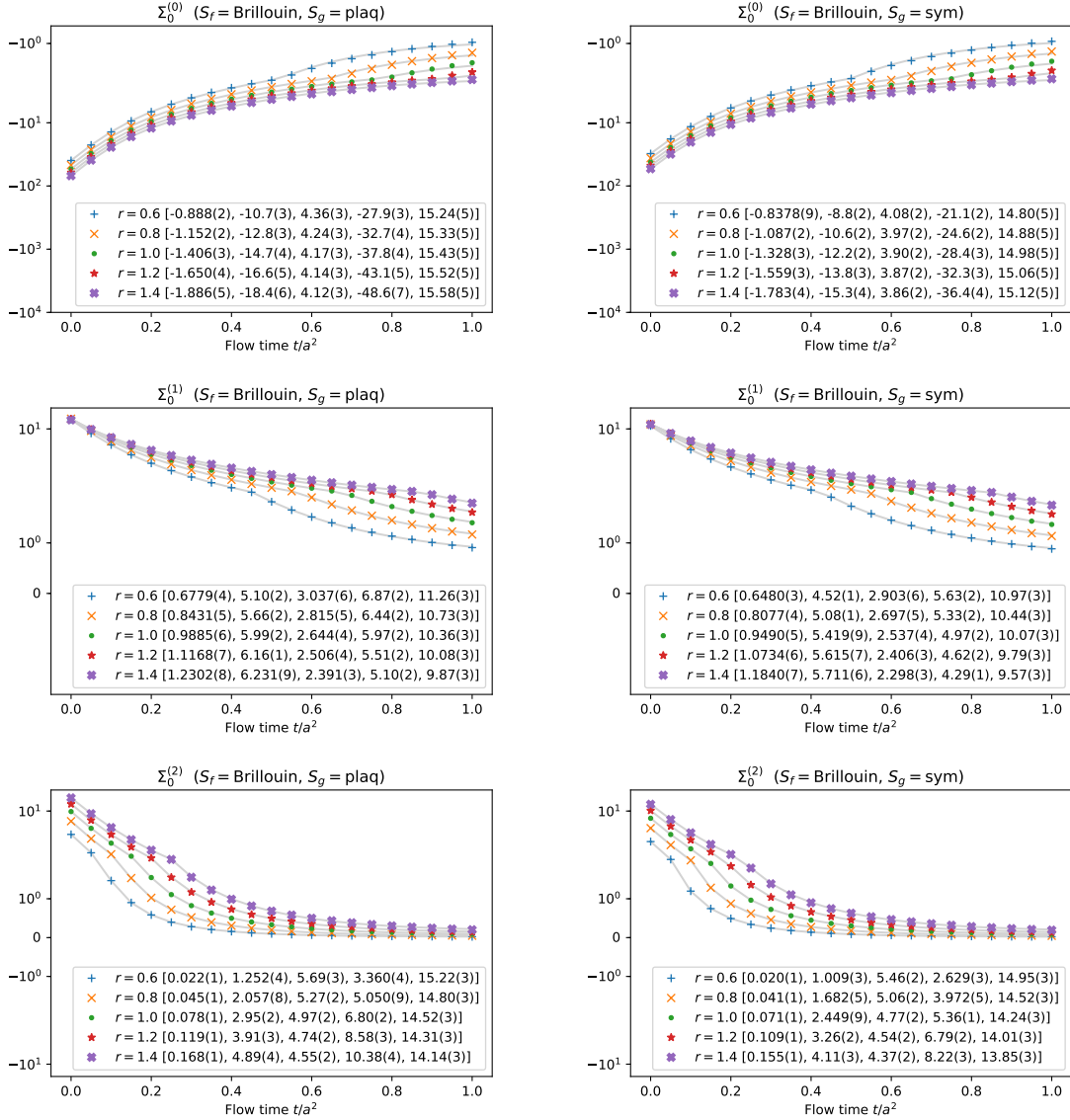


**Figure A.2:** The same as Figure A.1 but for Brillouin fermions .

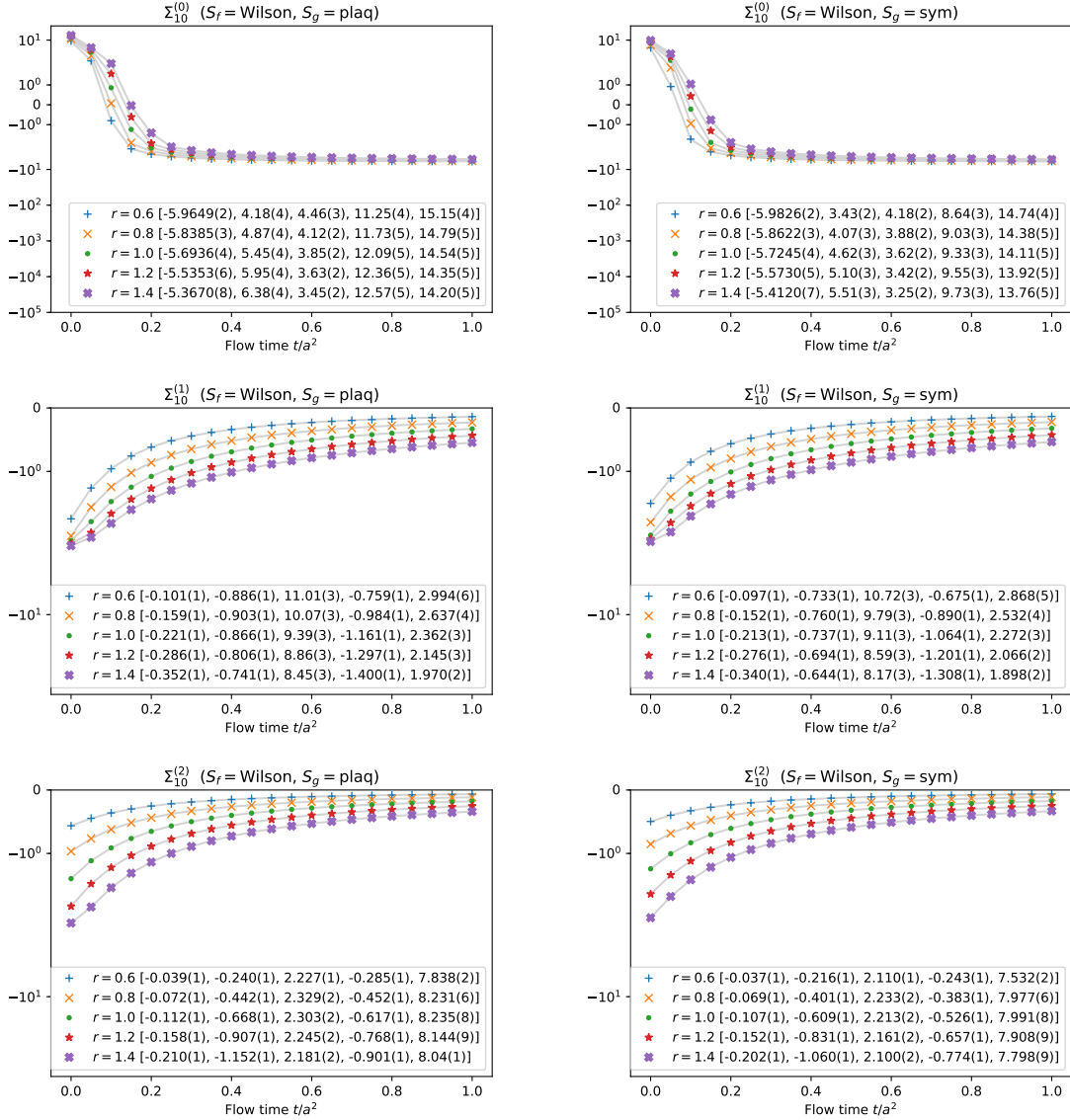


**Figure A.3:** The same as Figure A.1 but for  $\Sigma_{10}$ .

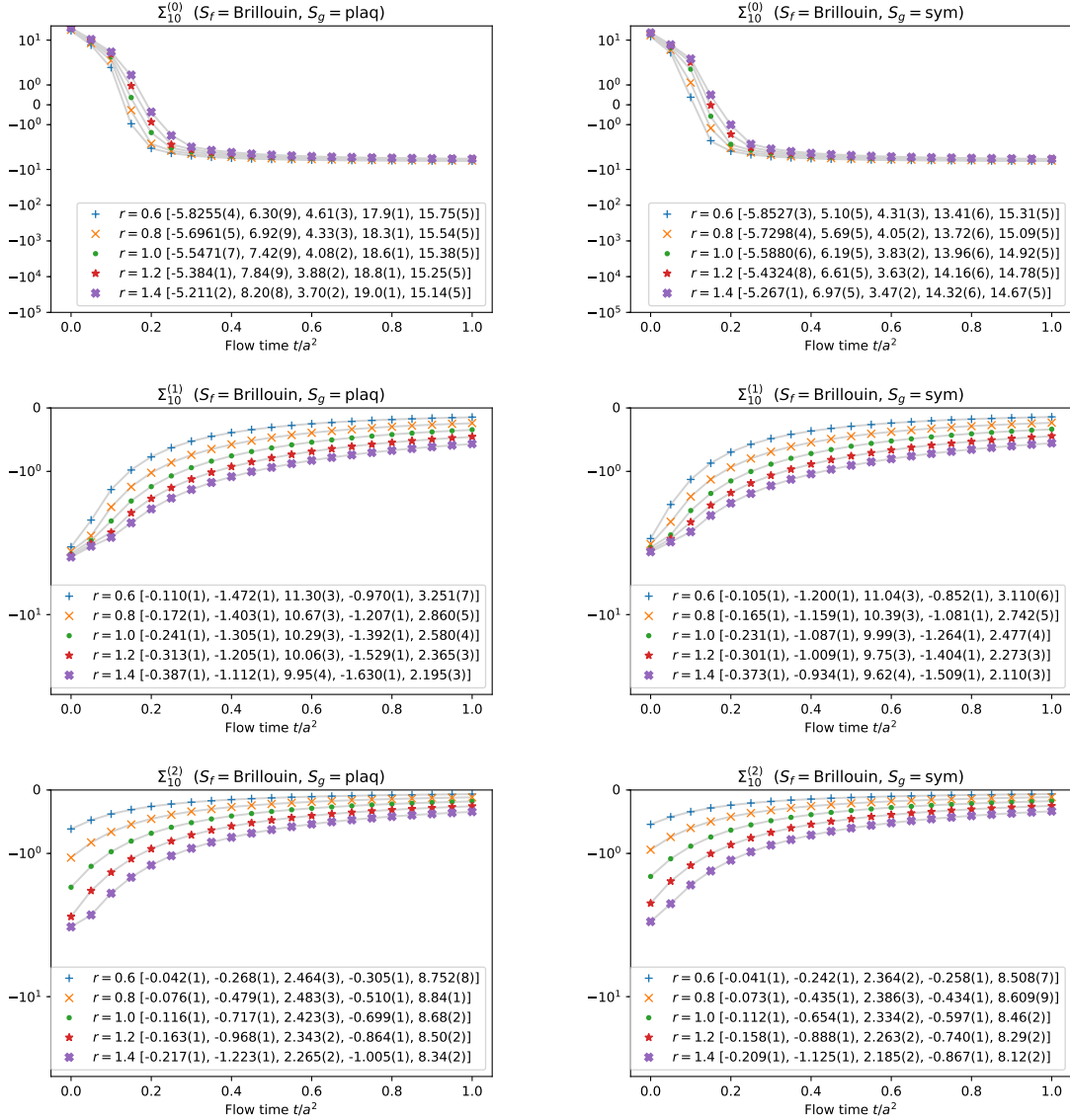


Figure A.4: The same as Figure A.3 but for Brillouin fermions.

## A.5 $c_{\text{SW}}^{(1)}$ with Stout Smearing

In this section we give some more complete data for  $c_{\text{SW}}^{(1)}$  with stout smearing. Table A.10 gives the results for  $c_{\text{SW}}^{(1)}$  with  $N_c = 3$  in terms of the coefficients of powers of the smearing parameter  $\varrho$ . For different values of  $N_c$  Tables A.11 and A.12 give the coefficients of  $N_c$  and  $1/N_c$  independently. Figures A.5 and A.7 show the  $r$ -dependence of those coefficients for Wilson fermions, Figures A.6 and A.8 for Brillouin fermions.

	Action	$n = 1$	$n = 2$	$n = 3$	$n = 4$
$\varrho^0$	Wil./plaq	0.2685882(5)	0.26859(3)	0.26859(3)	0.26859(1)
	Wil./sym	0.19624(3)	0.19624(3)	0.19624(3)	0.19624(3)
	Bri./plaq	0.1236257(8)	0.12362(2)	0.12362(2)	0.12362(2)
	Bri./sym	0.08859(3)	0.08859(3)		
$\varrho^1$	Wil./plaq	-3.634574(8)	-7.2691(5)	-10.9037(2)	-14.5383(8)
	Wil./sym	-2.5330(3)	-5.0659(5)	-7.5989(3)	-10.132(1)
	Bri./plaq	-1.69335(1)	-3.3867(3)	-5.0801(3)	-6.7734(6)
	Bri./sym	-1.1693(2)	-2.3387(3)		
$\varrho^2$	Wil./plaq	15.312641(2)	91.8758(4)	229.6894(8)	428.7537(5)
	Wil./sym	10.40969(4)	62.4581(4)	156.1454(9)	291.471(2)
	Bri./plaq	7.194783(3)	43.1685(5)	107.921(2)	201.453(2)
	Bri./sym	4.85384(6)	29.1231(5)		
$\varrho^3$	Wil./plaq		-584.2124(2)	-2921.0621(7)	-8178.974(2)
	Wil./sym		-390.84777(8)	-1954.2388(5)	-5471.869(2)
	Bri./plaq		-279.5358(4)	-1397.679(2)	-3913.501(3)
	Bri./sym		-185.6528(3)		
$\varrho^4$	Wil./plaq		1512.550(1)	22688.25(2)	105878.50(5)
	Wil./sym		1000.402(2)	15006.04(2)	70028.17(7)
	Bri./plaq		740.3087(9)	11104.63(2)	51821.62(7)
	Bri./sym		486.2348(6)		
$\varrho^5$	Wil./plaq			-99737.99(7)	-930887.4(8)
	Wil./sym			-65387.62(4)	-610283.8(9)
	Bri./plaq			-49950.77(3)	-466206.5(9)
	Bri./sym				
$\varrho^6$	Wil./plaq			191197.5(4)	5353537(6)
	Wil./sym			124452.9(3)	3484681(8)
	Bri./plaq			97831.9(2)	2739293(4)
	Bri./sym				
$\varrho^7$	Wil./plaq				-18245358(47)
	Wil./sym				-11804589(26)
	Bri./plaq				-9518117(43)
	Bri./sym				
$\varrho^8$	Wil./plaq				28031442(48)
	Wil./sym				18041502(41)
	Bri./plaq				14877196(7271)
	Bri./sym				

**Table A.10:** Coefficients of powers of  $\varrho$  in  $c_{\text{SW}}^{(1)}$  for Wilson and Brillouin clover fermions with  $N_c = 3$ .

	Action	$n = 1$	$n = 2$	$n = 3$	$n = 4$
$\varrho^0$	Wil./plaq	0.0988425(2)	0.098843(9)	0.098843(9)	0.098842(3)
	Wil./sym	0.071869(8)	0.071869(8)	0.071869(8)	0.071869(8)
	Bri./plaq	0.0457855(3)	0.045782(6)	0.045782(6)	0.045782(6)
	Bri./sym	0.032596(7)	0.032596(7)		
$\varrho^1$	Wil./plaq	-1.385889(3)	-2.7718(2)	-4.15766(5)	-5.5436(3)
	Wil./sym	-0.96522(8)	-1.9304(2)	-2.89567(9)	-3.8609(4)
	Bri./plaq	-0.665239(4)	-1.3305(1)	-1.99572(8)	-2.6610(2)
	Bri./sym	-0.45953(5)	-0.91906(8)		
$\varrho^2$	Wil./plaq	5.9430979(4)	35.6586(1)	89.1464(3)	166.4067(2)
	Wil./sym	4.04484(2)	24.2690(2)	60.6726(3)	113.2555(6)
	Bri./plaq	2.9145387(9)	17.4872(2)	43.7179(4)	81.6068(7)
	Bri./sym	1.97257(2)	11.8355(2)		
$\varrho^3$	Wil./plaq		-228.81860(5)	-1144.0929(3)	-3203.4604(6)
	Wil./sym		-153.37163(2)	-766.8582(1)	-2147.2028(4)
	Bri./plaq		-114.9556(1)	-574.7778(5)	-1609.3777(7)
	Bri./sym		-76.68337(8)		
$\varrho^4$	Wil./plaq		595.1488(4)	8927.232(5)	41660.43(2)
	Wil./sym		394.4523(5)	5916.784(7)	27611.66(3)
	Bri./plaq		306.4193(3)	4596.289(5)	21449.35(3)
	Bri./sym		202.1925(2)		
$\varrho^5$	Wil./plaq			-39331.71(3)	-367095.8(3)
	Wil./sym			-25837.98(2)	-241154.3(3)
	Bri./plaq			-20718.029(9)	-193368.0(3)
	Bri./sym				
$\varrho^6$	Wil./plaq			75472.9(2)	2113244(2)
	Wil./sym			49217.98(9)	1378103(3)
	Bri./plaq			40574.85(6)	1136096(2)
	Bri./sym				
$\varrho^7$	Wil./plaq				-7204527(15)
	Wil./sym				-4669018(8)
	Bri./plaq				-3943331(12)
	Bri./sym				
$\varrho^8$	Wil./plaq				11068717(16)
	Wil./sym				7134378(12)
	Bri./plaq				6154392(2424)
	Bri./sym				

**Table A.11:** The same as Table A.10 but for the Coefficient of  $N_c$  in  $c_{\text{SW}}^{(1)}$ .

	Action	$n = 1$	$n = 2$	$n = 3$	$n = 4$
$q^0$	Wil./plaq	-0.0838175(2)	-0.08382(2)	-0.08382(2)	-0.08382(2)
	Wil./sym	-0.05809(2)	-0.05809(2)	-0.05809(2)	-0.05809(2)
	Bri./plaq	-0.04119223(6)	-0.04119(3)	-0.04119(3)	-0.04119(3)
	Bri./sym	-0.02760(3)	-0.02760(3)		
$q^1$	Wil./plaq	1.5692766(2)	3.13856(7)	4.7078(2)	6.2771(2)
	Wil./sym	1.08814(6)	2.1763(2)	3.2644(2)	4.3526(3)
	Bri./plaq	0.90710168(4)	1.81420(3)	2.72131(9)	3.62840(6)
	Bri./sym	0.62772(2)	1.25545(3)		
$q^2$	Wil./plaq	-7.549958(5)	-45.2998(2)	-113.2494(5)	-211.3989(3)
	Wil./sym	-5.17448(3)	-31.0469(2)	-77.6172(4)	-144.8854(6)
	Bri./plaq	-4.64650062(3)	-27.87899(2)	-69.69752(8)	-130.1020(2)
	Bri./sym	-3.191648(2)	-19.149881(7)		
$q^3$	Wil./plaq		306.73007(4)	1533.6503(2)	4294.2212(7)
	Wil./sym		207.8014(2)	1039.007(2)	2909.219(3)
	Bri./plaq		195.9927(3)	979.963(1)	2743.897(3)
	Bri./sym		133.1918(2)		
$q^4$	Wil./plaq		-818.6903(7)	-12280.35(1)	-57308.34(7)
	Wil./sym		-548.8632(5)	-8232.950(7)	-38420.428(8)
	Bri./plaq		-536.8471(2)	-8052.701(6)	-37579.30(2)
	Bri./sym		-361.0282(2)		
$q^5$	Wil./plaq			54771.40(3)	511200(1)
	Wil./sym			36379.01(3)	339537.3(1)
	Bri./plaq			36609.95(4)	341692.9(4)
	Bri./sym				
$q^6$	Wil./plaq			-105663.9(5)	-2958589(2)
	Wil./sym			-69603.1(2)	-1948888(4)
	Bri./plaq			-71678.0(2)	-2006983(5)
	Bri./sym				
$q^7$	Wil./plaq				10104664(41)
	Wil./sym				6607391(43)
	Bri./plaq				6935625(78)
	Bri./sym				
$q^8$	Wil./plaq				-15524128(37)
	Wil./sym				-10084901(70)
	Bri./plaq				-10757942(118)
	Bri./sym				

**Table A.12:** The same as Table A.10 but for the Coefficient of  $1/N_c$  in  $c_{\text{SW}}^{(1)}$ .

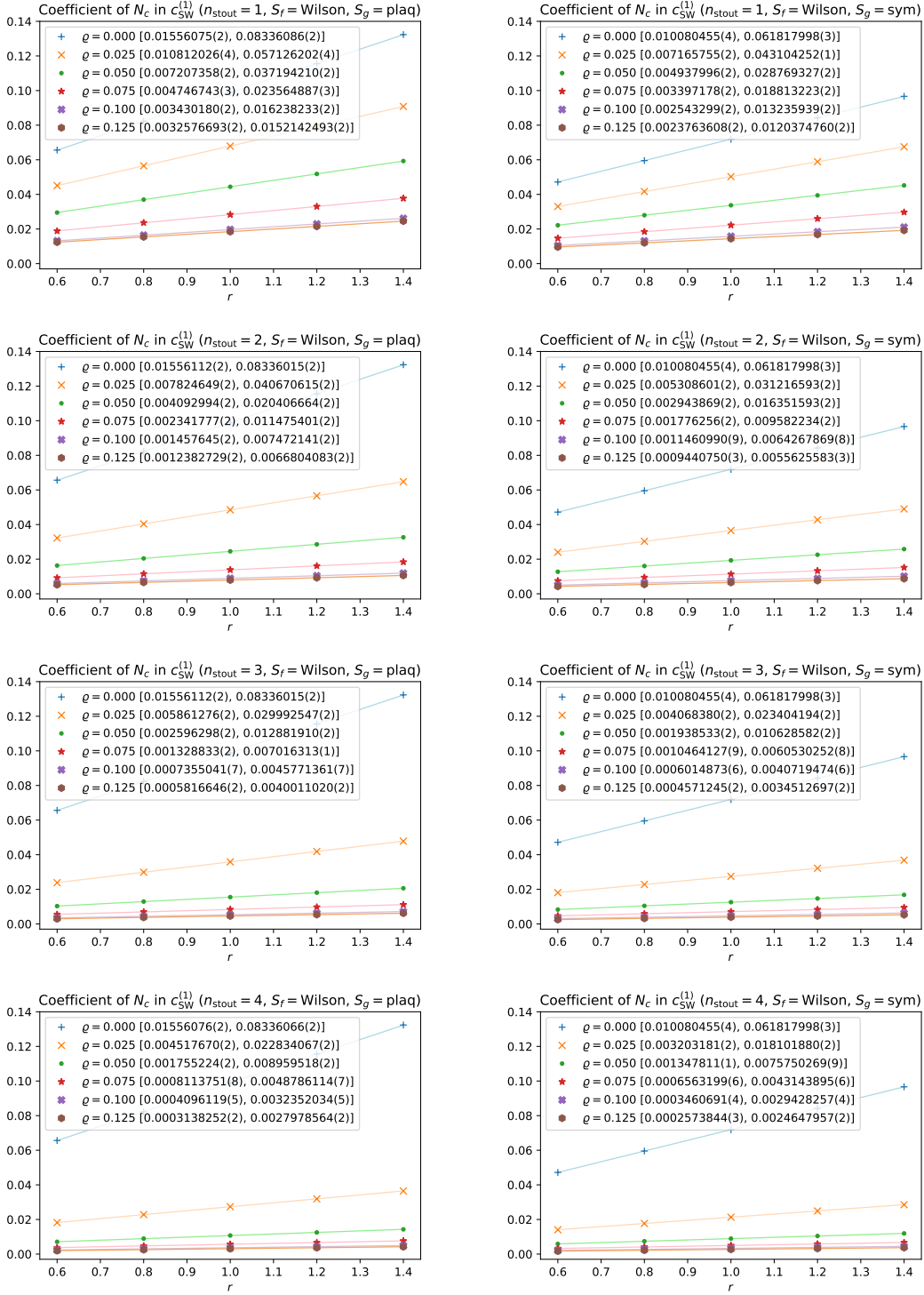


**Figure A.5:** The coefficient of  $N_c$  in  $c_{\text{SW}}^{(1)}$  as a function of the Wilson parameter  $r$  for Wilson fermions. The number of stout smearing steps increases from top to bottom, the left column showing results with the plaquette gauge action, the right column those with the Lüscher-Weisz action. Linear least-square fits of the form  $c_0 + c_1 \cdot r$  are also shown and the coefficients  $[c_0, c_1]$  given in brackets.

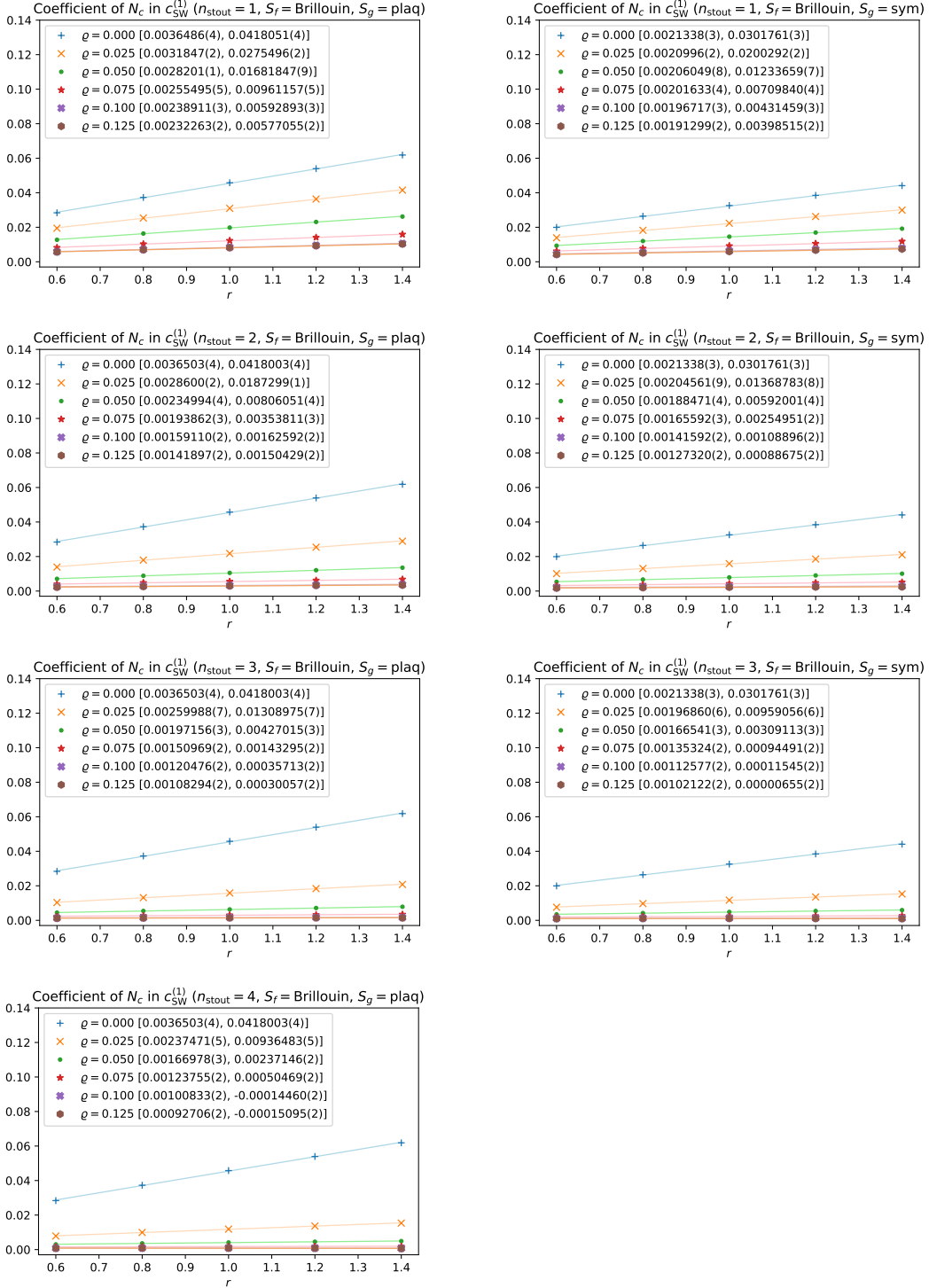


Figure A.6: The same as Figure A.5 but for Brillouin fermions.

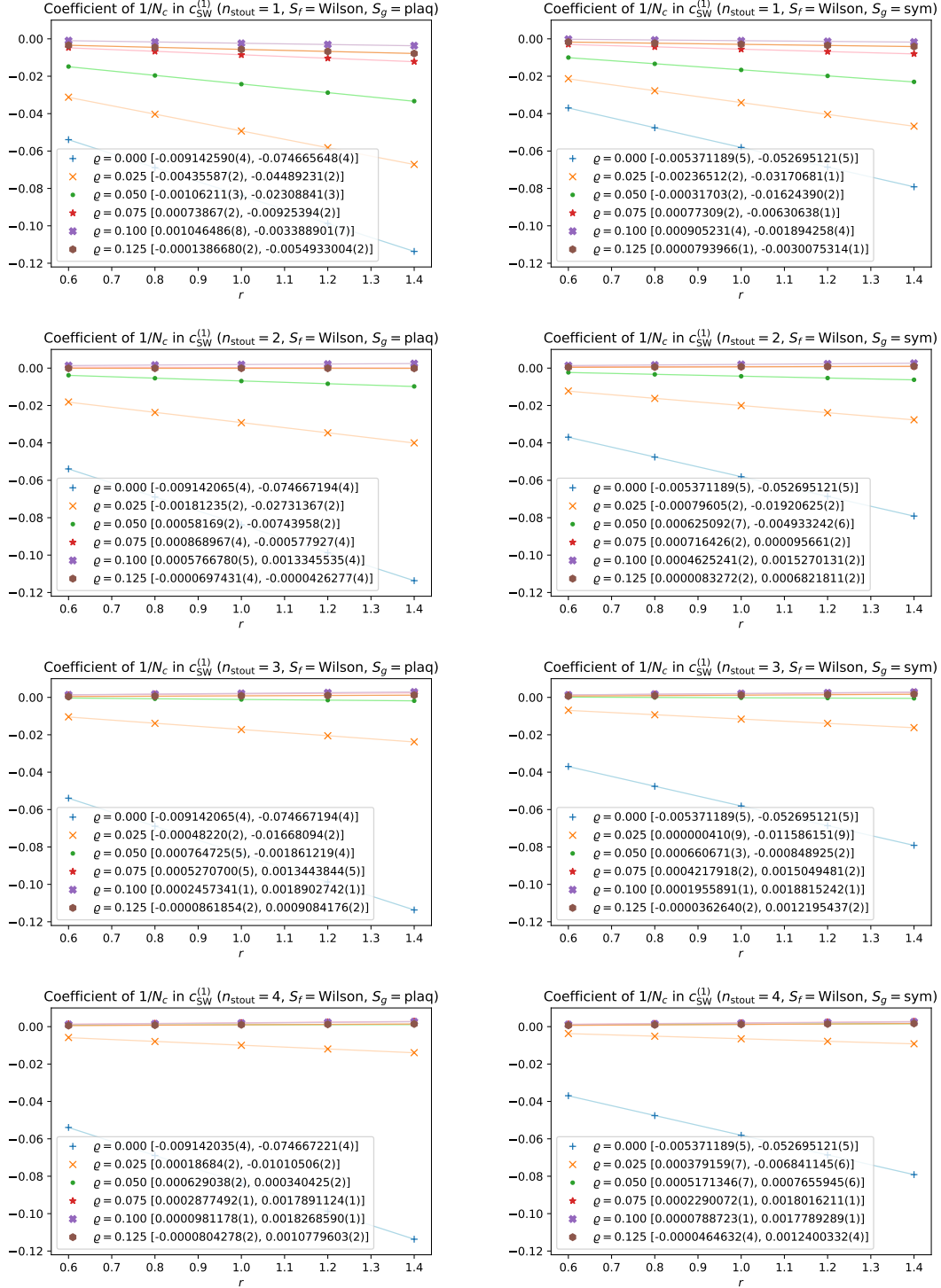


Figure A.7: The same as Figure A.5 but for the coefficient of  $1/N_c$ .

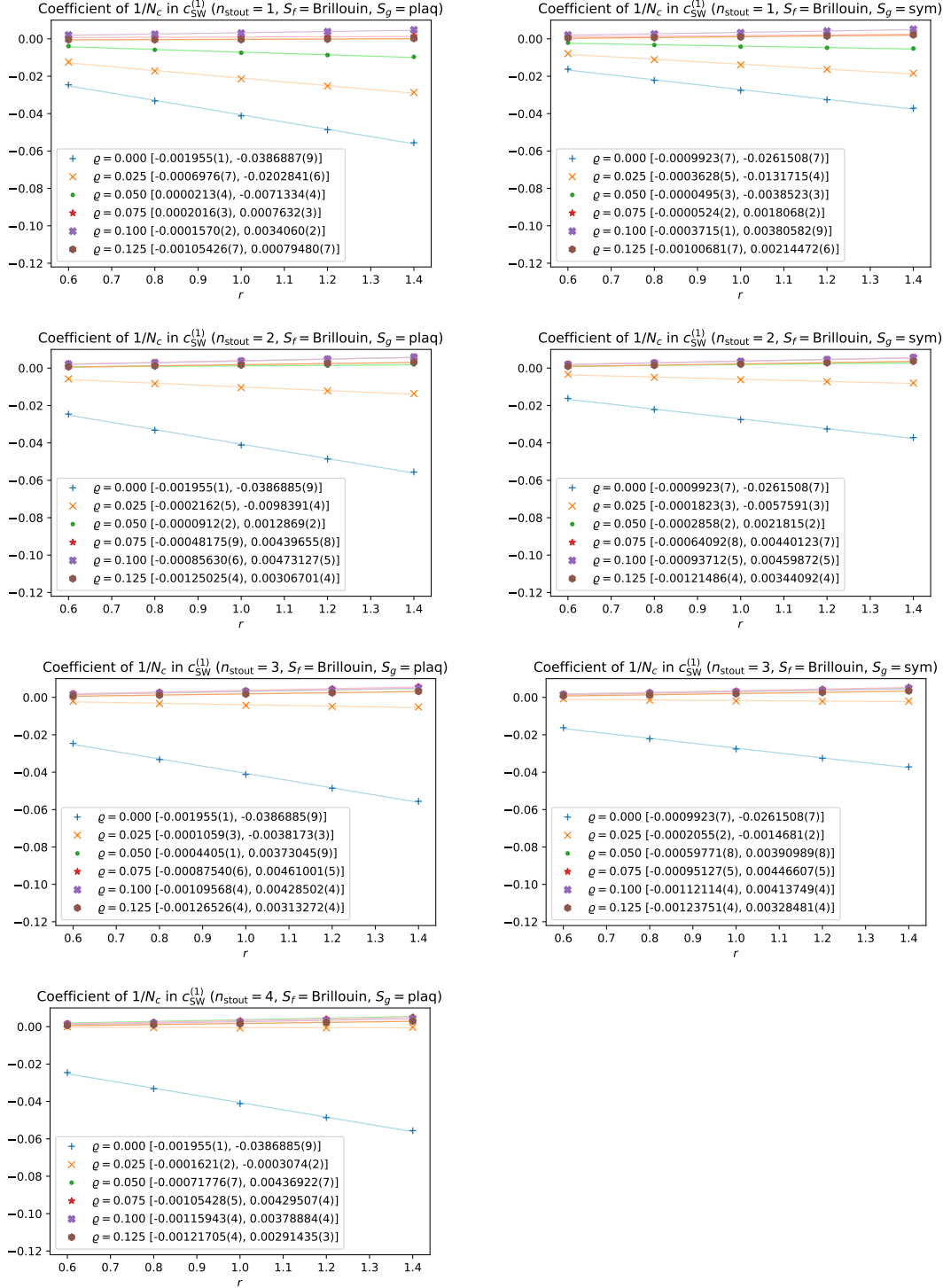
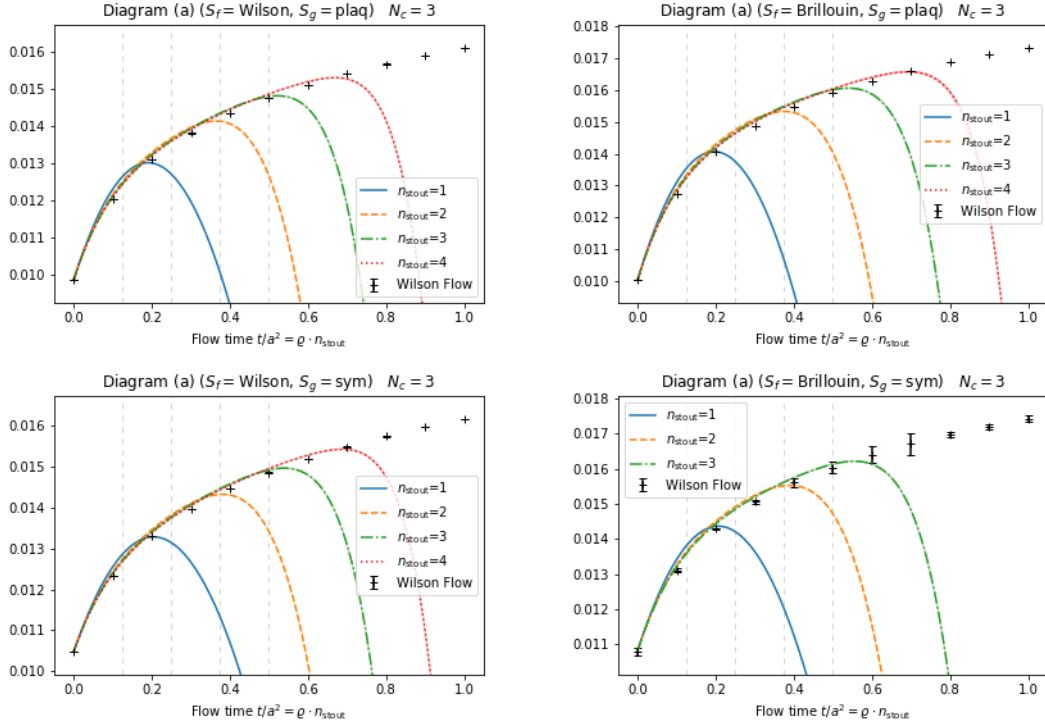


Figure A.8: The same as Figure A.7 but for Brillouin fermions.

## A.6 $c_{\text{SW}}^{(1)}$ with Wilson Flow

Here we show the individual results of the six diagrams that contribute to  $c_{\text{SW}}^{(1)}$  named (a) through (f), as depicted in Figure 4.4. Figures A.9 through A.13 show the constant part of each diagram plotted against  $t/a^2 = \varrho \cdot n_{\text{stout}}$  with stout smearing for up to  $n_{\text{stout}} = 4$  and the Wilson flow. The absolute values for the divergent diagrams (all except for diagram (d)) depend on our choice of regularisation (see Section A.6).

Figures A.14 and A.15 show the coefficients of  $N_c$  and  $1/N_c$  respectively with Wilson flow for five different values of  $r$  including double-exponential fit functions. Figures A.16 and A.17 show a part of the same data (for five flow times  $t/a^2$ ) as a function of  $r$  with linear fits.



**Figure A.9:** The constant part of diagram (a) with both Wilson flow and up to four stout smearing steps. Results are plotted against the flow time  $t$  or  $\varrho \cdot n_{\text{stout}}$  respectively. The four combinations of fermion (Wilson or Brillouin) and gluon (plaquette or Symanzik) actions are shown.

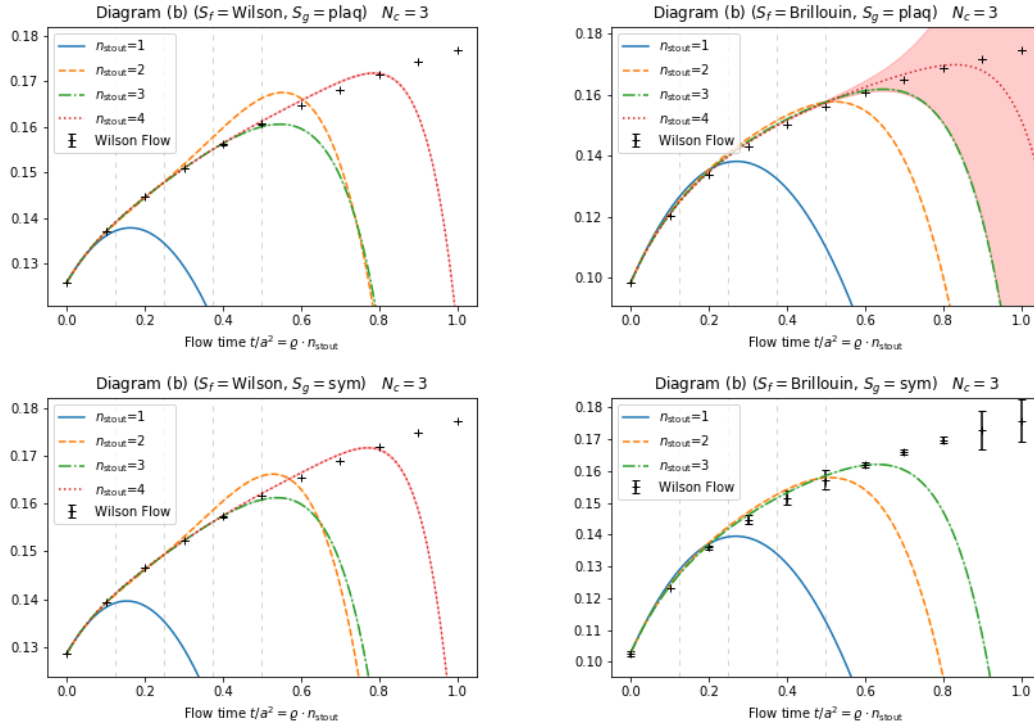


Figure A.10: The same as Figure A.9 but for diagram (b).

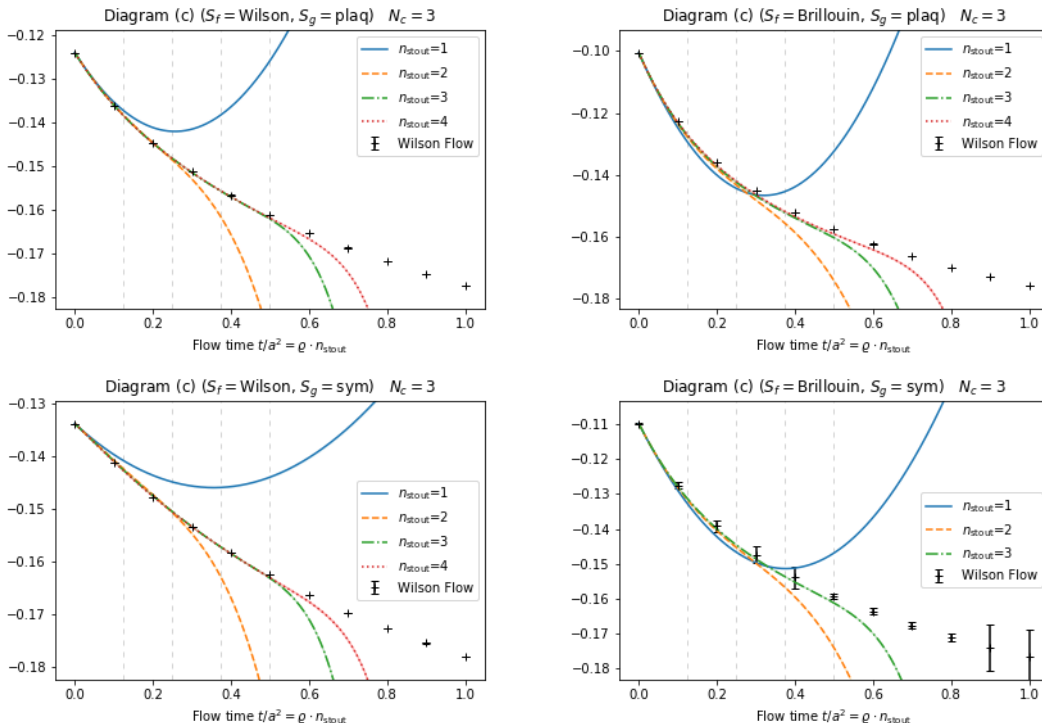


Figure A.11: The same as Figure A.9 but for diagram (c).

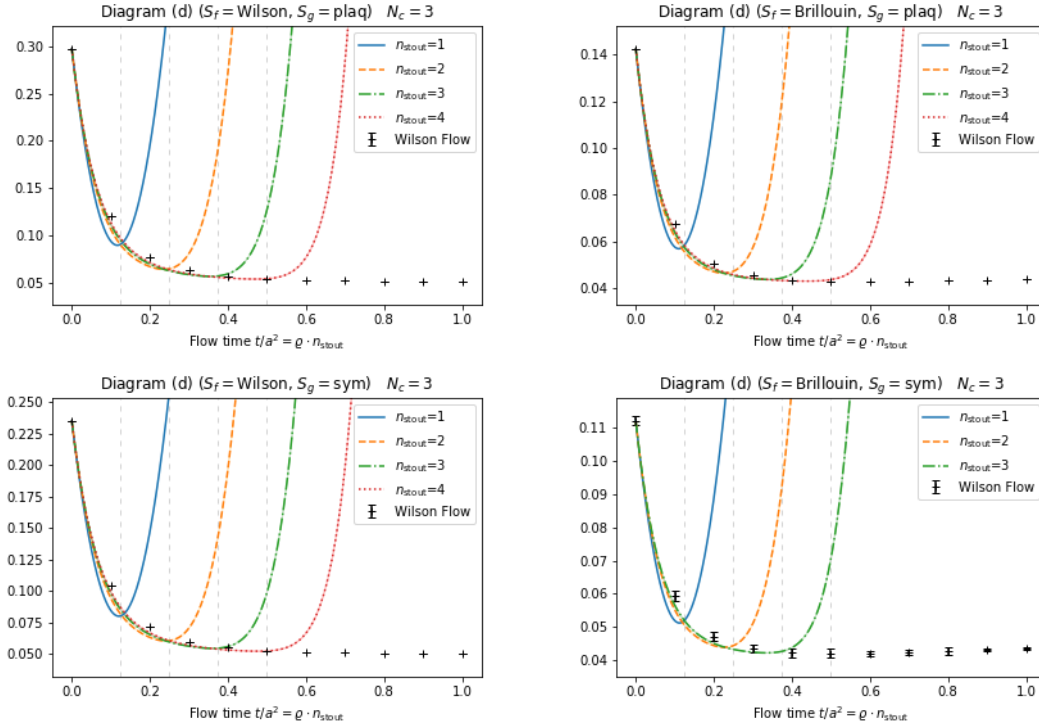


Figure A.12: The same as Figure A.9 but for diagram (d).

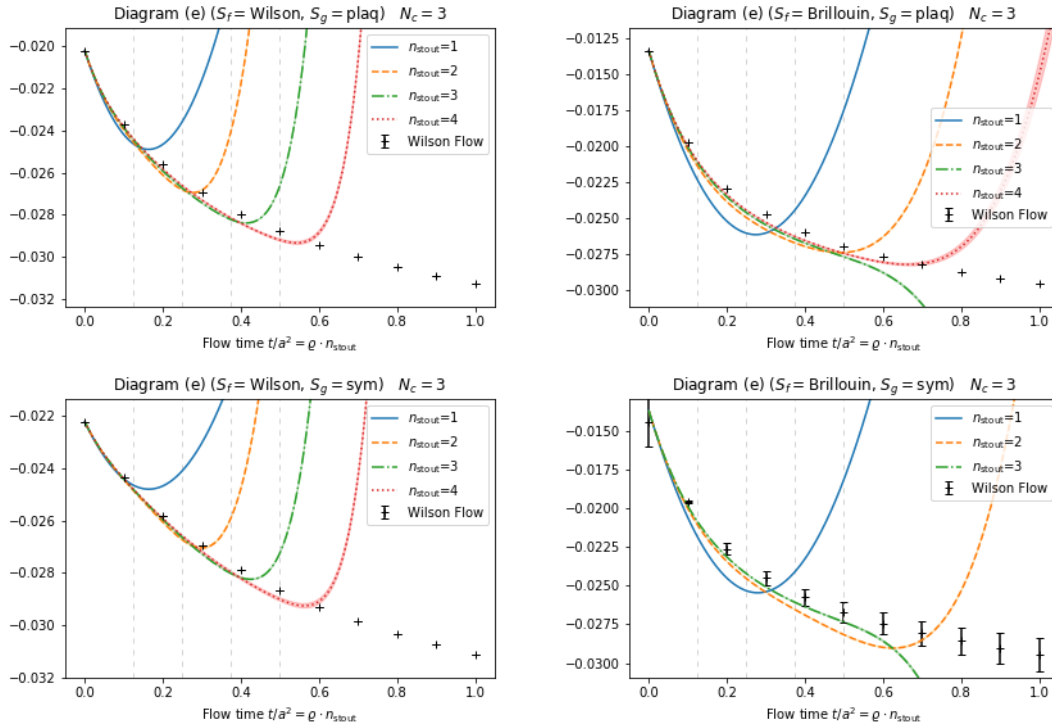
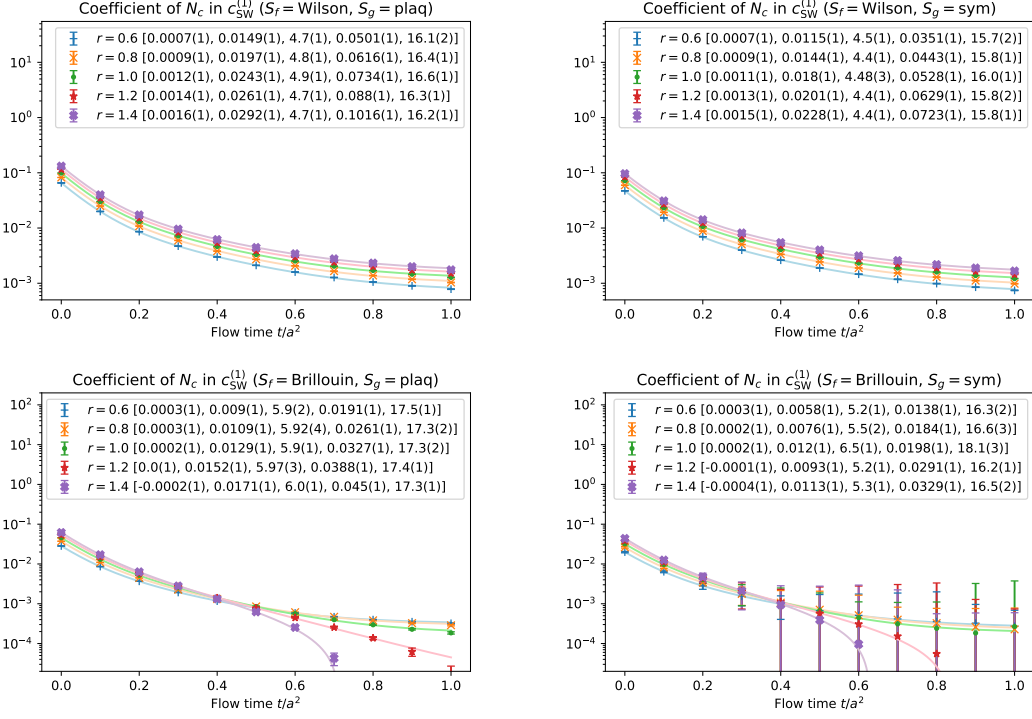
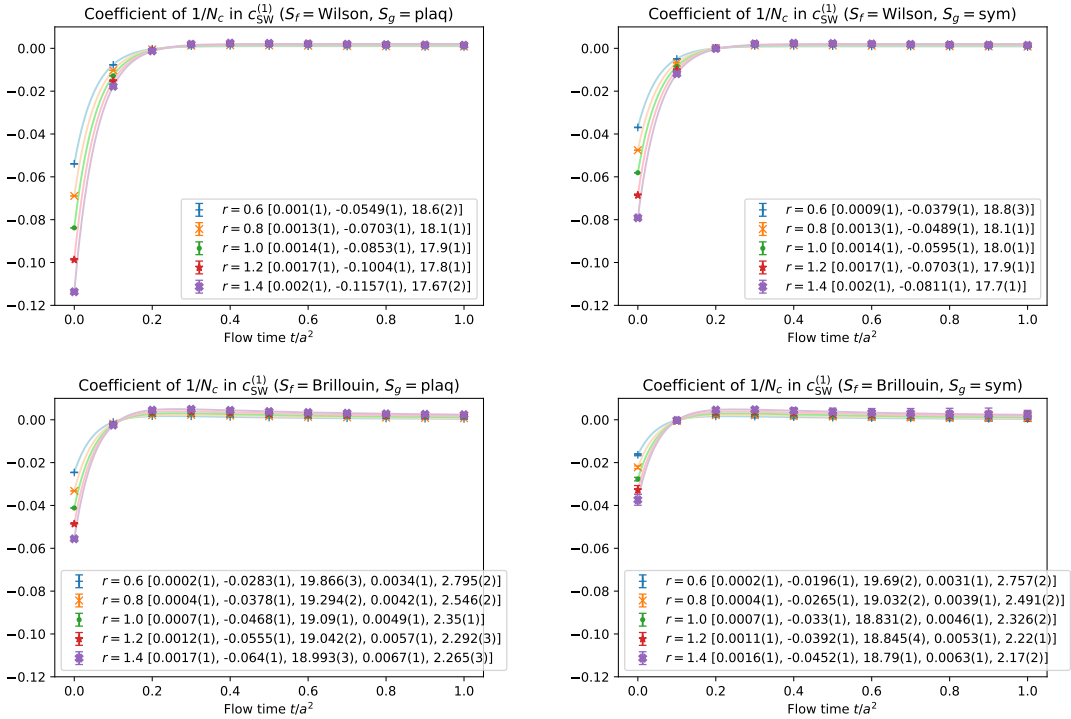


Figure A.13: The same as Figure A.9 but for diagrams (e) and (f), their results always being identical.



**Figure A.14:** Logarithmic plot of the coefficient of  $N_c$  in  $c_{SW}^{(1)}$  with Wilson flow as a function of the flow time  $t/a^2$  for five different values of  $r$ . Two-exponential fits of the form  $c_0 + c_1 e^{-c_2 t} + c_3 e^{-c_4 t}$  are also shown and the coefficients  $[c_0, c_1, c_2, c_3, c_4]$  given in brackets.



**Figure A.15:** The same as Figure A.14 but for the coefficient of  $1/N_c$ .

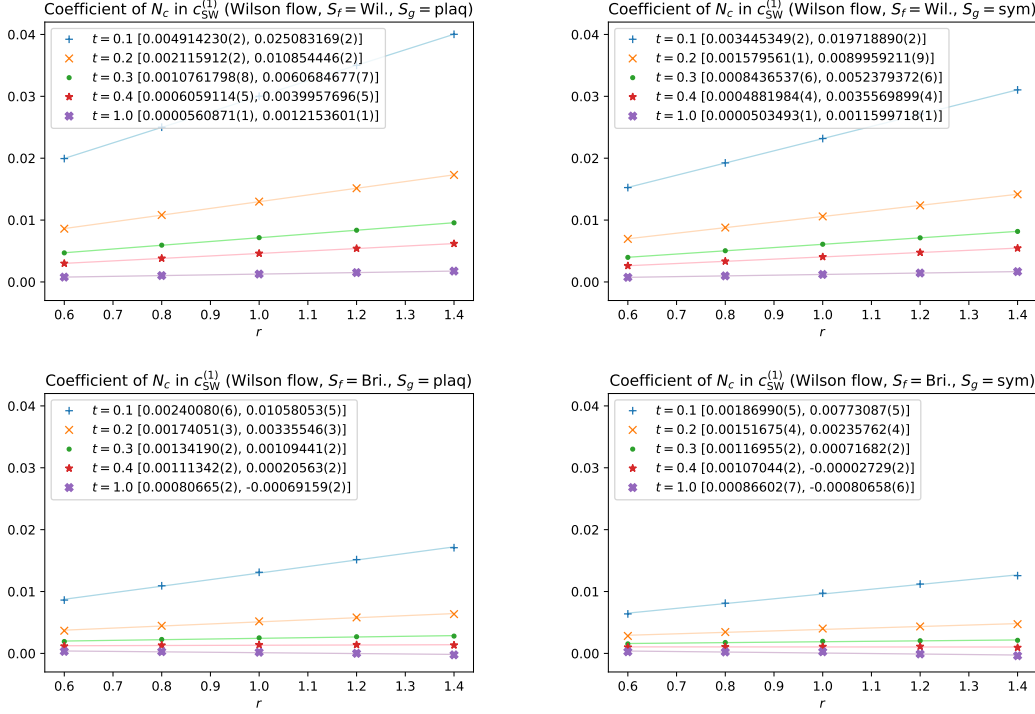


**Figure A.16:** The coefficient of  $N_c$  in  $c_{\text{SW}}^{(1)}$  as a function of  $r$  for a select number of values of the flow time  $t/a^2$ . Linear least-squares fits of the form  $c_0 + c_1 \cdot r$  are also shown and the coefficients  $[c_0, c_1]$  given in brackets.

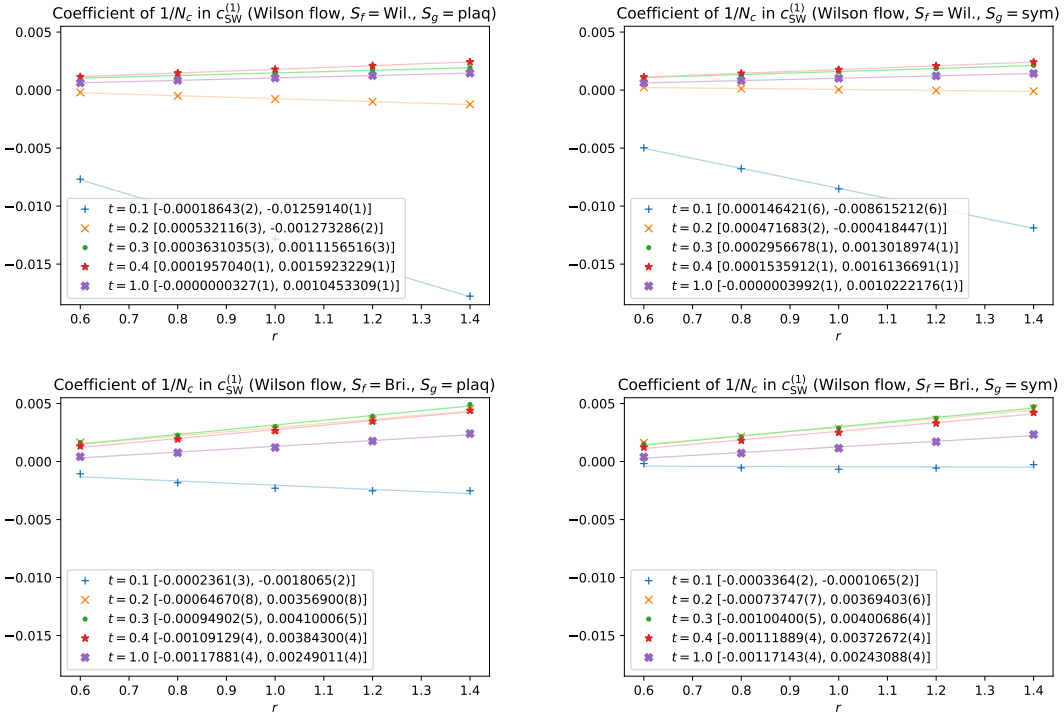


**Figure A.17:** The same as Figure A.16 but for the coefficient of  $1/N_c$ .

# Bibliography

- [1] Christof Gattringer and Christian B. Lang. *Quantum chromodynamics on the lattice*. Vol. 788. Berlin: Springer, 2010. ISBN: 978-3-642-01849-7, 978-3-642-01850-3.
- [2] I. Montvay and G. Munster. *Quantum fields on a lattice*. Cambridge Monographs on Mathematical Physics. Cambridge University Press, Mar. 1997. ISBN: 978-0-521-59917-7, 978-0-511-87919-7.
- [3] Kenneth G. Wilson. “Confinement of Quarks”. In: *Phys. Rev. D* 10 (1974). Ed. by J. C. Taylor, pp. 2445–2459.
- [4] Stephan Durr and Giannis Koutsou. “Brillouin improvement for Wilson fermions”. In: *Phys. Rev. D* 83 (2011), p. 114512. arXiv: 1012.3615 [hep-lat].
- [5] K. Symanzik. “Continuum Limit and Improved Action in Lattice Theories. 1. Principles and  $\varphi^4$  Theory”. In: *Nucl. Phys. B* 226 (1983), pp. 187–204.
- [6] B. Sheikholeslami and R. Wohlert. “Improved Continuum Limit Lattice Action for QCD with Wilson Fermions”. In: *Nucl. Phys. B* 259 (1985), p. 572.
- [7] Colin Morningstar and Mike J. Peardon. “Analytic smearing of SU(3) link variables in lattice QCD”. In: *Phys. Rev. D* 69 (2004), p. 054501. arXiv: hep-lat/0311018.
- [8] Martin Lüscher. “Properties and uses of the Wilson flow in lattice QCD”. In: *JHEP* 08 (2010). [Erratum: JHEP 03, 092 (2014)], p. 071. arXiv: 1006.4518 [hep-lat].
- [9] Maximilian Ammer and Stephan Dürr. “Calculation of cSW at one-loop order for Brillouin fermions”. In: *Phys. Rev. D* 109.1 (2024), p. 014512. arXiv: 2302.11261 [hep-lat].
- [10] Maximilian Ammer and Stephan Durr. “Stout smearing and Wilson flow in lattice perturbation theory”. In: (June 2024). arXiv: 2406.03493 [hep-lat].
- [11] Matthew D. Schwartz. *Quantum Field Theory and the Standard Model*. Cambridge University Press, Mar. 2014. ISBN: 978-1-107-03473-0, 978-1-107-03473-0.
- [12] C. P. Burgess and G. D. Moore. *The standard model: A primer*. Cambridge University Press, Dec. 2006. ISBN: 978-0-511-25485-7, 978-1-107-40426-7, 978-0-521-86036-9.
- [13] Steven Weinberg. *The Quantum theory of fields. Vol. 1: Foundations*. Cambridge University Press, June 2005. ISBN: 978-0-521-67053-1, 978-0-511-25204-4.
- [14] Steven Weinberg. *The quantum theory of fields. Vol. 2: Modern applications*. Cambridge University Press, Aug. 2013. ISBN: 978-1-139-63247-8, 978-0-521-67054-8, 978-0-521-55002-4.
- [15] R. L. Workman et al. “Review of Particle Physics”. In: *PTEP* 2022 (2022), p. 083C01.
- [16] L. D. Faddeev and V. N. Popov. “Feynman Diagrams for the Yang-Mills Field”. In: *Phys. Lett. B* 25 (1967). Ed. by Jong-Ping Hsu and D. Fine, pp. 29–30.

- [17] Holger Bech Nielsen and M. Ninomiya. “Absence of Neutrinos on a Lattice. 1. Proof by Homotopy Theory”. In: *Nucl. Phys. B* 185 (1981). Ed. by J. Julve and M. Ramón-Medrano. [Erratum: Nucl.Phys.B 195, 541 (1982)], p. 20.
- [18] Holger Bech Nielsen and M. Ninomiya. “Absence of Neutrinos on a Lattice. 2. Intuitive Topological Proof”. In: *Nucl. Phys. B* 193 (1981), pp. 173–194.
- [19] Holger Bech Nielsen and M. Ninomiya. “No Go Theorem for Regularizing Chiral Fermions”. In: *Phys. Lett. B* 105 (1981), pp. 219–223.
- [20] D. Friedan. “A PROOF OF THE NIELSEN-NINOMIYA THEOREM”. In: *Commun. Math. Phys.* 85 (1982), pp. 481–490.
- [21] John B. Kogut and Leonard Susskind. “Hamiltonian Formulation of Wilson’s Lattice Gauge Theories”. In: *Phys. Rev. D* 11 (1975), pp. 395–408.
- [22] David B. Kaplan. “A Method for simulating chiral fermions on the lattice”. In: *Phys. Lett. B* 288 (1992), pp. 342–347. arXiv: [hep-lat/9206013](#).
- [23] Herbert Neuberger. “Exactly massless quarks on the lattice”. In: *Phys. Lett. B* 417 (1998), pp. 141–144. arXiv: [hep-lat/9707022](#).
- [24] Michael Creutz. “Four-dimensional graphene and chiral fermions”. In: *JHEP* 04 (2008), p. 017. arXiv: [0712.1201 \[hep-lat\]](#).
- [25] Artan Borici. “Creutz fermions on an orthogonal lattice”. In: *Phys. Rev. D* 78 (2008), p. 074504. arXiv: [0712.4401 \[hep-lat\]](#).
- [26] Luuk H. Karsten. “Lattice Fermions in Euclidean Space-time”. In: *Phys. Lett. B* 104 (1981), pp. 315–319.
- [27] Frank Wilczek. “ON LATTICE FERMIONS”. In: *Phys. Rev. Lett.* 59 (1987), p. 2397.
- [28] Wolfgang Bietenholz et al. “Progress on perfect lattice actions for QCD”. In: *Nucl. Phys. B Proc. Suppl.* 53 (1997). Ed. by C. Bernard et al., pp. 921–934. arXiv: [hep-lat/9608068](#).
- [29] Stephan Durr. “Portable CPU implementation of Wilson, Brillouin and Susskind fermions in lattice QCD”. In: *Comput. Phys. Commun.* 282 (2023), p. 108555. arXiv: [2112.14640 \[hep-lat\]](#).
- [30] R. Wohlt. “IMPROVED CONTINUUM LIMIT LATTICE ACTION FOR QUARKS”. In: (July 1987).
- [31] Karl Jansen et al. “Nonperturbative renormalization of lattice QCD at all scales”. In: *Phys. Lett. B* 372 (1996), pp. 275–282. arXiv: [hep-lat/9512009](#).
- [32] Martin Luscher et al. “Chiral symmetry and O(a) improvement in lattice QCD”. In: *Nucl. Phys. B* 478 (1996), pp. 365–400. arXiv: [hep-lat/9605038](#).
- [33] Martin Luscher et al. “Nonperturbative O(a) improvement of lattice QCD”. In: *Nucl. Phys. B* 491 (1997), pp. 323–343. arXiv: [hep-lat/9609035](#).
- [34] R. G. Edwards, Urs M. Heller, and T. R. Klassen. “The Effectiveness of nonperturbative O(a) improvement in lattice QCD”. In: *Phys. Rev. Lett.* 80 (1998), pp. 3448–3451. arXiv: [hep-lat/9711052](#).

- [35] Karl Jansen and Rainer Sommer. “O(a) improvement of lattice QCD with two flavors of Wilson quarks”. In: *Nucl. Phys. B* 530 (1998). [Erratum: Nucl.Phys.B 643, 517–518 (2002)], pp. 185–203. arXiv: [hep-lat/9803017](#).
- [36] N. Yamada et al. “Non-perturbative O(a)-improvement of Wilson quark action in three-flavor QCD with plaquette gauge action”. In: *Phys. Rev. D* 71 (2005), p. 054505. arXiv: [hep-lat/0406028](#).
- [37] S. Aoki et al. “Nonperturbative O(a) improvement of the Wilson quark action with the RG-improved gauge action using the Schrödinger functional method”. In: *Phys. Rev. D* 73 (2006), p. 034501. arXiv: [hep-lat/0508031](#).
- [38] M. Lüscher and P. Weisz. “On-shell improved lattice gauge theories”. In: *Commun. Math. Phys.* 98.3 (1985). [Erratum: Commun.Math.Phys. 98, 433 (1985)], p. 433.
- [39] M. Albanese et al. “Glueball Masses and String Tension in Lattice QCD”. In: *Phys. Lett. B* 192 (1987), pp. 163–169.
- [40] Anna Hasenfratz and Francesco Knechtli. “Flavor symmetry and the static potential with hypercubic blocking”. In: *Phys. Rev. D* 64 (2001), p. 034504. arXiv: [hep-lat/0103029](#).
- [41] Martin Lüscher and Peter Weisz. “Perturbative analysis of the gradient flow in non-abelian gauge theories”. In: *JHEP* 02 (2011), p. 051. arXiv: [1101.0963 \[hep-th\]](#).
- [42] Robert V. Harlander and Tobias Neumann. “The perturbative QCD gradient flow to three loops”. In: *JHEP* 06 (2016), p. 161. arXiv: [1606.03756 \[hep-ph\]](#).
- [43] Johannes Artz et al. “Results and techniques for higher order calculations within the gradient-flow formalism”. In: *JHEP* 06 (2019). [Erratum: JHEP 10, 032 (2019)], p. 121. arXiv: [1905.00882 \[hep-lat\]](#).
- [44] Szabolcs Borsányi et al. “High-precision scale setting in lattice QCD”. In: *JHEP* 09 (2012), p. 010. arXiv: [1203.4469 \[hep-lat\]](#).
- [45] Rainer Sommer. “Scale setting in lattice QCD”. In: *PoS* LATTICE2013 (2014), p. 015. arXiv: [1401.3270 \[hep-lat\]](#).
- [46] Alberto Ramos. “The gradient flow running coupling with twisted boundary conditions”. In: *JHEP* 11 (2014), p. 101. arXiv: [1409.1445 \[hep-lat\]](#).
- [47] Martin Lüscher. “Future applications of the Yang-Mills gradient flow in lattice QCD”. In: *PoS* LATTICE 2013 (2014), p. 016.
- [48] Martin Lüscher. “Trivializing maps, the Wilson flow and the HMC algorithm”. In: *Commun. Math. Phys.* 293 (2010), pp. 899–919. arXiv: [0907.5491 \[hep-lat\]](#).
- [49] Stefano Capitani. “Lattice perturbation theory”. In: *Phys. Rept.* 382 (2003), pp. 113–302. arXiv: [hep-lat/0211036](#).
- [50] Colin J. Morningstar. “Lattice perturbation theory”. In: *Nucl. Phys. B Proc. Suppl.* 47 (1996). Ed. by T. D. Kieu, B. H. J. McKellar, and A. J. Guttmann, p. 92. arXiv: [hep-lat/9509073](#).
- [51] G. Martinelli and Yi-Cheng Zhang. “The Connection Between Local Operators on the Lattice and in the Continuum and Its Relation to Meson Decay Constants”. In: *Phys. Lett. B* 123 (1983), p. 433.

- [52] G. Martinelli and Yi-Cheng Zhang. “One Loop Corrections to Extended Operators on the Lattice”. In: *Phys. Lett. B* 125 (1983), p. 77.
- [53] Yusuke Taniguchi et al. “One loop renormalization factors and mixing coefficients of bilinear quark operators for improved gluon and quark actions”. In: *Nucl. Phys. B Proc. Suppl.* 73 (1999). Ed. by Thomas A. DeGrand et al., pp. 912–914. arXiv: [hep-lat/9809070](#).
- [54] C. Alexandrou et al. “One loop renormalization of fermionic currents with the overlap Dirac operator”. In: *Nucl. Phys. B* 580 (2000), pp. 394–406. arXiv: [hep-lat/0002010](#).
- [55] Sinya Aoki et al. “Perturbative renormalization factors in domain wall QCD with improved gauge actions”. In: *Phys. Rev. D* 67 (2003), p. 094502. arXiv: [hep-lat/0206013](#).
- [56] Sinya Aoki and Yoshinobu Kuramashi. “Perturbative renormalization factors of Delta  $S = 1$  four quark operators for domain wall QCD”. In: *Phys. Rev. D* 63 (2001), p. 054504. arXiv: [hep-lat/0007024](#).
- [57] Stefan Sint. “One loop renormalization of the QCD Schrodinger functional”. In: *Nucl. Phys. B* 451 (1995), pp. 416–444. arXiv: [hep-lat/9504005](#).
- [58] Yoshinobu Kuramashi. “Perturbative renormalization factors of bilinear operators for massive Wilson quarks on the lattice”. In: *Phys. Rev. D* 58 (1998), p. 034507. arXiv: [hep-lat/9705036](#).
- [59] N. Ishizuka and Y. Shizawa. “Perturbative renormalization factors for bilinear and four quark operators for Kogut-Susskind fermions on the lattice”. In: *Phys. Rev. D* 49 (1994), pp. 3519–3539. arXiv: [hep-lat/9308008](#).
- [60] Mauro Papinutto, Carlos Pena, and David Preti. “On the perturbative renormalization of four-quark operators for new physics”. In: *Eur. Phys. J. C* 77.6 (2017). [Erratum: Eur.Phys.J.C 78, 21 (2018)], p. 376. arXiv: [1612.06461 \[hep-lat\]](#).
- [61] Satchidananda Naik. “O(a) perturbative improvement for Wilson fermions”. In: *Phys. Lett. B* 311 (1993), pp. 230–234. arXiv: [hep-lat/9304013](#).
- [62] Sinya Aoki, Roberto Frezzotti, and Peter Weisz. “Computation of the improvement coefficient  $c(SW)$  to one loop with improved gluon actions”. In: *Nucl. Phys. B* 540 (1999), pp. 501–519. arXiv: [hep-lat/9808007](#).
- [63] Sinya Aoki and Yoshinobu Kuramashi. “Determination of the improvement coefficient  $c(SW)$  up to one loop order with the conventional perturbation theory”. In: *Phys. Rev. D* 68 (2003), p. 094019. arXiv: [hep-lat/0306015](#).
- [64] R. Horsley et al. “Perturbative determination of  $c(SW)$  for plaquette and Symanzik gauge action and stout link clover fermions”. In: *Phys. Rev. D* 78 (2008), p. 054504. arXiv: [0807.0345 \[hep-lat\]](#).
- [65] M. Luscher and P. Weisz. “Computation of the Action for On-Shell Improved Lattice Gauge Theories at Weak Coupling”. In: *Phys. Lett. B* 158 (1985), pp. 250–254.

- [66] P. Weisz. “Continuum Limit Improved Lattice Action for Pure Yang-Mills Theory. 1.” In: *Nucl. Phys. B* 212 (1983), pp. 1–17.
- [67] P. Weisz and R. Wohlert. “Continuum Limit Improved Lattice Action for Pure Yang-Mills Theory. 2.” In: *Nucl. Phys. B* 236 (1984). [Erratum: Nucl.Phys.B 247, 544 (1984)], p. 397.
- [68] R. Wohlert, P. Weisz, and Werner Wetzel. “Weak Coupling Perturbative Calculations of the Wilson Loop for the Standard Action”. In: *Nucl. Phys. B* 259 (1985), pp. 85–89.
- [69] M. Luscher and P. Weisz. “O(a) improvement of the axial current in lattice QCD to one loop order of perturbation theory”. In: *Nucl. Phys. B* 479 (1996), pp. 429–458. arXiv: [hep-lat/9606016](#).
- [70] Yusuke Taniguchi and Akira Ukawa. “Perturbative calculation of improvement coefficients to O( $g^{**2}a$ ) for bilinear quark operators in lattice QCD”. In: *Phys. Rev. D* 58 (1998), p. 114503. arXiv: [hep-lat/9806015](#).
- [71] Alois Grimbach et al. “O(a) improvement of the HYP static axial and vector currents at one-loop order of perturbation theory”. In: *JHEP* 03 (2008), p. 039. arXiv: [0802.0862](#) [[hep-lat](#)].
- [72] S. Aoki and Y. Kuramashi. “Perturbative determination of four parameters in relativistic heavy quark action”. In: *Nucl. Phys. B Proc. Suppl.* 119 (2003). Ed. by R. Edwards, John W. Negele, and D. Richards, pp. 583–585.
- [73] Sinya Aoki, Yasuhisa Kayaba, and Yoshinobu Kuramashi. “One loop calculation of mass dependent O(a) improvement coefficients for the relativistic heavy quarks on the lattice”. In: *Nucl. Phys. B Proc. Suppl.* 129 (2004). Ed. by S. Aoki et al., pp. 352–354. arXiv: [hep-lat/0310001](#).
- [74] Michael J. Glatzmaier, Keh-Fei Liu, and Yi-Bo Yang. “Perturbative Renormalization and Mixing of Quark and Glue Energy-Momentum Tensors on the Lattice”. In: *Phys. Rev. D* 95.7 (2017), p. 074513. arXiv: [1403.7211](#) [[hep-lat](#)].
- [75] Yi-Bo Yang et al. “The 1-loop correction of the QCD energy momentum tensor with the overlap fermion and HYP smeared Iwasaki gluon”. In: (Dec. 2016). arXiv: [1612.02855](#) [[nucl-th](#)].
- [76] G. Corbo, E. Franco, and G. C. Rossi. “Perturbative Renormalization of the Lowest Moment Operators of DIS in Lattice QCD”. In: *Phys. Lett. B* 221 (1989). [Erratum: *Phys.Lett.B* 225, 463 (1989)], p. 367.
- [77] G. Corbo, E. Franco, and G. C. Rossi. “Mixing of DIS Operators in Lattice QCD”. In: *Phys. Lett. B* 236 (1990), pp. 196–198.
- [78] Stefano Capitani and Giancarlo Rossi. “Deep inelastic scattering in improved lattice QCD. 1. The First moment of structure functions”. In: *Nucl. Phys. B* 433 (1995), pp. 351–389. arXiv: [hep-lat/9401014](#).
- [79] Giuseppe Beccarini et al. “Deep inelastic scattering in improved lattice QCD. 2. The second moment of structure functions”. In: *Nucl. Phys. B* 456 (1995), pp. 271–295. arXiv: [hep-lat/9506021](#).

- [80] R. C. Brower et al. “Calculation of moments of nucleon structure functions”. In: *Nucl. Phys. B Proc. Suppl.* 53 (1997). Ed. by C. Bernard et al., pp. 318–320. arXiv: [hep-lat/9608069](#).
- [81] Stefan Sint and Peter Weisz. “The Running quark mass in the SF scheme and its two loop anomalous dimension”. In: *Nucl. Phys. B* 545 (1999), pp. 529–542. arXiv: [hep-lat/9808013](#).
- [82] Achim Bode, Peter Weisz, and Ulli Wolff. “Two loop computation of the Schrodinger functional in lattice QCD”. In: *Nucl. Phys. B* 576 (2000). [Erratum: Nucl.Phys.B 608, 481–481 (2001), Erratum: Nucl.Phys.B 600, 453–453 (2001)], pp. 517–539. arXiv: [hep-lat/9911018](#).
- [83] Sergio Caracciolo, Andrea Pelissetto, and Antonio Rago. “Two loop critical mass for Wilson fermions”. In: *Phys. Rev. D* 64 (2001), p. 094506. arXiv: [hep-lat/0106013](#).
- [84] M. Luscher and P. Weisz. “Efficient Numerical Techniques for Perturbative Lattice Gauge Theory Computations”. In: *Nucl. Phys. B* 266 (1986), p. 309.
- [85] Matthew A. Nobes and Howard D. Trottier. “Progress in automated perturbation theory for heavy quark physics”. In: *Nucl. Phys. B Proc. Suppl.* 129 (2004). Ed. by S. Aoki et al., pp. 355–357. arXiv: [hep-lat/0309086](#).
- [86] Matthew A. Nobes. “Automated lattice perturbation theory for improved quark and gluon actions”. Other thesis. 2004.
- [87] A. Hart et al. “Automatically generating Feynman rules for improved lattice field theories”. In: *J. Comput. Phys.* 209 (2005), pp. 340–353. arXiv: [hep-lat/0411026](#).
- [88] A. Hart et al. “Automated generation of lattice QCD Feynman rules”. In: *Comput. Phys. Commun.* 180 (2009), pp. 2698–2716. arXiv: [0904.0375 \[hep-lat\]](#).
- [89] Dirk Hesse, Rainer Sommer, and Georg von Hippel. “Automated lattice perturbation theory applied to HQET”. In: *PoS LATTICE2011* (2011). Ed. by Pavlos Vranas, p. 229.
- [90] C. J. Monahan. “The Beauty of Lattice Perturbation Theory: The Role of Lattice Perturbation Theory in B Physics”. In: *Mod. Phys. Lett. A* 27 (2012), p. 1230040. arXiv: [1210.7266 \[hep-lat\]](#).
- [91] Hikaru Kawai, Ryuichi Nakayama, and Koichi Seo. “Comparison of the Lattice Lambda Parameter with the Continuum Lambda Parameter in Massless QCD”. In: *Nucl. Phys. B* 189 (1981), pp. 40–62.
- [92] Antonio Gonzalez Arroyo, F. J. Yndurain, and G. Martinelli. “Computation of the Relation Between the Quark Masses in Lattice Gauge Theories and on the Continuum”. In: *Phys. Lett. B* 117 (1982). [Erratum: Phys.Lett.B 122, 486 (1983)], p. 437.
- [93] Herbert W. Hamber and Chi Min Wu. “Some Predictions for an Improved Fermion Action on the Lattice”. In: *Phys. Lett. B* 133 (1983), pp. 351–358.
- [94] Giuseppe Burgio, Sergio Caracciolo, and Andrea Pelissetto. “Algebraic algorithm for the computation of one loop Feynman diagrams in lattice QCD with Wilson fermions”. In: *Nucl. Phys. B* 478 (1996), pp. 687–722. arXiv: [hep-lat/9607010](#).

- [95] Wolfram Research, Inc. *Mathematica 13.2*. Version 13.2. 2022. URL: <https://www.wolfram.com>.
- [96] Maximilian Ammer and Stephan Durr. “ $c_{\text{SW}}$  at One-Loop Order for Brillouin Fermions”. In: *PoS LATTICE2022* (2023), p. 289. arXiv: 2210.06860 [hep-lat].
- [97] Claude W. Bernard and Thomas A. DeGrand. “Perturbation theory for fat link fermion actions”. In: *Nucl. Phys. B Proc. Suppl.* 83 (2000). Ed. by M. Campostrini et al., pp. 845–847. arXiv: hep-lat/9909083.
- [98] Stefano Capitani, Stephan Durr, and Christian Hoelbling. “Rationale for UV-filtered clover fermions”. In: *JHEP* 11 (2006), p. 028. arXiv: hep-lat/0607006.
- [99] Maximilian Ammer and Stephan Durr. “Stout-smearing, gradient flow and  $c_{\text{SW}}$  at one loop order”. In: *PoS LATTICE2021* (2022), p. 407. arXiv: 2109.14562 [hep-lat].